IDENTIFICATION AND CHARACTERISATION OF A NOVEL, MULTI-POTENT, SKELETAL MUSCLE-DERIVED STEM CELL WITH BROAD DEVELOPMENTAL PLASTICITY

BEVERLEY JANE HENNING

A thesis submitted in partial fulfilment of the requirements of Liverpool John Moore's University for the degree of Doctor of Philosophy

March 2015

ACKNOWLEDGEMENTS

ABSTRACT

PW1$^+$/Pax7$^-$ skeletal muscle-derived interstitial progenitor cells (PICs) are myogenic *in vitro,* efficiently contribute to skeletal muscle regeneration *in vivo*, and are self-renewing *in vivo* whilst also giving rise to satellite cells (Mitchell et al. 2010). They have previously been identified in the mouse and pig and are bi-potent forming both smooth and skeletal muscle (Mitchell et al. 2010, Lewis et al. 2014). This study characterised murine PICs for stem cell properties of self-renewal, clonogenicity and multipotency. Furthermore, PW1 expression was assessed in cardiac tissue, and in an isolated Sca1$^+$ cardiac stem cell population.

Satellite cells and PICs were identified and quantified in hind limb skeletal muscle of 3, 10 and 21 day, and 2 year old mice: there was a decline in abundance of both SC and PICs with age. PICs were isolated by MACS technology from hind limb murine skeletal muscle of 21 day old mice, and their phenotype characterised. Isolated PICs expressed markers of pluripotency; Oct3/4, Sox2 and Nanog, were clonogenic and self- renewing over >60 population doublings *in vitro,* with a population doubling time of 15.8±2.9 hours. Furthermore, PICs demonstrated multipotency both *in vitro* and *in vivo* giving rise to cell types from the 3 germ layers.

PW1$^+$ cells were identified and quantified with respect to location in the heart on 3, 10 day, 21 day and 2 year old mice with the majority of cells found within the epicardium. There was rapid decline in abundance during postnatal development. CD45$^-$/Sca-1$^+$ CSCs were isolated from 6 week old mice via MACS technology and assessed for PW1 expression (83%).

In summary, this study showed PICs have broad developmental plasticity both *in vitro* and *in vivo*, and can be propagated and maintained in a primitive state in culture. Furthermore, PW1 also marks a stem cell population within the heart. These data opens new avenues for solid tissue engineering and regeneration utilising a single multi-potent stem cell type, isolated from an easily accessible source such as skeletal muscle.

TABLE OF CONTENTS

LIST OF TABLES

LIST OF FIGURES

ABBREVIATIONS

ASC   Adult Stem Cell

BMDC   Bone Marrow Derived Cell

BMT   Bone Marrow Transplant

cCFU   Cardiac-derived Colony Forming Unit

CDC   Cardiosphere Derived Cell

CNS   Central Nervous System

CPC   Cardiac Progenitor Cell (sca-1$^{+)}$

CSC   Cardiac Stem-progenitor Cell

cSP   Cardiac Side Population

DMD   Duchene's Muscular Dystrophy

DMSO   Dimethyl Sulfoxide

eCSC   Endogenous Cardiac Stem cell (c-kit^{+})

EPDC   Epicardial Derived Cell

ESC   Embryonic Stem Cell

ESCQ-FBS   Embryonic Stem Cell Qualified – Fetal Bovine Serum

FACS   Flow Assisted Cell Sorting

FAP   Fibro-adipogenic progenitor

FBS   Fetal Bovine Serum

FC   Flow Cytometry

hESC   Human Embryonic Stem cell

HSC   Hematopoietic Stem Cell

ICC   Immunocytochemistry

IHC   Immunohistochemistry

IF   Immunofluorescence

iPSC   Induced Pluripotent stem cell

LIF   Leukemia Inhibitory Factor

MAB   Mesoangioblast

MACS   Magnetic Activated Cell Sorting (Miltenyi)

MI   Myocardial Infarction

P   Passage

PBS   Phosphate Buffered Saline

PD   Population Doubling

PIC $PW1^+$/$Pax7^-$ interstitial cell

pPIC   Porcine derived $PW1^+$/$Pax7^-$ Interstitial Cell

qRT-PCR   Quantitative Real-Time Polymerase Chain Reaction

RT   Room Temperature

SC   Satellite cell

SP   Side Population

PUBLICATIONS

Waring, C.D., **Henning, B.J**., Smith, A.J., Nadal-Ginard, B., Torella, D., Ellison, G.M. (2015) Cardiac adaptations from 4 weeks of intensity-controlled vigorous exercise are lost after a similar period of detraining. *Physiological Reports*, 3 (2), e12302.

Ellison, G.M., Smith, A.J., Waring, C.D., **Henning, B.J**., Burdina, A.O., Polydorou, J., Vicinanza, C., Lewis, F.C., Nadal-Ginard, B., Torella, D. (2014) Adult Cardiac Stem Cells: Identity, Location and Potential. *Adult Stem Cells: Stem Cell Biology and Regenerative Medicine*, pp 47-90. Humana Press.

Lewis, F.C., **Henning, B.J**., Marazzi, G., Sassoon, D., Ellison, G.M., Nadal-Ginard, B. (2014) Porcine skeletal muscle-derived multipotent PW1pos/Pax7neg interstitial cells: isolation, characterization, and long-term culture. *Stem Cells Translational Medicine*, 3 (6), 702-12.

Ellison, G.M., Vicinanza, C., Smith, A.J., Aquila, I., Leone, A., Waring, C.D., **Henning, B.J**., Stirparo, G.G., Papait, R., Scarfò, M., Agosti, V., Viglietto, G., Condorelli, G., Indolfi, C., Ottolenghi, S., Torella, D., Nadal-Ginard, B. (2013) Adult c-kit(pos) cardiac stem cells are necessary and sufficient for functional cardiac regeneration and repair. *Cell,* 154(4):827-42.

Torella, D., Ellison, G.M., Torella, M., Vicinanza, C., Aquila, I., Iaconetti, C., Scalise, M., Marino, F., **Henning, B.J**., Lewis, F.C., Gareri, C., Lascar, N., Cuda, G., Salvatore, T., Nappi, G., Indolfi, C., Torella, R., Cozzolino, D., Sasso, F.C. (2014) Carbonic anhydrase activation is associated with worsened pathological remodeling in human ischemic diabetic cardiomyopathy. *Journal of the American Heart Association*, 3 (2), e000434.

Curcio, A., Torella, D., Iaconetti, C., Pasceri, E., Sabatino, J., Sorrentino, S., Giampà, S., Micieli, M., Polimeni, A., **Henning, B.J**., Leone, A., Catalucci, D., Ellison, G.M., Condorelli, G., Indolfi, C. (2013) MicroRNA-1 downregulation increases connexin 43 displacement and induces ventricular tachyarrhythmias in rodent hypertrophic hearts. *PLoS One*, 8 (7), e70158.

1. INTRODUCTION

1.1 Muscular Dystrophy and Heart Disease

1.1.1 Muscular Dystrophies

Muscular dystrophy is a term used to describe a range of genetic muscle diseases which result in progressive skeletal muscle weakness and wastage (Pearson 1963). The condition predominantly affects males and is inherited genetically, although roughly 1/3 of cases occur without any family history due to prenatal mutations (Bakker et al. 1989). The phenotypic manifestation of muscle wastage/weakness is mainly due to defects and/or the inability to make the protein dystrophin and other associated protein complexes. Dystrophin is a cytoplasmic protein located in the sarcolemma which forms part of a membrane spanning protein complex to connect the cytoskeleton to the basal lamina (Blake et al. 2002).

There are approximately 70,000 babies, children and adults in the UK suffering from some form of muscular disease (Table 1.1), with 12.6% of these being dystrophic disorders such as Duchenne's Muscular Dystrophy (DMD). DMD is a progressive muscle wasting disease which affects approximately 1:3500 boys and often results in death due to respiratory failure before 25 years of age (Blake et al. 2002). Current treatments include physiotherapy and corticosteroids to improve muscle strength, along with surgery to correct associated spinal curvature, these treatments however, are not a cure and only serve to manage the condition. Using stem cells as a regenerative therapy may be the key to providing a definitive cure for such genetic conditions.

To date there have been 6 clinical trials looking at the benefits of stem cell transplantation therapies in treating Duchene's muscular dystrophy (NCT01834040, NCT01834066, NCT02241434, NCT01610440, NCT02235844, NCT02285673), however results have not yet been published.

Table 1.1   Prevalence of muscular diseases within the UK (Muscular Dystrophy Campaign stats 2012).

Group of conditions	Patient number in UK	Percentage of total (%)
Muscular dystrophies	8,000-10,000	12.6
Myotonic disorders	9,500	13.3
Congenital myopathies	1,000	1.4
Distal myopathies	300	0.4
Mitochondrial myopathies	3,500	4.9
Metabolic myopathies	700	1.0
Periodic paralysis	900	1.3
Myositis	5,000-6,000	7.7
Spinal muscular atrophies	1,200	1.7
Hereditary neuropathies	23,000	32.0
Inflammatory and autoimmune neuropathies	6,400	8.9
Disorders of the neuromuscular junction	10,500	14.7
Myositis ossificans progressiva	60	0.1
Total number (prevalence)	**70,060-73,060**	**100**

1.1.2 Heart Failure and Disease

Heart failure occurs when the heart can no longer efficiently pump blood around the body resulting in a variety of symptoms including shortness of breath, dizziness, angina, weakness, nausea and eventually death. Caused by damage from an ischemic event such as a myocardial infarction (MI), cardiomyopathies of the muscle or disease of associated vessels and valves, heart failure is a chronic disease which gradually gets worse over time.

In 2011 there were 71,837 reported deaths from heart disease within the UK with more than 750,000 patients living with the condition (British Heart Foundation statistics 2012). Available treatments are currently highly ineffective, mainly given to reduce symptoms and slow down the progression of the disease, with the only 'cure' being organ transplantation (Jessup and Brozena 2003). A goal of cardiovascular research is to find a way to replace cardiomyocytes to prevent or reverse heart disease and failure, with many people looking promisingly to stem cell therapies as the solution (Nadal-Ginard et al. 2006).

In 2001 bone marrow derived stem cells (BMDCs) were found to give rise to new cardiomyocytes and vasculature (Orlic et al. 2001). A flurry of studies and clinical trials were conducted as a result of this paper, injecting BMDC's into patients after myocardial infarction (MI). Subsequent meta-analysis of the results showed a modest improvement in ventricular ejection fraction of 3 % (Lipinski et al. 2007, Kang et al. 2008, Abdel-Latif et al. 2007), however in 2004 two separate papers gave evidence that BMDCs do not form cardiac tissue (Murry et al. 2004, Balsam et al. 2004). Current clinical trials are mainly using bone marrow derived cells (BMDCs) of different origins in the hope of a positive paracrine effect (Nadal-

Ginard et al. 2006) and the hunt is still on to find the 'best' type of cell which will yield the most functional myocardial regeneration.

The discovery of an endogenous small cell population with the phenotype, behaviour and regenerative potential of bona fide cardiac stem cells (eCSCs) in adult mammalian myocardium, including in the human (Beltrami et al. 2003, Moretti et al. 2006) and their ability to regenerate contractile myocytes and microvascular both *in vitro* and *in vivo* (Ellison et al. 2007, Beltrami et al. 2003) may hold the key to producing functional regeneration of the myocardium damaged by an ischemic event.

Recently 2 clinical trials utilising cardiac stem/progenitor cells, (SCIPIO - NCT00474461) and CDC's (CADUCEUS - NCT00893360) have shown improvements in cardiac function in ischemic heart failure patients. The CADUCEUS trial looked at a total of 25 patients, of which with 17 received stem cell treatment. There was an 11% reduction in scar tissue compared to controls after 1 year, however this did not result in any improvement in global cardiac function (Makkar et al. 2012; Malliaras et al. 2014). The SCIPIO trial looked at 33 patients, 20 of which received stem cell treatment. They reported a higher reduction in scar tissue of 30%, and an increase in ejection fraction of 13.6 EF units after 1 year (Bolli et al. 2011; Chugh et al. 2012).

1.2 Stem Cells as Regenerative Medicines.

Stem cells are self-renewing cells capable of differentiation into a variety of cell types within the body. They can be unipotent or bipotent in that they can only make one or two cell types, or be multipotent being able to make a wider range of

cell types including those from other germ layers. Pluripotent stem cells are those with the highest level of potency and are able to give rise to any type of cell within the body. Due to these capabilities stem cells are currently at the forefront of research for regenerative medicines. Understanding the mechanisms by which these cells activate, proliferate and differentiate is fundamental in designing treatments for degenerative diseases and tissue repair. By utilising stem cell therapies we have the potential to save and improve lives of patients suffering from a wide array of medical conditions whether they are, acute, chronic, congenital or acquired. They may also be used to treat less 'life saving' but certainly 'life changing' conditions such as baldness or infertility (Ogawa et al. 2000; Yang et al. 2011).

To date there have been over 4500 registered stem cell related clinical trials of which around 1800 are currently in process, 500 of these being within Europe (www.clinicaltrials.gov). One of the most successful and best known stem cell therapies is bone marrow transplantation (BMT) which was first conducted in humans in 1968 and it still regularly used to treat blood and bone marrow diseases such as cancers and immune disorders, with approximately 60,000 BMT's taking place worldwide annually (Syed and Evans 2013).

It is hoped that the development of further cellular therapies may eventually reduce the need for invasive surgery and oversubscribed organ/tissue transplantations, as well as providing effective treatments for conditions for which there is currently none. Not only will this provide massive health benefits to the population but it will also reduce the economic burden of on-going illness and disease.

Unfortunately the reality of most stem cell trials to date (bar a few successful ones such as in BMT) have not yet shown striking results, mainly due to poorly controlled and commercially driven trials where results are inconclusive.

Stem cells can be used in regenerative therapies and treatments via a variety of avenues; the easiest and most commonly used is a direct infusion of cells either into the circulatory system or directly to the site of interest, this is the method of transfer used in BMTs and cellular based therapies and can be either autologous, where the donor and recipient are the same person, or allogeneic, when the donor is someone other than the recipient.

More recently stem cells have been used in tissue engineering to provide biologically functional grafts such as skin, bone and cartilage where the grafts main purpose is structural; this involves either growing the tissue *in vitro* before transplant, or using an artificial scaffold with incorporated stem cells for integration of the graft *in vivo*. However, the challenge lies in creating integrative tissues with a higher level of function such as the heart, liver or pancreas. Promisingly, recent research has shown the generation functional human liver in a mouse model when liver buds generated from human iPSCs were transplanted into non-obese diabetic/severe combined immunodeficient (NOD/SCID) Mice (Takebe et al. 2013). A similar study transplanting human stem-cell-derived β cells into NOD/SCID mice found that they went on to produce insulin, however insulin levels were lower than seen in cadaveric islet cell transplantation (Pagliuca et al. 2014).

In conditions such as muscular dystrophy or multiple sclerosis, where the condition affects the whole or a large area of the body, tissue grafts may not be a viable solution and therefore it is imperative that we develop cellular therapies that can repair damage and restore function *in situ* (Cossu and Sampaolesi 2007)

One avenue for achieving this in genetic conditions may be gene therapy, where the genetic content of a patient's own cells is altered by the insertion/replacement or removal of genes using a vector. Examples of Vectors used include adenoviruses, retroviruses, adeno-associated viruses and plasmids (Chamberlain et al. 2002). Such therapies can be targeted at mature myofibres, however to ensure long-lasting results they must also be targeted at muscle stem-progenitor cells (Bertoni 2014).

In non-genetic conditions or injury such as a myocardial infarction (MI), it may be possible to activate patients' functional endogenous stem cells using stimuli such as growth factors and cytokines to encourage and/or increase *in situ* regeneration. Such a therapy has previously been shown to improve ventricular function in pigs that have received intracoronary insulin-like growth factor (IGF-1) and hepatocyte growth factor (HGF) after an induced MI (Ellison et al. 2011). A more recent study found that sustained delivery of IGF-1, delivered via a hydrogel had a similar effect in a pig chronic MI model, with a 4 fold increase in the number of cardiac stem cells, increased ventricular function, new myocyte formation and increased capillarization (Koudstall et al. 2014).

Furthermore, stem cells may be used as a stepping stone between animal studies and clinical trials; cultivated and differentiated *in vitro* they can be utilised to test

and help in the development of new drugs and medicines, allowing us to see cell responses and possible side effects before testing on patients. One example of this is cholangiocytes derived from human induced pluripotent stem cells, which were found to have a similar reaction *in vitro* as seen in patients, to two drugs used to treat cystic fibrosis associated cholangiopathy: verapamil and octreotide (Sampaziotis et al. 2015).

Stem cells can be acquired from a number of sources which are generally divided into 3 categories. Embryonic stem cells (ESCs), induced pluripotent stem cells (iPSCs) and adult stem cells (ASCs), with each type having its own benefits, drawbacks and relevant applications.

1.2.1 Embryonic Stem Cells

ESCs are pluripotent stem cells found within the epiblast tissue of the inner cell mass of a blastocyst; in humans this is 5-6 days post fertilization (Hardy et al. 1989). They are universally recognised as the most pluripotent of all stem cells due to their indefinite self-renewal capacity and differentiation efficacy into derivatives of the 3 primary germ layers; endoderm, mesoderm and ectoderm (Thomson et al. 1998; Amit et al. 2000). ESCs have been successfully isolated from numerous mammalian species including the mouse (Evans and Kaufman 1981), primate (Müller at al. 2009) and human (Thomson et al. 1998) and although initially hailed as a new tool for tissue engineering and regenerative therapies, they have since proved to be problematic. The production, harvest and subsequent use of human ESCs is highly controversial and raises many ethical, religious and moral questions, these however are not the only limitations. Autologous cell transplantations are not possible; indeed there are problems with

histocompatibility and immunological response within the recipient (Taylor et al. 2011). Furthermore, the sheer attribute of their assured pluripotency may also be their downfall with reports of malignant teratoma formation (Shih et al. 2007; Knoepfler 2009). Whilst much research has been conducted on ESCs from a number of sources, the first approved human clinical trial using human ESC-derived (hESC) oligodendrocyte progenitor cells to treat spinal cord injuries was halted due to financial issues (NCT01217008), affirming that ESC research still needs to overcome many hurdles before it can be supported and translated to a clinical setting.

1.2.2 Induced Pluripotent Stem Cells

iPSCs are artificially derived from non-pluripotent adult somatic cells, such as skin fibroblasts, via forced expression of pluripotency genes. The most commonly used are Oct3/4, Sox2, c-Myc and Klf4 (Takahashi and Yamanaka 2006; Takahashi et al. 2007) although transfection of Nanog and LIN28 alongside Oct4 and Sox2, has also been shown to induce pluripotency (Yu et al. 2007). iPSCs produce morphologically similar colonies to ESCs and contribute to a variety of tissues within the developing embryo when injected into the blastocyst (Takahashi and Yamanaka 2006). Since their initial production in 2006 in the mouse, they have since also been produced in rats (Li et al. 2009), rhesus monkeys (Lui et al. 2008), Pigs (Ezashi et al. 2009) and importantly in humans (Yu et al. 2007; Takahashi et al. 2007). Initially iPSCs were hailed as the new saviour of stem cell research, allowing a patient's own cells to be utilized for autologous transplantation. While it was thought this would eliminate problems associated with allogeneic transplants it seems that some immunological responses still occur,

possibly due to epigenetic alterations within the cells during *ex vivo* processing (Zhao et al. 2011).

As with ESCs, iPSCs form teratomas, one suggested reason being the use of oncogenic factors such as c-Myc to induce these cells (Kneopler 2009), However it should be noted that teratoma forming ESC's do not over express c-Myc and therefore the exact reason behind this is still unknown. Initially most iPSCs were induced using retroviral transfection, which carried risks associated with using any viral vector (Cornetta et al. 1991), however more recently safer integration free methods have been devised.

1.2.3 Adult Stem Cells

ASCs are tissue-specific stem-progenitor cells found throughout the tissues and organs of the body after embryonic development, usually residing within a specific cellular niche (Snippert and Clevers 2011). They are self-renewing through mitotic cell division and multipotent; giving rise to mature, differentiated cell types of the tissue from which they are derived. It is generally accepted that they are responsible for maintaining homeostasis of the wear-and-tear renewal and repair of aged or damaged tissue and have been identified in most adult tissue types (Table 1.2), including skeletal muscle (Tedesco et al. 2010), heart (Beltrami et al. 2003), brain (Paspala et al. 2011), liver (Kordes and Häussinger 2013), kidneys (Gupta et al. 2006), skin (Fuchs 2008), gut (Wang et al. 2013), lung (Liu et al. 2006) and eyes (Secker and Daniels 2009).

One of the most well documented and clinically successful ASC is the hematopoietic stem cell (HSC), capable of giving rise to cells of myeloid and lymphoid lineages (Osawa et al. 1996; Iwasaki and Akashi 2007). HSCs are found

in the bone marrow, peripheral blood and cord blood. First identified in 1961 in the mouse (Till and McCulloch 1961), HSCs have since been used to treat over 50 diseases including leukaemia, inflammatory bowel disease and osteogenesis imperfecta (Thomas 1999).

Each of the above ASC population has a distinctive marker profile on which they can be identified (Table 1.2).

Table 1.2   Tissue specific ASC populations and their phenotype throughout the mammalian body.

Organ/Tissue	Stem/Progenitor Cell	Phenotype
Muscle	Satellite Cell	$CD45^-/Pax7^+$
Heart	Cardiac Stem Cell	$CD45^-/c\text{-}kit^+/Sca\text{-}1^+$
Brain	Neural Stem Cell	$CD45^-/CD34^-$ $CD133^+/Nestin^+/Sox2^+$
Liver	Hepatic Progenitor Cells	$EpCAM^+$
Kidneys	Multipotent Renal Progenitor Cell	$CD45^-/CD133^-/CD106^-/CD31^-$ $CD56^-/CD90^+/CD44^+$
Skin	Keratinocyte Stem Cell (Bulge, SG and epidermal)	$Ck5^+/Ck14^+/p63^+/\alpha6\beta4^+$
Gut	Intestinal Stem Cell	$CD44^+/CD24^{low}/CD166^+$
Lung	Basal Stem cell Clara Stem Cell	$Ck5^+/Ck14^+$ $CCSP^+/Cyp2f2^+$
Eyes	Limbal Epithelial Stem Cell	$Ck3^-/Ck12^-/Cn43^-/p63^+$
Blood/Bone Marrow	Hematopoietic Stem Cell	$Lin^-/CD34^+/c\text{-}kit^+/Sca\text{-}1^+$

1.2.4 Adult Stem Cells vs Embryonic Stem Cells and Induced Pluripotent Stem Cells

Interestingly, unlike ESCs and iPSCs, pluripotent ASCs such as cCFUs do not independently form teratomas (Chong et al. 2011). Whilst many consider teratoma formation a measure of pluripotency, a stem cell capable of trans-germ layer differentiation without teratoma formation is surely ideal in the formation of viable, safe clinical therapies. As with iPSCs, ASCs provide us with a source for autologous therapies, and with minimal manipulation these cells may not incite any undesirable immunological response, as demonstrated by HSC therapies used to date. Finally, ASCs do not carry the same ethical issues associated with ESCs, with both host and donor able to give informed consent.

Current human trails aimed at muscle regeneration of both skeletal and cardiac muscle primarily use either cord blood or adult stem cells of multiple origins, however some studies using iPSCs have recently begun. Much of this research is still on-going and the best cell type is yet to be determined.

1.3 Stem Cell Properties and Characteristics

1.3.1 Pluripotency

ESCs and iPSCs are pluripotent, with the ability to differentiate into cell types from the three primary germ layers; the mesoderm, ectoderm and endoderm, which appear during early embryonic development *in vivo*. Pluripotency and self-renewal in stem cells is usually associated with phenotypic expression of three important markers, Sox2, Oct3/4 and Nanog, which act together and individually to maintain stem cells in a pluripotent state. They are thought to function as molecular rheostats in inhibiting stem cell differentiation and promoting self-

renewal and pluripotency, although the exact mechanisms by which they do this are very complex and not yet fully understood (Rizzino 2009). The presence of these markers in ESCs, alongside forced expression in iPSCs, is well documented; however their function within ASC populations needs to be further fortified. Together these three factors have become somewhat of a proxy for stemness.

SRY-high mobility group box 2 (Sox2) is a transcription factor concomitant to the maintenance of self-renewal and pluripotency. Indeed, down regulation of Sox2 has been shown to promote differentiation in murine ESCs (Avilion et al. 2003). Initially expressed in blastomeres it continues to persist in the epiblast, with further expression reported in some multipotential and precursor cells (Avilion et al. 2003). Sox2 deletion during embryonic development proves lethal with murine embryos unable to develop an epiblast (Avilion et al. 2003), thus showing the importance of Sox2 during embryogenesis and development. It is surmised that Sox2 acts in synergy with Oct3/4 to activate Oct-Sox enhancers capable of regulating pluripotency genes such as Nanog, Oct4 and Sox2 itself (Bosnali et al. 2009).

Octomer binding transcription factor 4, also commonly known as Oct3, Oct4 or Oct3/4, belongs to the Pit-Oct-Unc (POU) transcription factor family (Schöler et al. 1990). It is attributed to the maintenance of pluripotency and is almost exclusively expressed in ESC and germ line cells (Schöler et al. 1990; Nichols et al. 1998). Oct3/4 knockout embryos are incapable of development beyond the blastocyst stage exhibiting irregular inner cell mass formation; subsequently ESCs cannot be derived from Oct3/4 deficient blastocysts (Nichols et al. 1998). While a 50% reduction in Oct3/4 seems to promote trophectodermal differentiation within

ESCs, a two fold increase in Oct3/4 similarly results in primitive endoderm and mesoderm differentiation (Niwa et al. 2000) suggesting that a precise expression level of Oct3/4 is needed to maintain pluripotency of ESCs and the functionality of Oct3/4 does not operate in an on/off mechanism.

The transcription factor Nanog is a homeobox protein and the third key player in pluripotency, it is expressed in the inner cell mass of blastocysts, the epiblast and germ cells (Chambers et al. 2003; Hart et al. 2004). Unlike Oct3/4 and Sox2, Nanog is not homogeneously distributed in ESCs with cells being a mix of Nanog high or Nanog low. Overexpression of Nanog can alleviate LIF (leukaemia inhibitory factor) dependence of mouse ESCs (Chambers et al. 2003; Mitsui et al. 2003) which neither Oct3/4 nor Sox2 have been shown to do. Furthermore, Nanog ablation results in decelerated cell growth of murine ESCs (Mitsui et al. 2003). This correlates with the reported enhanced proliferation of Nanog expressing cells via promotion of cells into s-phase (Zhang et al. 2005).

1.3.2 Self-renewal

Stem cells can self-renew by either symmetrical or asymmetric division, dependant on intrinsic and extrinsic influences (Morrison and Kimble 2006)

Stem cell self-renewal capability can be assessed by a number of methods *in vitro*: Clonogenicity is the ability of a single cell to clone itself and subsequently form a colony, generally shown as a percentage or number of colonies per initial cell population, it is assessed via colony scoring (Preisler et al. 1975), where cells are plated at a very low density and later assessed via microscopy for colony formation. Alternatively single cells are seeded, usually within individual wells of

a 96-well plate, and the percentage of single cells that go on to form colonies is counted, with the benefit of generating 100% pure single cell derived colonies which can be used for further experimentation.

The total number of possible population doublings (PDs) can also be an indicator of stemness, with true stem cells capable of indefinite self-renewal and therefore infinite population doublings. It should however be noted that non-optimum culture conditions can severely affect proliferation *in vitro* with cells displaying a PD below their intrinsic potential.

Hayflick and Moorhead (1961) first described that human cells derived from embryonic tissues are only capable of between 40-60 PDs in culture before growth arrest or replicative senescence occurs. This data has subsequently been used to define 'Hayflicks limit' (Hayflick 1979), which is the number of times any normal cell can divide. These initial studies were conducted using human fibroblasts but have since been conducted in many other tissues and a variety species. Further research by Hayflick (1973) suggested that this 'limit' is in fact correlated to the maximum lifespan of a species, with a PD limit of 14-28 in mice which can live to 3.5 years of age, and 15-35 in chickens which can reach 30 years old . In agreement with this, in longer-living species such as the Galapagos tortoise the limit extends to 90-130 doublings (Goldstein 1974).

As well as passing the species specific 'limit' of PDs, to demonstrate true 'self-renewal' the phenotype of the cell after long-term culture should be the same as the starting cell population.

1.3.3 Trans-germ Layer Differentiation

Some purported ASCs share more characteristics with progenitor cells than *bona fide* stem cells, whilst they may be multipotent and have self-renewal capability most are incapable of trans-germ layer differentiation (Figure 1.1). Promisingly however, an increasing number of ASCs have shown such capability indicating that there may be a pool or several populations of pluripotent ASCs residing within the adult mammalian body.
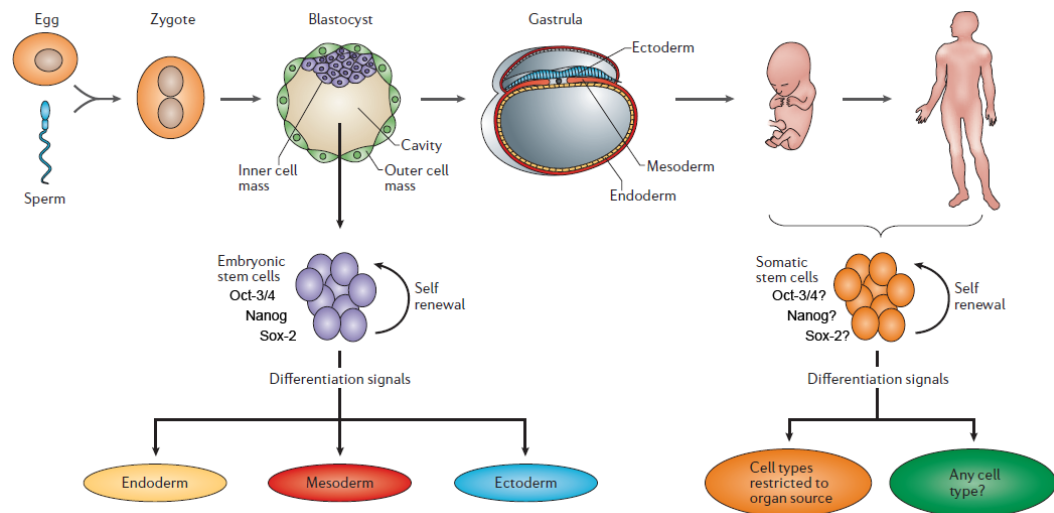
Figure 1.1   Plutipotent potential of ESCs and proposed pluripotency of ASCs (Adapted from O'Connor and Crystal 2006).

In 1997, Eglitis and Mezey transplanted labelled HSCs (of mesoderm origin) into sub lethally irradiated mice which were then seen to be widely distributed throughout multiple regions of the brain at 3 days post-transplant, with the number of cells detected rising over several weeks. 10% of the HSC derived cells found in the brain regions went on to express astroglial marker GFAP suggesting

that HSCs are capable of trans-germ layer differentiation. Further to this, human derived HSCs implanted into lesions of the developing spinal cord of chick embryos differentiate into neurons with neuronal expressing neuronal markers NeuN and MAP2 (Sigurjonsson et al. 2005).

More recently, Neural stem cells taken from the adult mouse brain have been shown to contribute in the formation of chimeric chick and mouse embryos, concurrently giving rise to cells of all germ layers (Clarke et al. 2000). Similarly cardiac derived colony forming units (cCFUs) from mouse hearts also show differentiation into mesodermal, endodermal and ectodermal cells when injected alongside ESCs in teratoma formation assays (Chong et al. 2011). These data support the hypothesis that like ESCs and iPSCs, some adult stem cells may be pluripotent. It should be noted that these few studies have not yet been replicated and therefore their conclusions should be treated with caution.

1.4 Stem Cell Aging

There are two main types of stem cell aging: replicative and chronological aging (Figure 1.2). Replicative aging is related to the number of cell divisions a cell has been through, whilst chronological aging is the actual age of the cell. Stem cells that undergo more cycles (e.g intestinal stem cells) due to a higher cell turnover, show both replicative and chronological aging. Those which undergo fewer divisions because of a lower cell turnover (e.g CSC's) are chronologically aged but not necessarily replicative senescent.
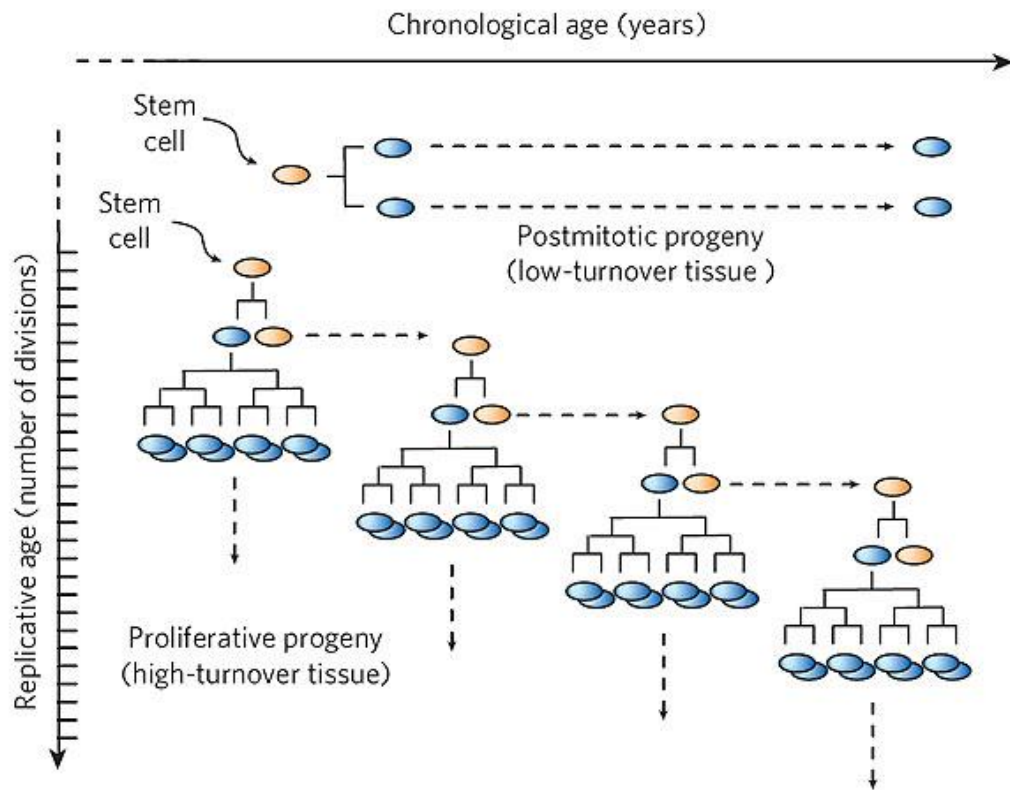
Figure 1.2   Replicative and Chronological aging of Stem Cells. (Rando. 2006).

The reason why stem cells become dysfunctional or senescent during replicative aging may be linked to telomere shortening, genetic mutations or other changes that occur with each cell division (Rando 2006). Telomeres are nucleotide sequences at the end of chromosomes which act like a buffer to prevent changes to the functional section. They can become shortened during replication as DNA polymerase does not start at the beginning of the strand, however they can also become shortened following oxidative stress (von Zglinicki et al. 1995)

In contrast, chronologically aged cells may become dysfunctional due to changes in their niche or systemic environment which can cause epigenetic changes and

effect intrinsic cell processes, such as Notch signaling which controls satellite cell activation (Conboy and Rando 2002; Rando. 2006; Liu and Rando 2011).

1.5 Skeletal Muscle

Skeletal muscle is comprised of striated multinucleated myofibers, formed by the fusion of mononucleated myoblasts during development (Hawke and Garry 2001) and is capable of contraction, controlled by the somatic nervous system. Each myofiber is composed of myofibrils, which contain sarcomeres made up of actin and myosin heavy chain (MHC) filaments. MHC exists in a number of isoforms which dictates the physiological properties of individual fibres via ATPase activity (Jones and Round 1990). Fibres can be divided into Type I, Type IIa or Type IIb fibres dependent on the MHC isoform present, with Type I fibres classed as slow-twitch due to their slow speed of contraction, whilst Types IIa and IIb are fast-twitch fibres. Skeletal muscles throughout the body use a combination of these fibres in different proportions to achieve the desired physiology required for the function of that individual muscle.

1.5.1 Skeletal Muscle Regeneration

In the normal healthy adult, homeostasis of skeletal muscle is mediated by resident stem-progenitor cells called satellite cells (SCs), however as we age our body's ability to replace muscle fibres decreases and there is a progressive loss of muscle mass called sarcopenia, with a reduction in the cross sectional area of muscle fibres (Faulkner et al. 1995). Indeed, 20% of all 60-70 year olds have sarcopenia, this figure rises to 50% in those over 75 (Berger and Doherty 2010). One explanation for this may be that the SCs have a maximum proliferative capacity so as we age and our SCs are activated to repair wear and tear over our

lifetime, the pool of competent SCs becomes depleted. In agreement with this, Renault et al. (2002) reported a significant reduction in the number of satellite cells between young (23±1 years) and old (74±4 years) individuals in both bicep and masseter muscle. Furthermore it has been demonstrated that SCs isolated from aged muscle display a lag time before proliferation suggesting compromised activation (Schultz and Lipton 1982).

SCs are small round mononuclear ASCs located between the basal lamina and sarcolemma of individual muscle fibres accounting for 2-7% of the nuclei associated with a fibre (Péault et al. 2007; Mauro. 1961). They are universally identified by their expression of Pax7 (Seale et al. 2000).

Pax7 (paired box-7) is a transcription factor that is involved in the specification of SCs during development (Relaix et al. 2005), with Pax7 germline mutant mice having few SCs (Seale et al. 2000) and reduced muscle regeneration (Oustanina et al. 2004).

SCs are also known to express other markers such as CD56, M-Cadherin, CXCR4, c-met and CD34 (Beauchamp et al. 2000; Tedesco et al. 2010) and are mitotically quiescent until stimulated following acute/chronic injury or stress (Figure 1.3). Upon activation they initiate MyoD and Myf5 expression, losing CD34 before becoming myoblasts (Zammit et al. 2006; Tedesco et al. 2010). During this process they also undergo asymmetric division and are capable of rounds of pronounced stem cell proliferation (Zammit et al. 2006) allowing the SC pool to be replenished (Figure 1.3).
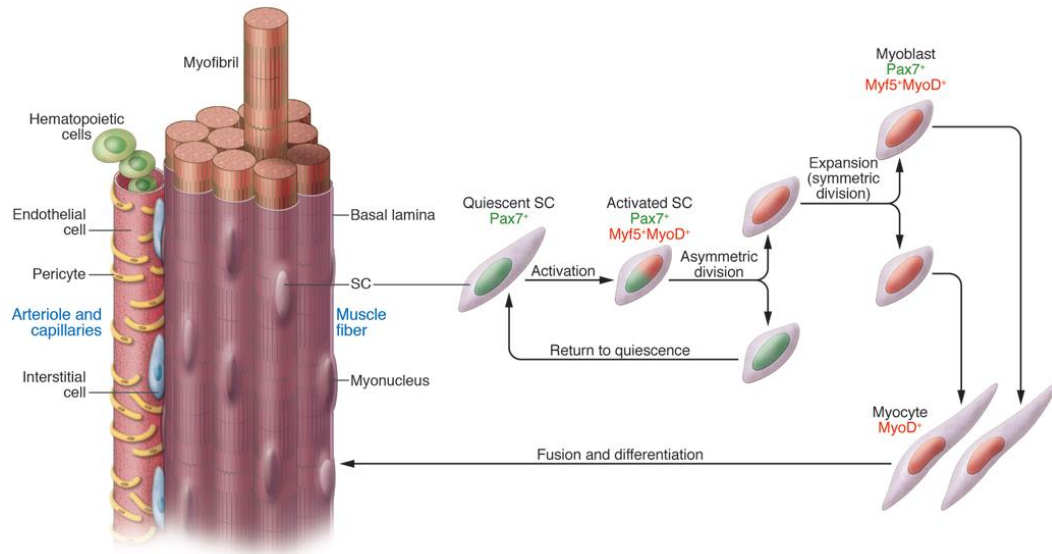
Figure 1.3 **Muscle fibre anatomy and SC activation** (Tedesco et al. 2010).

Whilst SCs are capable of myogenic differentiation *in vitro* and *in vivo* and extensively contribute to new muscle fibre formation (Collins et al. 2005), transplanted SCs have limited migration capacity with an inability to cross the endothelial wall (Price et al. 2007; Tedesco et al. 2010). SCs that have undergone culture *ex vivo* also have decreased proliferative capacity and a reduction in myofiber production when transplanted *in vivo* (Shadrach and Wagers 2011; Montarras et al. 2005); therefore SCs are not currently regarded as a viable source for systemic regenerative cellular therapies until at least part of these problems are solved.

1.5.2 Muscle-resident Stem Cell Populations

Since the first discovery of SCs 50 years ago (Mauro. 1961), a variety of other muscle-resident stem cells have been identified and described with varied differential and clinical potentials. These include vessel-associated cells such as

mesoangioblasts (Cossu and Bianco. 2003) and pericytes (Dellavalle et al. 2007, 2011), alongside interstitial cells such as; side population cells (Asakura et al. 2002), fibro/adipogenic progenitors (Joe et al. 2010) and PW1 positive interstitial cells (Mitchell et al. 2010). Whilst we may not know the exact role of each cell type in the normal healthy individual, many appear to interact with satellite cells to regulate myogenisis, adipogenisis and fibrogenisis during regeneration (Joe at al. 2010; Murphy et al. 2011; Uezumi et al. 2010). Understanding these mechanisms may allow us to utilise these cell types in developing therapies for damaged or diseased muscle and its surrounding environment.

Embryonic mesoangioblasts (MABs) are a mesodermal stem cell population primarily found during development in embryonic vessels, which express CD34, stem cell antigen 1 (Sca-1), and Flk-1 (Cossu and Bianco 2003). However, a similar population of 'adult MABs' has also been isolated from adult tissue of mouse, dog and human (Tonlorenze et al. 2007). Adult MABs also express pericyte markers neural/glial antigen 2 (NG2) and alkaline phosphatase (AP) (Dellavalle et al. 2007) and are a candidate for cellular therapies due to their ability to migrate extensively in the muscle bed, crossing vascular walls whilst also self-renewing. Indeed, when injected through the femoral artery of DMD (Duchenne's muscular dystrophy) dogs, Sampaolesi et al. (2006) reported a significant amelioration and preservation of motility.

Pericytes are vessel associated cells located in postnatal micro-vasulature, that express AP, NG2 and Beta-type platelet-derived growth factor receptor (PDGFRβ) (Dellavalle et al. 2011). Their main function is to create, maintain and re-model

blood vessels, although they have also been shown to integrate into skeletal muscle of mice (Dellavalle et al. 2011).

Side Population (SP) muscle stem cells are identified by their exclusion of Hoechst 33342 and give rise to dystrophin positive myofires when injected intravenously into mice with a mutation of the dystrophin gene (MDX mice) (Gussoni et al. 1999). Residing in the muscle interstitium with close proximity of the endothelium, subsets of SP cells have been shown to express Sca-1, CD34 and Pax7 (Judson et al. 2013), although there is some controversy over the use of Hoechst 33342 dye exclusion as a defining parameter (Kallestad and McLoon 2010).

Fibro-adipogenic precursors (FAPs) are interstitial cells, which are lineage negative, Sca-1$^+$, CD34$^+$ and display both adipocyte and fibroblast differentiation potential *in vitro* (Joe et al. 2010). Uezumi et al (2010) further described this FAP population as PDGFRα$^+$ with both groups further demonstrating adipogenic differentiation *in vivo* (Joe et al. 2010; Uezumi et al. 2010).

Similarly to FAPs, skeletal muscle fibroblasts, which are positive for TE-7 and PDGFRα and negative for CD56, form adipocytes when cultured in adipocyte differentiation medium or with fatty acids (Agley et al. 2013).

Finally, in 2010, a population of muscle-resident PW1$^+$/Pax7$^-$ interstitial cells (PICs) was identified in the mouse which are bi-potent, efficiently contributing to smooth and skeletal muscle regeneration *in vivo*, whilst also generating SCs and replenishing the PIC population (Mitchell et al. 2010). Since their discovery in

mice, PICs have also been described in hind-limb muscle of pigs (Lewis et al. 2014).

Many of the described muscle stem-progenitor cell populations share a similar phenotype, expressing the same markers and are isolated using similar techniques, therefore it may be expected that there is some overlap between these cell types.

1.5.3 PICs

Apart from their ability to effectively contribute to skeletal muscle regeneration, and their compatibility with a systemic delivery (Mitchell et al. 2010), PICs have not yet been characterized in detail. How they fit in and compare with other muscle stem cell populations is unclear and therefore they are of much interest. Their main defining characteristics are their location within the muscle interstitium and their expression of PW1.

PW1, or paternally expressed gene 3 (peg3), encodes a large Kruppel-type zinc finger transcription factor with a proline-rich domain which is widely expressed during fetal development and later persists in adult neurons and skeletal muscle (Kuroiwa et al. 1996, Relaix et al. 1996). PW1 knockout mice are 20% smaller at birth and go on to develop impaired maternal behaviour due to a reduction in oxytocin neurons in the hypothalamus, indicating that PW1 is involved with modulation of mammalian growth and behaviour (Li et al. 1999).

PW1 is expressed in both PICs and quiescent SCs (93% of SC's at 2 week postnatal) although it is not known if activated SCs continue to express PW1 (Mitchell et al. 2010; Lewis et al. 2014). Utilising PW1- reporter transgenic mice, PW1 expression has also been described in multiple adult stem cell niches

throughout the body including the gut, skin, cental nervous system (CNS) and early HSCs (Besson et al. 2011). Therefore, it has been implicated as a possible marker for stem-progenitor cell populations throughout the adult mammalian body.

PICs and SCs are distinguishable by both location and molecular markers (Table 1.3); SCs express Pax7 and are located under the basal lamina (Mauro. 1961), whilst PICs do not express Pax7 and are located in the interstitium (Mitchell. et al 2010, Lewis et al. 2014). PICs are also positive for stem cell antigen -1 (Sca-1), whilst both SC's and PICs are negative for CD45 and positive for CD34. Furthermore, in contrast to satellite cells which only give rise to myofibres, PICs have bi-potent differential potential giving rise to both striated and smooth muscle (Mitchell et al 2010; Lewis et al. 2014).

Table 1.3   Marker expression and location of PICs vs quiescent SCs.

	PIC	SC
PW1	+	+
CD45	-	-
Pax7	-	+
Sca-1	+	-
CD34	+	+
Location	Interstitial	Under Basal Lamina

Upon $CD45^-/CD34^+$ isolation by flow assisted cell sorting (FACS) murine PICs can be further split into 2 distinct PIC populations based on their level of Sca-1 expression. Sca-1^{MED} PICs from 1 week old mice demonstrate higher myogenic differential potential *in vitro* (fusion index = 40%) than their Sca-1^{HIGH} counterparts (fusion index = 25%), however the Sca-1^{MED} PIC population declines rapidly (from ~9% of lineage negative cells) during early postnatal development and is no longer detectable at 5 weeks of age. In contrast the Sca-1^{HIGH} PICs persist into adulthood (7 weeks) increasing from ~18% to ~28% of all lineage negative cells (Pannérec et al. 2013). Importantly both young and adult Sca-1^{HIGH} populations have a similar gene profile (Pannérec et al. 2013). These data suggest that the Sca-1^{MED} fraction may be integral for the rapid growth needed in post-natal development, whilst the Sca-1^{HIGH} PICs persist to maintain the muscle throughout adulthood.

Importantly, Mitchell et al. (2010) demonstrated, by using Pax3^{Cre} mice crossed with Rosa^{lacZ} mice, that PICs are not derived from a Pax3 lineage and therefore are not derived from satellite cells. They do however go on to express Pax3 on entry into the skeletal muscle lineage suggesting they are upstream of SC's in lineage differentiation. Indeed, PICs isolated from Rosa^{lacZ} mice and injected into focally injured tibialis anterior of nude mice were not only found to participate as efficiently as SC's in myofibre formation, but also gave rise to Pax7$^+$ SCs as well as replenishing the PIC population (Mitchell et al. 2010).

Transcriptome and gene ontology analyses of PICs and SCs from 1 week old mice show that both cell types have distinct transcriptome signatures, with SC specific genes belonging primarily to the skeletal muscle lineage whilst PICs express

genes from multiple cell fates (Pannérec et al. 2013). In agreement with these differences in transcriptomes, Lewis et al. (2014) found that PICs isolated from 2 month old pig hind limb skeletal muscle (pPICs) expressed the three pluripotency markers, Oct3/4, Sox2, and Nanog alongside the stem/progenitor marker c-kit by both quantitative real-time polymerase chain reaction (qRT-PCR) and immunocytochemistry (ICC). When propagated in culture they maintained a stable phenotype and normal karyotype over 40 passages and were clonogenic throughout, thus indicating that they can be maintained in a primitive state in culture. Moreover, in addition to giving rise to skeletal and smooth muscle, pPICs were also capable of differentiation *in vitro* into other mesodermal cell types including endothelial and cardiomyocyte-like cells when cultured in lineage specific growth media. Furthermore, a subpopulation of PDGFRα$^+$ PICs displays adipogenic properties (Pannérec et al. 2013).

1.6 Cardiac Muscle

Cardiac muscle is made up of striated cardiomyocytes and like skeletal muscle this striation is due to MHC and actin filaments. However unlike skeletal muscle which exhibit linear striations, cardiomyocyte filaments can have a more 'branched' appearance and arrange themselves differently. The two MHC isoforms found within cardiac muscle are α-MHC and β-MHC, which display different shortening velocities and isometric forces (Malmqvist et al. 2004).

1.6.1 Cardiac Muscle Regeneration

The adult heart was, until recently, thought to be a post mitotic organ without any regenerative capability, with the belief that all cardiomyocytes were formed during fetal and early post-natal development (Nadal-Ginard 1978; Chien and

Olson 2002), and all cardiomyocytes within the heart being the same age as the individual (Oh et al. 2001). Any increase in size with growth was attributed to hypertrophy of the existing myocytes (Soonpaa and Field 1998; Hunter and Chien 1999; Laflamme and Murry 2011). However, myocytes undergoing mitosis have been found in the hearts of rats (Overy and Priest 1966), mice (Anversa and Kajstura 1998) and humans (Kajstura et al. 1998). Moreover, it has since been reported using carbon dating techniques that human cardiomyocytes renew with a gradual decrease in annual turnover from 1% at the age of 25 to 0.45% at 75 with less than 50% of cardiomyocytes being replaced over a lifetime (Bergmann et al. 2009).

Mature cardiomyocytes are terminally differentiated, although there are a number of reports that claim ventricular cardiomyocytes can re-enter the cell cycle and divide by mitosis (Anversa and Kajstura 1998; Senyo et al. 2013). Myocyte replacement was originally attributed to a stem cell population (Beltrami et al. 2003), this theory has since been confirmed by utilizing cell fate mapping demonstrating that newly formed myocytes are not derived from existing cardiomyocytes (Hsieh et al. 2007; Ellison et al. 2013) and are indeed formed by a resident stem cell population (Ellison et al. 2013, Koudstall et al. 2013).

1.6.2 Cardiac stem-progenitor cells populations

To date there have been numerous cardiac stem-progenitor cell populations identified in the mammalian heart (Ellison et al. 2014). These include c-kit positive, Sca-1 positive, cardiac side population, cardiosphere-derived and epicardial-derived cells (Table 1.4).

Table 1.4   Phenotype and properties of CSC populations (Adapted from Ellison et al. 2014)

PHENOTYPE	CO-EXPRESSION	SPECIES	*In vitro* STEM CELL PROPERTIES			*In vivo* CARDIAC REGENERATIVE POTENTIAL
			Self-Renewal	Cardiomyocyte Differentiation	Multipotency	
c-kit	Nkx2.5, MEF2C, GATA4, Sca-1, MDR1, CD90, CD166, Flk-1, Isl-1.	Neonatal and Adult rat, mouse, Porcine, Dog. Postnatal and Adult Human.	Yes	Yes	Yes	Yes
Cardiosphere derived	CD105, CD90, CD34, CD31, c-kit, ABCG2, Flk-1, GATA4, Nkx2.5, Isl-1.	Neonatal and Adult Rodent and human. Adult Dog, Primate and Porcine.	Yes	Yes	Yes	Yes
Sca-1	CD31, CD29, Pdgfrα, CD45, c-kit, Isl-1, CD105.	Neonatal and Adult Mouse. Foetal and Adult Human.	Yes	Yes	Yes	Yes
Epicardial	c-kit, CD34, GATA4, Nkx2.5, Sca-1, CD44, CD90, CD105, Wt1, Isl1.	Fetal and Adult Human and Mouse Adult Rat and fish Fetal Chick.	Yes	Yes	Yes	Yes
Side population	Sca1, CD31, Tie1/2, Nkx2.5, Gata4	Neonatal and Adult Mouse.	Yes	Yes	Yes	Yes
Isl-1	CD31, CD144, Flk1, GATA4, Nkx2.5.	Foetal, Postnatal, and Adult Mouse. Foetal, Postnatal and Adult Rat. Foetal and Postnatal Human.	Yes	Yes	Yes	ND

c-kit+ cardiac stem/progenitor cells

The first endogenous small cell population with the phenotype, behaviour and regenerative potential of *bona fide* cardiac stem and progenitor cells was discovered within adult rat myocardium in 2003 by the group of Anversa and Nadal-Ginard (Beltrami et al. 2003). Subsequent populations have since been reported in the mouse (Fransioli et al. 2008), dog (Linke et al. 2005), pig (Ellison et al. 2011) and human (Torella et al. 2006a, 2006b). These endogenous cardiac stem cells (eCSCs) express the stem cell markers c-kit and Sca-1 and are lineage negative being negative for surface markers CD45, CD34 and CD31 (Beltrami et al. 2003); c-kit is a tyrosine kinase receptor which regulates cell fate (Roskoski 2005). eCSCs are found at a ratio of between ~1:1000 cardiomyocytes with significantly more located in the left and right atria's than the left and right ventricle (Arsalan et al. 2012; Ellison et al. 2011). They can be successfully expanded *in vitro* (Beltrami et al. 2003) and are clonogenic, self-renewing and multipotent (Torella et al. 2007), capable of generating the three major cell types of the myocardium : myocytes, smooth muscle and endothelial vascular cells (Figure 1.4) (Nadal-Ginard et al. 2003; Ellison et al. 2007). Furthermore, they form cardiospheres in suspension which, after directed myogenic differentiation in defined culture medium, attach and differentiate into beating myocytes (Smith et al. 2014). When injected into the heart following a myocardial infarction (MI) they display significant regenerative potential, giving rise to new myocytes and vasculature and restoring cardiac function (Beltrami et al. 2003).
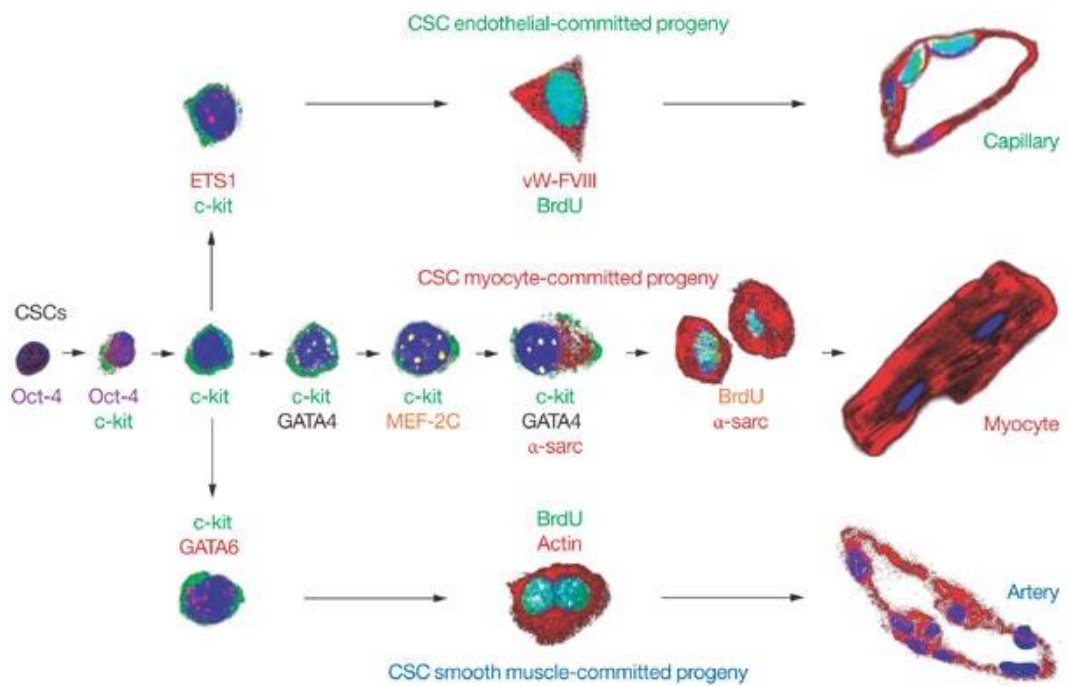
Figure 1.4   Schematic representation of eCSCs differentiation into the three cardiac lineages (Ellison et al. 2007).

Sca-1⁺ cardiac stem/progenitor cells

Sca-1 positive cardiac stem/progenitor cells are resident non-myocyte cells that express stem cell antigen 1 (Sca-1) and have been identified in adult murine hearts (Oh et al. 2003). They are small, round cells approximately 2-3µm wide ,with a high nucleus to cytoplasm ratio (Samal et al. 2012) and express early cardiac specific factors such as Gata-4 and MEF2C (Oh et al.2003; Matsurra et al. 2004). Similar to c-kit⁺ eCSCs they are self-renewing (Matsuura et al. 2004; Ye et al. 2012) and capable of myocyte formation both *in vitro* (Oh et al. 2003; Ye et al.2012, Matsuura et al. 2004; Takamiya et al. 2011, Chong et al. 2011, Wang et al. 2006), and *in vivo,* showing homing to injured myocardium and formation of new cardiomyocytes (Oh et al. 2003). Furthermore, 4 weeks post MI, animals injected intramyocardially with Sca-1⁺ eCSCs exhibit increased cardiac function and increased wall thickness of the infarcted area (Takamiya et al. 2011). Interestingly, Sca-1⁺ eCSCs have demonstrated differentiation into non-cardiac lineages *in vitro* and *in vivo* (Takamiya et al.2011; Chong et al. 2011), with Sca-1^{HIGH} eCSCs demonstrating a broader differentiation potential over Sca-1^{LOW} eCSCs, with the former being capable of osteogenic, chondrogenic, smooth muscle, endothelial and cardiac differentiation *in vitro* (Takamiya et al. 2011). As the homology of Sca-1 has not yet been confirmed in any other mammalian species other than the mouse, it is difficult to directly translate this research to human biology.

Side population cells

Cardiac side population cells (cSPs), which efflux Hoechst 33342, account for ~1% of total cardiac cells in the mouse heart (Hierlihy et al. 2002) and have

subsequently been isolated (Asakura et al. 2002). They express Sca-1 and low levels of c-kit, but are negative for CD34 and CD45 (Martin et al. 2004). 75% of cSPs are positive for the endothelial markers CD31, whilst the CD31 negative fraction displays the most cardiomyogenic potential (Wang et al. 2006). These CD31 negative cSPs express Sca-1 and the cardiac-specific markers Nkx2.5 and GATA4 and are capable of cardiogenic differentiation *in vitro* undergoing spontaneous contraction (Pfister et al.2005; Oyama et al. 2007).

Cardiosphere-derived cells

Messina et al. (2004) described the isolation of cardiosphere-derived cells (CDCs) from postnatal cardiac tissue that migrate and grow as clusters or 'cardiospheres'. CDCs are clonogenic, self-renewing and differentiate into cardiomyocyte, endothelial and smooth muscle lineages (Beltrami et al. 2003; Messina et al. 2004; Davis et al. 2009). CDCs represent a mixed population with some cells expressing c-kit (Beltrami et al. 2003), mesenchymal markers CD105 and CD90 and a small population expressing endothelial markers CD34 and CD31 (Messina et al. 2004; Smith et al. 2007; Carr et al. 2011). It is thought that the growth of different cardiac stem-progenitor cell populations in cardiospheres mimics the stem cell niche (Ellison et al. 2014) with CDCs demonstrating a higher oxidative stress resistance over monolayer cultured cells (Bartosh et al. 2008) and a 2-fold increase in stem cell markers Nanog and Sox2 (Li et al. 2010). When injected intramyocardial into mice following MI, cardiosphere treated mice showed a significant increase in left ventricular ejection fraction after 3 weeks whilst monolayer cells did not (Li et al. 2010).

Epicardial-derived cells

Epicardial-derived cells (EPDCs) have a fibroblastic appearance in culture and adhere to plastic dishes (van Tuyn et al. 2007). Human EPDCs express CD44, CD90, CD105 and GATA4 but are negative for Isl-1 (van Tuyn et al. 2007). When injected into infarcted mouse hearts they improve cardiac function and differentiate into endothelial and smooth muscle cells, however they do not make cardiomyocytes (Winter et al. 2007, 2009). Limana et al. (2007) identified a c-kit$^+$/CD45$^-$ stem cell population in the adult epicardium, however, in contrast to previously described EPDCs, they are non-adherent. When injected into the mouse MI model, they proliferate and migrate towards the site of injury where they differentiate into myocardial and vascular cells significantly reducing left ventricular remodelling (Limana et al. 2007). Sca-1$^+$ cardiac-derived colony forming units (cCFU's) as described by Chong et al. (2011) are also derived from the epicardium.

Isl-1+ cells

Finally, a population of resident progenitor cells in the heart expressing the marker Islet-1 (Isl-1) was identified in rodent and human postnatal myocardium (Laugwitz et al. 2005). Isl-1 expression is involved in the direction of primitive cardiac progenitors to specific lineages (Bondue et al. 2011). The role of Isl-1 in development has been clearly documented (Moretti et al. 2006) however there is some doubt as to the role Isl-1 cells play in adult life. Isl-1 positive cells found in the heart of adult (11-13 weeks) rats are positive for cardiac troponin I (cTnI) suggesting they are commited to cardiomyogenic differentiation (Genead et al. 2010).

While these cardiac stem-progentior cell populations are described individually, there is in fact significant overlap and co-expression with each other, with the main differences being due to the isolation techniques used. This raises the possibility that these cell types may constitute a single stem-progenitor cell, displaying different phenotypes with lineage sequence (Ellison et al. 2014).

It should be noted that bone marrow derived stem cells (BMDCs), although initially thought to give rise to new myocytes and vasculature in a mouse MI model (Orlic et al. 2001) have not been found to directly form cardiac tissue (Murry et al. 2004; Balsam et al. 2004). 1.7 Skeletal Muscle Vs Cardiac Muscle

Although both striated muscles composed of myosin and actin filaments, cardiac and skeletal muscles contain several distinct differences (Table. 1.5)

Firstly, both muscle types are comprised of different isoforms of MHC (although MHC1 and β-MHC are products of the same gene), and are controlled via different nervous pathways with skeletal muscle being controlled voluntarily whilst cardiac muscle is controlled autonomously. Furthermore skeletal muscle is composed of multi-nucleated myocytes in comparison to single or bi-nucleated cardiomyocytes.

Skeletal muscle shows a much higher growth and regenerative capacity than cardiac muscle, with an average turnover of ~1-2% of myonuclei per week (Schmalbruch and Lewis. 2000) compared to a 50% turnover of cardiomyocytes over an individual's lifetime (Bergmann et al. 2009). This regenerative capacity is apparent in the ability for muscle to adapt and change with damage caused by

exercise and mechanical stresses (Morton et al. 2009), such as in body builders and athletes. Although the heart has also shown some adaptation to exercise (Waring et al. 2012), regeneration of new myocytes are much more subtle.

In agreement with differences in regenerative capacity of the two muscle types, the presence and frequency of endogenous stem/progenitor cell populations (SCs and eCSCs) is also dramatically different. SCs are found at a frequency of 1 SC for every 2-7 myonuclei (Peault et al. 2007) dependant on the type of muscle, whereas eCSCs are extremely rare at only 1 per ~1000 cardiomyocytes (Torella et al. 2007). This raises the question: is the regenerative capacity of a muscle limited by the frequency of stem/progenitor cells?

Finally, the embryological origin of these two muscle types is different with skeletal muscle derived from the somites of the paraxial mesoderm, whilst cardiac tissue one of the earliest tissues formed from the lateral plate mesoderm.

Table 1.5   Skeletal Muscle vs Cardiac Muscle and their Regenerative capacity.

	Skeletal Muscle	**Cardiac Muscle**
Myosin Isoforms	MHCI, MHC IIa, MHC IIb	α-MHC, β-MHC
Nervous System	Somatic	Autonomous
Nuclei	Multinucleated	Single/Binulcleated
Myocyte Turnover	1-2% of myonuclei Per week	50% over lifetime
Regenerative Capacity	High	Very Low
Regeneration Mediator	Satellite cells	eCSC
Stem Cell Frequency	2-7% of myonuclei	~1 eCSC:1000 myocytes
Embryological origin	Paraxial mesoderm	Lateral plate mesoderm

The roles that these two muscles play within the body and subsequent consequences of damage to the two tissues are markedly distinct from each other, with the homeostasis of the heart being imperative to survival. As the heart is a critical organ in sustaining life, it could be expected that it should have a superior regenerative capacity; however this is clearly not the case. There are a number of reasons why the heart might not need to possess this, with the first being that in individuals with an active lifestyle and good diet, injuries and disease simply do not, or are very unlikely to occur, whereas skeletal muscle is constantly put under stress and subject to injury. With more people leading unhealthy lifestyles and surviving to an older age, the need to find cures for heart conditions is a relatively

new problem in human evolution. Having a low turnover of cells may in fact be beneficial to the heart as with less cycling cells the probability of developing cancer is low. Indeed, primary angiosarcomas are one of the rarest forms of cancer, and most tumours reported in the heart are secondary tumours that originated in another tissue (Cancer Research UK).

If PW1 marks 'muscle stem cells', and Sca-1 is a marker shared between $PW1^+$ PICs and eCSCs, then it may be expected that it should also be a marker expressed in eCSCs. PW1 has previously been detected in embryonic and early postnatal cardiac tissue (Besson et al. 2011), however what population of cells this actually marks has not been determined. Therefore, do PICs and eCSCs, both being muscle-resident stem cells, belong to the same ASC population?

1.8 Aims and Objectives

The main aims of this study are:

1. Quantify PW1 expression in skeletal muscle of postnatal and aged mice.

2. Successfully isolate murine PICs and characterise their phenotype *in vitro*.

3. Test PICs for stem cell properties, i.e. multipotency and self-renewal *in vitro* and *in vivo*.

4. Determine the presence of 'PIC like' cells in cardiac tissue, and their overlap with previously described CSCs.

2. METHODS

2.1 Animals

C57BL/6 Mice derived from a conventional colony at Liverpool John Moores University were housed under controlled conditions of 19-23°C and 45-55% relative humidity with water and food (containing 22% protein) available ad libitum.

All regulated animal procedures were carried out under the Home Office project licence PPL70/8273 and personal licence I0916B98D.

2.2 Tissue collection and processing

Animals were sacrificed at 3 day (2.6 ± 0.1 g), 10 day (5.4 ± 0.2 g), 21 day (7.8 ± 0.4 g) and 2 years (35.7 ± 1.2 g) of age via CO_2 asphyxiation or cervical dislocation. Immediately after sacrifice skeletal hind limb muscle and whole hearts were dissected and fixed in formalin for 24 hours before tissue processing.

After 24 hour formalin fixation, tissue was cut transversely (skeletal muscle) or longitudinally (cardiac) and processed in a tissue processor (Leica, Nussloch, Germany; TO 1020) on the following cycle:

1. Formalin – 1 hour
2. Formalin – 1 hour
3. Alcohol 70% – 1 hour 30 minutes
4. Alcohol 80% – 1 hour 30 minutes

5. Alcohol 96% – 1 hour 30 minutes

6. Alcohol 100% – 1 hour

7. Alcohol 100% – 1 hour

8. Alcohol 100% – 1 hour

9. Xylene – 1 hour 30 minutes

10. Xylene – 1 hour 30 minutes

11. Paraffin – 2 hours

12. Paraffin – 2 hours

After processing, tissue samples were embedded in paraffin wax blocks using an embedding station (Leica; EG 1160A) after which 5 μm tissue sections were cut using a microtome (Leica; RM 2235) and mounted on polysine™ microscope slides (Menzel-Gläser, Braunschweig, Germany) using a waterbath.

2.3 Immunohistochemistry

Immunohistochemistry is the process of detecting antigens in cells/tissues using primary (target antigen) and secondary (fluorochrome) antibodies (Figure 2.1).

It is based on the principle that primary antibodies bind to specific antigens on the protein of interest. Primary antibodies are synthesised in animals by repeat immunization with the antigen of interest, the animals immune response then produces antibodies (B lymphocytes) against the antigen which are harvested and purified; most primary antibodies are now available commercially. When introduced to the tissue, the primary antibodies bind to the specific epitopes where they come in contact with them. The primary antibodies also contain isotype

specific antigens from the host animal in which they were made (e.g. Mouse IgG) and it is to these epitopes that secondary antibodies, made via the same process, which have been conjugated to fluorescent tags, are able to bind. Due to the nature in which the secondary antibody is made it is good practice to perform a blocking step with serum from the host of the secondary antibody (most commonly goat or donkey), prior to staining to prevent non-specific binding of the fluorescently tagged antibody. The more protein expressed by a cell/tissue the more primary and secondary antibody attachment and the greater the fluorescent signal will be.
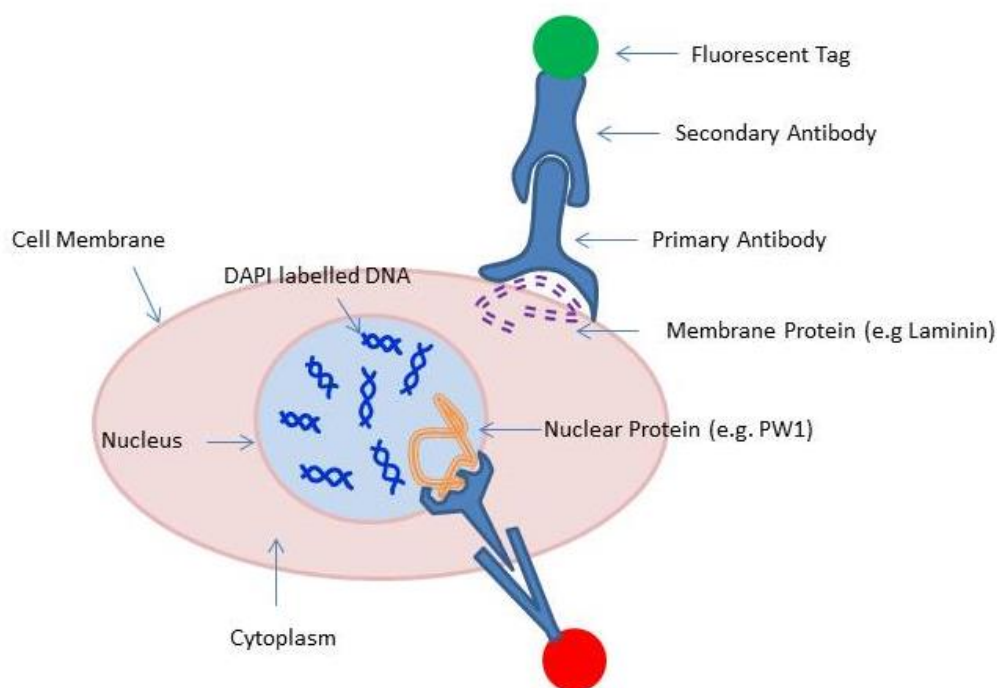
Figure 2.1   Schematic to show antibody binding and immunofluorescence on cell/tissue proteins.

Deparaffinisation and rehydration was achieved by incubation at 70°C for 30 minutes, followed by immersion in the following:

1. Xylene – 2 x 5 minutes

2. 96% ethanol – 1 x 4 minutes, 1 x 3 minutes

3. 90% ethanol – 3 minutes

4. 80% ethanol – 3 minutes

5. H_2O – 4 minutes

Antigen retrieval was achieved using pre-heated citric acid buffer (0.35 g/L citric acid monohydrate, Sigma, St Louis, USA; 2.4 g/L Citric acid trisodium, Sigma; pH 6) and heating on full power for 10 minutes in a microwave. Slides were allowed to cool to room temperature (RT) for ~45 minutes then rinsed in distilled water for 1 minute followed by 5 x 2 minute washes in PBS (Sigma).

A hydrophobic barrier was created around each tissue section using an ImmEdge™ Pen (Vector) before blocking with 10% donkey serum (Sigma) in PBS for 30 minutes at RT. Directly after blocking, the donkey serum was discarded and the first primary antibody applied for either 1 hour at 37°C or overnight at 4°C (see sections 3.2, 4.2, 5.2, 6.2) and washed in PBS for 5 x 2 minutes. The relevant secondary antibody was then applied (1/100 dilution) for 1 hour at 37°C followed by 5 x 2 minute washes in PBS.

Nuclei were counterstained with DNA binding dye, 4, 6-diamidino-2-phenylindole (DAPI) (1:1000, Sigma) for 15 minutes at RT, followed by 6 x 2

minutes PBS washes before mounting in Vectashield™ mounting medium (Vector laboratories).

All quantification was conducted at x40 magnification on a fluorescence microscope (Nikon, Surrey, UK; E1000M Eclipse) and representative Z stack micrographs imaged on a confocal microscope (Zeiss, Cambridge, UK; LSM 710)

2.3.1 Haematoxylin and eosin staining

After deparaffinisation and rehydration, slides were immersed in haematoxylin (Sigma) for 3 minutes at RT and rinsed with running water for 5 minutes. Slides were counterstained with eosin (Sigma) for 5 minutes at RT and rinsed in running water for 5 minutes before air-drying for 1 hour at 37°C. Slides were cleared in Xylene for 5 minutes at RT before mounting with Distyrene Plasticizer Xylene (DPX; Sigma).

2.3.2 DAB staining

To determine which tumour cells arose from GFP[+] PICs and were not a result of the ESC's, paraffin embedded tumour tissue sections were prepared and stained for green fluorescent protein (GFP) (Abcam, Cambridge, UK; 1 hour at 37°C) as previously described (see section 2.3), after the GFP primary antibody and 5 x 2 min wash in PBS, endogenous peroxidase activity was blocked using 1 part H_2O_2: 3 parts PBS for 15 minutes at RT. After 5 x 2min washes in PBS donkey-anti-Rabbit HRP (Santa Cruz, Texas, USA) was applied for 1 hour at 37° and SigmaFast DAB (3,3'-diaminobenzidine; Sigma) tablets were used to visualise the GFP (5 minutes at RT). Slides were washed in PBS (5 x 2 minutes), allowed to

dry (1 hour at 37°C) and cleared in xylene (5 minutes) before mounting and cover slipping using DPX (Sigma).

2.4 Immunocytochemistry

Cells grown on chamber slides were fixed with 4% formaldehyde (TAAB laboratory and microscopy, Berkshire, UK) for 20 minutes at room temperature and rinsed in PBS for 5 x 2 minutes before staining. For ICC of cytospin preparations: 200 µl of 50,000 cells/ml cell suspension per spot (2 spots per slide), were spun down onto polysine™ (Menzel-Gläser) using a Cytospin 4 centrifige and Shandon EZ double cytofunnels (Thermo Scientific, Massachusetts, USA), slides were then rapidly fixed with Shandon cellfix spray (Thermo Scientific) and allowed to air dry. The fixative was removed by soaking the slides in 95% ethanol for 15 minutes, followed by 5 x 2 minutes washes in PBS. For staining of nuclei proteins, cells were permeabilised with 0.1% triton for 10 minutes at RT and washed for 5 x 2 minutes in 0.1% Tween PBS.

Cells were blocked with 10% donkey serum in 0.1% Tween PBS for 30 minutes at RT. Directly after blocking, the donkey serum was discarded and the first primary antibody applied for 1 hour at 37°C and washed in PBS for 5 x 2 minutes. The relevant secondary antibody was then applied (1/100 dilution) for 1 hour at 37°C followed by 5 x 2 minute washes in PBS. Nuclei were counterstained with DAPI, rinsed in PBS for 6 x 2 minutes before mounting with vectashield™ (Vector laboratories).

All quantification was conducted at x 40 magnification on a fluorescence microscope (Nikon; E1000M Eclipse) and representative Z stack micrographs imaged on a confocal microscope (Zeiss; LSM 710)

2.5 Cell Isolation

2.5.1 Isolation of PICs from murine skeletal muscle

Skeletal muscle hind limb was dissected and rinsed in basic buffer (Table 2.1). The tissue was minced extensively with scissors and then stirred at 37°C for 30 minutes in digestion buffer (Table 2.1). Following digestion, the preparation was centrifuged at 300 g for 1 minute (brake 3). The supernatant, containing the small cells, was filtered (40 μM) and the pellet discarded. The cell suspension was then topped up to 30 ml with incubation buffer (Table 2.1) and spun at 1500 rpm for 7 minutes (brake 7) after which the supernatant was discarded and the pellet re-suspended in 1ml incubation medium (Table 2.1). The small cell population was then sorted for the PIC cell population using Magnetic Activated Cell Sorting (MACS) as per standard protocol (Miltenyi, Bergisch Gladbach, Germany). Briefly, using direct mouse CD45 microbeads (Miltenyi) the CD45$^+$ cells were depleted from the cell preparation, leaving the CD45$^-$ fraction, from this, the Sca-1$^+$ cells were then enriched using an indirect (FITC) mouse Sca-1 microbead kit (Miltenyi).

2.5.2 Isolation of Sca-1$^+$ CSCs from murine hearts

6 week old mice were given an injection of 200 U heparin (MP biomedicals) 15 minutes prior to euthanasia with 50 μl of pentobarbitone. Hearts were then

dissected and the aorta cannulated as described in Smith et al. (2014). Cannulated

hearts were retrograde coronary perfused (11.6 ml/minute) on an adapted

lagendorff system with basic buffer (Table 2.1) until all blood was removed (~5

minutes), followed by digestion buffer (Table 2.1) for 12 minutes and incubation

buffer (Table 2.1) for 5 minutes. Digested hearts were then placed in incubation

buffer (Table 2.1) and minced extensively before centrifugation at 300 g for 1

minute (brake 3). Further filtration, centrifugation and MACs sorting for CD45$^-$

cells and Sca-1$^+$ cells were as described for PIC isolation (section 2.4.1)

Table 2.1   Cell Isolation Media

Media	Components
Basic Buffer	MEM (Sigma), 2.93 mM Hepes (Sigma), 2.05 mM Glutamine (Sigma), 9.99 mM Taurine (Sigma), pH 7.3
Digestion Buffer	Basic Buffer (as above), 7 mg/ml Collagenase II (Worthington, Lakewood, USA)
Incubation Buffer	Basic Buffer (as above), 0.5% BSA (Sigma), pH 7.3
Incubation Medium	PBS (Life Technologies, Carlsbad, USA), 0.5% BSA (Sigma), 2 µM EDTA (Life Technologies)

2.6 Cell culture

Cells were cultured on 1.5% gelatin (Sigma) coated dishes in growth medium

(Table 2.2). Cultures were incubated at 37°C in 5% CO_2 and passaged 1 in 3 when

they reached ~80% confluency using 0.25% trypsin-EDTA solution (Sigma).

Once cells were detached, trypsin activity was quenched with passage medium

(Table 2.2) before centrifugation (300 g for 3 minutes). The supernatant was

aspirated and the cell pellet suspended in fresh growth media, for re-plating in a

new dish at ~ 20,000 cells per cm^2.

Mouse ESC's (Gifted from Agi Grigoriadis, Kings College London) were

cultured on 1% gelatin coated dishes in ESC growth medium (Table 2.2).

Table 2.2   Cell Culture Media

Media	Components
Growth Medium	45% DMEM/F12 Ham (Sigma), 1 X ITS (Life Technologies), 45% Neurobasal Medium (Life Technologies), 0.5% Glutamax (Life Technologies), 1 X B27 (Life Technologies),1 X N2 (Life Technologies), 20 ng/ml EGF (Peprotech, Rocky Hill, USA), 10 ng/ml bFGF (Peprotech), 10% ESCQ-FBS (Life Technologies), 10 ng/ml LIF (Millipore, Darmstadt, Germany), 1% PenStrep (Life Technologies), 0.1% Fungizone (Life Technologies), 0.1% Gentamicin (Sigma)
Passage Medium	DMEM (Life Technologies), 10% FBS (Life Technologies), 1% PenStrep (Life Technologies), 0.1% Fungizone (Life Technologies), 0.1% Gentamicin (Sigma)
ESC Growth Medium	10% FBS (Hyclone, Utah, USA), 1mM sodium pyruvate (Sigma), MEM non-essential amino acids (Life Technologies), 50 mM β-mercaptoethanol (Sigma), 1000 U/ml GSK-inhibitor (Stemgent, Cambridge, USA) 1000 U/ml MEK-inhibitor (Stemgent) 1000 U/ml LIF (Millipore).

2.6.1 Clonogenicity

Clonogenicity was determined using a clonogenicity assay in which, through

serial dilution, a single cell was deposited into a well of a 96-well plate (~ 50 cells

seeded per plate). The number of wells which formed single-cell derived colonies

by 14 days was quantified, and expressed as a percentage of the total number of

single cells deposited (n=3 per assay).

2.6.2 Population Doubling

Doubling time is a measure of proliferation, giving the average time it takes for a

cell to replicate. The population doubling time was calculated at every 5th passage

(n=3 per time point) using the following formula, where: t= time in culture, x= starting population, y= final population.

$$\text{Doubling time} = t * \frac{\log(2)}{\log\left(\frac{y}{x}\right)}$$

2.6.3 Cardiosphere formation

To generate cardiospheres; C9 PICs (P5) were treated with 100 nM Oxytocin in normal growth media for 72 hours prior. LIF and Oxytocin were then removed from the medium and cells re-plated in bacteriological dishes for a further 72 hours.

2.6.4 Directed Differentiation

C9 PICS (P5) were plated at 2×10^4 cells/cm^2 in dishes as described (Table 2.3) and cultured in specific differentiation media listed in Table 2.4.

Table 2.3   Directed Differentiation: Dishes and Coatings

Differentiation	Dish Coating	Dishes
Myogenic	1.5% Gelatin (Sigma)	3 x 10cm dish, 1 x 4 well glass chamber slide
Cardiomyogenic	1 µg/ml Laminin (Sigma)	3 x 10cm dish, 1 x 4 well glass chamber slide
Adipogenic	1.5% Gelatin (Sigma)	1 x 4 well glass chamber slide
Endothelial	10 µg/ml Fibronectin (Sigma)	3 x 10cm dish, 1 x 4 well glass chamber slide
Hepatic	10 µg/ml Fibronectin (Sigma)	4 x 10cm dish, 1 x 4 well glass chamber slide
Neuronal	1 µg/ml Laminin (Sigma)	3 x 10cm dish, 1 x 4 well glass chamber slide

Table 2.4   Directed Differentiation Media

Media	Medium Components	Duration
Myogenic Medium	High Glucose (4.5 g/L) DMEM(Life Technologies), 2% Horse serum (Life Technologies), 1% PenStrep (Life Technologies).	5 days
Cardiomyogenic Medium	<u>Days 1-4;</u> α-MEM (Sigma), 1 μM dexamethasone (Sigma), 50 μg/ml ascorbic acid (Sigma), 10 mM β-glycerophosphate (Sigma) and 2% FBS (Life Technologies) 5 ng/ml TGF-β1 (Peprotech), 10 ng/ml BMP2 (Peprotech), and 10 ng/ml BMP4 (R&D Systems, Minneapolis, USA). <u>Day 5-14;</u> α-MEM (Sigma), 1 μM dexamethasone (Sigma), 50 μg/ml ascorbic acid (Sigma), 10 mM β-glycerophosphate (Sigma) and 2% FBS (Life Technologies), 150 ng/ml Dkk-1 (R&D Systems)	14 days
Adipogenic Medium	Low glucose (1g/L) DMEM (Sigma), 10% FBS (Invitrogen), 50μM Hydrocortisone (Sigma), 1μM Dexamethazone) (Sigma).	14 days
Endothelial Medium	DMEM (Invitrogen), 10 ng/ml VEGF (Peprotech), 1% PenStrep (Invitrogen).	7 days
Hepatic medium	Low glucose DMEM (Sigma), 25% F12K media (Invitrogen), 20ng/ml HGF (Peprotech), 10 ng/ml Oncostatin (Peprotech), 1x ITS (Invitrogen), 5 mM Nicotinamide (Sigma), 2.5% FBS (Invitrogen), 1% PenStrep (Invitrogen).	14 days
Neuronal Medium	medium (low glucose DMEM, 10% horse serum, 300 ng/ml Retinoic acid)	14 days

2.6.5 GFP transduction

C9 PICs (P10) were transduced with the construct for green fluorescent protein (GFP) via lentiviral transduction: 10^6 293T cells (Clontech, California, USA) at 70% confluency were treated with 5 μg Delta 8.9 plasmid, 10 μg GFP plasmid, 2 μg VSV-g plasmid (pre-prepared plasmids gifted from Daniele Torella, Magna Graecia University, Italy) and 30 μl Lipofectamine2000 (Life Technologies) in 6 ml of OptiMEM-I (Life Technologies) for 4 hours. A further 5 ml of OptiMEM-I containing 10% FBS (Life Technologies) and 1% PenStrep (Life technologies)

was then added. After 24 hours the media was changed for normal 293T growth media and left for a further 24 hours, after which the lentiviral supernatant was collected. PICs were transduced for 24 hours using a 1: 5 ratio of; lentiviral supernatant: PIC media containing 8 µg/ml of Polybrene (Sigma). The tranduction efficiency was checked by flow cytometry.

2.7 Flow Cytometry

Cells were blocked with 10% donkey serum in incubation medium (Table. 2.1) immediately before incubation with the primary antibody. For nuclear expression of PW1, cells were permeabilised with BD fixation/permeabilisation kit (BD, New Jersey, USA) as per manufacturer's instructions prior to the blocking step. All antibodies were incubated at 4°C for 15 minutes and washed in incubation buffer after incubation. Flow cytometry was conducted on a BD FACS Calibur and 10,000 events recorded for each analysis. Results were plotted and analysed using Flowing Software (Turku Centre for Biotechnology). Isotype controls were used to determine expression.

The FACS Calibur is a 4 colour flow cytometer and contains two lasers; a 15mW air-cooled argon-ion laser with an excitation of 488 nm and a 9mW red diode laser with an excitation of 635 nm. It also contains four filters: FL1= 530/30, FL2= 585/42, FL3= 650LP and FL4= APC- 661nm.

2.8 Quantitative RT-PCR (qRT-PCR)

Total mRNA was obtained from cell pellets using the QIAshredders and RNeasy mini kit (Qiagen, Venlo, Netherlands) with a DNase step (Qiagen) to remove any

residual DNA, as per manufacturers instructions. Briefly, cell pellets were lysed with RLT buffer containing 1% β-mercaptoethanol before transfer to a QIAShredder tube and spun at top speed for 2 minutes. 70% ethanol was added to the flow through and transferred into an RNeasy column. This was then spun at >8000 g for 15 seconds. The flow through was discarded and the column washed with RW1 buffer and spun (>8000 g for 15 seconds, flow through discarded) immediately followed by a 15 minute incubation with DNase. Following this, the column was once again washed with RW1 buffer, spun (>8000 g for 15 seconds) and the flow through discarded. The column was then washed twice with RPE buffer and the flow through discarded (1st wash spun at >8000 g for 15 seconds, and the second spin for 2 min's). Finally the RNeasy column filter was placed inside a new collection tube, 30 μl of RNase free water added to the filter and spun at >8000 g for 1 minute.

Final mRNA concentration (ng/μl) and quality (260/280 and 260/230 ratio) of the resulting flow though was measured using a Nanodrop 2000 (Thermo scientific).

cDNA was synthesised via reverse transcription, using a Taqman reverse transcription (RT) kit (Life technologies). Each reaction contained 10ng/μl RNA, 10μl of 10xRT Buffer, 22μl of $MgCl_2$ (25mM), 20μl dNTP mix (2.5mM), 5μl Random hexamers (50μM), 2μl RNase inhibitor (20U/l), 2.5μl Multiscribe RT enzyme (50U/μl) and DNase/RNase free H_2O. The reaction was performed on a Biorad i-cycler (Bio-rad, Hercules, USA), on the following program:

1. 25°C - 10 minutes
2. 48°C - 30 minutes

51

   3. 95°C - 5 minutes

qRT-PCR was peformed on a Biorad i-cycler with a MyIQ detection system, using IQ SYBR Green supermix (Bio-rad). The PCR-reaction included 1µl of template cDNA and 500nM of forward and reverse primers with the following program:

   1. 95°C – 5 minutes

   2. 40 cycles of:

         a. 95°C – 15 seconds

         b. 60°C – 30 seconds

         c. 72°C – 30 seconds

Florescence was detected as the end of each amplification cycle (step 2c).

Melt curve analysis was performed on all reactions, at 0.5°C increments between 55-95°C, to detect any genomic DNA contamination, primer dimers and/or non-specific amplification.

Data were analysed using BioRad IQ software, and the transcript copy number estimated by normalising results to the housekeeping gene (HKG) GAPDH, using the following equation where Ct= cycle threshold.

Copy number of target = 2500*1.93^(HKi - target Ct)

Where 2500 is an empirical estimation of the number of HKG transcripts, 1.93 reflects a typical reaction amplification efficiency of 93%, and HKi is the geometric mean Ct of the HKG (Aguilar et al. 2007).

Fold change of differentiated cells over undifferentiated cells was calculated as below:

$$\text{Fold Change} = \frac{\text{Differentiated copy number}}{\text{Undifferentiated copy number}}$$

All primers were designed using NCBI Primer-BLAST software , with melting temperatures of 60ºC and primer lengths of ~20. All reactions were performed in triplicate.

2.9 Surgery

12 week old C57BL/6 were anaesthetised via inhalation of isoflurane and immediately given antibiotics (0.5ml Betamox LA) and pain relief (5mg/kg Carprieve) subcutaneously and Visotears used on the eyes to prevent drying. Animals were placed on a heat mat throughout surgery and recovery. Hair was removed prior to incision using clippers and Nair™ hair removal cream (3 minutes), before disinfection with Hibiscrub. A small (~10mm) incision was made midline on the mouse right hand side just under the ribcage, followed by a slightly smaller incision (~7mm) in the peritoneum directly underneath. The kidney was then gently exposed using small non-toothed forceps to hold it in place. A small incision was made to the kidney capsule using a 27 gauge needle without piercing the kidney itself: The kidney capsule was kept moist with PBS containing 0.05% gentamicin throughout. A small space was then made between the kidney and its capsule using a fine pipette tip containing the cell mix. The cell mix was deposited slowly, forming a gel like ball as the matrigel solidified, and the entry site cauterized to prevent leakage. The peritoneum and skin were individually

closed using 5-0 Vicryl sutures and the animal allowed to recover. 10 out of 12

animals operated on survived (1 did not recover, 1 died 24 hours post-surgery).

Animals were sacrificed 4 weeks post-surgery and assessed for tumour formation.

Tumours were removed and fixed and processed for immunostaining as

previously described (see section 2.2).

2.10 Statistical Analysis

Data is presented as Mean ±SD. Significance between 2 groups was determined

using an independent T-test. For analysis of more than 2 groups, One-Way

ANOVA was performed with tukey post hoc method to locate the differences.

Significance was reported when $p < 0.05$.

RESULTS

3. PIC location and distribution

3.1 Introduction

Growth velocity is highest in early postnatal development than at any subsequent stage with a rapid growth and maturation of skeletal muscle occurring during this time (Lui and Baron. 2011). To enable this growth, it has previously been shown that there is an abundance of SCs present at birth, which sharply decline in frequency to adult levels (Suzuki et al. 2010), after which point there is a gradual decline with age (Neal et al. 2012) and in age-related sarcopenia (Shefer et al. 2010).

PICs are identified by their expression of PW1 and interstitial location (see Table 1.3) and are found at a similar frequency to SCs with ~22, ~13 and ~16 PICs per 100 fibres compared to 19, 14 and 11 SCs at birth, 7, and 14 days respectively (Mitchell et al. 2010). Similarly, our group found a 1:1 ratio of PICs: SCs in the hind-limb muscle of 2 month old pigs (Lewis et al. 2014). The abundance of PICs declines in aged mice (18 months) to <1 per 100 fibres (Formicola et al. 2014) with the PIC: SC ratio decreasing to ~1:3.

This study determined PW1 expression, PIC and SC abundance in murine hind-limb up to 21 days post-natal development, which is when SC abundance per muscle fibre falls to adult levels in mice (Cardasis and Cooper 1975). Formicola et al. (2014) previously looked at PIC and SC abundance in 18 month old mice;

however mice can live for 2 years or more. Therefore, to properly encapsulate the abundance of PICs and SCs in aged muscle their presence in 2 year old mice was also investigated.

3.2 Methods

3.2.1 Quantitative Immunohistochemistry

Skeletal muscle sections of 3, 10, 21 day and 2 year old mice (n=3 per age group) were stained as described in (see Section 2.3) for antibodies listed in Table 3.1. Total nuclei, PW1$^+$ nuclei, PW1$^+$ interstitial nuclei and total muscle fibres were counted (3, 10 and 21 days: n=10 fields of view per animal, 2 years: n=20 fields of view per animal). Muscle fibres were identified by a fully intact basal lamina, delineated by laminin, PW1 staining was seen in nuclei. PW1$^+$ cells located in the interstitium were counted as PICs, whilst PW1$^+$ cells located under the basal lamina of the muscle fibres were counted as satellite cells. Standard deviation was calculated from the mean of each animal per group (n=3).

Table 3.1   Antibodies used on paraffin embedded skeletal muscle tissue sections.

Primary Antibody	Dilution	Incubation	Secondary Antibody
PW1 (Gifted by David Sassoon, Inserm, Paris)	1:3000	Overnight at 4°C	Alexa Fluor 488 Donkey anti-Rabbit, (Stratech)
Laminin (Sigma)	1:50	1 Hour at 37°C	Alexa Fluor 594 Donkey anti-Chicken (Stratech)

3.3 Results

Expression of PW1 in hind-limb skeletal muscle cross sections was assessed by immunohistochemistry (IHC) at 3, 10 and 21 days and 2 years. PW1 was seen as nuclear staining, co-expressed with DAPI (Figure 3.1).

PW1 expression was quantified as a percentage of total nuclei in all locations of the hind limb muscle, inclusive of SCs and PICs. At 3 days ~9% of nuclei were positive for PW1, this abundance decreased ~1.5 fold between 3 and 10 days, with subsequent decreases of ~1.5 fold between 10-21 days and ~3 fold between 21days and 2 years. This equated to a ~6 fold reduction in PW1 expression from 3 days to 2 years, with PW1 expressed in less than ~1.5% of nuclei in aged animals (Figure 3.2).

The number of $PW1^+$ nuclei per muscle fibre was calculated: Muscle fibres were identified as delineated by laminin staining. Similar to PW1 abundance, there was a ~11 fold decrease in the number of $PW1^+$ nuclei/muscle fibre (cross-sectional area), between 3 days and 2 years; Specifically, a ~2 fold decrease between 3-10 days, ~1.5 fold decrease between 10- 21 days and ~4 fold decrease between 21 days and 2 years (Figure 3.3). These data translated to a reduction from 1 $PW1^+$ nuclei: 3 fibres at 3 days, to 1 PIC: 31 fibres at 2 years (Figure 3.4).
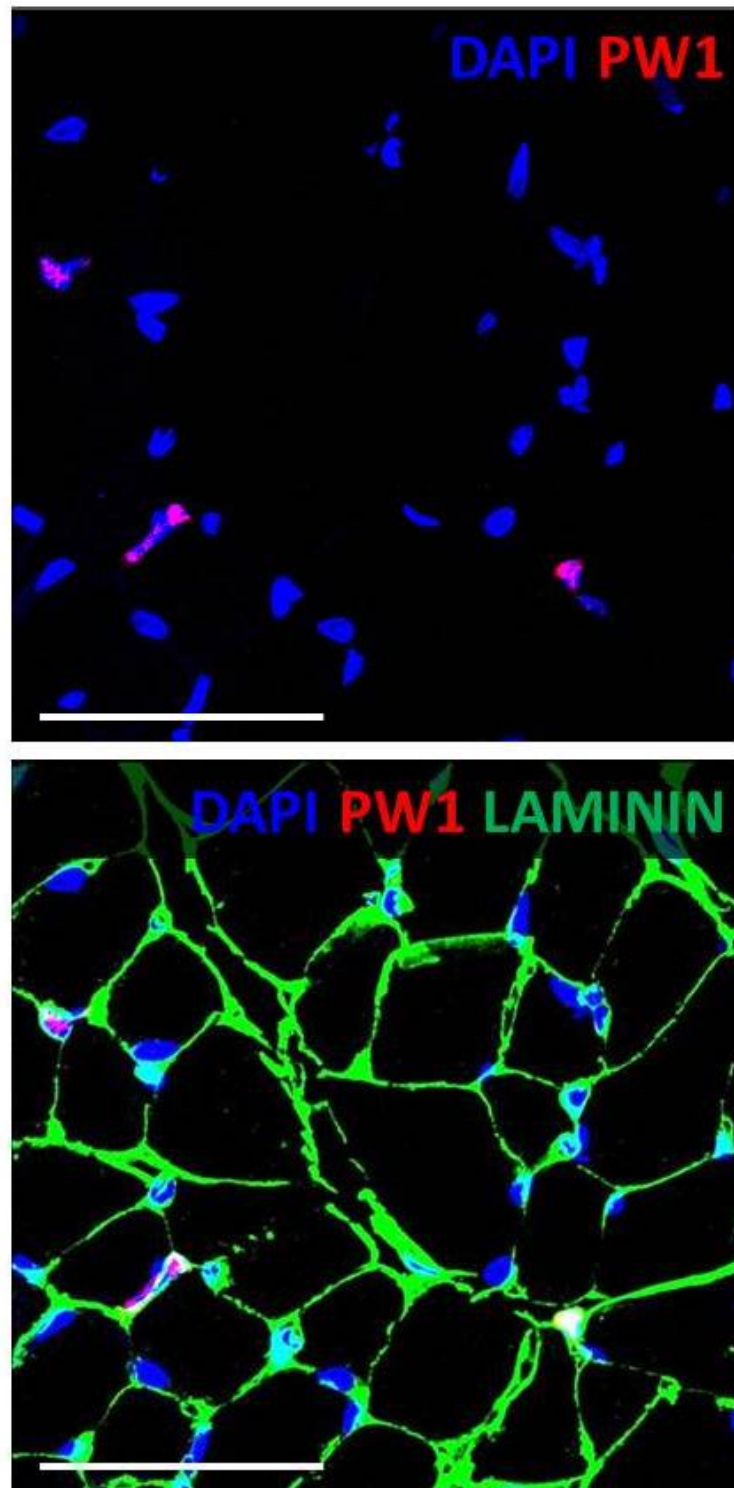
Figure 3.1   Identification of PW1 in murine hind-limb muscle. 10 day old

mouse paraffin embedded hind limb muscle, stained by IHC for PW1 (red) and

laminin (green). Nuclei are stained in blue by DAPI. Scale = 50µm.
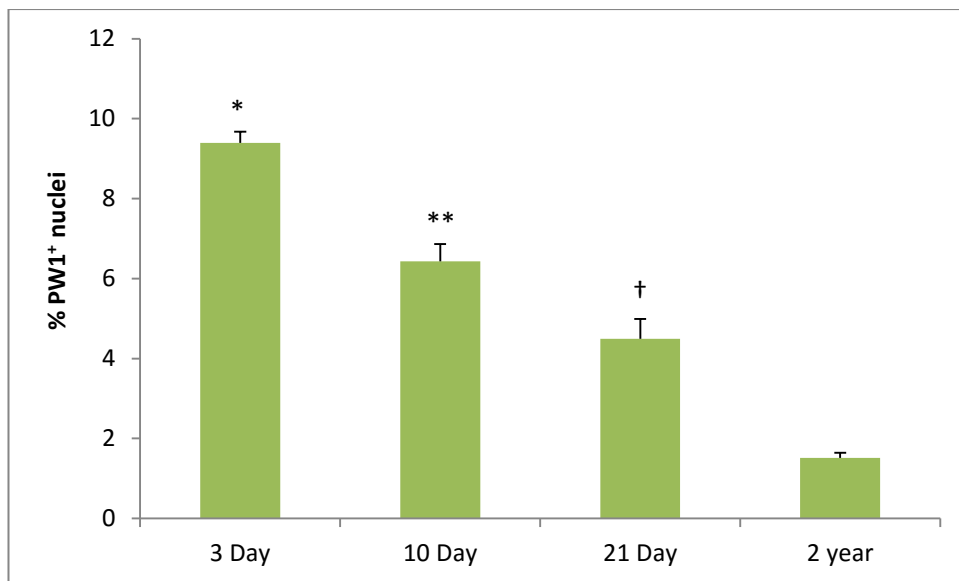
Figure 3.2   Total PW1 abundance in hind-limb muscle from postnatal to ageing. PW1 expression as a percentage of total nuclei (inclusive of PICs and SCs) in 3, 10 and 21 day, and 2 year old mice. Data is mean ±SD, n=3 per group. * denotes significant differences (p<0.05) vs 10 day, 21 day and 2 year, ** denotes significant differences (p<0.05) vs 21 day and 2 year, † denotes significant differences (p<0.05) vs 2 year.

Figure 3.3 **The number of PW1 nuclei per muscle fibre from postnatal to**

ageing. The number of PW1^{+} nuclei (inclusive of PICs and SCs) per cross

sectional muscle fibre in 3, 10, and 21 day and 2 year old mice. Data is mean ±SD,

n=3 per group. * denotes significant differences (p<0.05) vs 10 day, 21 day and 2

year, ** denotes significant differences (p<0.05) vs 21 day and 2 year, † denotes

significant differences (p<0.05) vs 2 year.
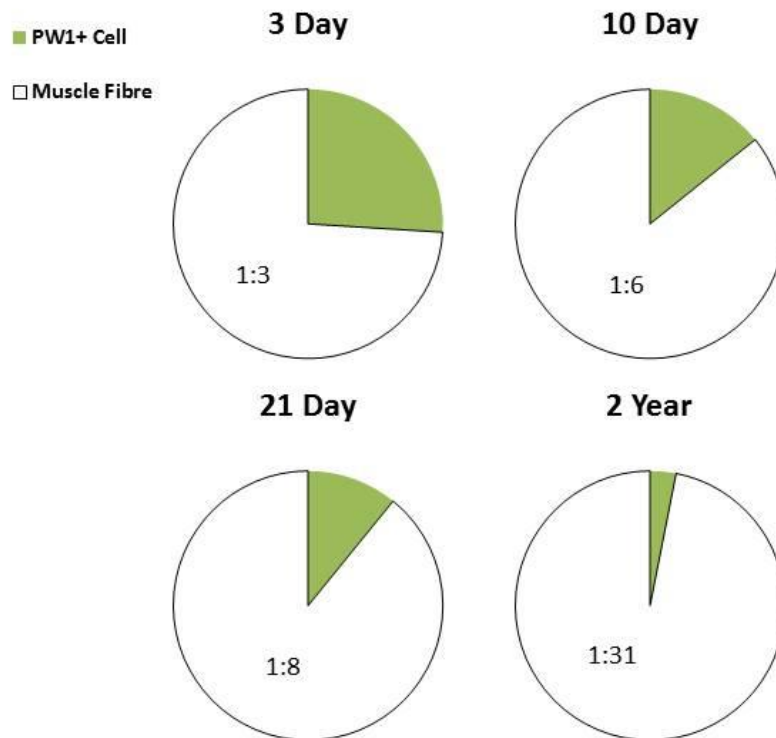
Figure 3.4   The ratio of PW1 nuclei: Muscle fibre from postnatal to ageing.

The ratio of PW1$^+$ nuclei: muscle fibre (cross-sectional area) in hind limb skeletal muscle of 3, 10 and 21 day, and 2 year old mice. Data is mean, n=3 per group.

Cells positive for nuclear PW1 staining were identified as being either:

A) PIC – located within interstitial spaces

or

B) SC – located directly under the basal lamina of muscle fibres, with at least one side free of laminin (Figure 3.5).

To account for activated satellite cells that may have moved into interstitial spaces Pax7 staining was utilized to further distinguish between PICs and SC's, however no interstitial cells expressing both Pax7 and PW1 were found.

At 3 days ~5% of total nuclei were identified as $PW1^+$ PICs, this reduced ~ 12 fold by 2 years to ~0.5% (Figure 3.6). PICs represented ~57% of $PW1^+$ nuclei assessed between 3 and 21 days, however this number dropped to ~30% in 2 year old animals (Figure 3.7).

Similar to total PW1 expression, there was a progressive decrease with age (~21 fold between 3 days and 2 years) in the number of PICs per muscle fibre (Figure 3.8). This equated to a total reduction from 1 PIC: 5 muscle fibres at 3 days, to 1 PIC: 104 fibres at 2 years of age (Figure 3.9).
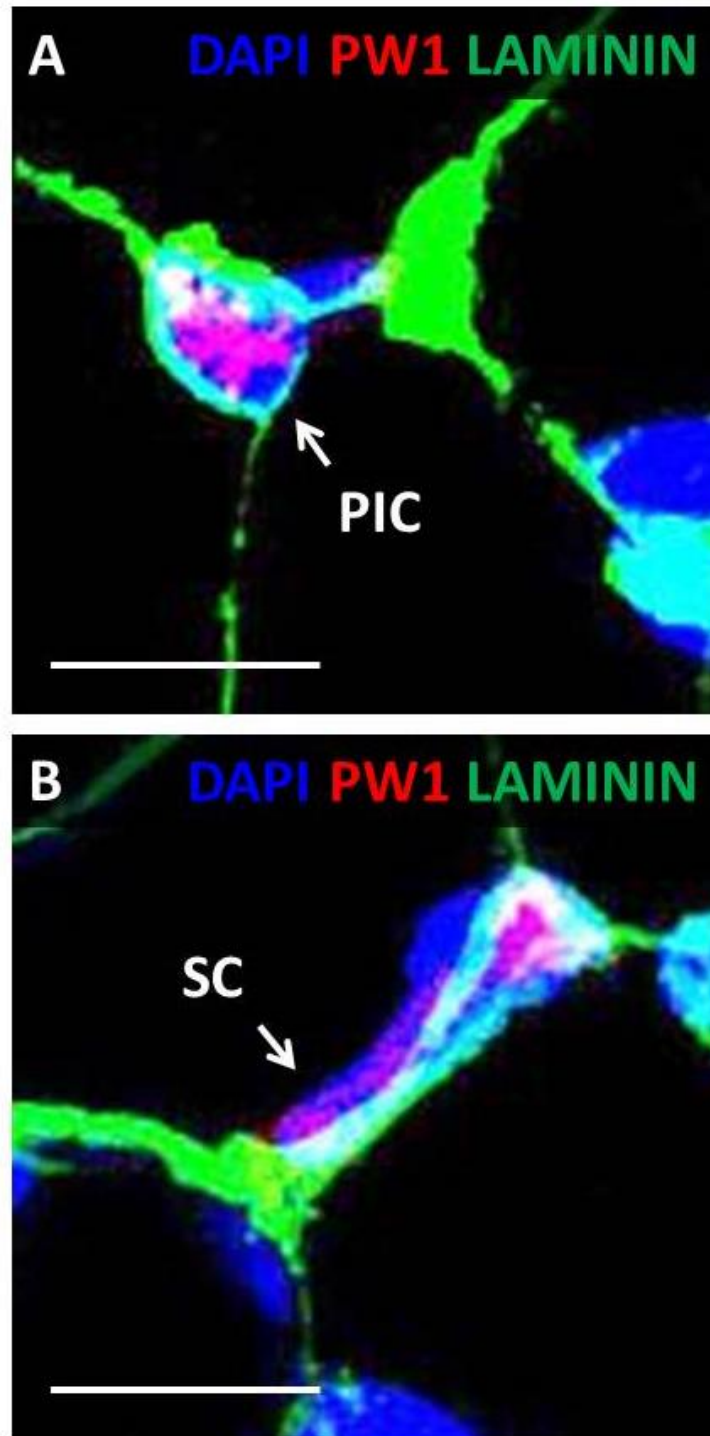
Figure 3.5   The identification of PICs and SCs in murine hind limb muscle.

10 day old mouse hind limb muscle stained for PW1 (red), laminin (green) and

DAPI (blue), showing A. PW1$^+$ interstitial PIC and B. PW1$^+$ satellite cell under

the basal lamina. Scale = 10µm.
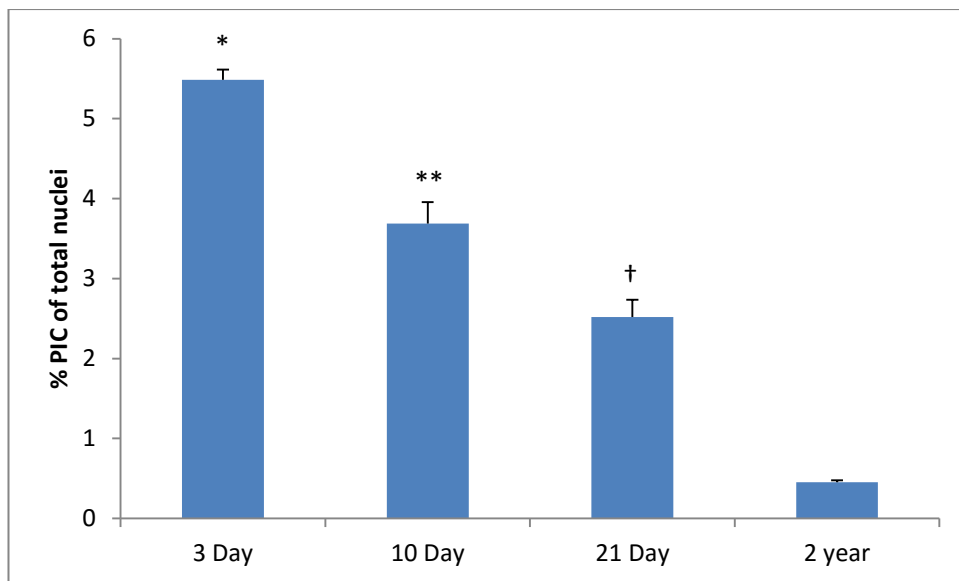
Figure 3.6   PIC abundance in hind-limb muscle from postnatal to ageing.

The percentage of total nuclei identified as interstitial PICs in 3, 10 and 21 day, and 2 year old mice. Data is mean ±SD, n=3 per group. * denotes significant differences (p<0.05) vs 10 day, 21 day and 2 year, ** denotes significant differences (p<0.05) vs 21 day and 2 year, † denotes significant differences (p<0.05) vs 2 year.
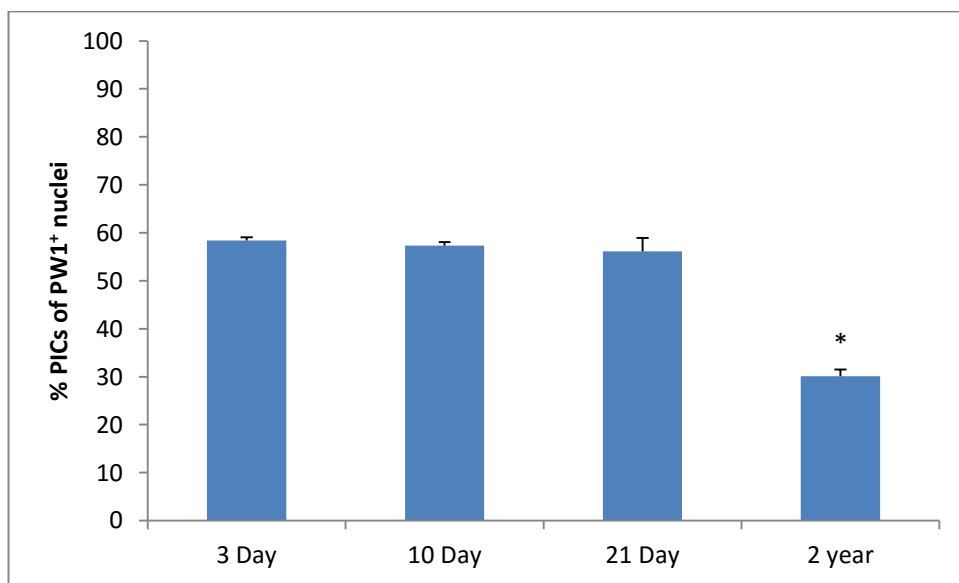
Figure 3.7   Percentage of PICs in the PW1$^+$ cell fraction from postnatal to ageing. The percentage of PW1$^+$ nuclei identified as interstitial PICs in hind limb skeletal muscle in 3, 10 and 21 day, and 2 year old mice. Data is mean ±SD, n=3 per group. * denotes significant differences (p<0.05) vs 3, 10 and 21 day.
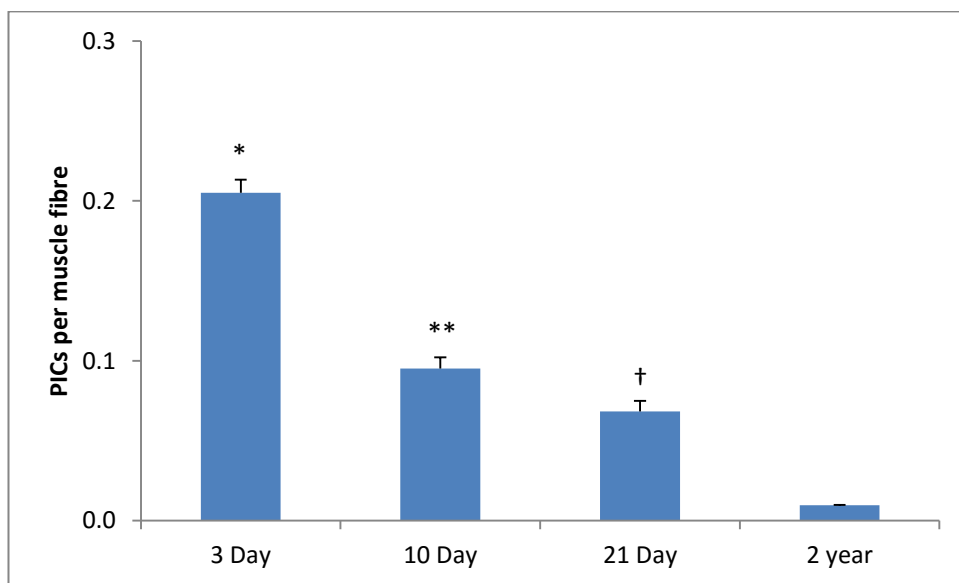
Figure 3.8 **The number of PICs per muscle fibre from postnatal to ageing.**

The number of interstitial PICs per muscle fibre in hind limb skeletal muscle of 3, 10, and 21 day, and 2 year old mice. Data is mean ±SD, n=3 per group. * denotes significant differences (p<0.05) vs 10 day, 21 day and 2 year, ** denotes significant differences (p<0.05) vs 21 day and 2 year, † denotes significant differences (p<0.05) vs 2 year.
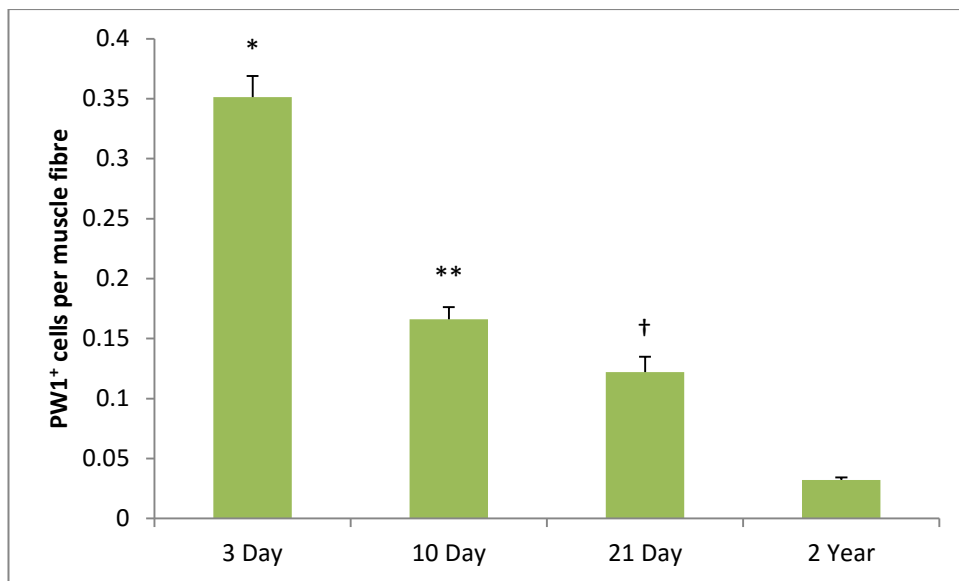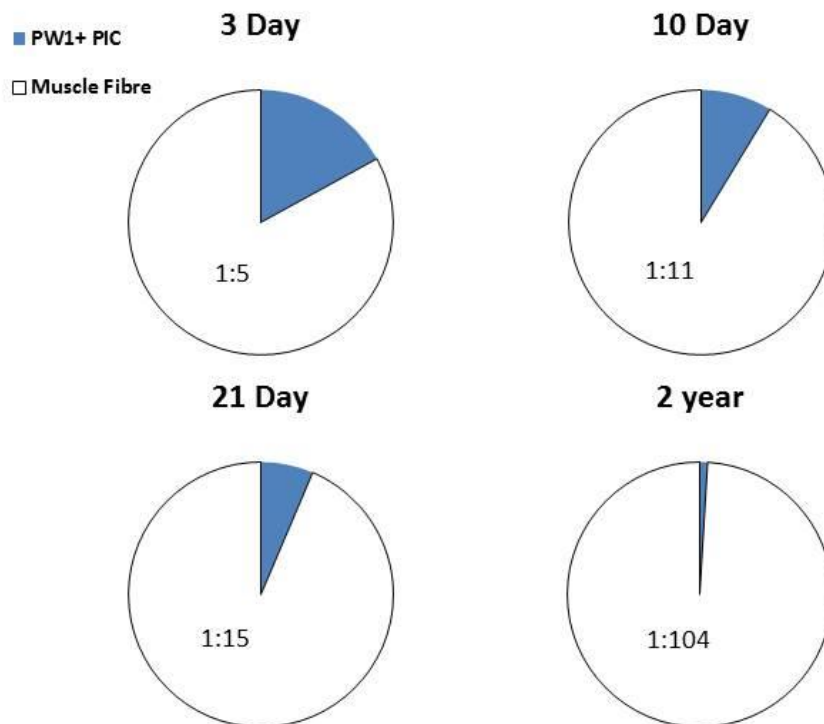
Figure 3.9   The ratio of PIC: Muscle fibre from postnatal to ageing. The ratio of interstitial PIC: muscle fibre (cross-sectional area) in hind limb skeletal muscle of 3, 10 and 21 day, and 2 year old mice. Data is mean, n=3 per group.

The abundance of SC's followed a similar trend with age as PICs: SCs reduced from ~4% of all nuclei at 3 days, to ~1% by 2 years (Figure 3.10). However, they showed an inverse trend in the percentage of PW1$^+$ nuclei that they represented being 43% of the PW1$^+$ nuclei between 3-21 days, rising to ~70% in aged mice (Figure 3.11).

Again, similar to PICs, the number of SCs per muscle fibre decreased ~6 fold between 3 days and 2 years (Figure 3.12). This equated to a total reduction from 1 SC: 7 muscle fibres at 3 days, to 1 SC: 44 fibres at 2 years of age (Figure 3.13).

Overall, the ratio of PICs: SCs remained constant (~13:10) during the first 3 weeks of postnatal development, however this dropped to ~4:10 in 2 year old mice (Figure 3.14).
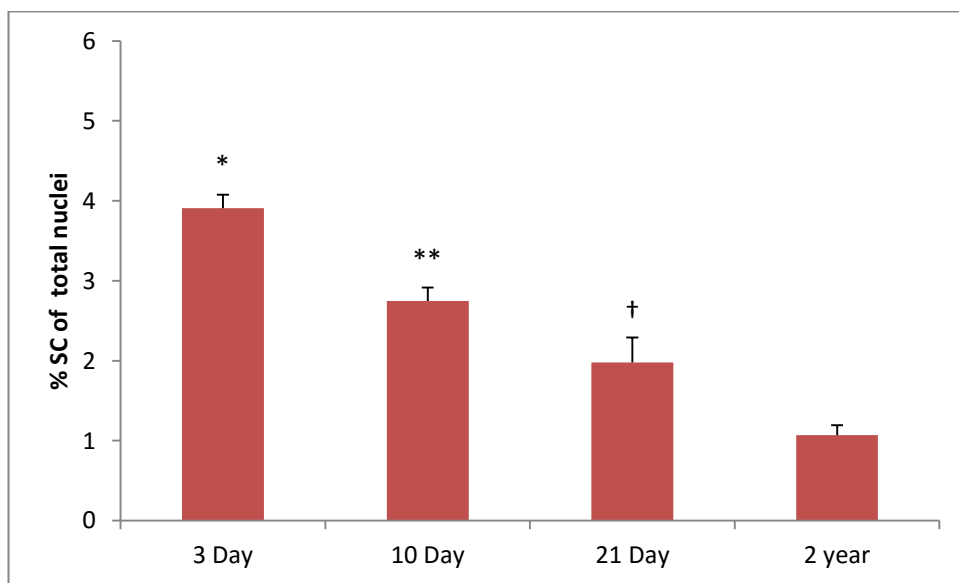
Figure 3.10   SC abundance in hind-limb muscle between from postnatal to ageing. The percentage of total nuclei identified as SCs under the basal lamina in 3, 10 and 21 day, and 2 year old mice. Data is mean ±SD, n=3 per group. * denotes significant differences (p<0.05) vs 10 day, 21 day and 2 year, ** denotes significant differences (p<0.05) vs 21 day and 2 year, † denotes significant differences (p<0.05) vs 2 year.
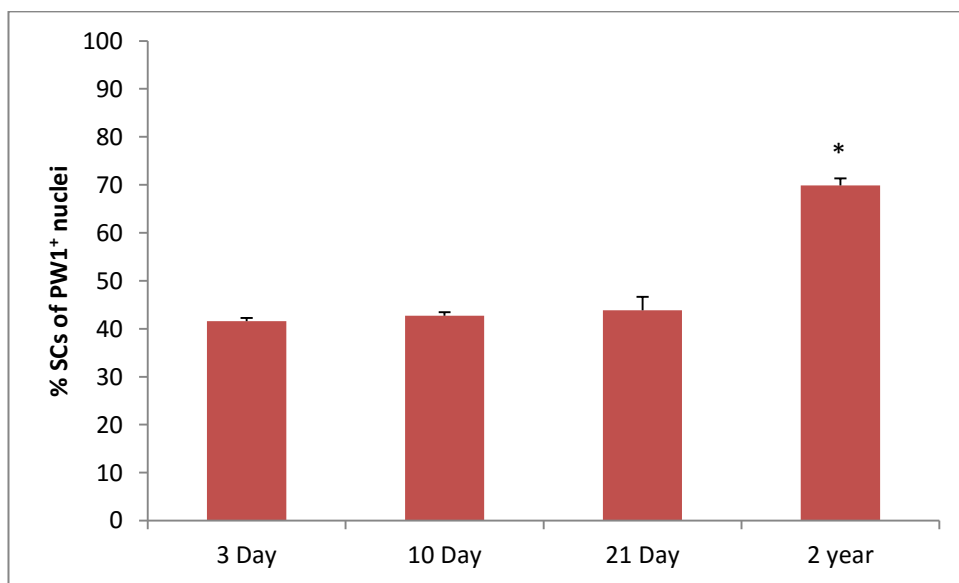
Figure 3.11 **Percentage of SCs in the PW1$^+$ fraction between 3 days and 2 years.** The percentage of PW1$^+$ nuclei identified as SCs under the basal lamina in hind limb skeletal muscle in 3, 10 and 21 day, and 2 year old mice. Data is mean $\pm$SD, n=3 per group. * denotes significant differences (p<0.05) vs 3, 10 and 21 day.
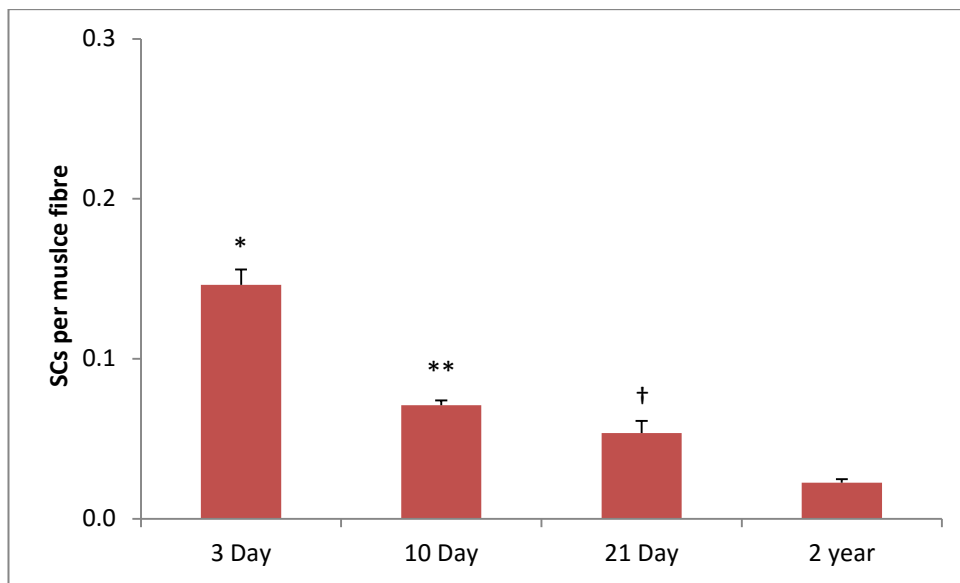
Figure 3.12   The number of SCs per muscle fibre between 3 days and 2

years. The number of SCs under the basal lamina per muscle fibre in hind limb

skeletal muscle of 3, 10, and 21 day, and 2 year old mice. Data is mean ±SD, n=3

per group. * denotes significant differences (p<0.05) vs 10 day, 21 day and 2 year,

** denotes significant differences (p<0.05) vs 21 day and 2 year, † denotes

significant differences (p<0.05) vs 2 year.
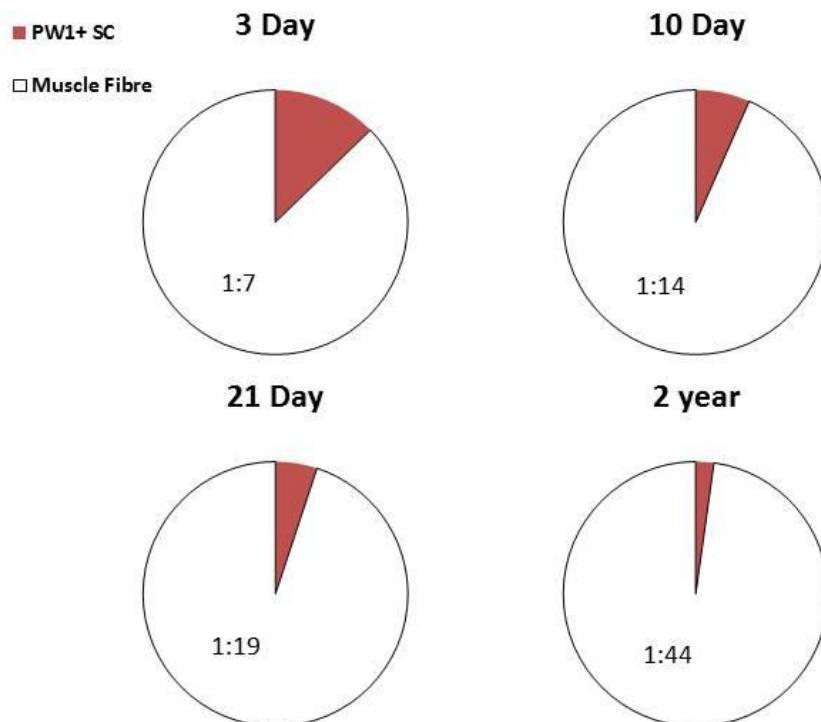
Figure 3.13   The ratio of SC: Muscle fibre between 3 days and 2 years. The

ratio of SC: muscle fibre (cross-sectional area) in hind limb skeletal muscle of 3,

10 and 21 day, and 2 year old mice. Data is mean, n=3 per group.
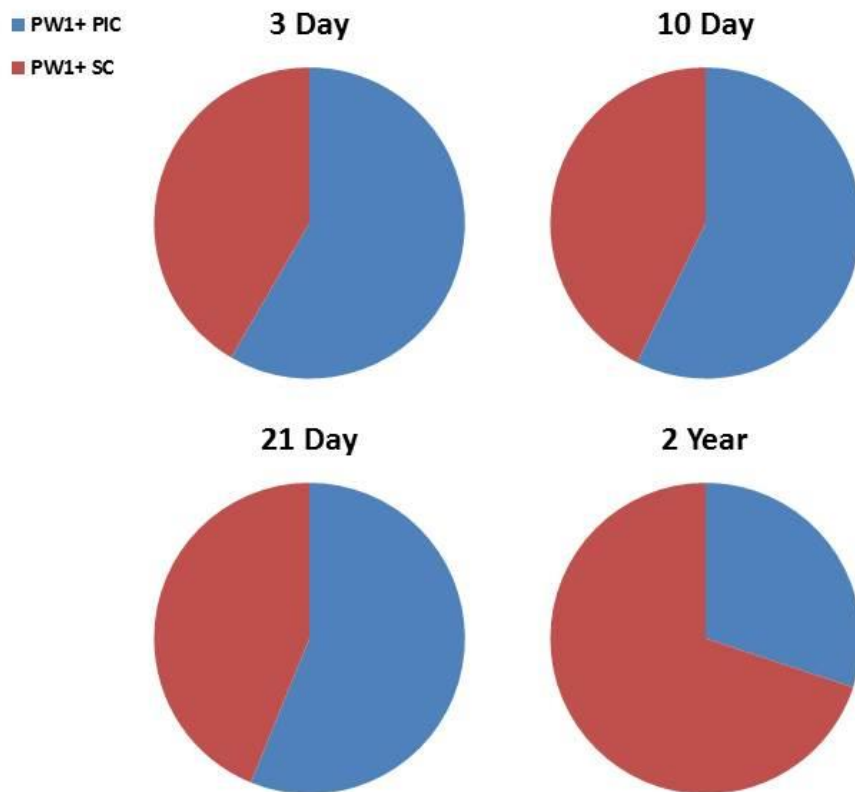
Figure 3.14   PIC to SC ratio between 3 days and 2 years. The ratio of PICs:
SCs in hind limb skeletal muscle in 3, 10 and 21 day and 2 year old mice. Data is
mean, n=3 per group**.**

3.3 Discussion

The main findings that emanated from this study are:

1. There was a decrease in PW1 expression in skeletal muscle over the 2 year lifespan of the mouse.

2. The number of PICs and SCs per muscle fibre decreased with age.

3. The ratio of PICs: SC's remained constant during the first 3 weeks of postnatal development.

4. The PIC: SC ratio declined in aged animals.

3.3.1 PW1 abundance in skeletal muscle

The abundance of PW1 expression in hind-limb tissue, and its decrease with age, was in agreement to that previously reported (~1.5 fold between 0-14 days) during early postnatal development (Mitchell et al. 2010). Jones et al. (2014) described a similar decrease of PW1 transcripts in skeletal muscle of mice between 0-21 days. Transcripts further decreased from 21- 42 days; however there was no difference between 42-70 days suggesting PW1 expression stabilises at adult levels.

In aged animals (2 Years), PW1 protein expression decreased further; a similar decline (~3.6 fold) was recently reported between 7 weeks and 18 months (Formicola et al. 2014). This decrease was due to a reduction in the abundance of both PICs and SCs: It was noted that SCs demonstrated a visually weaker PW1 signal than PICs, suggesting there may be a difference in PW1 protein expression between the two cell populations, although this was not quantified.

3.3.2 Reduction in PIC abundance with age

PICs declined in abundance from 3 days to 2 years. This trend was previously shown in mice between 0-14 days (Mitchell et al. 2010) and 7 weeks to 18 months (Formicola et al. 2014). The mechanism behind this change in abundance is unknown, however chronological and replicative aging may account for the reduction of cells in the stem cell pool (Rando 2006).

3.3.3 Reduction in SC abundance with age

It is well documented that SCs decline with age: Formicola et al. (2014) reported a ~2.5 fold reduction in the number of SCs per muscle fibre, in young and old mice (7 weeks to 18 months) with other groups showing similar results: ~2.5 fold decrease between 3.5 and 27 months (Day et al. 2010); ~ 3 fold decrease between 3.5 and 16 months (Shefer et al. 2010). Furthermore, Neal et al. (2012) found a greater reduction (~6 fold) between juvenile (2 weeks) and aged mice (2.5 years), which is in agreement with this study. It is thought that SCs become less efficient at proliferation and myotube formation with age due to the aging of their environment, rather than intrinsic aging of the SCs themselves (Carlson and Faulkner 1989, Conboy et al. 2005).

3.3.4 PICs vs SCs

The present study found that SCs and PICs were found at a ratio of ~1:1 throughout the first 3 weeks of postnatal life in the mouse, with a similar ratio documented in 0, 7, 14 day and 7 week old mice (Mitchell et al 2010; Formicola et al. 2014) and 2 month old pigs (Lewis et al. 2014).

However, the PIC: SC ratio changed in aged animals to ~1:3, as previously described in 18 month old mice (Formicola et al. 2014), demonstrating that PICs decline at a faster rate than SC's in old age; the exact time point this occurs, and the mechanism behind this change is unknown.

This steady ratio during early post-natal development suggests that it may be the decrease in the PIC population that is directly affecting the SC cell pool. Indeed, PICs have been shown to give rise to SCs (Mitchell et al. 2010); however, pericytes have also been shown to contribute to the SC pool (Cappellari and Cossu. 2013), which may account for a lesser reduction in SCs than PICs in 2 year aged mice.

The link between SCs and PICs is apparent, however, it has not yet been fully explored. To further elucidate how these two cell types are linked, their abundance in relation to each other should be studied throughout adulthood. Thus providing us with a clear picture as to when the ratio of PICs: SC cells changes; Do PICs slowly decline at a slightly faster rate than SCs? Or is there a sudden drop in PIC abundance at a specific time point?

Furthermore, Pax7 germline knockout mice have an increased abundance of PICs, and a lesser number of SCs, with a ~3:1 ratio of PIC: SC (Mitchell et al. 2010). Whether this occurs as PICs are less efficient at generating SCs without Pax7, or whether the PIC population is elevated by another mechanism to counteract the SC depletion has not yet been determined. However, the reduced capacity for muscle regeneration seen in Pax7 germline knockout mice (Oustanina et al. 2004) would indicate that it may be the former.

Lineage tracing studies would help identify and describe this link between PICs and SCs, however to do this we would first need to identify a PIC exclusive marker to enable labelling of the PIC population solely.

If the decline in PICs is directly responsible for the subsequent decline in SCs with age, can PICs be replenished? And would this counteract the effects of sarcopenia?

4. PICs are self-renewing and clonogenic in *vitro*

4.1 Introduction

The phenotype and behaviour of murine PICs *in vitro* is not yet well documented. Previous studies have identified the phenotype and regenerative capacities of PICs in *vivo,* such as their expression of PW1/Sca-1 and CD34 and ability to contribute to the regeneration of skeletal muscle following an injury (Mitchell et al. 2010, Pannérec et al. 2013). Our group was the first to demonstrate that porcine PICs (pPICs) maintain a stable phenotype and karyotype over long term cell culture, and express stemness markers, however as no Sca-1 homologue has been identified in pig, pPICs were not selected by positive expression of Sca-1, but CD34 instead (Lewis et al. 2014).

Isolating adult stem cells (ASCs) from solid tissues can be achieved by enzymatic digestion, which requires an initial mechanical breakdown of the tissue into smaller pieces prior to treatment. Enzymatic digestion breaks down tissues using proteolytic enzymes such as trypsin and collagenase, releasing small cells held within the tissue compartment. The use of such enzymes has been well documented as far back as 1974 in isolating myogenic cells from adult rat muscle (Bischoff. 1974) and has since been used to isolate cells from a variety of tissues. Mitchell et al. (2014) first isolated PICs using 0.15%/g Pronase before purification, whilst subsequent studies used 2 µg/ml collagenase A, 2.4U/ml dispase I and 10ng/ml DNase I (Pannérec et al. 2013) or 100 mg/ml collagenase A

and 3mg/ml of dispase I (Lewis et al. 2014). Cells obtained by this method can be further purified using an enrichment protocol.

Affinity based separation methods utilize known surface markers of target stem cell populations, applying antibodies to label them with either magnetic or fluorescent tags. Fluorescence activated cell sorting (FACS) labels target cells with antigen specific fluorescent tags, and sorts them based on fluorescent signal and light scattering by flow cytometry. Similarly, Magnetic activated cell sorting (MACS) labels cells with an antibody coated magnetic bead. When passed through a magnetic field, any magnetically labelled cells are captured, and unwanted cells discarded. MACS purity is ~75% and allows for a higher output and faster separation of ~10^{11} cells/hour compared to 10^{7} cells/hour using FACS (Zhu et al. 2013).Furthermore, MACS sorting is less stressful on the cells than FACS with improved cell viability post-sorting (Li et al. 2013). PICs have previously been isolated by FACS (Mitchell et al. 2010, Pannérec et al. 2013) for negative expression of CD45 and TER119 and positive expression of Sca-1 and CD34. Our group isolated pPICs via MACS for CD34 positive expression and CD45 negative expression (Lewis et al. 2014).

Ordinarily, ASCs are cultured at 37°C in 5% CO_2 to mimic conditions within the mammalian body. Cell culture treated flasks/plates are coated with a substrate such as gelatin to aid cell attachment prior to plating in growth media. Growth media are specific for each ASC cell type, and traditionally contain media supplements and growth factors known to encourage proliferation and/or maintain pluripotency. A number of ASC populations isolated from either skeletal or

cardiac muscle have been cultured *in vitro* long term including eCSCs, which have a PD of ~22 hours and can proliferate over 65 passages (Ellison et al. 2011).

It has not yet been shown that murine PICs can be propagated and maintained in culture, or if they express stem cell properties. For the first time, this study characterises the phenotype and *in vitro* characteristics of murine PICs to answer the following:

a) Can they be propagated in culture long term?

b) Do they display stem cell characteristics of self-renewal and clonogenicity?

4.2 Methods

PICs were isolated and cultured as described (see Sections 2.5.1 and 2.6) and their

phenotype confirmed and further characterised by immunocytochemistry, flow

cytometry and qRT-PCR.

4.2.2 Immunocytochemistry of cytospin slides

Immunocytochemistry was conducted as per methods (Section 2.4). Antibodies

used and their applications are listed in table 4.1.

Table 4.1   Antibodies used in immunocytochemistry of cytospin slides.

Primary Antibody	Dilution	Incubation	Secondary Antibody
Sca-1 (Abcam)	1/50	1 hour at 37°	Alexa Fluor 488 Donkey anti-Rat (Stratech)
PW1 (Gifted by David Sassoon, Inserm, Paris)	1/3000	1 hour at 37°	Cy 3 Donkey anti-Rabbit (Stratech)
Sox2 (Santa Cruz)	1/50	1 hour at 37°	Dylight 488 Donkey anti-Goat (Stratech)
Nanog (Abcam)	1/50	1 hour at 37°	Alexa Fluor 488 Donkey anti-Rabbit (Stratech)
Oct3/4 (Santa Cruz)	1/50	1 hour at 37°	FITC Donkey anti-Mouse IgG (Stratech)
Pax7 (DSHB)	1/50	1 hour at 37°	FITC Donkey anti-Mouse IgG (Stratech)
CD45 (Santa Cruz)	1/50	1 hour at 37°	Alexa Fluor 594 Donkey anti-Rat (Stratech)

4.2.3 Flow Cytometry

Flow cytometry was conducted as per methods (Section 2.7), using antibodies and

relevant controls described in Table 4.2.

Table 4.2   Antibodies used in Flow Cytometry

Antibody	Conjugate/ Secondary	Control	Dilution	Incubation
PW1 Inserm, Paris	Alexa Fluor 488 Donkey anti-Rabbit Stratech	Alexa Fluor 488 Donkey anti-Rabbit Stratech	1/20	15 minutes at 4°C
Sca-1 Miltenyi	FITC conjugated	FITC Mouse IgG Isotype control Miltenyi	1/20	15 minutes at 4°C
Albumin Abcam	FITC Conjugated	FITC Rat IgG Isotype control Abcam	1/20	15 minutes at 4°C
CD45 Biolegend	FITC Conjugated	FITC Mouse IgG Isotype control Abcam	1/20	15 minutes at 4°C
Pdgfrβ Abcam	PE Conjugated	PE Mouse IgG Isotype Control Abcam	1/20	15 minutes at 4°C
CXCR4 Abcam	Alexa Fluor 488 Donkey anti-Rat Stratech	Alexa Fluor 488 Donkey anti-Rat Stratech	1/20	15 minutes at 4°C
NG2 Santa Cruz	Alexa Fluor 488 anti-Rabbit Stratech	Alexa Fluor 488 Donkey anti-Rabbit Stratech	1/20	15 minutes at 4°C
Pdgfrα Santa Cruz	Dylight 488 Donkey anti-Goat Stratech	Dylight 488 Donkey anti-Goat Stratech	1/20	15 minutes at 4°C
CD146 RnD	FITC Donkey anti-Mouse IgG Stratech	FITC Donkey anti-Mouse IgG Stratech	1/20	15 minutes at 4°C
c-kit Santa Cruz	Alexa Fluor 488 Donkey anti-Rabbit Stratech	Alexa Fluor 488 Donkey anti-Rabbit Stratech	1/20	15 minutes at 4°C
CD34 eBioscience	FITC Conjugated	FITC Rat IgG isotype Control Abcam	1/20	15 minutes at 4°C
CD31 Miltenyi	PE Conjugated	PE Rat IgG Isotype Control Miltenyi	1/20	15 minutes at 4°C
CD31 eBioscience	FITC Conjugated	FITC Rat IgG isotype Control Abcam	1/20	15 minutes at 4°C
Pax7 DSHB	FITC Donkey anti-Mouse IgG Stratech	FITC Donkey anti-Mouse IgG Stratech	1/20	15 minutes at 4°C
c-kit Miltenyi	PE Conjugated	PE Rat IgG isotype Control Miltenyi	1/20	15 minutes at 4°C

4.2.4 qRT-PCR

qRT-PCR was conducted as per methods (Section 2.8), using primers listed in Table 4.3.

Table 4.3   Primer sequences

Gene	Accession Number	Forward	Reverse
Sox2	NM_011443.3	CACAACTCGGAGATCAGCAA	CTCCGGGAAGCGTGTACTTA
Oct3/4	NM_013633.2	CCAATCAGCTTGGGCTAGAG	CTGGGAAAGGTGTCCCTGTA
Nanog	NM_028016.2	TACCTCAGCCTCCAGCAGAT	GTGCTGAGCCCTTCTGAATC
PW1	NM_008817.2	TTTTGGTGAGTTGCTTGCAG	ACGTTCTTGGGCATAACTGG
CD34	NM_133654.3	GGGTAGCTCTCTGCCTGATG	TCTCTGAGATGGCTGGTGTG
SCA1	NM_001271446.1	CCATCAATTACCTGCCCCTA	AAGGTCTGCAGGAGGACTGA
CD45	NM_011210.3	CCTGCTCCTCAAACTTCGAC	GACACCTCTGTCGCCTTAGC
CD146	NM_023061.2	GAGCTCATCTCCCCTCACAG	TCCTGACCACTACCCAAAGG
GAPDH	NM_008084.2	ACCCAGAAGACTGTGGATGG	CACATTGGGGGTAGGAACAC
β-actin	NM_007393.3	AGCCATGTACGTAGCCATCC	TCTCAGCTGTGGTGGTGAAG

4.2.5 Self-renewal

To determine self-renewal, C9 PICs were cultured (see Section 2.6) for 20 passages, with their clonogenicity (see Section 2.6.1) and population doubling time (see Section 2.6.2) calculated every 5th passage. Furthermore, their morphology was observed and phenotype assessed throughout their time in culture by qRT-PCR (at P1, P10 and P20) and FC (at P2 and P20).

4.2 Results

4.2.1 Isolation and Characterisation of CD45$^-$/Sca-1$^+$ PICs

Murine hind limb muscle obtained from both legs of 21 day old mice was enzymatically digested before the CD45$^-$/Sca1$^+$ fraction was obtained through MACS technology (See section 4.2.1), ~ 800,000 CD45$^-$/Sca-1$^+$ cells were obtained per mouse.

Isolated cells were plated in 35mm dishes in one of 2 medias: Promocell complete skeletal muscle media or a defined stem cell growth media, as optimised by our laboratory for the expansion of eCSCs. After 6 days cells cultured in Promocell media had a >50% decrease in number since plating, whilst in contrast, the cells plated in defined stem cell growth media had increased 10-fold to ~$1.5x10^5$ cells per dish (Figure 4.1).

CD45$^-$/Sca-1$^+$ cells cultured in growth media contained a high number of small, round and bright cells with a very high nucleus to cytoplasmic ratio, which adhered to the culture dish whilst those cultured in Promocell media did not show any small rounded, bright cells and appeared flattened (Figure 4.2).

Our defined growth medium was chosen for all subsequent culture due to the growth rate and morphology of the cells observed. There was an initial visual increase in the abundance of small, round, bright cells observed between P0 and P3 (Figure 4.3) which maintained for the duration of time in culture. These small cells detached quickly when trypsinised with very little cell death occurring at each passage.
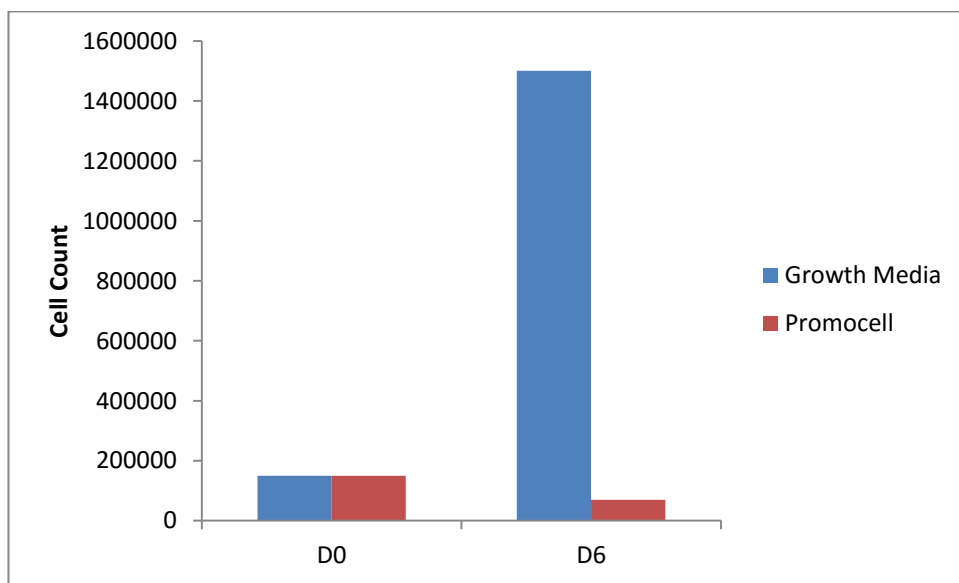
Figure 4.1   PIC population growth in Promocell vs Growth media. Cell count at initial plating (D0) and after 6 days (D6) of culture in PIC and Promocell growth medias (n=1 culture dish).
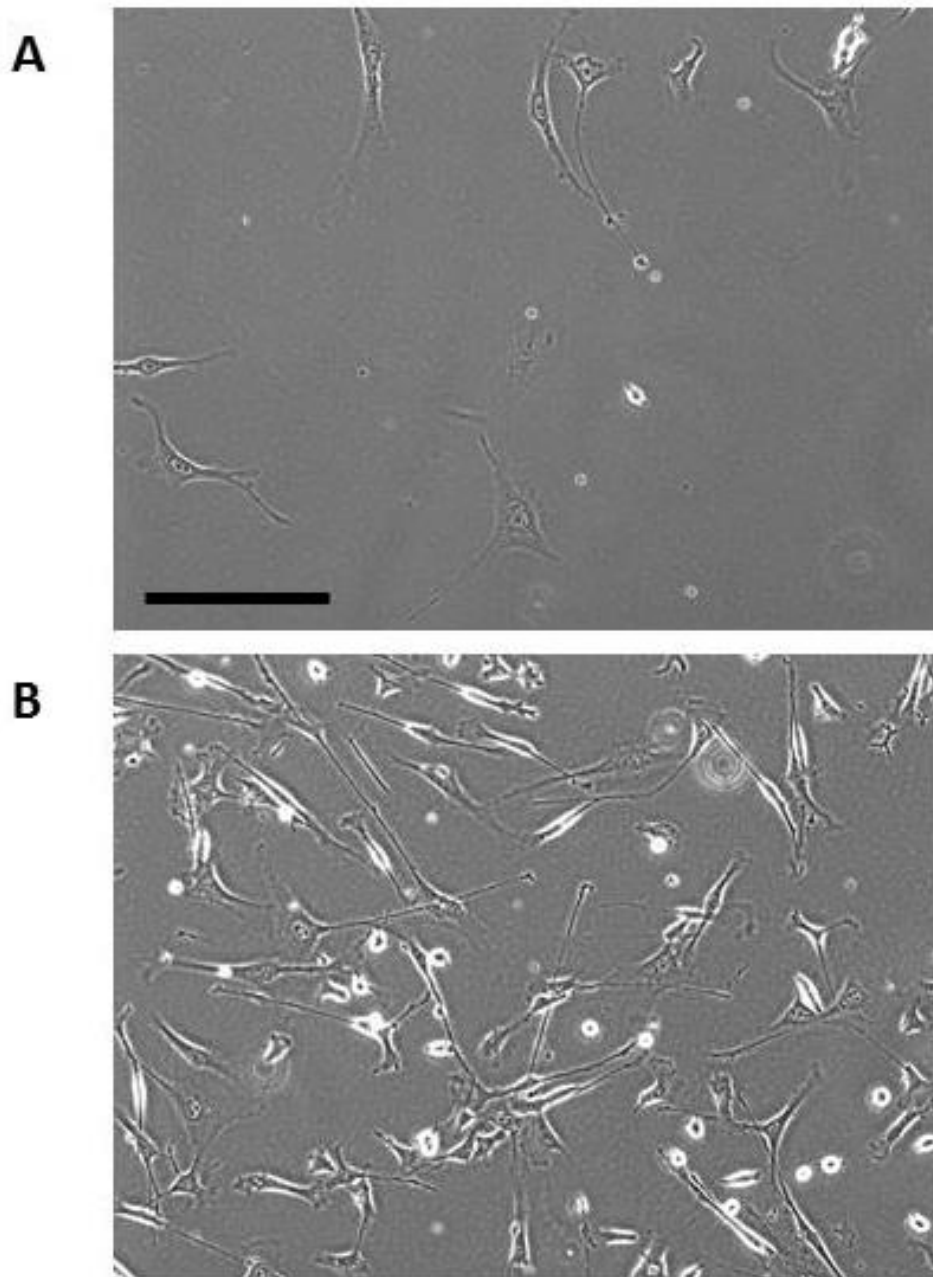
Figure 4.2 **Cell Morphology in Promocell vs Growth Media.** Transmitted

light microscope observation of CD45$^-$/Sca-1$^+$ cells isolated from 21 day old mice

after 6 days in culture with A. Promocell media and B. growth media. Scale

=200μm.
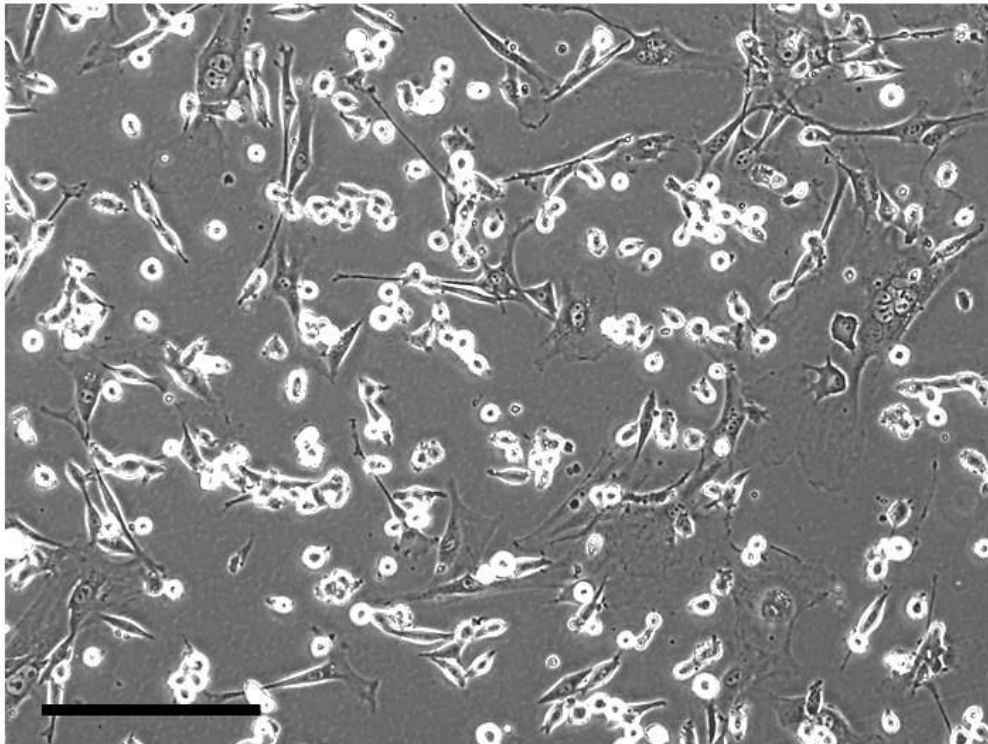
Figure 4.3   Cell morphology at P3. Transmitted light microscope observation

of CD45⁻/Sca-1⁺ cells isolated from 21 day old mice and cultured to P3. Scale

=200μm.

Immunocytochemistry (ICC) of cytospin slides (Figure 4.4), and FC analysis (Figure 4.5) of P3 cells from 21 day old mice, confirmed the isolated cells were CD45$^-$/Sca-1$^+$. In agreement with PIC phenotype, cells were also confirmed as being Pax-7$^-$ and PW1$^+$, and are thereafter referred to as 'PICs'.

To further elucidate the phenotype of PICs, an array of markers previously described in PIC populations (Figure 4.6) and other muscle related cells (Figure 4.7) was carried out at P4. Results showed PICs did not express endothelial markers CD31 or CD146, nor pericyte markers NG2 and PDGFRβ ($< 3\%$), but did express PDGFRα (19%), CD34 (51%) and CXCR4 (59%) as expected based on previous studies (Lewis et al. 2014).
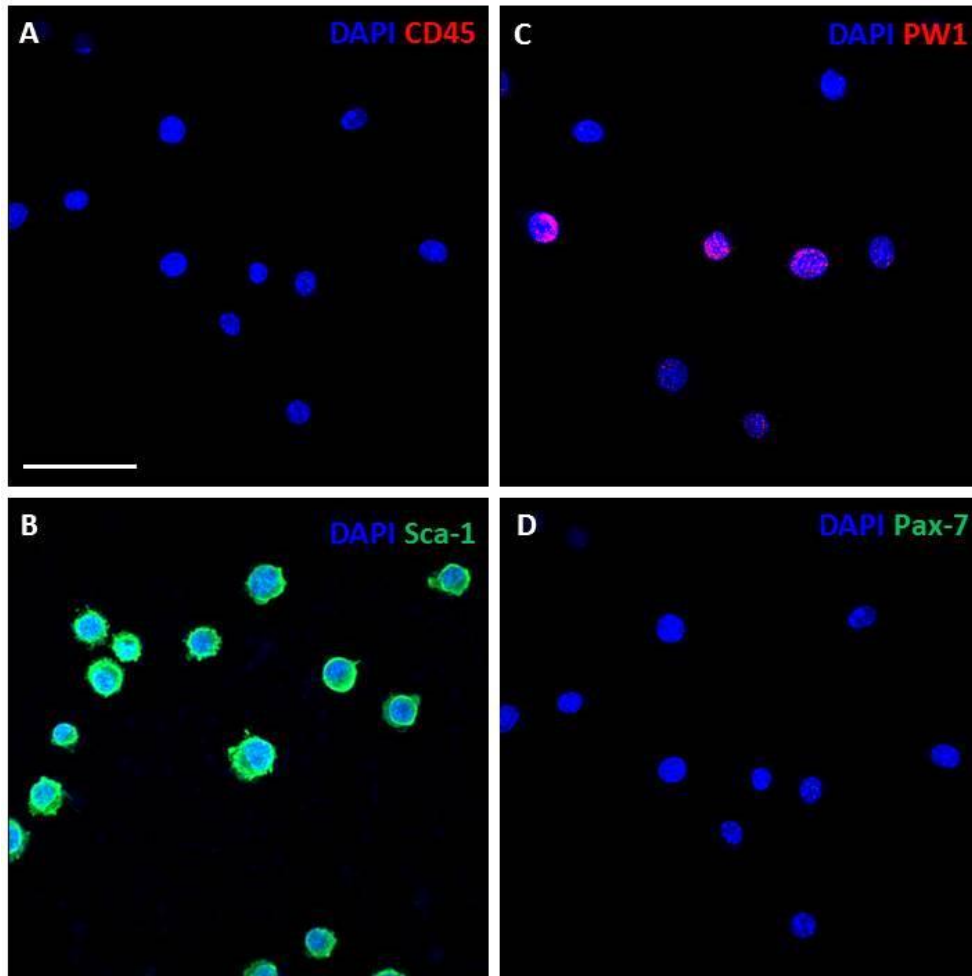
Figure 4.4   Confirmation of PIC isolation by ICC. Protein expression of

CD45$^-$/Sca-1$^+$ cells by ICC at P3: showing negativity for CD45 (red) (A),

positivity for Sca-1 (green) (B) and PW1 (red) (C), and negativity for Pax-7

(green) (D). Nuclei visualised with DAPI (blue). Scale =50µm.
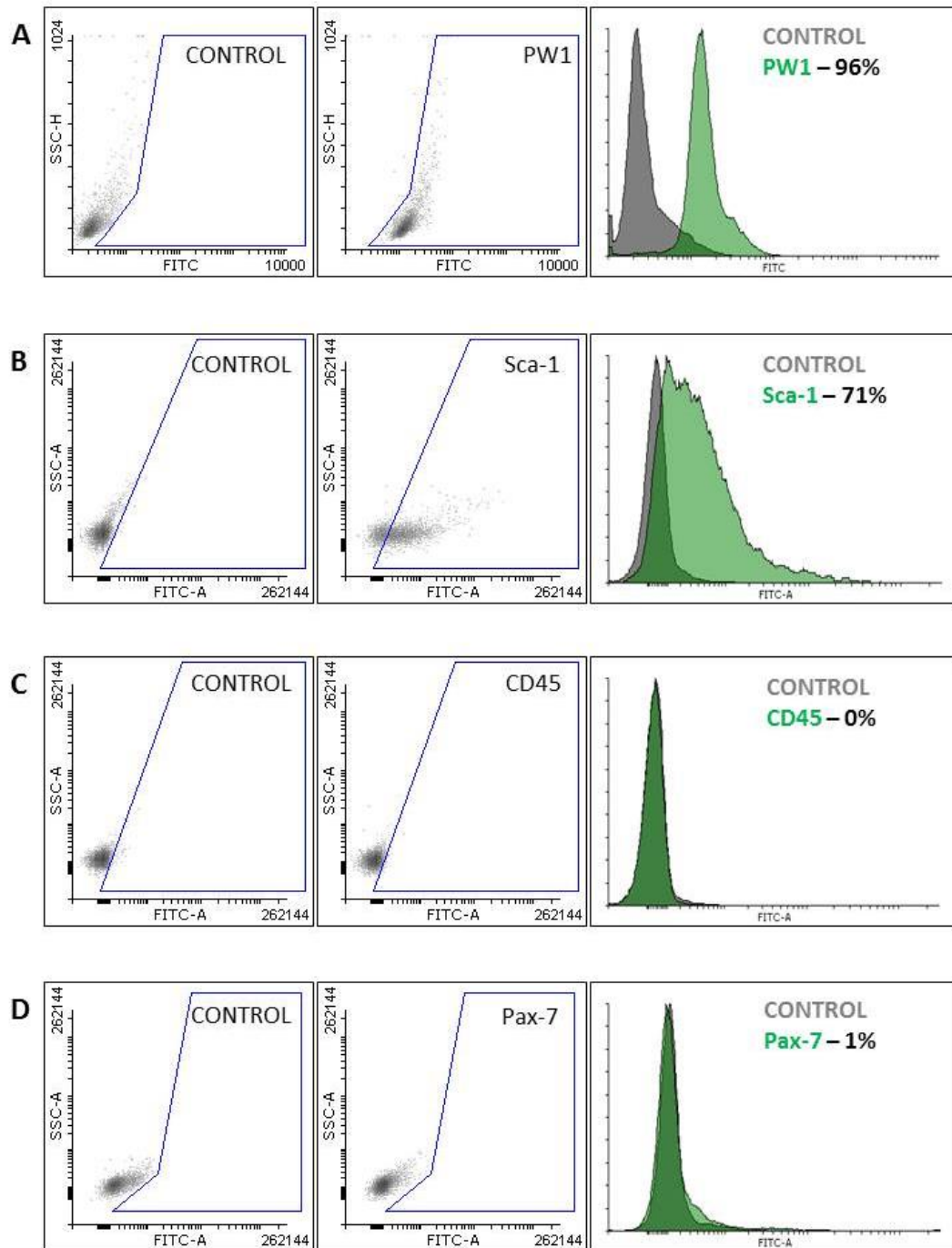
Figure 4.5 **Confirmation of PIC isolation by FC.** FC analysis of CD45⁻/Sca-1⁺ cells at P3: showing positivity for PW1 (A) and Sca-1 (B), and negativity for CD45 (C) and Pax-7 (D).
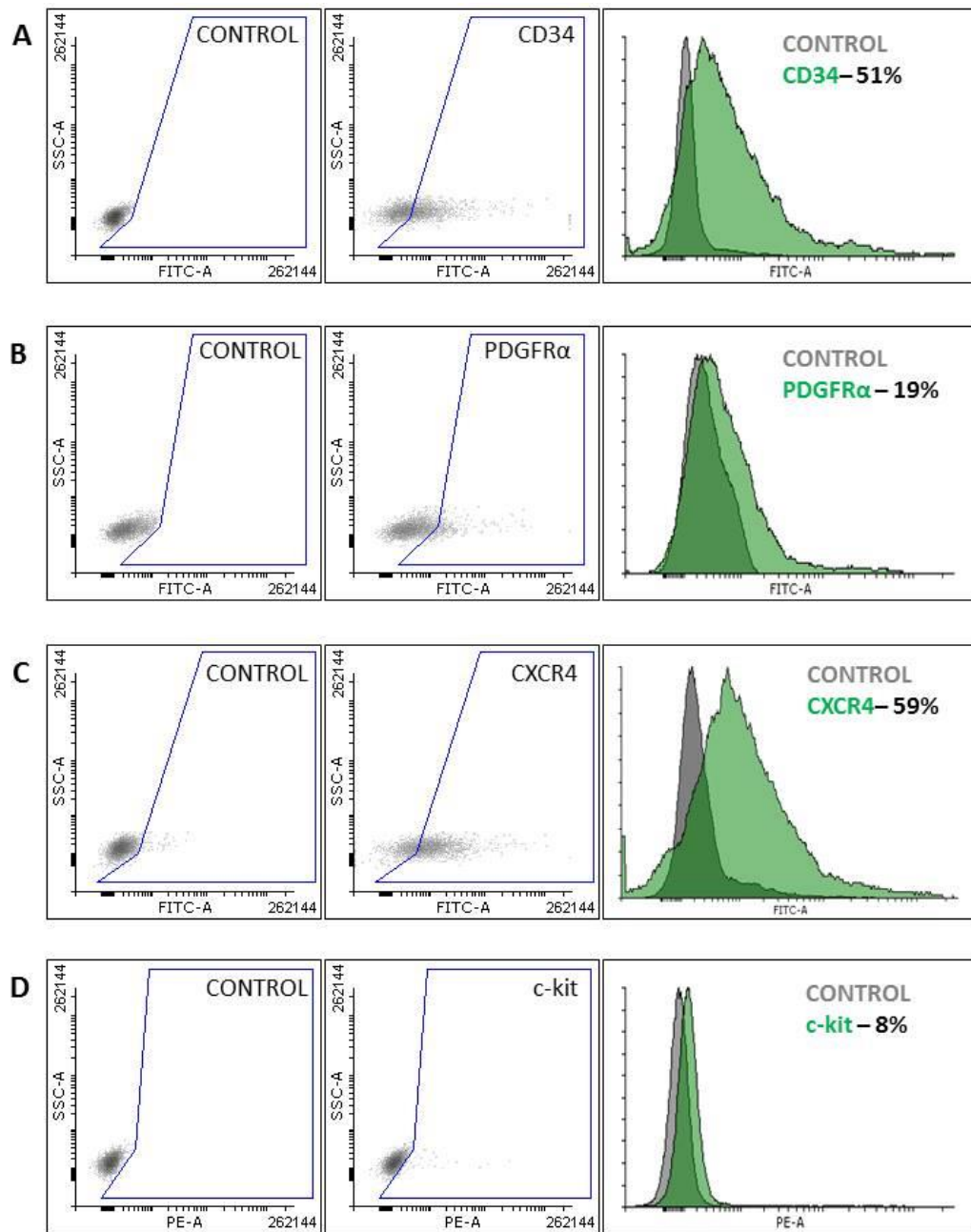
Figure 4.6 **Flow Cytometry analyses for known PIC markers.** FC analysis of PICs at P4 for surface marker expression CD34 (A), PDGFRα (B), CXCR4 (C) and c-kit (D).
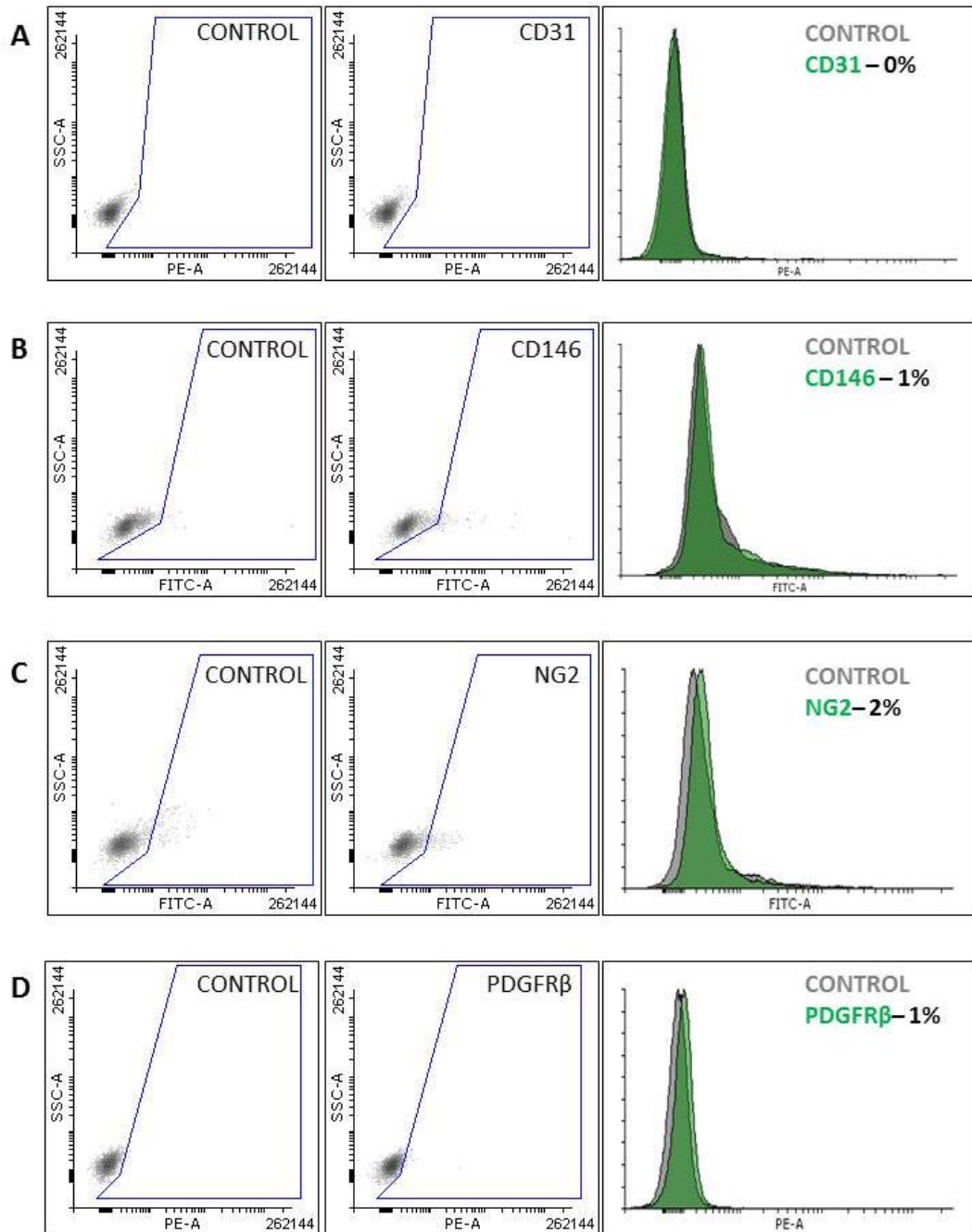
Figure 4.7. **Flow Cytometry analysis for non-PIC markers.** FC analysis of PICs at P4 for surface marker expression of CD31 (A), CD146 (B), NG2 (C) and PDGFRβ (D).

Next, PICs were assessed for markers of stemness and pluripotency (Sox2, Oct3/4 and Nanog), ICC revealed nuclear staining for all 3 of these markers in > 98% of cells at P3 (Figure 4.8).

In addition, gene transcription was assessed by qRT-PCR; PICs expressed transcripts for the PIC markers PW1, Sca-1 and CD34 whilst being negative for CD45 (Transcript copy number < 1). Furthermore, they expressed all three transcripts for Sox2 , Oct3/4 and Nanog. PW1 was the most highly expressed with a CT (19.9) similar to that of GAPDH (19.8) (see appendix for all CT values). Nanog displayed the highest transcript number out of the pluripotency genes being 12 times higher than Sox2 and 2 times higher than Oct3/4 (Figure 4.9).

The levels of transcripts was compared to that of mouse ESCs, which exhibited higher levels of the pluripotency markers, comparable levels of Sca-1 and a lesser amount of PW1 than seen in PICs (Figure 4.9).
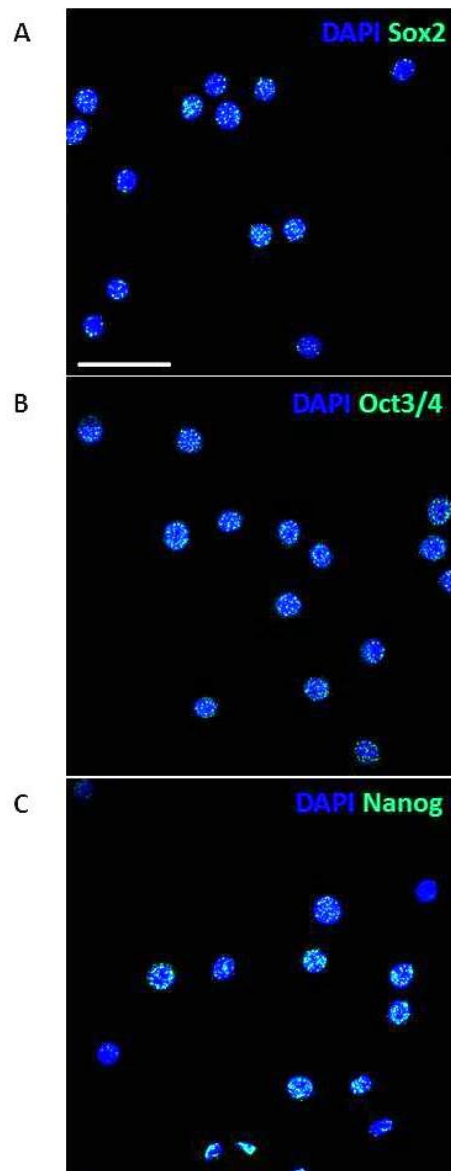
Figure 4.8   Pluripotency marker expression in PICs. Expression at P3 of

pluripotency markers Sox2 (A), Oct3/4 (B) and Nanog (C) as shown in green.

Nuclei are stained blue by DAPI. Scale =50µm.
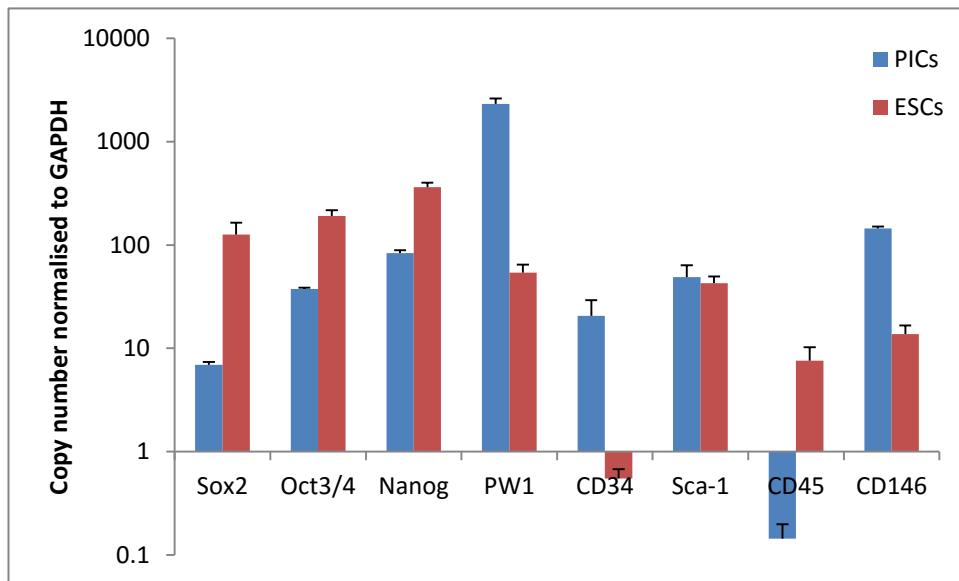
Figure 4.9   PIC transcript profile. Transcript analysis by qRT-PCR of PICs at P3 (blue) and mouse ESCs (red). Bars represent the transcript copy number normalised to GAPDH. Error bars represent the standard deviation of the mean, n=triplicate.

4.2.2 Single cell derived clonal cell lines from PICs

Clonogenicity assays were conducted at P5 to allow cells to recover from the isolation protocol, and also to activate their proliferation, as described by Smith et al. (2014) when isolating and cloning CSCs. Isolated PICs were deposited as a single cell/well by serial dilution into 96 well cloning plates (n=3). 34 ±11% of single cells (PICs) went on to form clonal populations of small rounded cells, which formed aggregates at high density (Figure 4.10). The 12 fastest growing and morphologically 'best' looking (comprised of small, rounded bright cells) cell lines were chosen for further propagation, these were labelled C1 – C12. Of the initial 12 clone lines selected, seven (C1, C2, C3, C4, C5, C9 and C12) continued to exhibit good morphology (Figure 4.11) and population growth over 3 passages, and were used for further analysis.
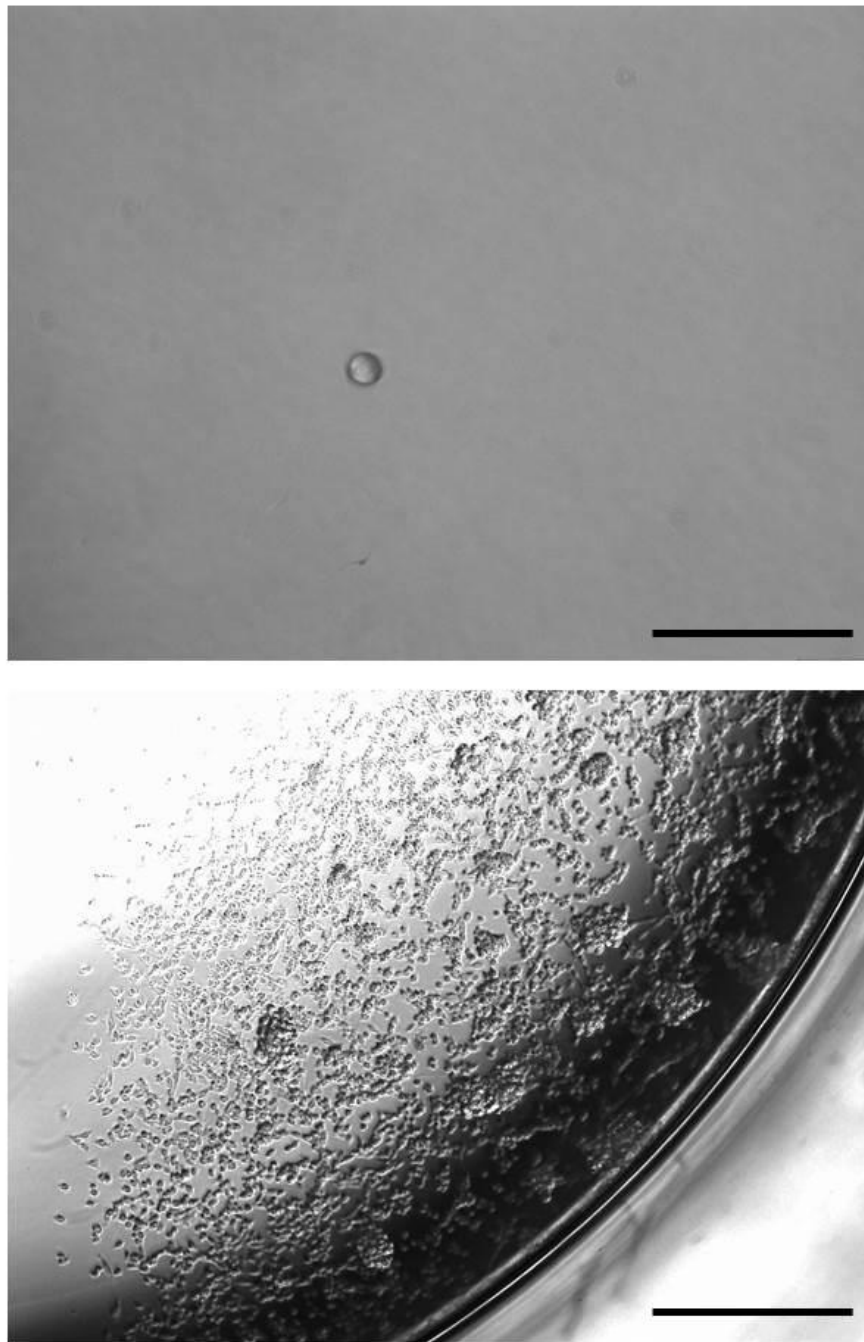
Figure 4.10   Single cell-derived PIC clones. Transmitted light microscope

observation of a single PIC (top, scale =100µm), and subsequent clonal

population after 12 days cultured in a 96 well plate (bottom, scale =500µm).
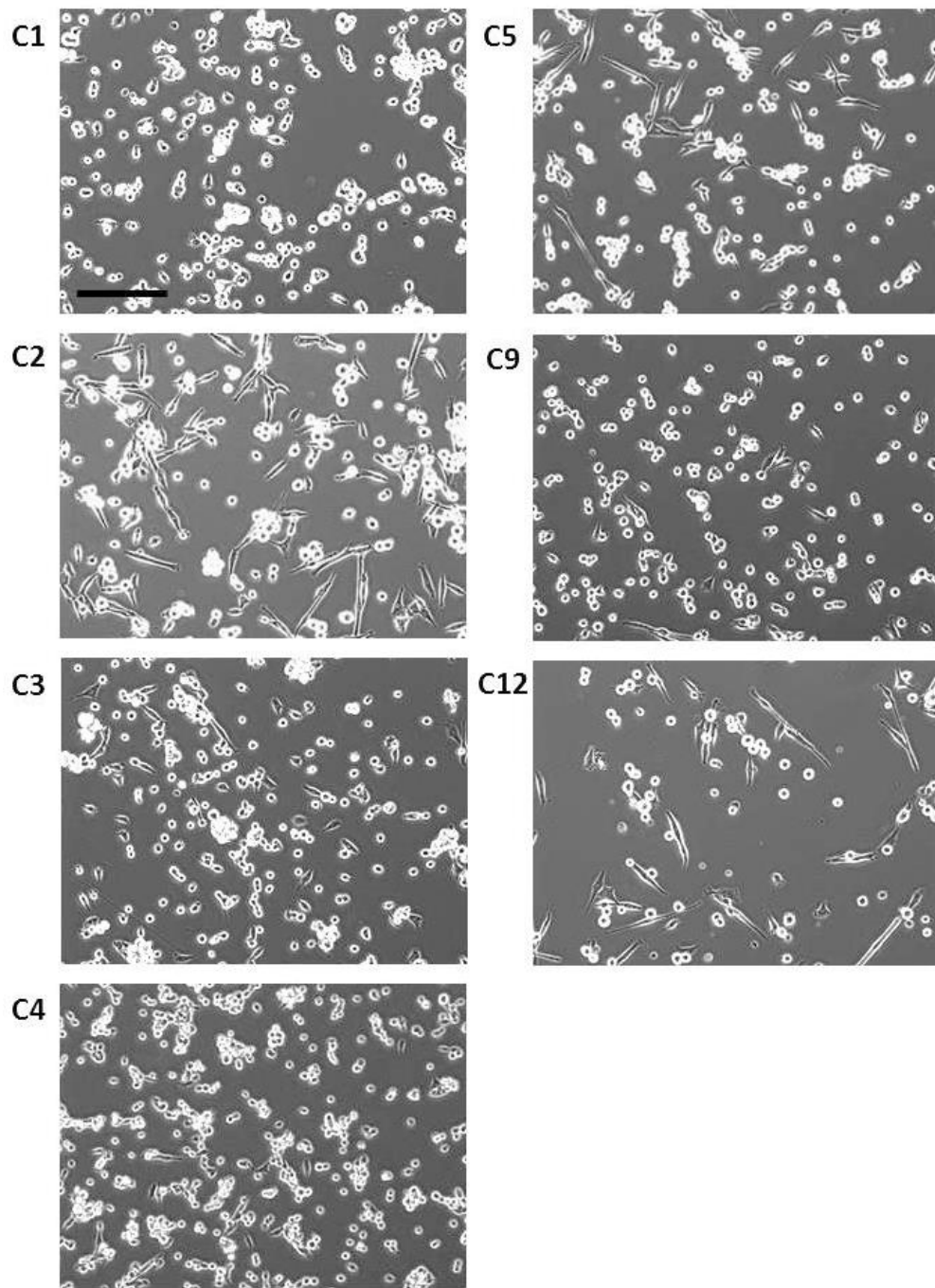
Figure 4.11   PIC Clone morphology. Transmitted light microscope

observation of clonal PIC populations (C1-C12). Scale =200µm.

The PW1 expression of each clonal line was evaluated at P2 post-cloning by ICC, with all 7 clonal cell lines being positive for PW1 (Figure 4.12). When quantified by flow cytometry all clones had >90% expression of PW1. C9 and C12 had the highest expression (99%) of PW1, whilst C1 and C3 had the lowest expression at 94% and 95% respectively (Figure 4.13).

Sca-1 was also expressed in all clonal lines (Figure 4.14) with the lowest being C3 (65%) and the highest C12 (97%).

Transcript profiles of the 7 clonal PIC cell lines was assessed by qRT-PCR and compared to un-cloned 'bulk' cultured PICs. Levels of PIC specific transcripts (PW1, Sca-1 and CD34) remained high in all clones (Figure 4.15) with the exception of C1 which had a marked decrease in Sca-1 and CD34. Although bulk cultured PICs had a higher copy number PW1, Sca-1 and CD34 than any of the clonal cell lines, Clone 9 had the highest expression for both PW1 and Sca-1 with values closest to that of bulk PICs.

Transcript levels of pluripotency genes (Sox, Oct3/4 and Nanog) appeared lower in all clonal cell lines than in bulk PICs (statistical analysis not performed as results are a triplicate of n=1 for all groups). Levels of Nanog and Oct3/4 were largely comparable between all clonal PICs, however Sox2 detection was negligible in all lines except C9 (Figure 4.16).

Therefore, C9 was selected for further investigation due its comparable transcriptome profile to that of bulk PICs; moreover, it displayed high expression of Sca-1 and the highest expression of Nanog, Oct/3/4, Sox2 and PW1, than all other clones.
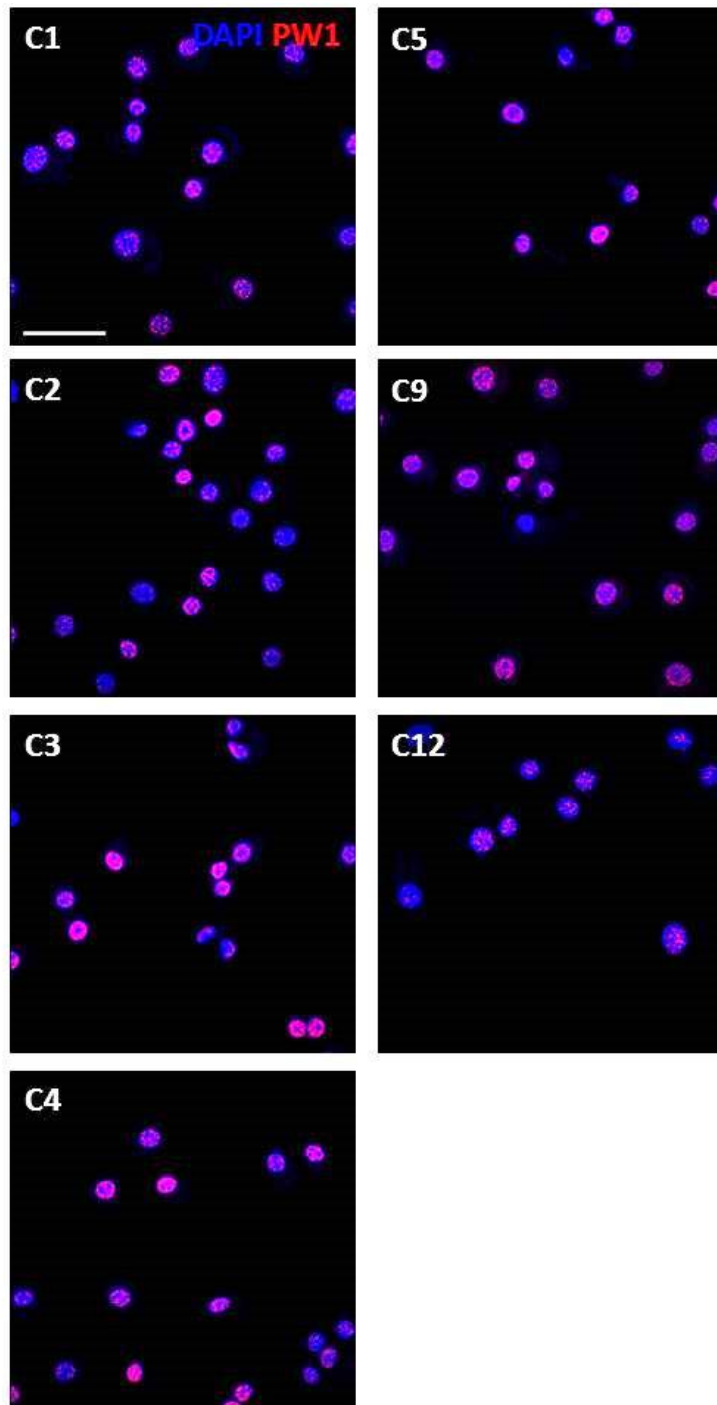
Figure 4.12   PW1 expression in clones by ICC. Expression of PW1 (red) by immunocytochemistry in clonal PIC populations, Nuclei visualised with DAPI (blue). Scale=50μm.
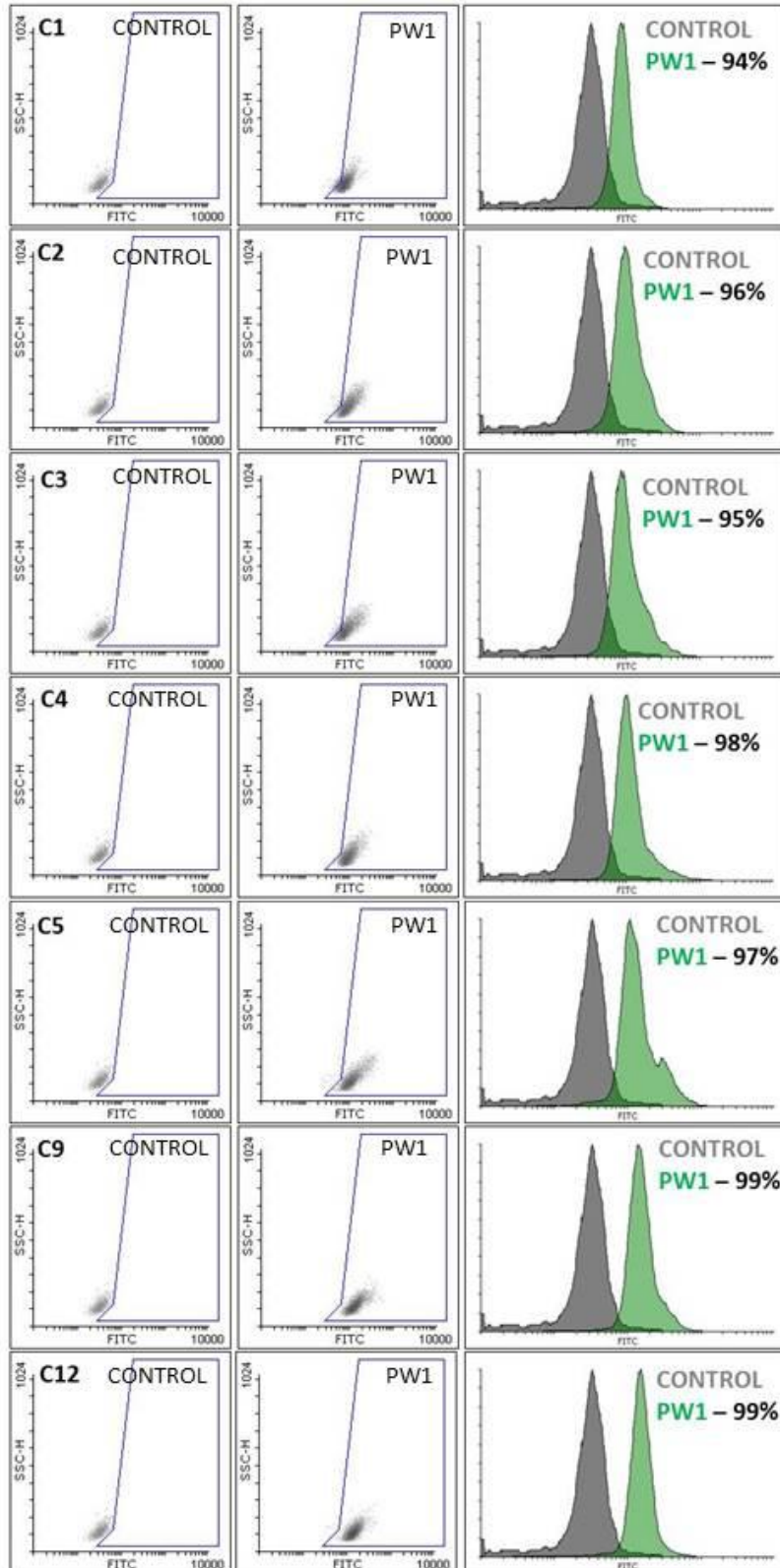
Figure 4.13   PW1 expression in PIC clones by FC. PW1 expression in clonal
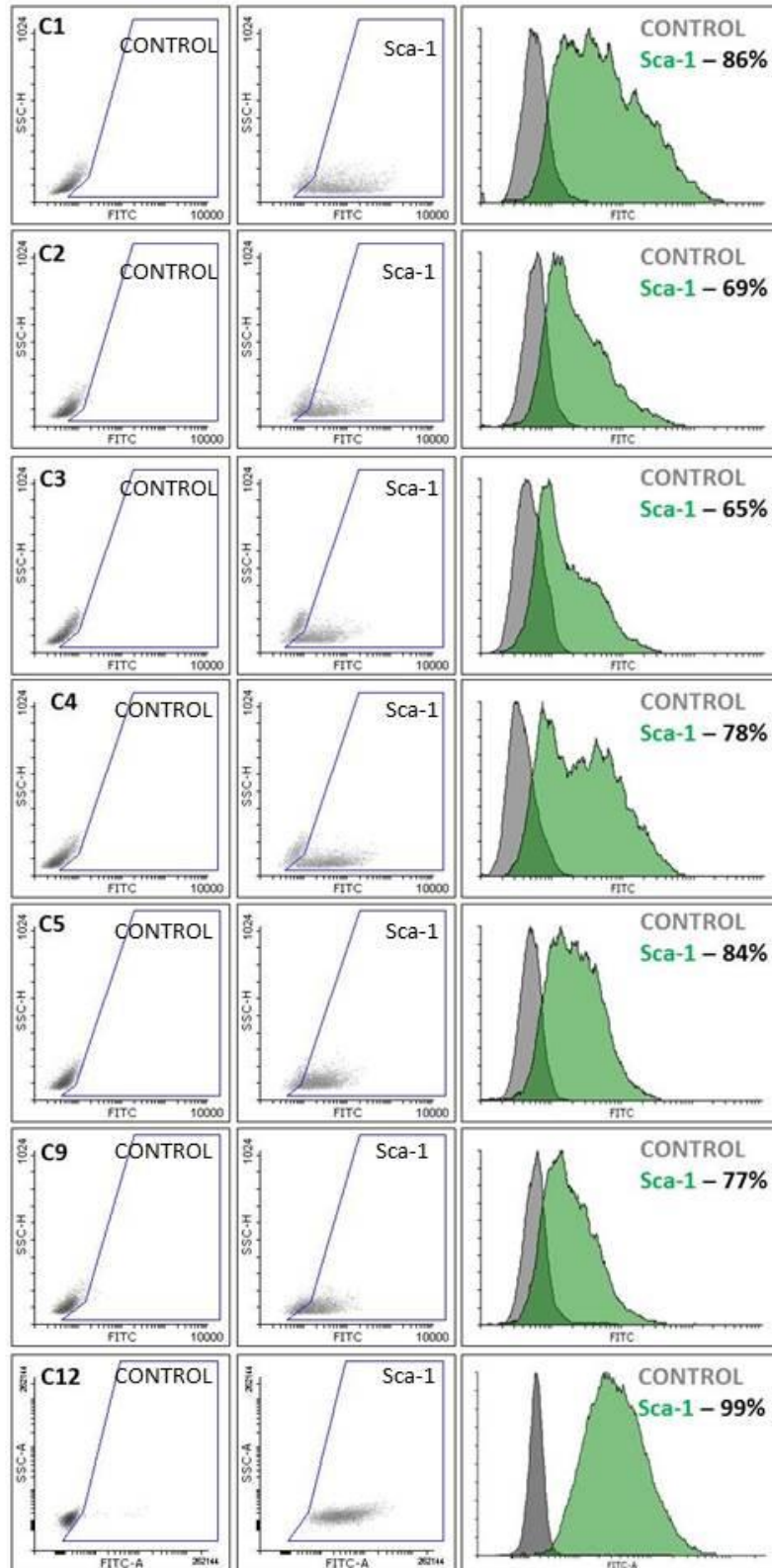
PIC populations.

Figure 4.14   Sca-1 expression in PIC clones by FC. Sca-1 expression in clonal

PIC populations.
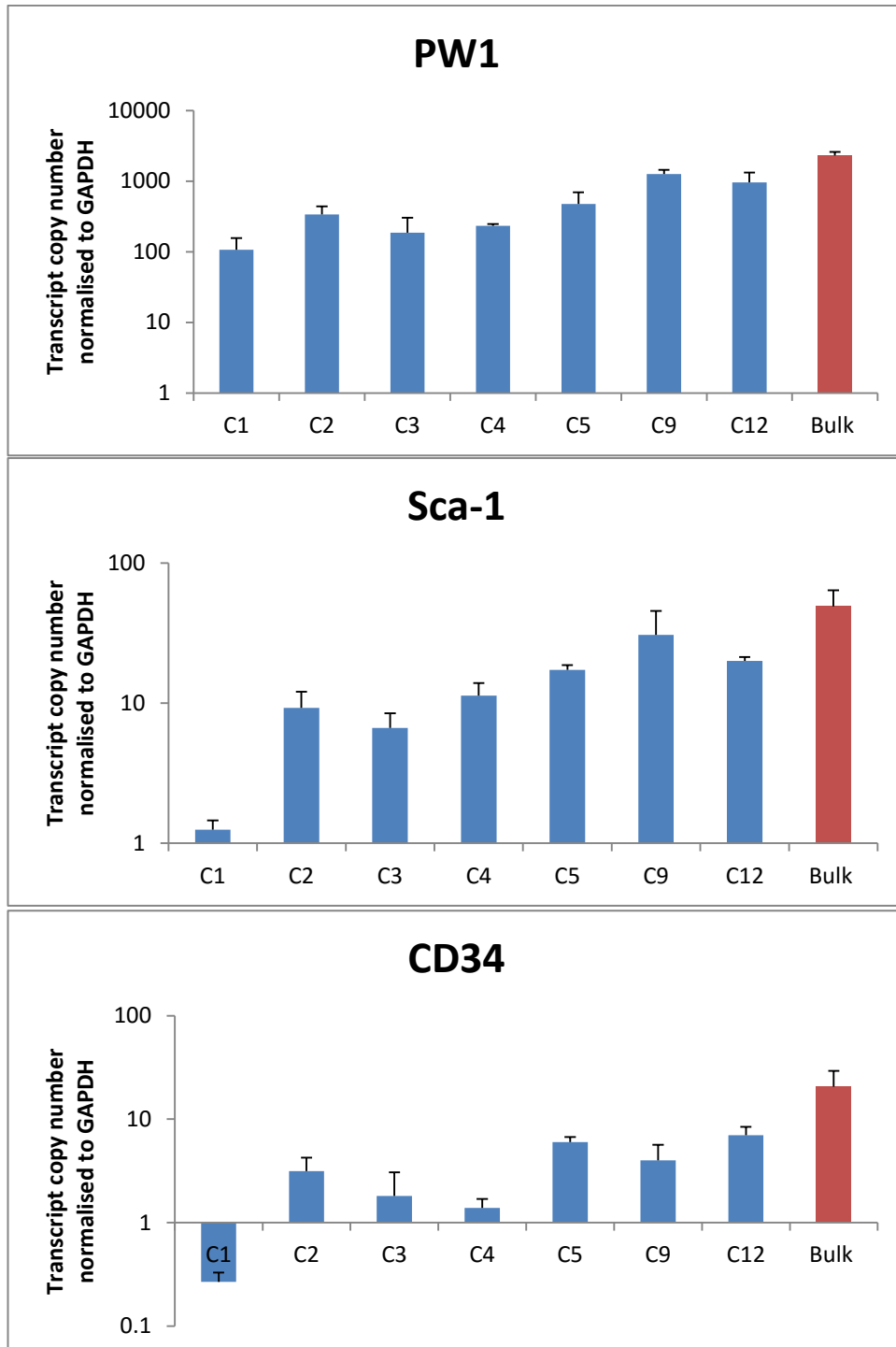
Figure 4.15 **Transcription of PIC markers in clonal vs bulk PICs.** Transcript analysis by qRT-PCR of PW1. Sca-1 and CD34 in clonal PICs, compared to bulk PICs. Bars represent the transcript copy number normalised to GAPDH. Error bars represent the standard deviation of the mean, n=triplicate.
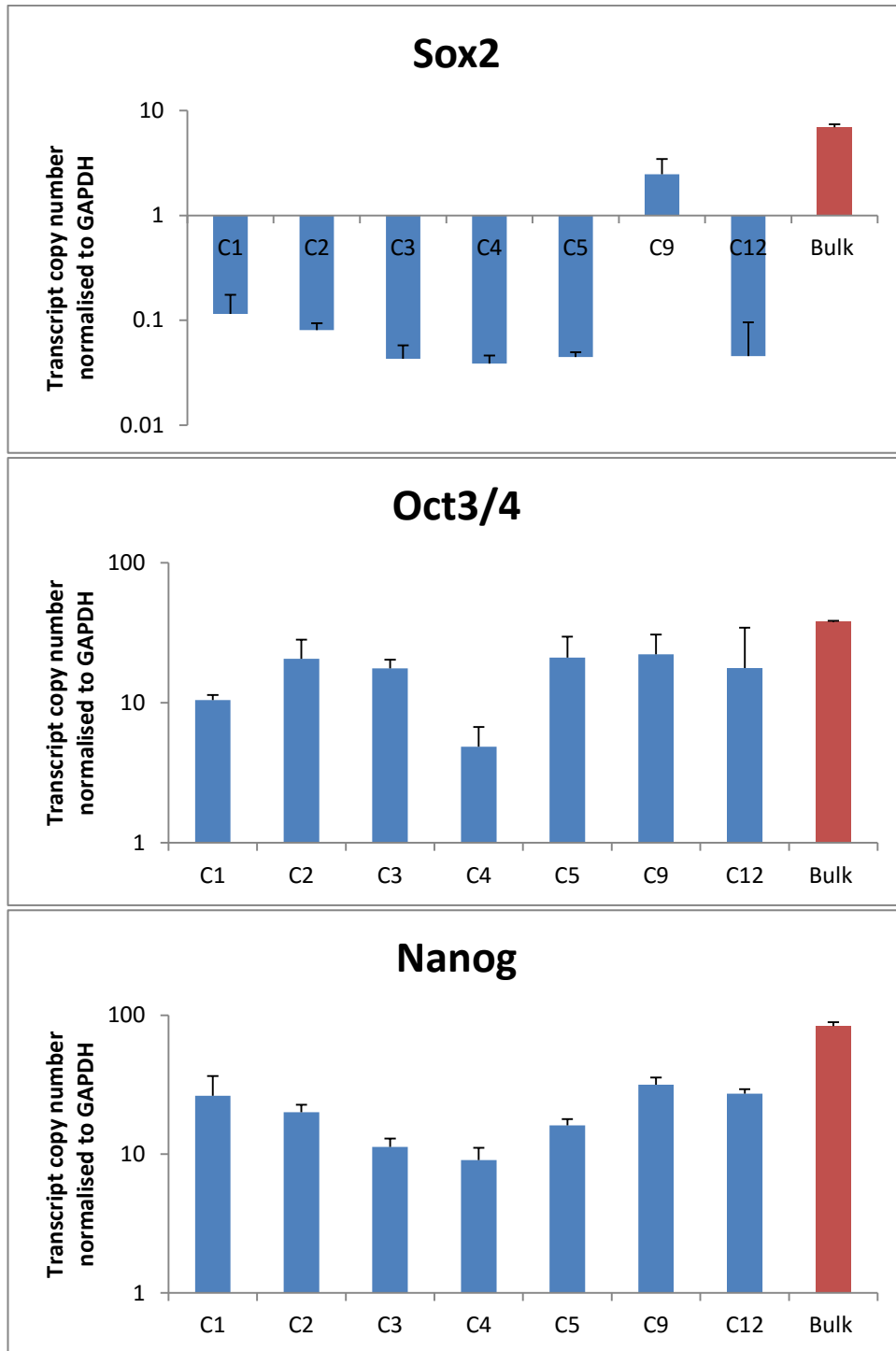
Figure 4.16   Transcription of pluripotency genes in clonal vs bulk PICs.

Transcript analysis by qRT-PCR of Sox2, Oct3/4 and Nanog in clonal PICs compared to bulk PICs. Bars represent the transcript copy number normalised to GAPDH. Error bars represent the standard deviation of the mean, n=triplicate.

4.2.3 Maintaining a clonal cell line.

The morphology of C9 PICs remained consistently small, round and bright (Figure 4.17) with a stable doubling time of 16±3 hours over 20 passages (Figure 4.18). C9 PICs were passaged every 48 hours which equated to ~64 population doublings over 20 passages. C9 PICs were able to produce single-cell derived sub-clones with an efficiency of 91±2%, assessed at every 5th passage (Figure 4.19). Furthermore, they maintained a stable expression of Sca-1 (Figure 4.20) and PW1 (Figure 4.21) by FC analysis at P2, P10 and P20.
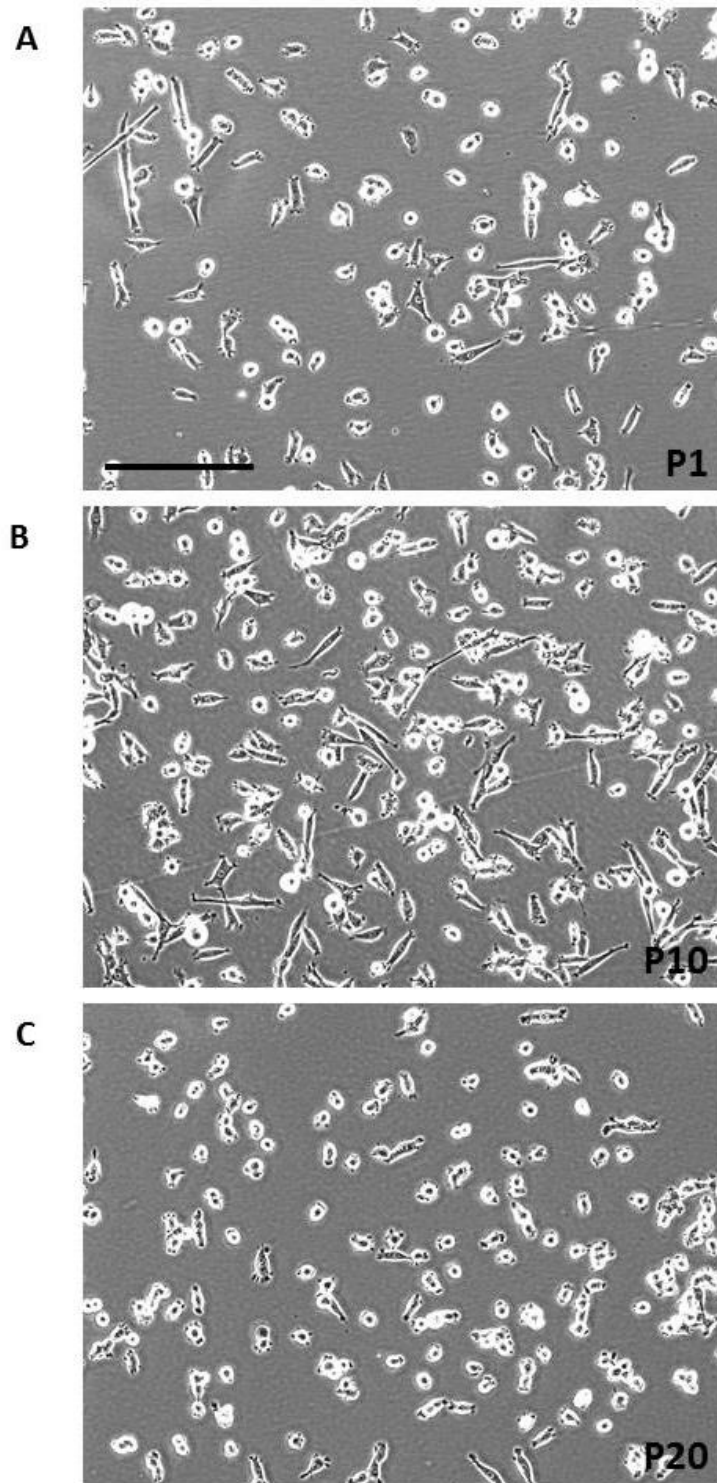
Figure 4.17   C9 morphology over time in culture. Transmitted light

microscope observation of C9 PICs at P1 (**A**), P10 (**B**) and P20 (**C**). Scale

=200µm.
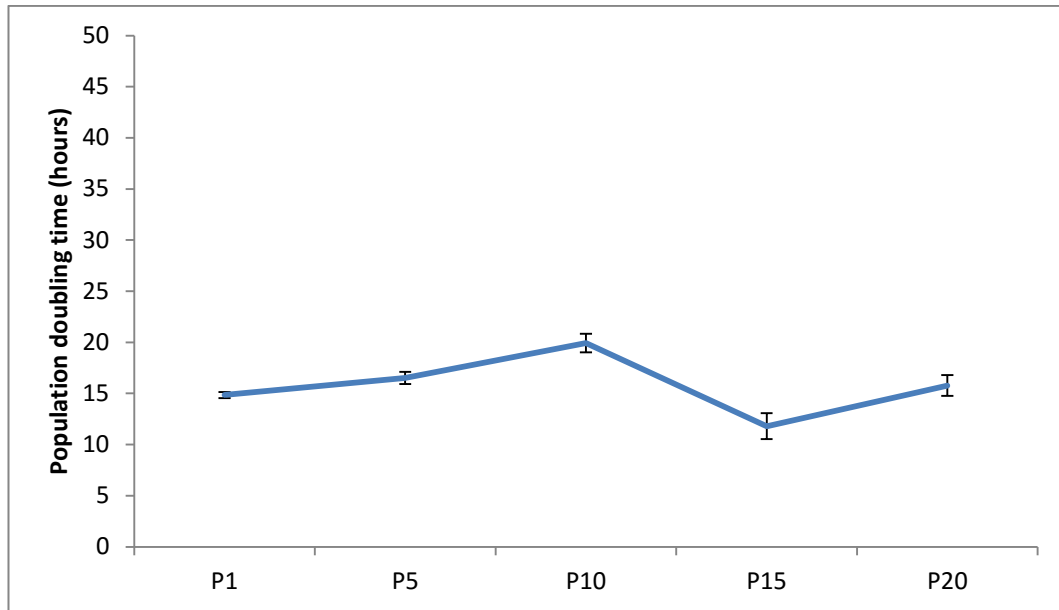
Figure 4.18   C9 Population doubling time. Doubling time of C9 PICs between

P1 and P20. Data is mean ±SD, n=3.
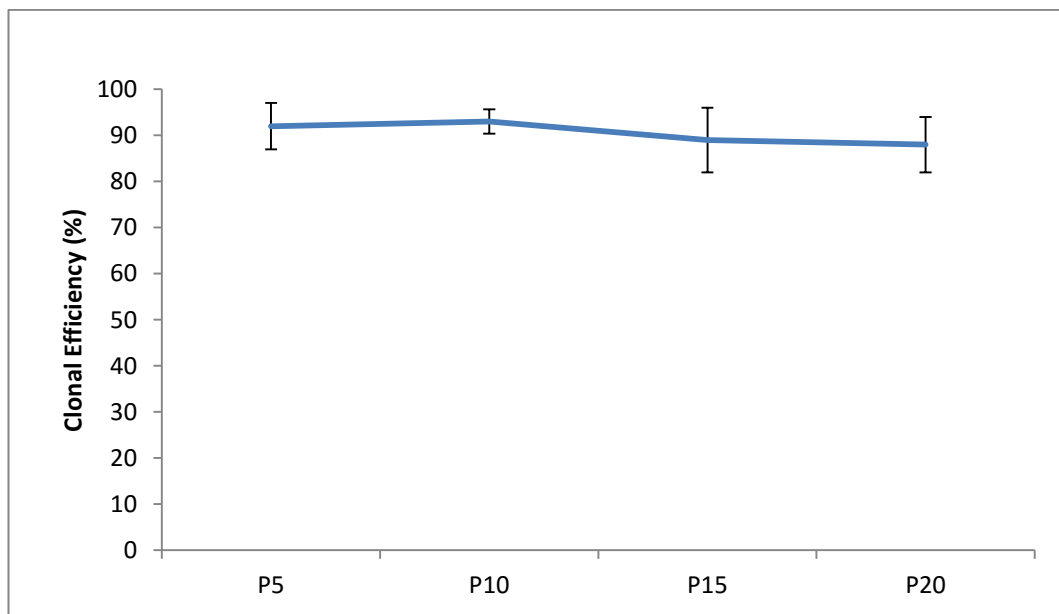
Figure 4.19   C9 Clonogenicity. Clonogenicity of C9 PICs at 5 passage

intervals between P5 and P20. Data is mean ±SD, n=3.
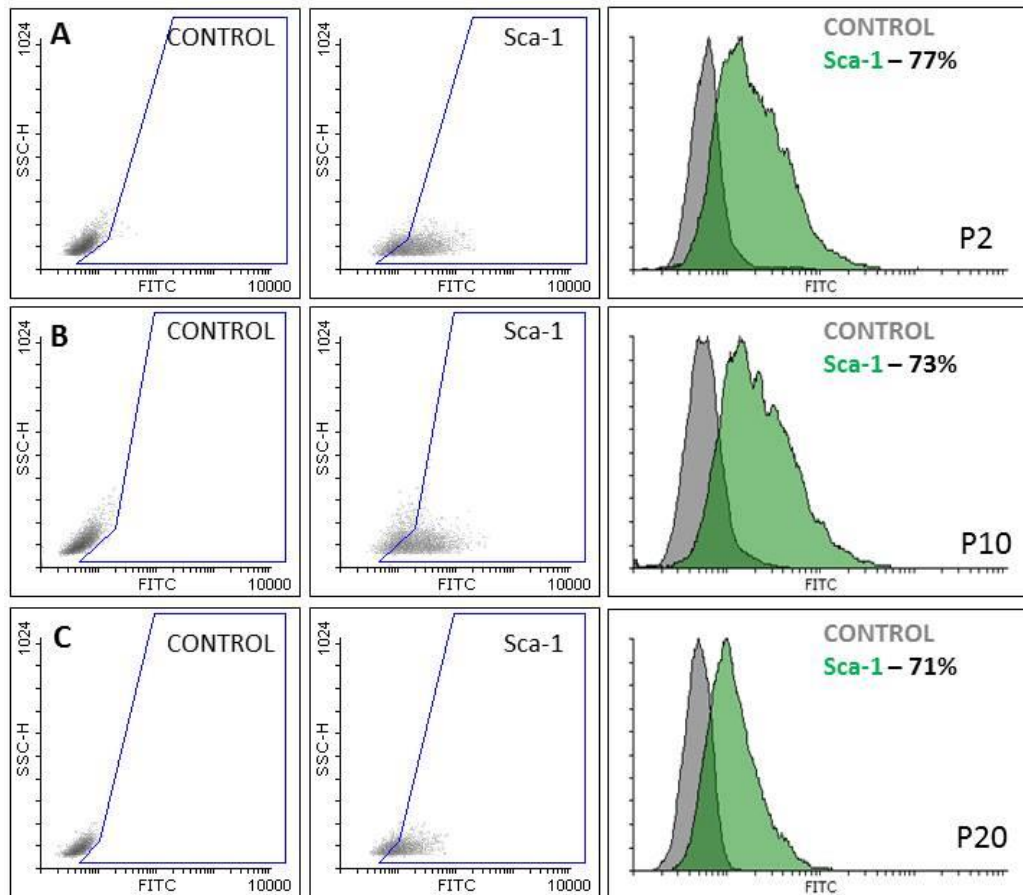
Figure 4.20   Sca-1 expression of C9 over time in culture. FC analysis

showing expression of Sca-1 in C9 PICs at P2 (A), P10 (B) and P20 (C).
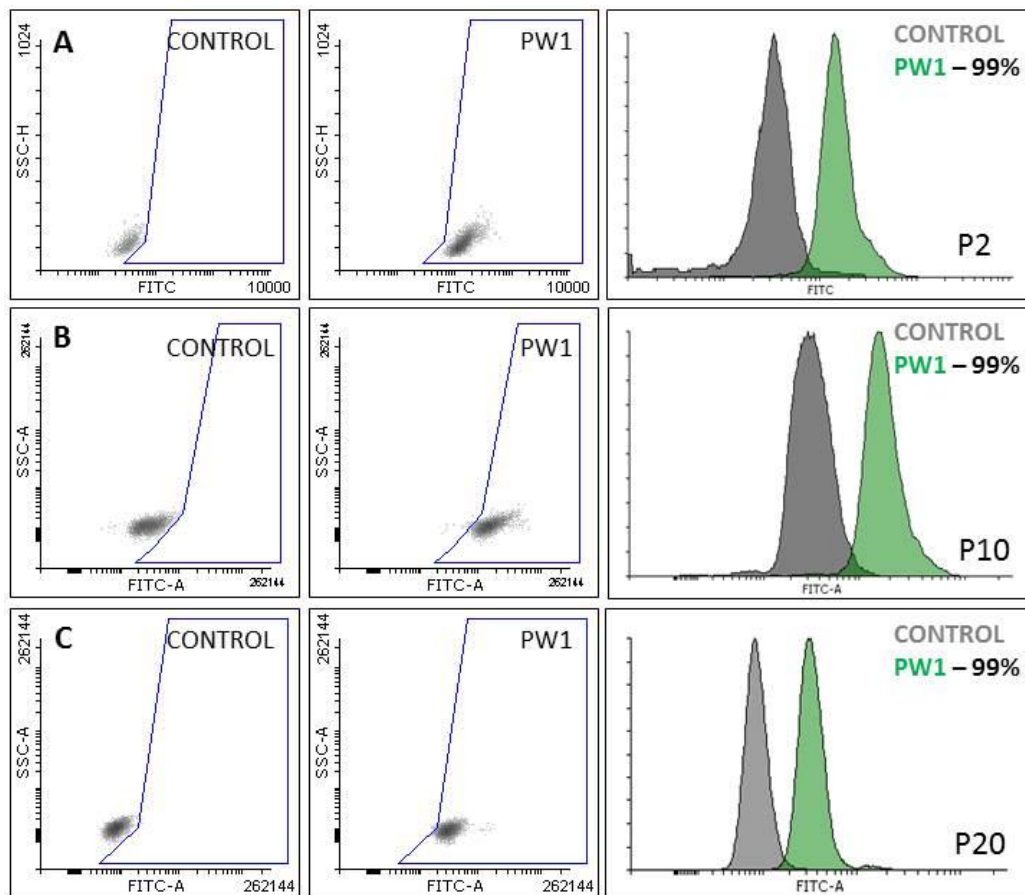
Figure 4.21   PW1 expression of C9 over time in culture. FC analysis showing

expression of PW1 in C9 PICs at P2 (**A**), P10 (**B**) and P20 (**C**).

To further show the stability of C9 PICs in culture, FACs analysis for surface markers previously screened for in bulk PICs was conducted at P2 and P20. When compared to bulk PICs; CD34 and CXCR4 expression had increased by ~6% and ~20% respectively, whilst C9 PICs no longer expressed PDGFRα. There were no notable changes of more than 5% between, P2 and P20 for PIC markers CD34 (Figure 4.22), PDGFRα (Figure 4.23), CXCR4 (Figure 4.24) and c-kit (Figure 4.25). Furthermore C9 PICs remained negative for CD31 (Figure 4.26), CD146 (Figure 4.27), PDGFRβ (Figure 4.28) and NG2 (Figure 4.29).
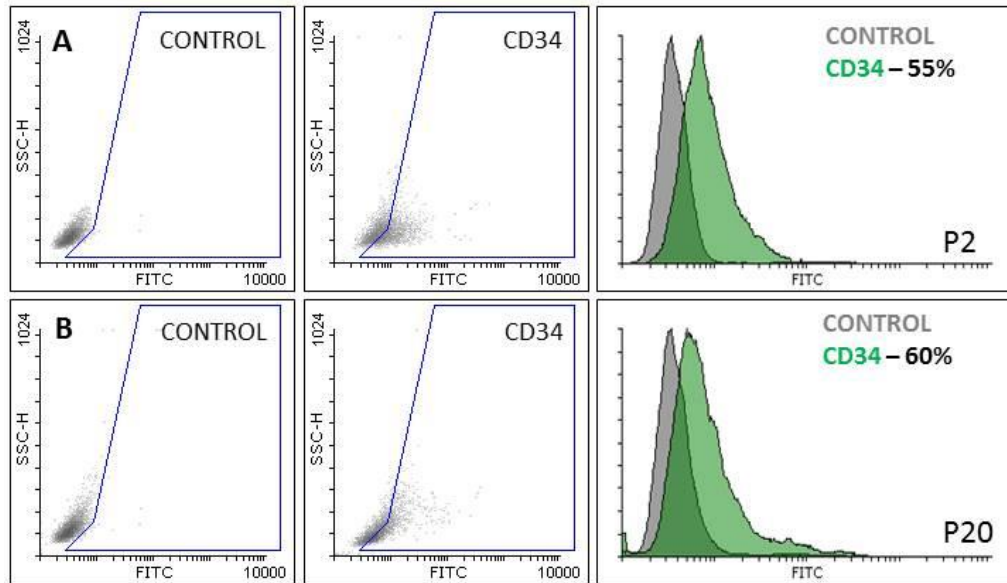
Figure 4.22   CD34 expression over time in culture. Expression of CD34 in C9 PICs by FC at P2 (**A**) and P20 (**B**).
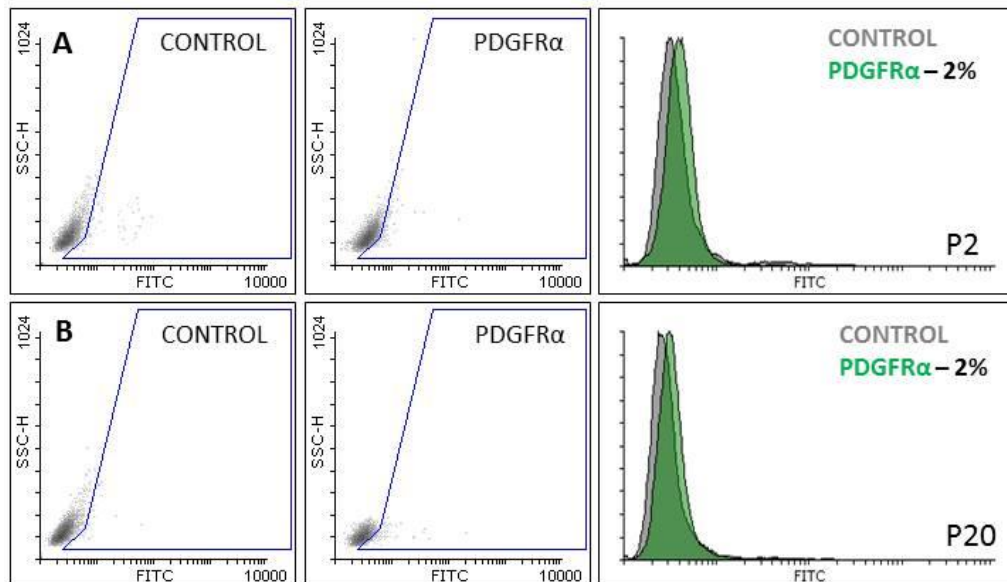
Figure 4.23   PDGFRα expression over time in culture. Expression of PDGFRα in C9 PICs by FC at P2 (**A**) and P20 (**B**).
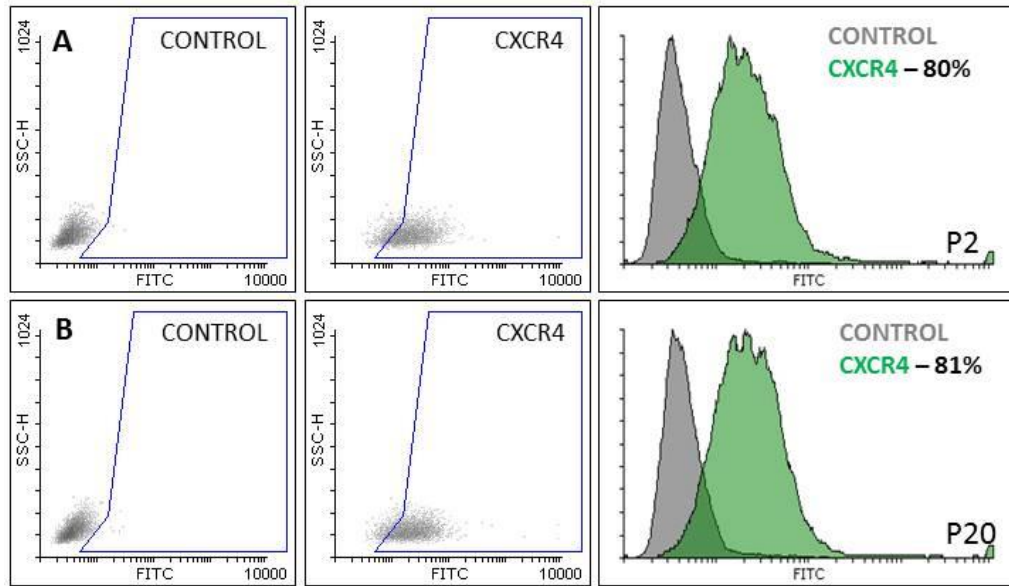
Figure 4.24   CXCR4 expression over time in culture. Expression of CXCR4 in C9 PICs by FC at P2 (**A**) and P20 (**B**).
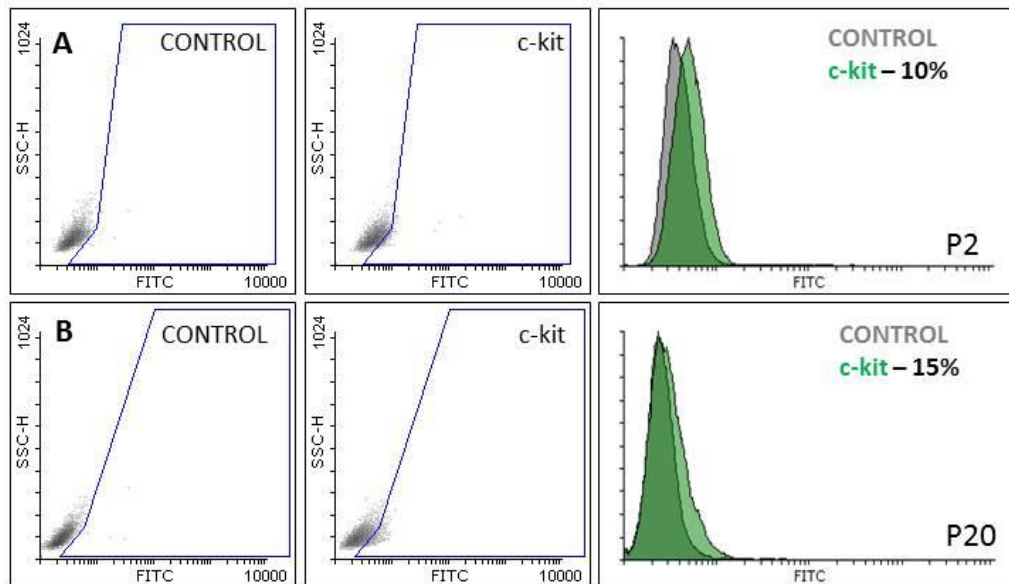
Figure 4.25   c-kit expression over time in culture. Expression of c-kit in C9 PICs by FC at P2 (**A**) and P20 (**B**).
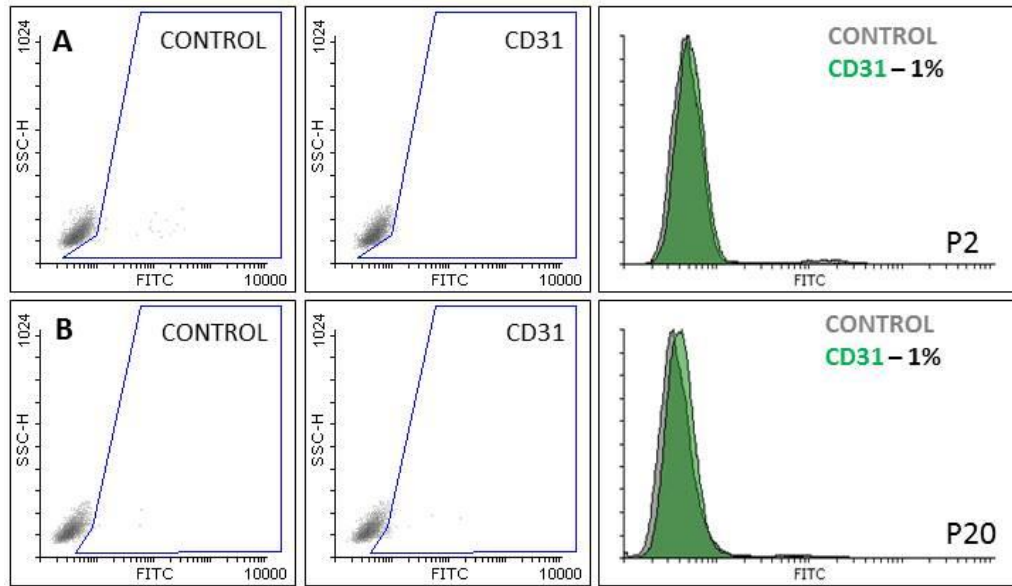
Figure 4.26 **CD31 expression over time in culture.** Expression of CD31 in C9 PICs by FC at P2 (**A**) and P20 (**B**).
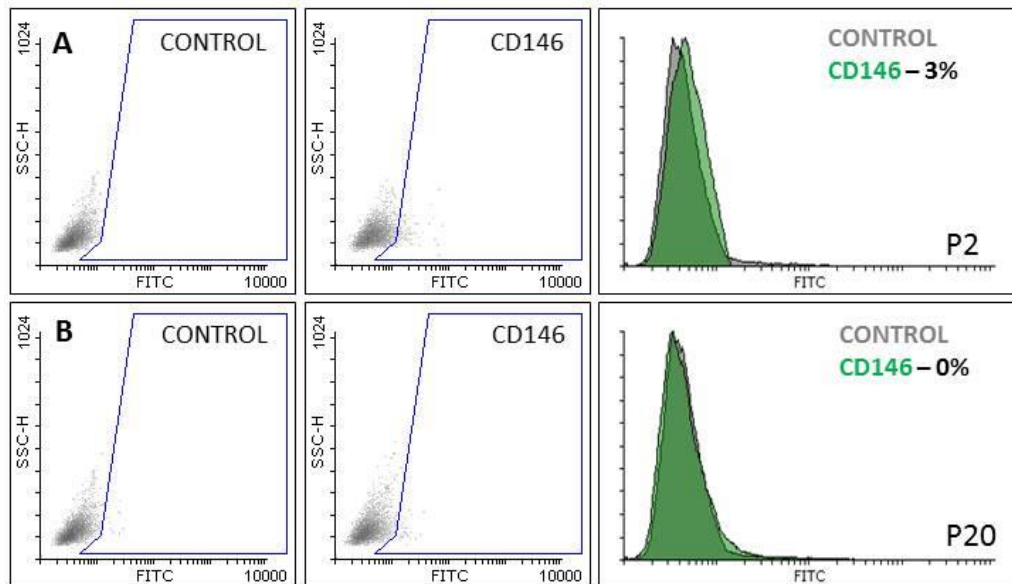
Figure 4.27 **CD146 expression over time in culture.** Expression of CD146 in C9 PICs at P2 (**A**) and P20 (**B**).

114
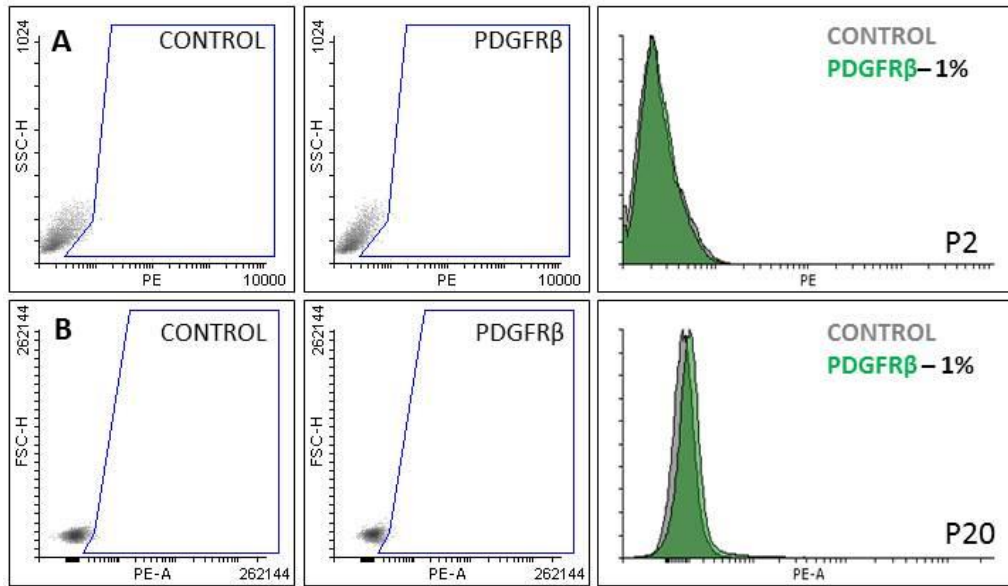
Figure 4.28   PDGFRβ expression over time in culture. Expression of

PDGFRβ in C9 PICs by FC at P2 (**A**) and P20 (**B**).
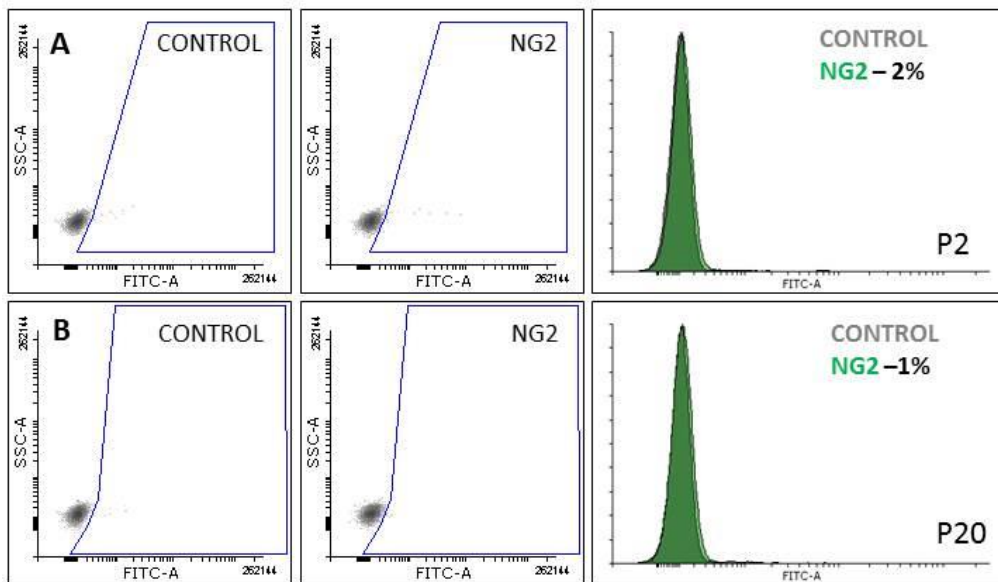
Figure 4.29   NG2 expression over time in culture. Expression of NG2 in C9

PICs by FC at P2 (**A**) and P20 (**B**).

The stability of the transcriptome profile of C9 PICs was assessed by qRT-PCR at P1, P10 and P20. PW1, Sca-1, CD34, Oct3/4 and Nanog were all expressed throughout the 20 passages, with slight fluctuations in transcript levels at each passage. Sox2 however had dropped below a copy of number of 1 by P10 indicating the transcript was no longer present (Figure 4.30).
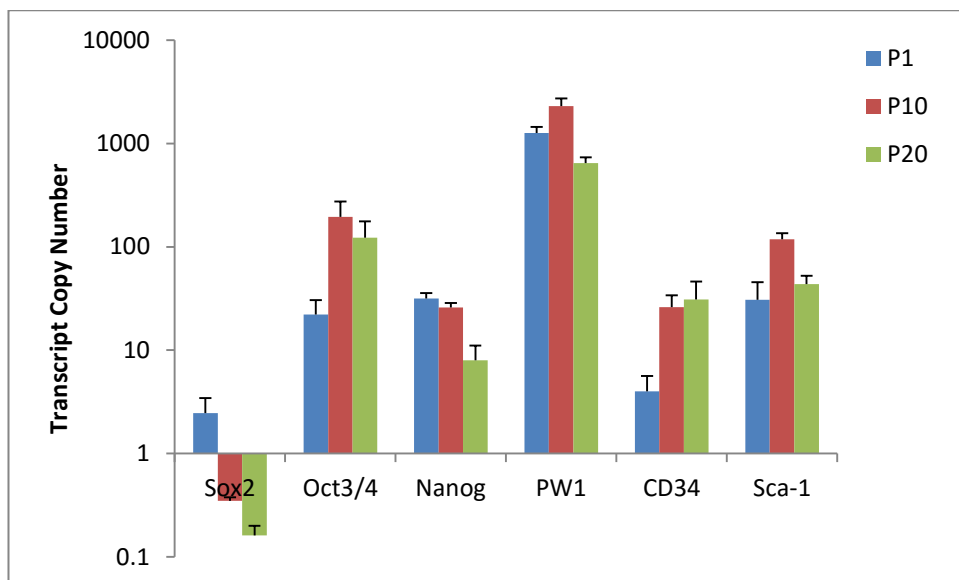
Figure 4.30   C9 Transcription profile over time in culture. Transcriptome analysis by qRT-PCR of C9 PICs at P1, P10 and P20. Bars represent the transcript copy number normalised to GAPDH. Error bars represent the standard deviation of the mean, n=triplicate.

Sub clones of C9 PICs generated at P10 (C9A, C9B, C9C) were found to have a similar morphology to that of C9 PICs from which they originated (Figure 4.31), and were propagated for further investigation.

Sub-clones had a Sca-1 expression of 95±1% by FC at P2 (Figure 4.32) and a PW1 expression of 99±0% (Figure 4.33). There was no change in Sca-1 (Figure 4.34) or PW1 (Figure 4.35) between bulk, clonal and sub-clonal PICs.

The transcriptome profile of C9A, C9B and C9C was analysed by qRT-PCR at P2 post cloning: CD34, and PW1 expression was similar in C9 and sub-clones whilst, supporting the FC data, Sca-1 was increased in sub-clones over the original C9 population. The pluripotency genes Sox2 and Oct3/4 were not detectable in sub-clones and levels of Nanog were greatly reduced (Figure 4.36).
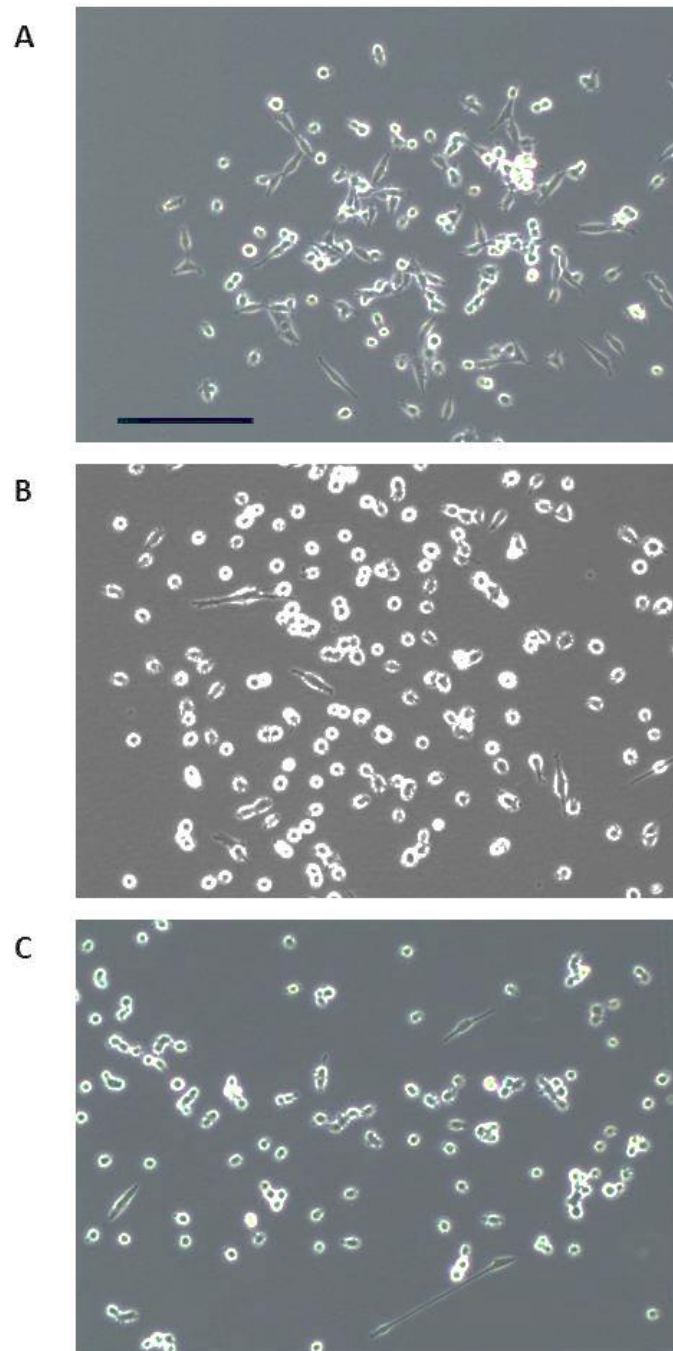
Figure 4.31   C9 Sub-clone Morphology. Morphology of sub-clones at P1,

generated from C9 at P10: C9A (**A**), C9B (**B**), and C9C (**C**). Scale = 200um.
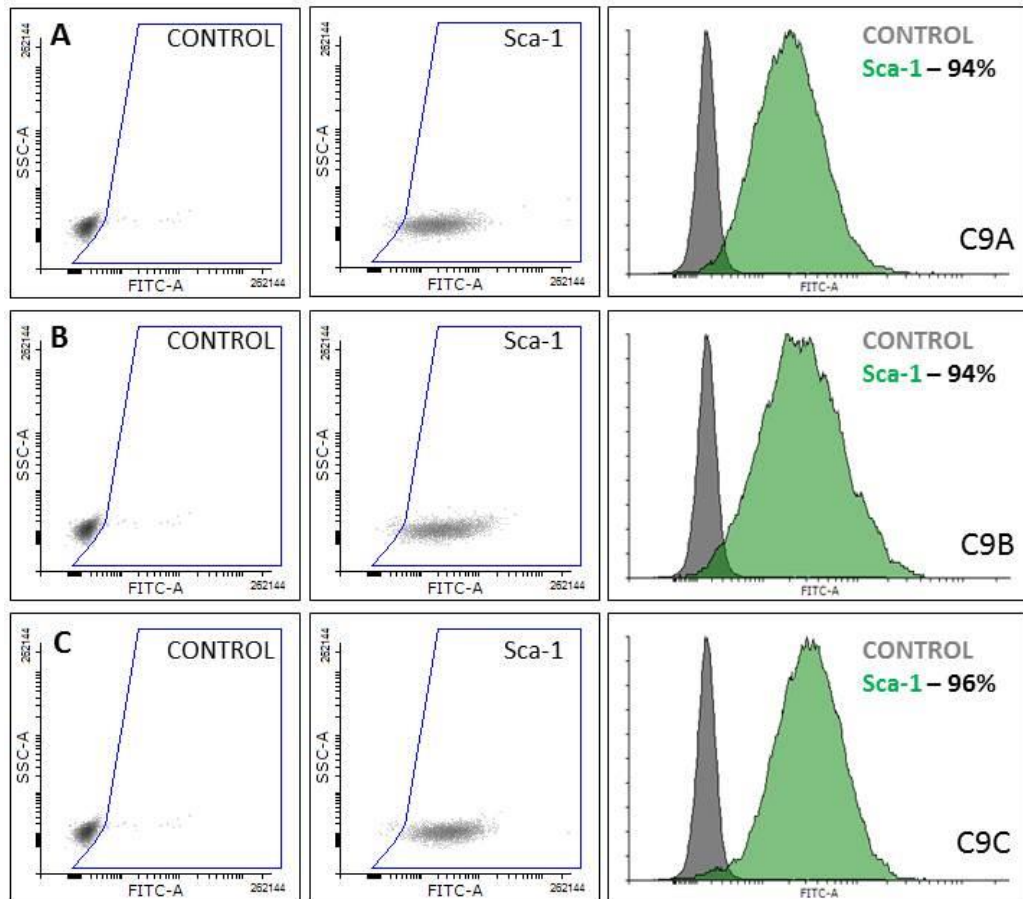
Figure 4.32 Sca-1 expression in C9 sub-clones. Expression of Sca-1 by FC at

P2 of C9A (**A**), C9B (**B**), and C9C (**C**).
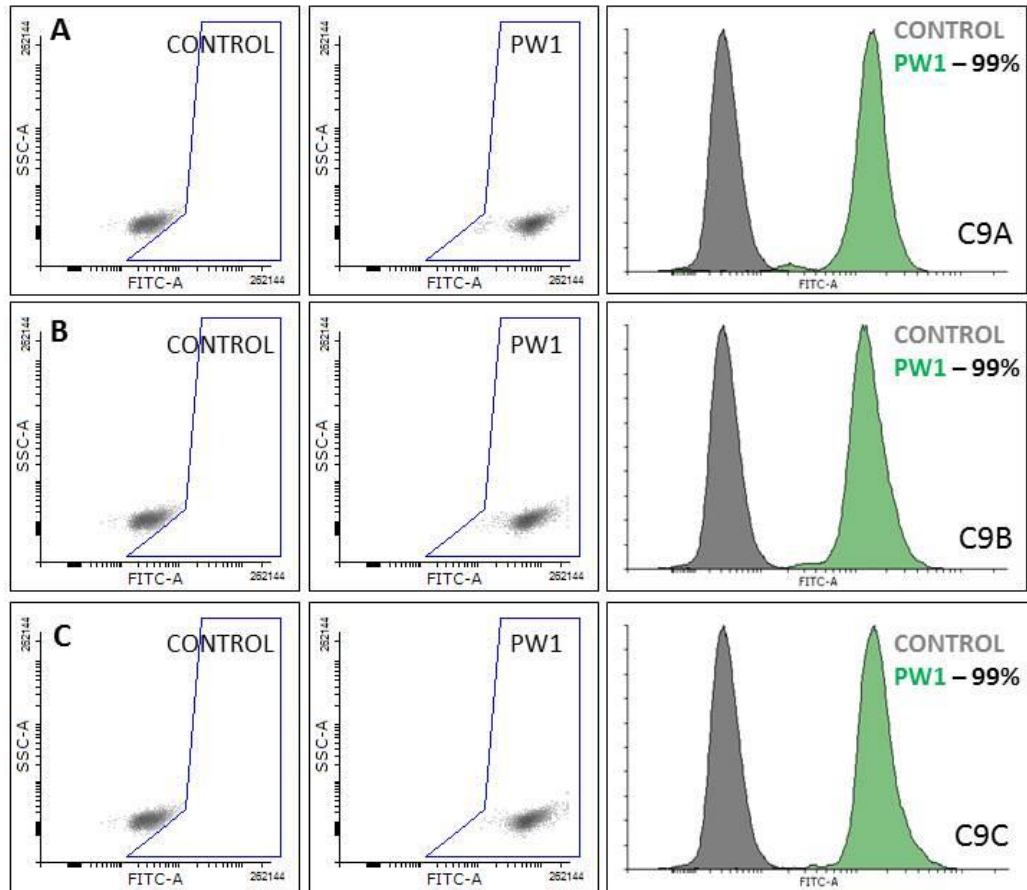
Figure 4.33   PW1 expression in C9 sub-clones. Expression of PW1 by FC at

P2 of C9A (**A**), C9B (**B**), and C9C (**C**).
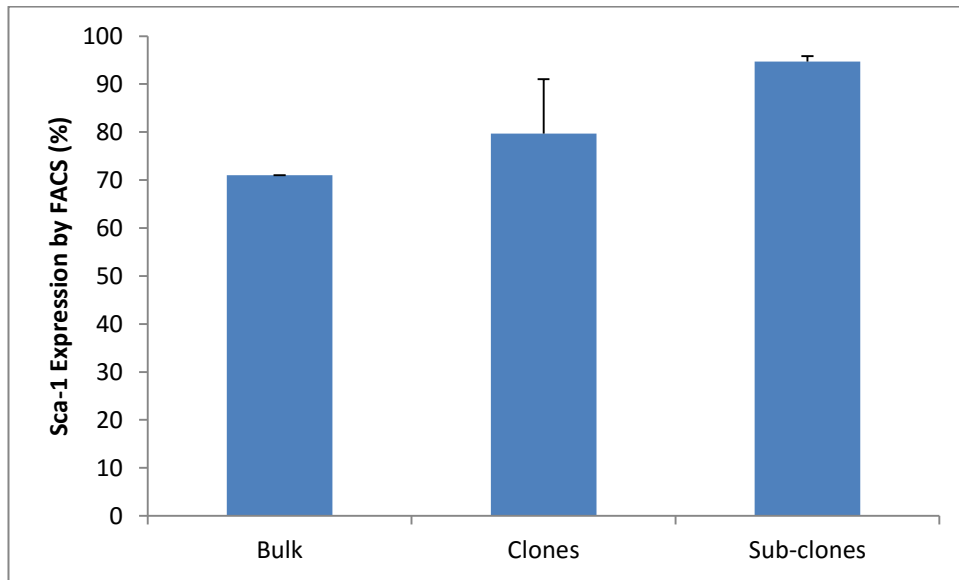
Figure 4.34 **Sca-1 expression in bulk vs. clonal vs. subclonal PICs.** Sca-1 expression by FC in bulk, clonal and sub-clonal PICs. Bars represent the mean for each group. Error bars represent the standard deviation of the mean, bulk n=1, clones, n=7, sub-clones n=3.
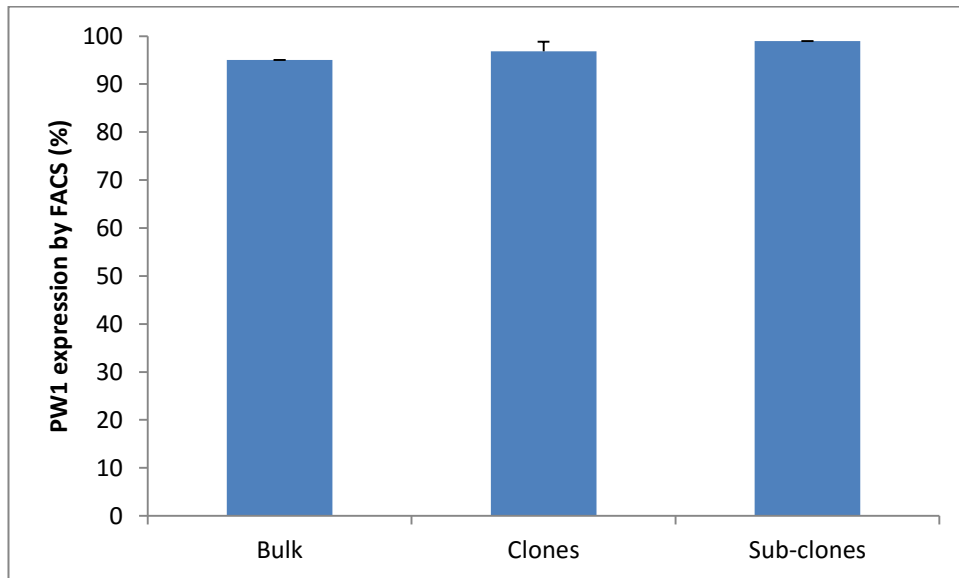
Figure 4.35 **PW1 expression in bulk PICs vs clones vs sub-clones.** PW1
expression by FC in bulk, clonal and sub-clonal PICs. Bars represent the mean for
each group. Error bars represent the standard deviation of the mean, bulk n=1,
clones, n=7, sub-clones n=3.
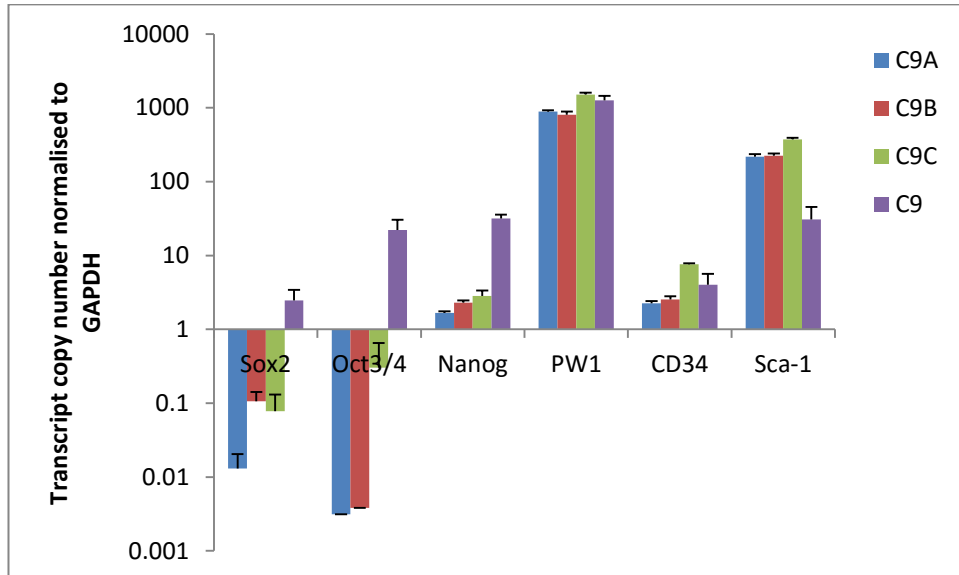
Figure 4.36   Transcription profile of C9 PIC sub-clones vs C9 PICs.

Transcriptome analysis by qRT-PCR analysis of sub-clones (C9A-C) compared to

original C9 PICs. Bars represent the transcript copy number normalised to

GAPDH. Error bars represent the standard deviation of the mean, n=triplicate.

When all data were merged to form one group for clones, one group for subclones and bulk PICs, there seemed to be a reduction in transcript levels for all 3 pluripotency genes with each cloning stage, with only Nanog remaining above a copy number of 1 in all groups. PIC markers PW1, CD34 and Sca-1 were present in all PIC populations and whilst there was some fluctuation between groups, no obvious trend was observed (Figure 4.37).
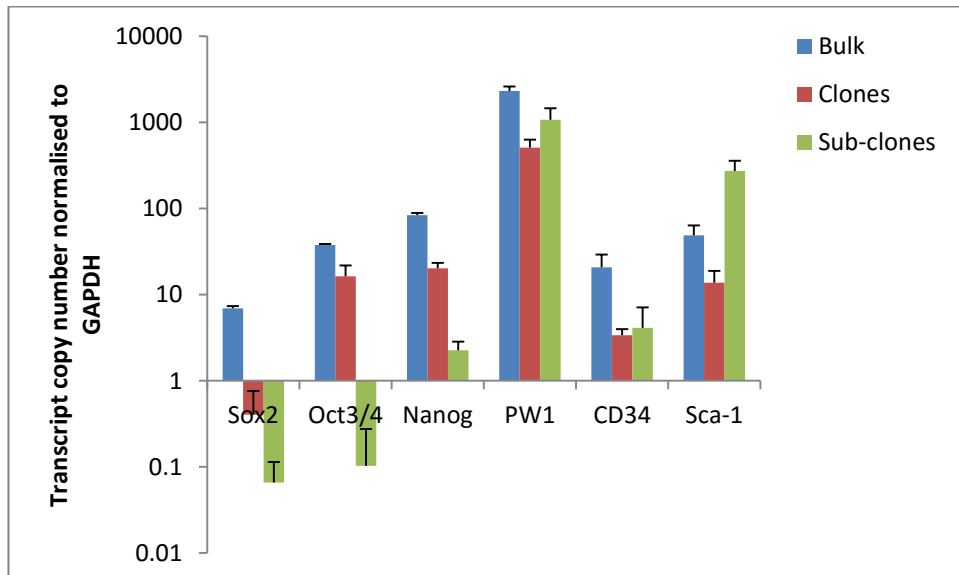
Figure 4.37   **Transcription profile of bulk PICs vs clones vs sub-clones.**

Transcriptome analysis by qRT-PCR of bulk (n=1 in triplicate), clones (n=7) and sub-clones (n=3). Bars represent the transcript copy number normalised to GAPDH. Error bars represent the standard deviation of the mean.

4.4 Discussion

The main findings of this study are:

1. PICs were successfully isolated from murine hind-limb tissue.

2. PICs can be propagated in culture for long periods whilst maintaining a stable phenotype.

3. PICs are clonogenic and self-renewing *in vitro*.

4. PICs express markers of pluripotency.

4.4.1 Isolation and characterisation of PICs

The confirmation of isolated PICs as CD45$^-$/Sca-1$^+$/Pax7$^-$/PW1$^+$ by FC analysis and ICC, whilst being morphologically small, round and bright, is consistent with that previously described (Mitchell et al. 2010; Pannérec et al. 2013; Lewis et al. 2014). PICs in this study were not sorted for CD34$^+$ expression, unlike in previous studies (Mitchell et al 2010; Pannérec et al 2013; Lewis et al 2014) as MACs sorting does not allow for 2 positive sorts. In line with this, FC analysis confirmed they contained a mix of CD34$^-$ and CD34$^+$ cells.

A low percentage of bulk PICs expressed PDGFRα, this is in contrast to that described previously in murine PICs and pPICS (33%) (Pannérec et al. 2013; Lewis et al. 2014), which both contain PDGFRα$^+$ and PDGFRα$^-$ cells. Furthermore, C9 PICs didn't express PDGFRα which suggests the process of cloning selected for a PDGFRα$^-$ population. In light of this, C9 PICs are distinct from the FAP population described as CD45$^-$/Sca-1$^+$/CD34$^+$/ PDGFRα$^+$ (Uezumi et al. 2010; Joe et al. 2010; Pannérec et al. 2013), whilst *in vitro* characteristics of

previously described PICs have contained a subset of FAPs (Mitchell et al. 2010; Pannérec et al. 2013; Lewis et al. 2014)(Figure 4.38).
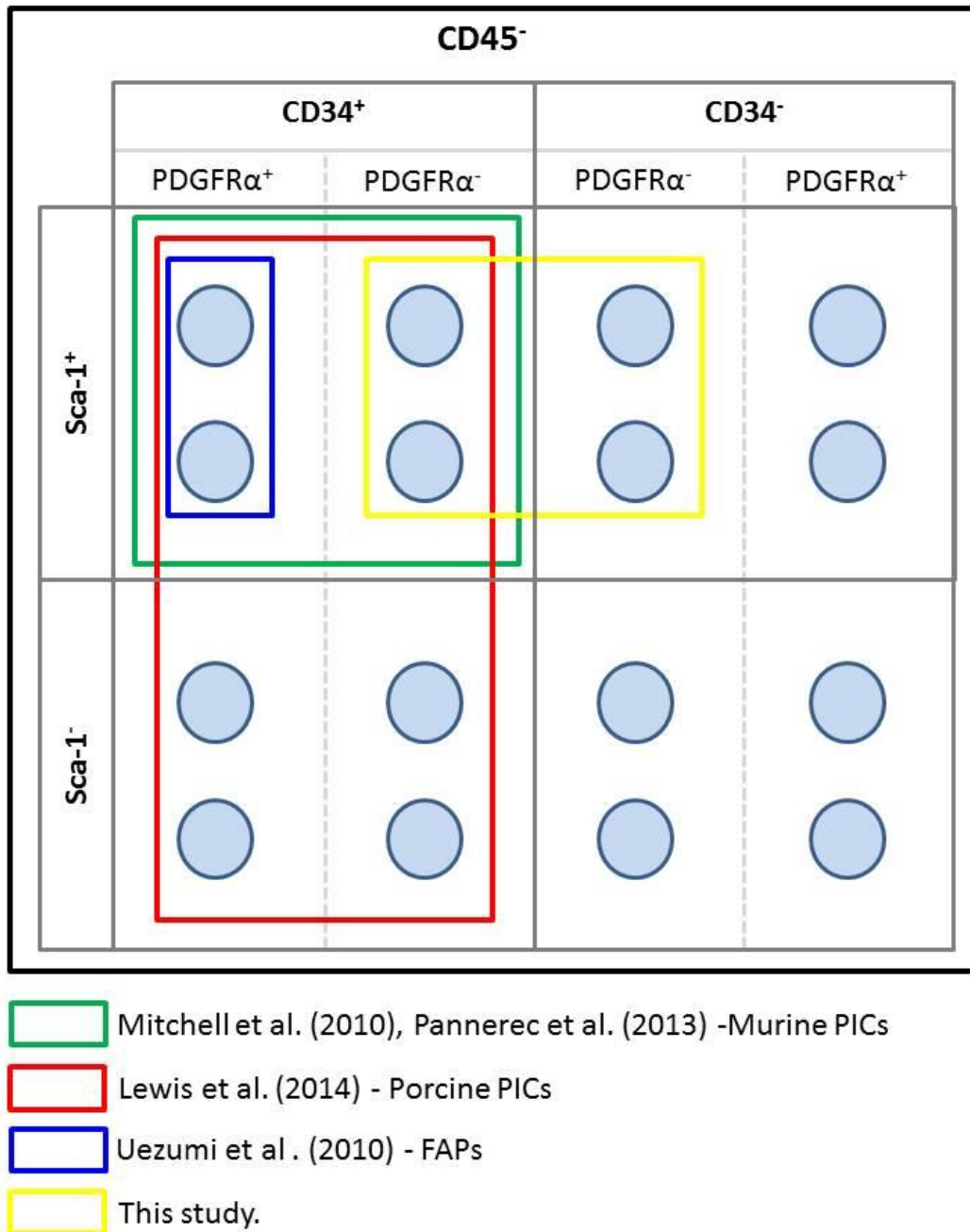
Figure 4.38   Overlap of previously described PIC populations.

The protein expression of CXCR4 in this study was similar to levels reported in pPICs (59% vs 55%) (Lewis et al. 2914). CXCR4 (C-X-C chemokine receptor type 4), is a receptor for SDF-1 (stromal-derived-factor-1) and is implicated in the homing of multiple ASC populations including: HSC's (Sharma et al. 2011), adipose derived stem cells (Stuermer et al. 2015), MSC's (Shi et al. 2007) and eCSCs (Ellison et al. 2013). PICs also express the gene for CXCR4 but at a lower intensity than SC's (Pannérec et al 2013). Interestingly, C9 PICs showed increased positivity for CXCR4 over their un-cloned bulk counterparts, suggesting that the process of cloning selected for a CXCR4$^+$ population. It is not known if this was true for all clone lines, however an increase in CXCR4 has been shown to increase clonogenicity of neuroblastoma cell lines *in vitro* (Liberman et al. 2012).

In agreement with Lewis et al. (2014) PICs are not of haematopoietic or endothelial lineage, being negative for CD45 and CD31 and furthermore they are distinct from pericytes and adult MABs as they did not express NG2, PDGFRβ or CD146.

4.4.2 PICs can be propagated *in vitro*

Previously, Mitchell et al (2010) had reported differentiation of freshly isolated PICs with time in culture with 30% of cells expressing MyoD and Pax7 after 4 days suggesting they had undergone differentiation; however PICs were cultured for 3-4 days in BIOAMF-2 media, which is specifically optimized for primary culture of human amniotic fluid cells and is not designed to maintain self-renewal.

This study is the first to show that murine PICS can be propagated and maintained in long term culture. The media used in this study is one optimised by our group

and has previously been used to culture pPICS (Lewis et al. 2014) and eCSCs (Ellison et al. 2013). Indeed, we previously demonstrated pPICs were capable of maintaining a stable phenotype and karyotype over 40 passages (Lewis et al. 2010). The importance of using the correct growth media was further reinforced in this study by the growth senescence of PICs when placed in promocell growth media.

Clonal PIC cell lines displayed a similar morphology and phenotype to both bulk PICs, and each other, as did their sub-clonal counterparts. A clonal population was chosen for assessment over time in culture to ensure that results were characteristic of PICs and were not an artefact of a mixed cell population. C9 was subsequently chosen for further analysis due to it being the most similar to the transcription profile of non-cloned 'bulk' cells, and the phenotype of PICs in general.

The ability to propagate PICs *in vitro* culture is in contrast to that seen in SCs which rapidly lose their self-renewal properties and under-go differentiation (Cosgrove et al. 2009). SCs were not isolated during this study.

4.4.3 PICs are self-renewing and clonogenic

When propagated in culture PICs displayed characteristics of stem cells: clonogenicity and self-renewal.

PICs demonstrated an ability to form single-cell derived clonal populations; their clonal efficiency of ~34% was less than reported in pPICS (53%) (Lewis et al. 2014), but is within the range previously reported for other adult stem cell populations such as porcine skin stem cells (23% - Dyce et al. 2004). Moreover,

C9 PICs retained a subsequent clonogenicity of ~91%, substantiating their clonogenic properties, and self-renewal ability. This is the first study propagate and compare clones, and subsequently sub-clone PICs.

C9 PICs exhibited a stable PD over 20 passages, demonstrating each generation is as proliferative as its predecessor. A shorter PD is indicative of a higher rate of proliferation: The PD of murine ESCs is ~10-14 hours (Pauklin et al. 2011), porcine iPSCs derived from fetal fibroblasts have a PD of ~17hours (Ezashi et al. 2009), whilst pPICS have a PD of ~22 hours (Lewis et al. 2014).

The doubling time of PICs isolated from the mouse (~16 hours) was shorter than that reported in pPICs, which could be because a) Murine PICs are more proliferative than pPICs or b) The pPIC population was not a clonal cell line, not sorted for Sca-1, and therefore heterogeneous.

In heterogeneous populations, different cell types divide at different rates, therefore affecting the overall doubling time. In contrast C9 PICs were derived from a single cell, thus all cells would display a similar rate of proliferation.

The total number of population doublings over 20 passages was calculated to be ~64, far surpassing hayflicks limit of 14-28 doublings for cells of murine origin, as well as also extending beyond the 40-60 doublings initially reported as the maximum in human cells (Hayflick. 1973).

Importantly, in addition to maintaining their PD, C9 PICs also retained their morphology and phenotype over time in culture, displaying comparable levels of PW1 and Sca-1 at P2 and P20. Sca-1 and PW1 are both genes associated with ASC populations and stemness (Holmes and Stanford 2007; Besson et al. 2011).

129

4.4.4 PICs express markers of pluripotency

This is the first study to describe the presence of pluripotency markers in murine PICS. The levels of pluripotency gene transcripts were lower in PICs than in ESCs as expected, although they were still substantial. It was noted that there was a decrease in transcript levels of all 3 pluripotency genes, over time in culture. Whether the pluripotent potential of the cells differed with time was not tested. Despite these discrepancies, the growth kinetics and morphology did not change. This therefore suggests they could be artefacts of the *in vitro* environment rather than an inability of the PICs to self-renew competently. *In vivo* PICs would naturally inhabit a 3D environment interacting with many other cell types. Whilst *in vitro* conditions are optimised to mimic the *in vivo* environment, ultimately cell culture cannot currently provide an identical niche to that in which they naturally reside within the body.

Bulk PICs had the highest number of transcripts for pluripotency markers, however bulk PICs were not cultured long term. Therefore, it is not known if PICs self-renew more efficiently in a heterogeneous culture.

In summary, for the first time these data suggest that murine PICs display properties of *bona fide* stem cells being clonogenic and self-renewing *in vitro*. Furthermore, similar to PICs isolated from the pig (Lewis et al. 2014), they expressed markers of pluripotency (Nanog, Oct3/4 and Sox2) which is the final attribute of a true stem cell. The pluripotent potential of PICs will be investigated in the next chapter.

5. PICs display multipotent potential

5.1 Introduction

Potency (bi-potent, multipotent or pluripotent) is the third measure of stemness and can be determined *in vitro* by inducing differentiation down specific cell lineages of the 3 germ layers, using defined culture media.

Mitchell et al (2010) originally demonstrated that PICs were bi-potent, differentiating into both skeletal and smooth muscle *in vitro* after 24-36 hours in myogenic differentiation media (DMEM, 2% horse serum), with approximately 30% of PICs expressing MHC, whilst the majority went on to express SMA. Our group found a similar ratio, with 76% of pPICs differentiating into smooth muscle vs. 24% into skeletal muscle (Lewis et al. 2014). Furthermore, Sca-1^{Med} PICs have a higher fusion index (40%) than that of Sca-1^{High} PICs (20%) in 1 week old mice. This fusion index of 20% in maintained in Sca-1^{High} PICs from adult (7 week old) mice (Sca-1^{Med} PICs do not persist into adulthood) (Pannérec et al. 2013).

Most recently, our group demonstrated that skeletal muscle derived pPICs have cardiomyogenic potential, forming cardiospheres that upon further differentiation express cTnI and Cx43 (Lewis et al. 2014). Furthermore, pPIC generated cardiospheres showed they could also differentiate into endothelial and smooth muscle cells (Lewis et al. 2014), similar to eCSCs that can generate all 3 cardiac lineages (Ellison et al. 2013).

In addition to their myogenic potential, PICs also demonstrate an adipogenic differentiation potential of 60% in *vitro* (Pannérec et al 2013), with lipid droplet formation also seen in pPICs (Lewis et al. 2014).

On further investigation, Pannérec et al (2013) reported that PDGFRα^+ PICs were capable of adipogenic differentiation but did not display myogenic differentiation potential, whilst PDGFRα^- PICs had myogenic potential but lacked adipogenic differentiation capability. These findings are in agreement with previous data that PDGFRα^+ cells in adult muscle interstitium are fibro-adipogenic progenitor (FAP) cells (Uezumi et al. 2010; Joe et al. 2010).

Other muscle derived progenitors, including satellite cells, have previously been reported to undergo osteogenic differentiation *in vitro* (Asakura et al. 2001, Oishi et al 2013). Similarly to adipogenic differentiation, Oishi et al (2013) identified PDGFRα^+ cells as having osteogenic differentiation capabilities, whilst CD56$^+$ cells did not.

All three of these cell types (myogenic, adipogenic and osteogenic) originate from the mesoderm layer and what has not yet been described is the ability of PICs to differentiate the trans- germ layer into cells types from the other two germ layers, the endoderm and the ectoderm. The endoderm gives rise to gastrointestinal and the respiratory tract as well as pancreatic beta cells and hepatocytes, whilst the third primary germ layer, the ectoderm, gives rise to cells of the nervous system, skin and teeth amongst others (Gao et al. 2013).

PICs express the pluripotency markers Oct3/4, Nanog and Sox2 (Figure 4.8; Lewis et al. 2014); therefore for the first time, this study will assess the trans-germ layer differentiation potential and potency of PICs both *in vitro* and *in vivo*.

5.2 Methods

5.2.1 Directed Differentiation in vitro

C9 PICs (P5) were plated in dishes and chamber slides as described (see Table 2.3) at ~20,000 cells per cm^2. Undifferentiated C9 PICs (P5) were used as controls for all *in vitro* differentiation experiments. Chamber slides were stained by ICC, and cell pellets were analysed by qRT-PCR as previously described in the methods (Section 2.4 and 2.8 respectively). Antibodies and their applications are listed in Table 5.1; Primers are listed in Table 5.2.

For ICC: the number of positive cells/nuclei was counted and expressed as a percentage of total nuclei (n=100 nuclei counted per marker)

For qRT-PCR: Copy number normalised to GAPDH and βactin, and fold change over undifferentiated PICs was calculated as described (see Section 2.8).

Myogenic differentiation

Once cells achieved 80% confluency, normal growth media was changed for myogenic differentiation medium (Table 2.4). After 5 days chamber slides were fixed for ICC staining of MHC, α-sarc and SMA. Cell pellets made from the 10cm dishes, were pooled and analysed by qRT-PCR for the same markers.

Cardiomyogenic differentiation

Cardiospheres were formed (see Section 2.6.3) prior to transfer to dishes for cardiomyogenic differentiation. After 14 days in cardiomyogenic differentiation medium (Table 2.4); chamber slides were fixed for ICC staining for Cx43, cTnI

and Desmin. Cell pellets made from the 10cm dishes, were pooled and analysed by qRT-PCR for Cx43, cTnI and α-sarc.

Adipogenic differentiation

After 14 days in adipogenic differentiation media (Table 2.4) cells were fixed for histological Oil Red O staining: Fixed chamber slides were immersed in Propanediol (Sigma) for 5 minutes at RT followed by Oil red O (Sigma) for 8 minutes at 60°C. This was again rinsed in Propanediol for a further 5 minutes, followed by running water for 5 minutes. Cells were then counter stained using Haematoxylin (Sigma) for 3 minutes at RT and rinsed in running water for 5 minutes before mounting with vectashield™ (Vector laboratories).

Endothelial differentiation

After 7 days in endothelial differentiation medium (Table 2.4); chamber slides were fixed for ICC staining of CD31, Cd34, CD146 and vWF. Cell pellets made from the 10cm dishes, were pooled and analysed by qRT-PCR for the same markers.

Hepatic differentiation

After 14 days in hepatic differentiation medium (Table 2.4); chamber slides were fixed for ICC staining of CK18, CK19, HNF1α and Albumin. 1 x 10cm dish was used for flow cytometry (see Section 2.7) to detect Albumin Expression (Abcam; 1:20 dilution). Cell pellets made from 3 x 10cm dishes, were pooled and analysed by qRT-PCR for the same markers.

Neurogenic differentiation

After 14 days in hepatic differentiation medium (Table 2.4); chamber slides were fixed for ICC staining of ChAT, β-3 tubulin, GFAP and γ-Enolase. Cell pellets made from 3 x 10cm dishes, were pooled and analysed by qRT-PCR for the same markers.

Table 5.1   **Directed Differentiation: Immunocytochemistry Antibodies**

Primary Antibody	Dilution	Incubation	Secondary Antibody
α-sarc (Sigma)	1/50	1 hour at 37°	Dylight 594 Donkey anti-Mouse IgM (Stratech)
MHC (Sigma)	1/50	1 hour at 37°	Cy3 Donkey anti-Mouse IgG (Stratech)
SMA (Sigma)	1/500	1 hour at 37°	Cy3 Donkey anti-Mouse IgG (Stratech)
Cx43 (Cell Signalling)	1/50	1 hour at 37°	Alexa Fluor 488 Donkey anti-Rabbit (Stratech)
cTnI (Santa Cruz)	1/50	1 hour at 37°	Alexa Fluor 488 Donkey anti-Rabbit (Stratech)
Desmin (Santa Cruz)	1/50	1 hour at 37°	FITC Donkey anti-Mouse IgG (Stratech)
CD31 Santa Cruz	1/50	1 hour at 37°	Dylight 488 Donkey anti-Goat (Stratech)
vWF Millipore	1/50	1 hour at 37°	Alexa Fluor 488 Donkey anti-Rabbit (Stratech)
CD34 Santa Cruz	1/50	1 hour at 37°	Dylight 488 Donkey anti-Goat (Stratech)
CD146 RnD	1/50	1 hour at 37°	FITC Donkey anti-Mouse IgG (Stratech)
CK18 Abcam	1/50	1 hour at 37°	FITC Donkey anti-Mouse IgG (Stratech)
CK19 Santa Cruz	1/50	1 hour at 37°	Dylight 488 Donkey anti-Goat (Stratech)
HNF-1α Santa Cruz	1/50	1 hour at 37°	Alexa Fluor 488 Donkey anti-Rabbit (Stratech)
Albumin Abcam	1/50	1 hour at 37°	FITC conjugated
ChAT Abcam	1/50	1 hour at 37°	Alexa Fluor 488 Donkey anti-Rabbit (Stratech)
GFAP Dako	1/50	1 hour at 37°	Alexa Fluor 488 Donkey anti-Rabbit (Stratech)
β3-Tubulin Abcam	1/50	1 hour at 37°	FITC Donkey anti-Mouse IgG (Stratech)
γ-Enolase Santa Cruz	1/50	1 hour at 37°	Dylight 488 Donkey anti-Goat (Stratech)

Table 5.2   Directed Differentiation: Primer sequences

Gene	Accession Number	Forward	Reverse
α-sarc	NM_009606.2|	AAGTGCGACATCGACATCAG	AAGTGCGACATCGACATCAG
MHC	NM_001039545.2	CCAAGCTGACCAAGGAGAAG	CCAAGCTGACCAAGGAGAAG
SMA	NM_007392.3	GCTGTCCCTCTATGCCTCTG	GAAGGAATAGCCACGCTCAG
Cx43	NM_010288.3	GTGGCCTGCTGAGAACCTAC	GAGCGAGAGACACCAAGGAC
cTrl	NM_009406.3	GAAGCAGGAGATGGAACGAG	TTAAACTTGCCACGGAGGTC
CD31	NM_001032378.1	GCCTCACCAAGAGAACGGAAGGC	TGGGCCTTCGGCATGGAACG
vWF	NM_011708.4	TGCCCTTGTGTGTGCACGGG	GTACCCTGGCTGCTGCACCG
CD146	NM_023061.2	GAGCTCATCTCCCCTCACAG	TCCTGACCACTACCCAAAGG
Ck18	NM_010664.2	CGAGGCACTCAAGGAAGAAC	CTTGGTGGTGACAACTGTGG
Ck19	NM_008471.2	CTCGGATTGAGGAGCTGAAC	TCACGCTCTGGATCTGTGAC
Albumin	NM_009654.3	GACAAGGAAAGCTGCCTGAC	TTCTGCAAAGTCAGCATTGG
HNF1α	NM_009327.3	ACTTGCAGCAGCACAACAT	GAATTGCTGAGCCACCTCTC
β-3-tubulin	NM_023279.2	CATGGACAGTGTTCGGTCTG	TGCAGGCAGTCACAATTCTC
ChAt	NM_009891.2	GTAACAGCCCAGGAGAGCAG	AGGTGTTGCATGCACTGAAG
ENO2	NM_013509.2	TCTATCGCCACATTGCTCAG	AGGGTGTGGTACACCTCTGC
GFAP	NM_001131020.1	CACGAACGAGTCCCTAGAGC	ATGGTGATGCGGTTTTCTTC
GAPDH	NM_008084.2	ACCCAGAAGACTGTGGATGG	CACATTGGGGGTAGGAACAC
β-actin	NM_007393.3	AGCCATGTACGTAGCCATCC	TCTCAGCTGTGGTGGTGAAG

5.2.2 Teratoma assay

Cells were injected in 10μl of 70% Matrigel (Sigma) with PBS under the kidney capsule of mice for tumour formation (see Section 2.9). PICs were labelled with GFP as per methods (Section 2.6.5). Groups were as follows:

Group A – SHAM - no cells (n=2).

Group B – 1 x 10^6 GFP PICs (n=3).

Group C – 5 x 10^5 GFP PICs/ 5 x 10^5 ESCs (n=3).

Group D – 1 x 10^6 ESCs (n=2).

Teratomas' were stained as previously described (see Section 2.3) for lineage specific antibodies (Table 5.3).

Table 5.3   Table of antibodies used in IHC of teratomas

Primary Antibody	Dilution	Incubation	Secondary Antibody
GFP (Abcam)	1/50	1 hour at 37°	Alexa Fluor 488 Donkey anti-Rabbit (Stratech)
β-3-Tubulin (Abcam)	1/50	1 hour at 37°	Cy3 Donkey anti-Mouse IgG (Stratech)
Desmin (Santa Cruz)	1/50	1 hour at 37°	Cy3 Donkey anti-Mouse IgG (Stratech)
αFP (Life Technologies)	1/50	1 hour at 37°	Cy3 Donkey anti-Mouse IgG (Stratech)
SMA (Sigma)	1/500	1 hour at 37°	Cy3 Donkey anti-Mouse IgG (Stratech)
GFP (Abcam)	1/50	1 hour at 37°	HRP Donkey anti-Rabbit (Santa Cruz)

138

5.2 Results

5.2.1 Myogenic differentiation

Clonal PICs (C9 P10) were placed in myogenic differentiation media: Transmitted light observations revealed the formation of elongated myotubes after 24 hours in culture, which continued to grow and align themselves to form fibres with neighbouring myotubes for the first 5 days in culture (Figure 5.1). At this point muscle fibres were observed to spontaneously twitch *in vitro* without any external stimulus (see video). Further culture past day 5 resulted in gradual degeneration of fibre structures and cell detachment, probably due to over confluence.

Cells were fixed at Day 5 for immunofluorescent (IF) staining to determine the fibre type using antibodies against myosin heavy chain (MHC) and alpha-sarcomeric actin (α sarc) for striated skeletal muscle, and smooth muscle actin (SMA) to detect smooth muscle. Confocal microscopy of stained fibres showed that ~80% of fibres expressed proteins for MHC and α-sarc whilst ~20% expressed proteins for SMA (Figure 5.2). It should be noted that SMA is also expressed in undifferentiated skeletal myoblasts, however the morphology was consistent with smooth muscle cells.

qRT-PCR analysis of fibres at day 5 for the corresponding genes for MHC, α-sarc and SMA found all 3 were highly expressed (Figure 5.3). The fold change in these transcripts (over un-differentiated cells) was calculated, and all showed increases over undifferentiated cells (Figure 5.4).
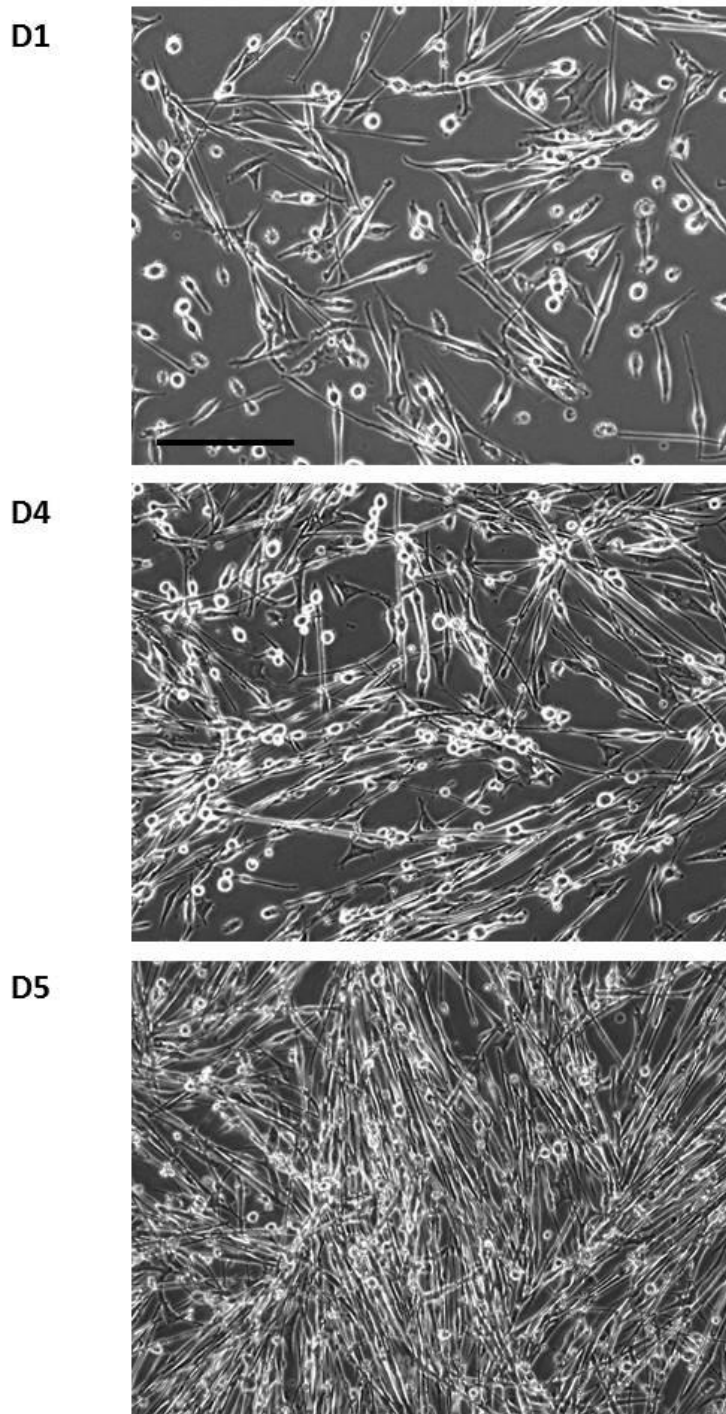
Figure 5.1   Cell morphology after myogenic differentiation. Transmitted

light microscope observations after myogenic differentiation of C9 PICs at day 1,

4 and 5. Scale = 200µm.
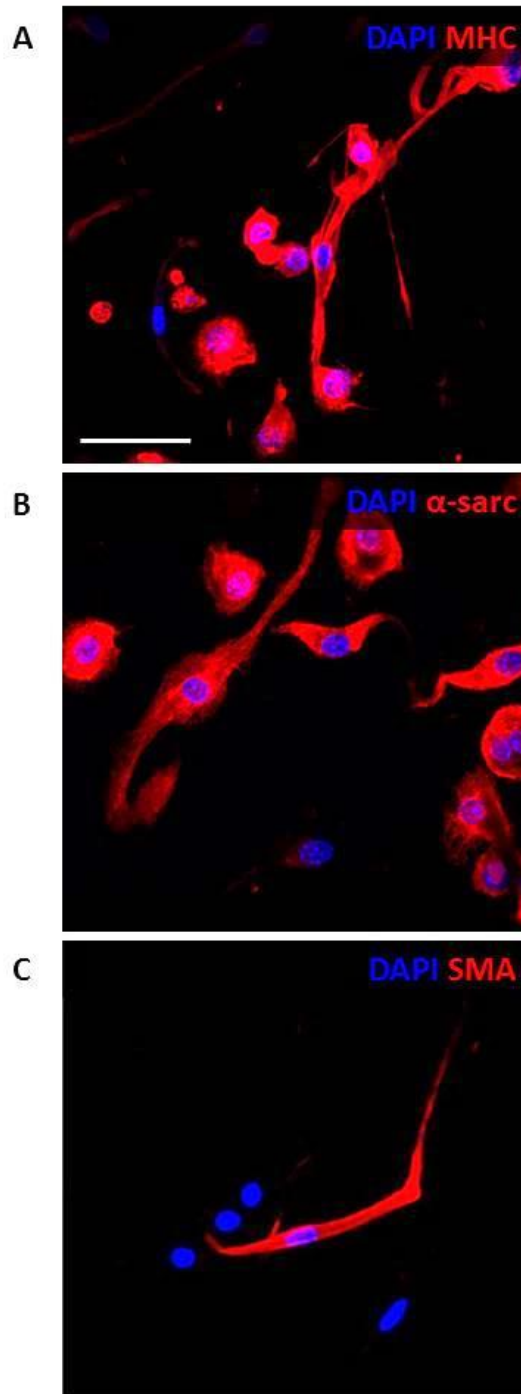
Figure 5.2 **Myogenic protein expression.** IF staining of cells after 5 days of directed myogenic differentiation, for MHC (**A**); red, α-sarc (**B**); red and SMA (**C**); red. Nuclei were counterstained with DAPI (blue). Scale = 50μm.
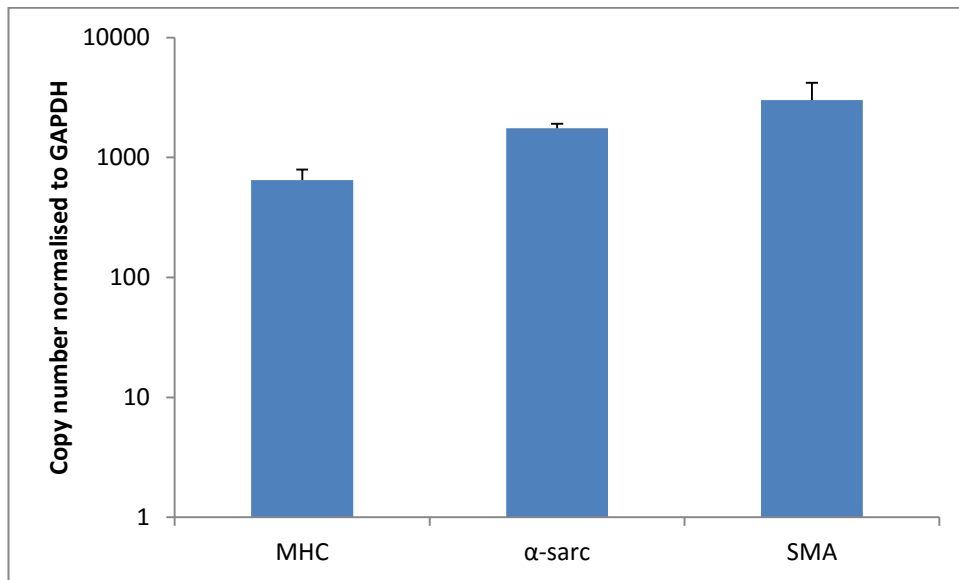
Figure 5.3 **Myogenic transcript expression.** Transcript analysis by qRT-PCR for muscle markers MHC, α-sarc and SMA after 5 days of directed myogenic differentiation of C9 PICs. Bars represent the transcript copy number normalised to GAPDH. Error bars represent the standard deviation of the mean, n=triplicate.
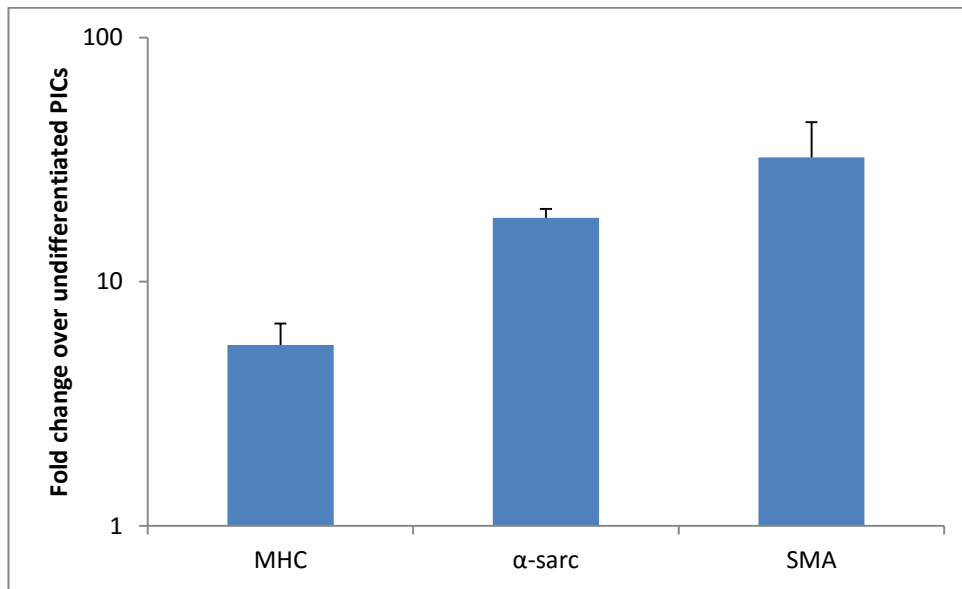
Figure 5.4   **Fold change increase in myogenic marker transcripts.** The fold change increase in transcript copy number of MHC, α-sarc and SMA after 5 days of directed myogenic differentiation of C9 PICs. Bars represent the fold change over undifferentiated PICs. Error bars represent the standard deviation of the mean, n=triplicate.

To demonstrate cardiomyogenic differentiation potential, firstly cardiospheres were generated (see section 2.6.3) from PICs (Figure 5.5). After 14 days of cardiomyogenic differentiation, a small number of cells expressed cardiac gap junction protein connexin 43 (Cx43), cardiomyocyte marker cardiac troponin I (cTnI) and desmin (Figure 5.6). Furthermore, transcripts were detected for Cx43, cTnI and α-sarc (Figure 5.7), with an increase in all three transcripts over undifferentiated cells (Figure 5.8); however cardiospheres were not seen to beat.
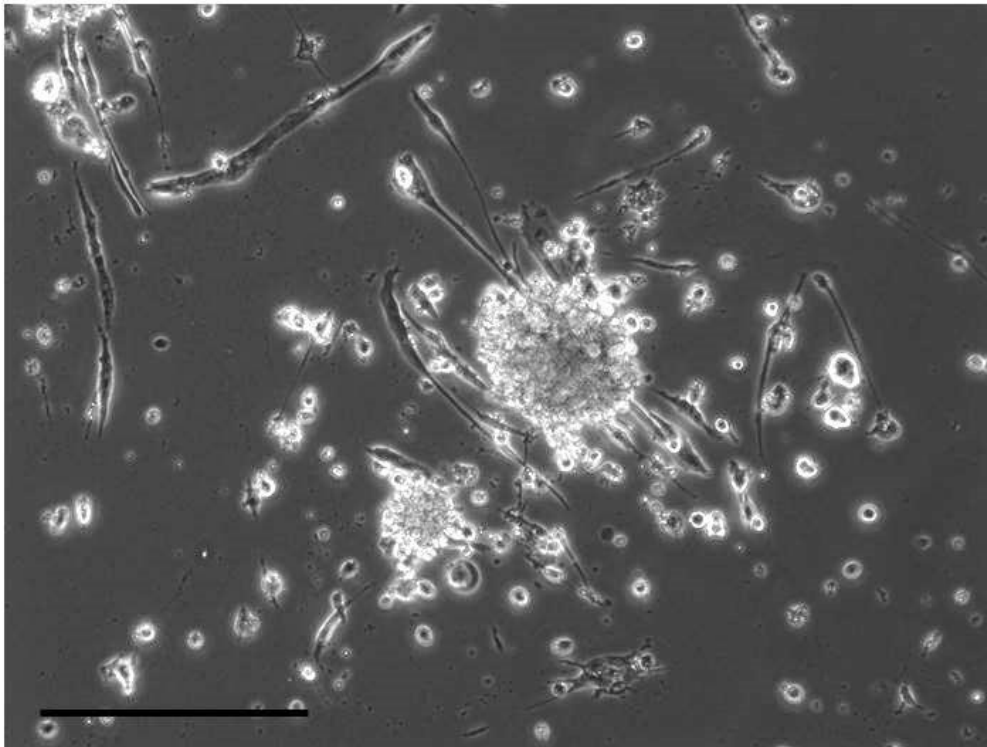
Figure 5.5 **Cell morphology after cardiosphere formation.** Transmitted light microscope observations of C9 PICs after cardiosphere formation and 14 days of cardiomyogenic differentiation. Scale = 200µm.
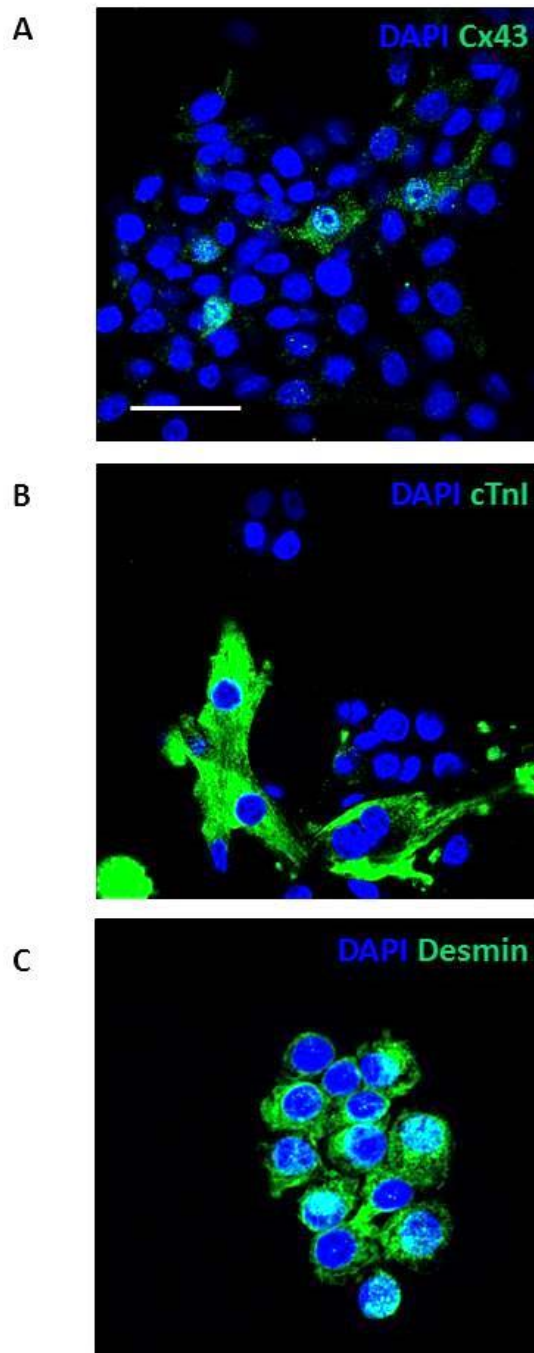
Figure 5.6   Cardiomyogenic protein expression. IF staining of C9 PICs after

14 days of directed cardiogenic differentiation for cardiac markers Cx43 (**A**);

green, cTnI (**B**); green and Desmin (**C**); green. Nuclei were counterstained with

DAPI (blue). Scale = 50µm.
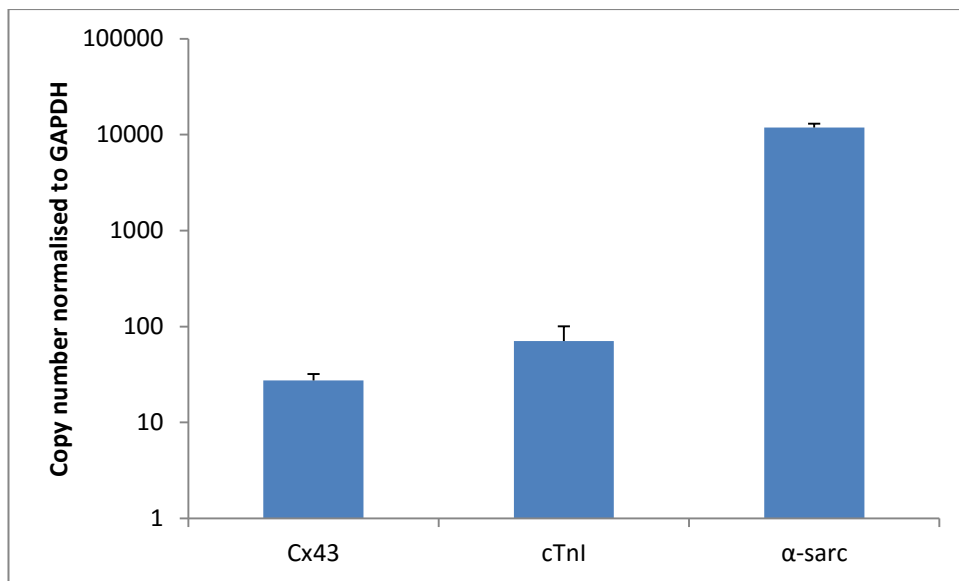
Figure 5.7 **Cardiomyogenic transcript expression.** Transcript analysis of C9

PICs by qRT-PCR for cardiac markers Cx43, cTnI and α-sarc after 14 days of

directed cardiomyogenic differentiation. Bars represent the transcript copy

number normalised to GAPDH. Error bars represent the standard deviation of the

mean, n=triplicate.
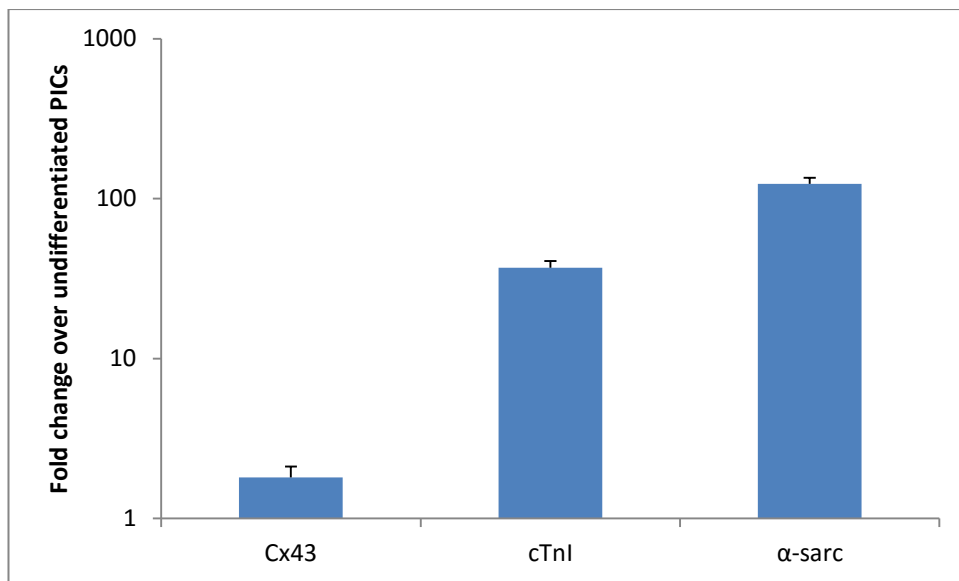
Figure 5.8 Fold change increase in cardiomyogenic marker transcripts.

The fold change in transcript copy number of Cx43, cTnI and α-sarc after 14 days

of directed cardiomyogenic differentiation of C9 PICs. Bars represent the fold

change over undifferentiated PICs. Error bars represent the standard deviation of

the mean, n=triplicate.

5.2.2 Differentiation into other Mesoderm cell types

To demonstrate an ability to form non-myogenic cells from the mesoderm layer,

PICs were placed in either adipogenic or endothelial differentiation.

After 14 days of directed adipogenic differentiation, cells were fixed and stained

with Oil red O, revealing the formation of lipid droplets (Figure 5.9), however

true mature adipocyte morphology was not seen.
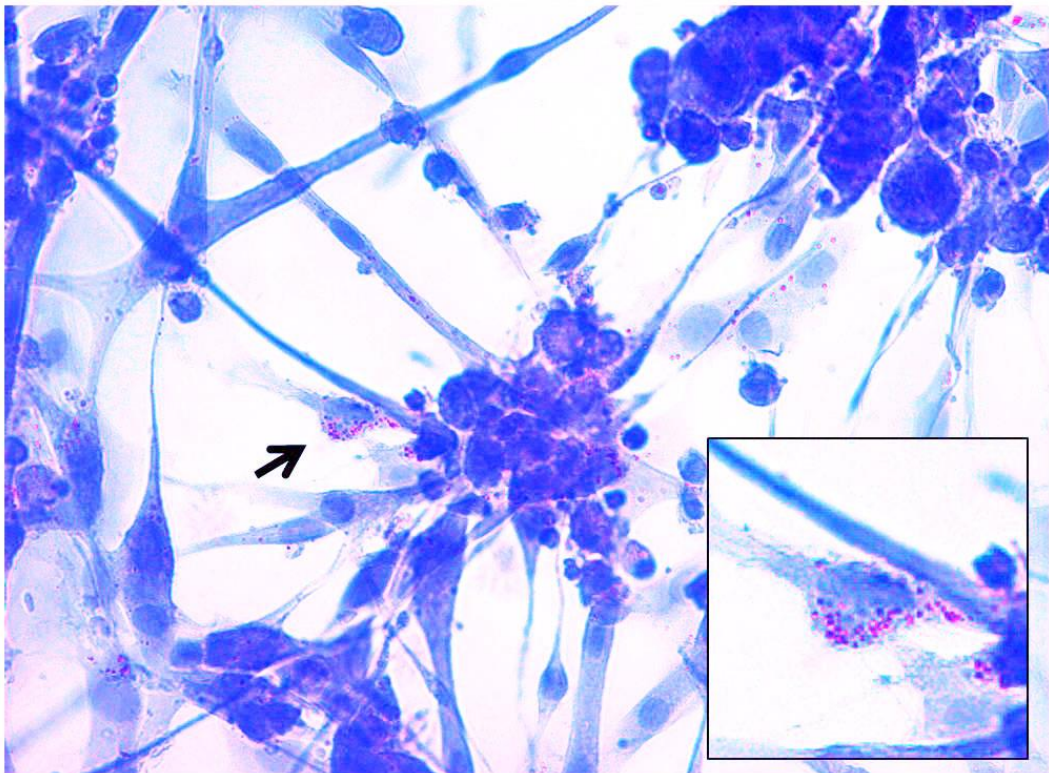
Figure 5.9   Lipid formation following adipogenic differentiation.

Transmitted light microscope observation of Oil red O staining (red) to detect

lipid droplets after 14 days of directed adipogenic differentiation. Nuclei are

counterstained with haemotoxilin (blue). Inset is a x 2 zoom of the cell identified

by an arrow.

148

After culture in endothelial differentiation media (see section 2.11.4) for 7 days PICs formed vessel like structures (Figure 5.10), which when imaged after IF staining were found to express proteins for CD31 (98%), vWF (98%), CD34 (99%) and CD146 (97%) (Figure 5.11). Transcripts for all four of these markers were found by qRT-PCR in differentiated cells (Figure 5.12), however fold changes over undifferentiated cells were quite small (Figure 5.13).
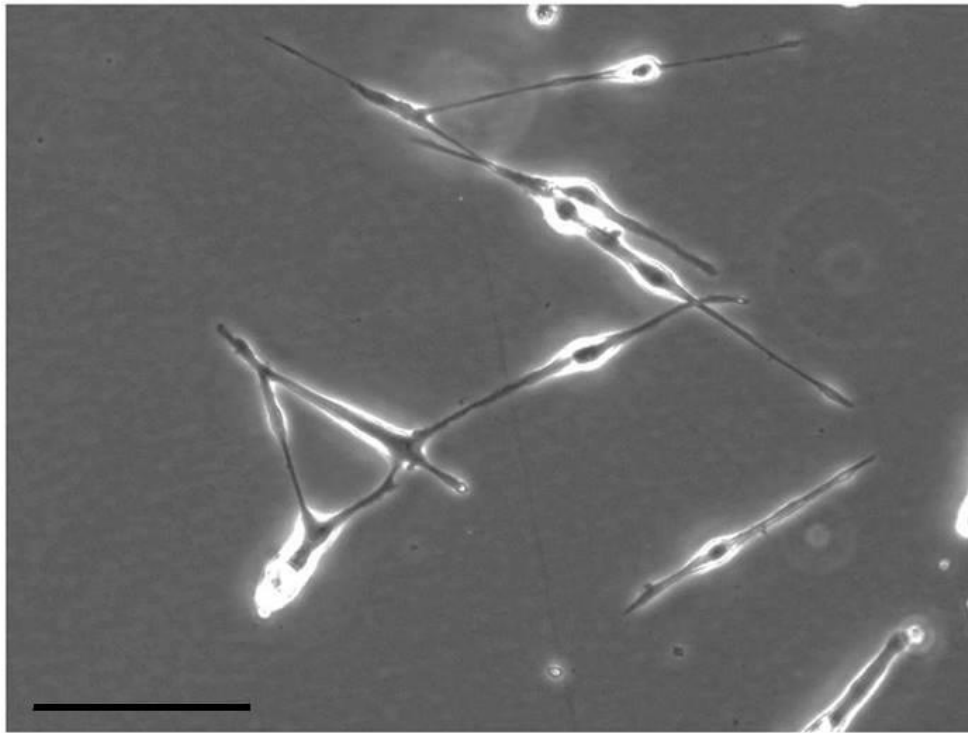
Figure 5.10   Cell morphology after endothelial differentiation. Transmitted light microscope observations after 7 days of endothelial differentiation. Scale = 100µm.
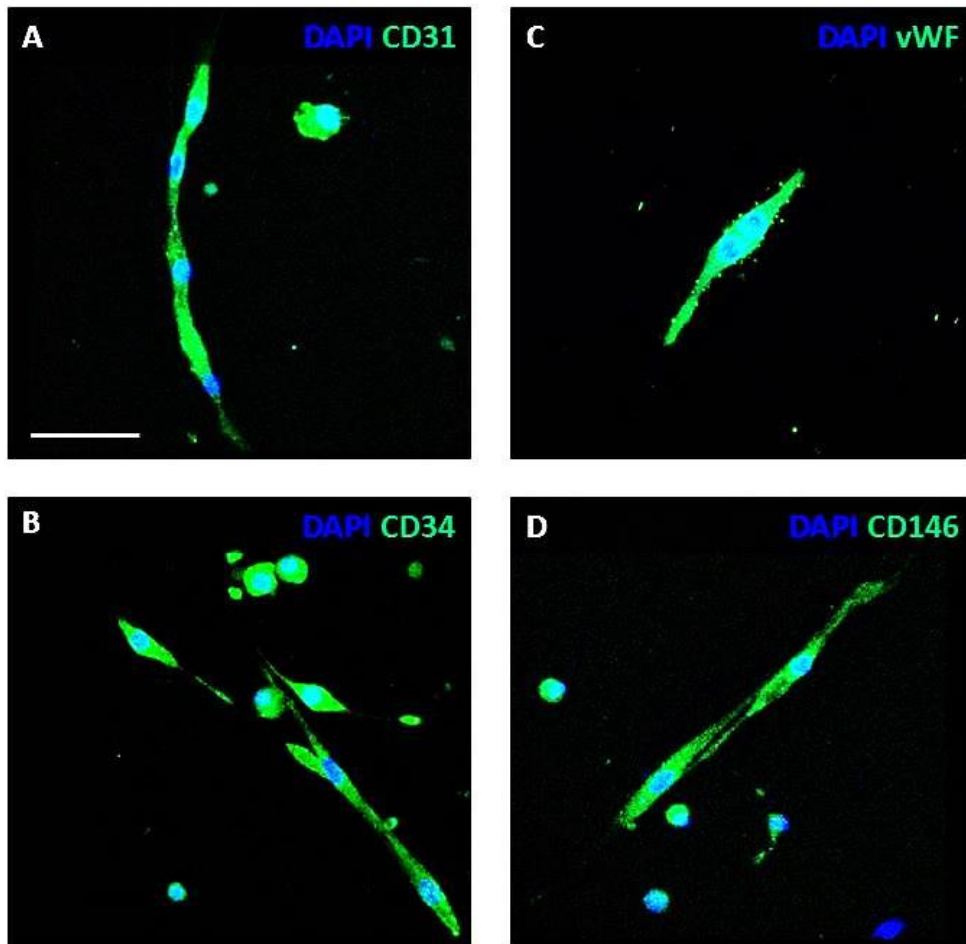
Figure 5.11   Endothelial protein expression. IF staining of C9 PICs after 7 days of directed endothelial differentiation for surface markers CD31 (**A**); green, CD34 (**B**); green, vWF (**C**); green and CD146 (**D**); green. Nuclei were counterstained with DAPI (blue). Scale = 50μm.
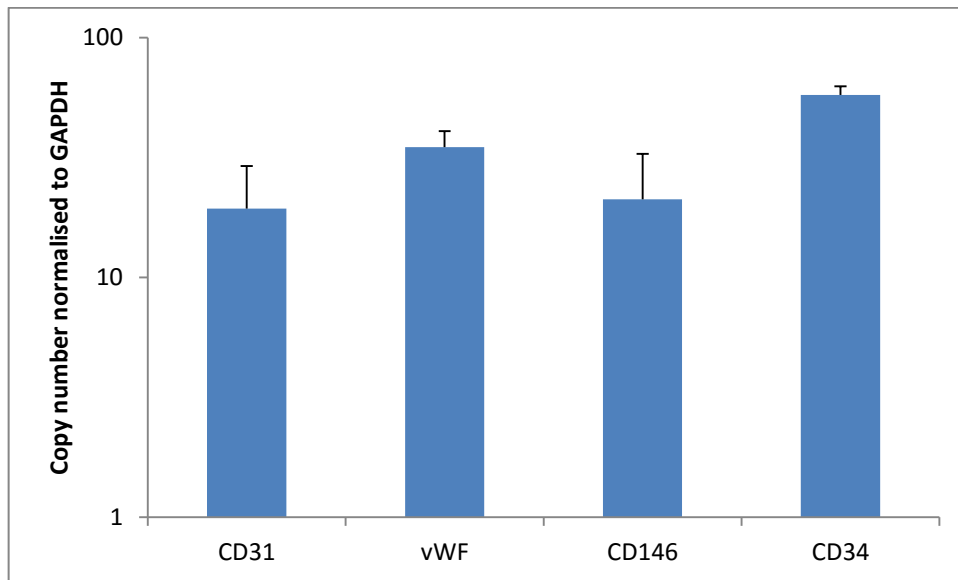
Figure 5.12   Endothelial transcript expression. Transcript analysis by qRT-PCR for endothelial markers CD31, vWF, CD146 and CD34 after 7 days of directed endothelial differentiation of C9 PICs. Bars represent the transcript copy number normalised to GAPDH. Error bars represent the standard deviation of the mean, n=triplicate.
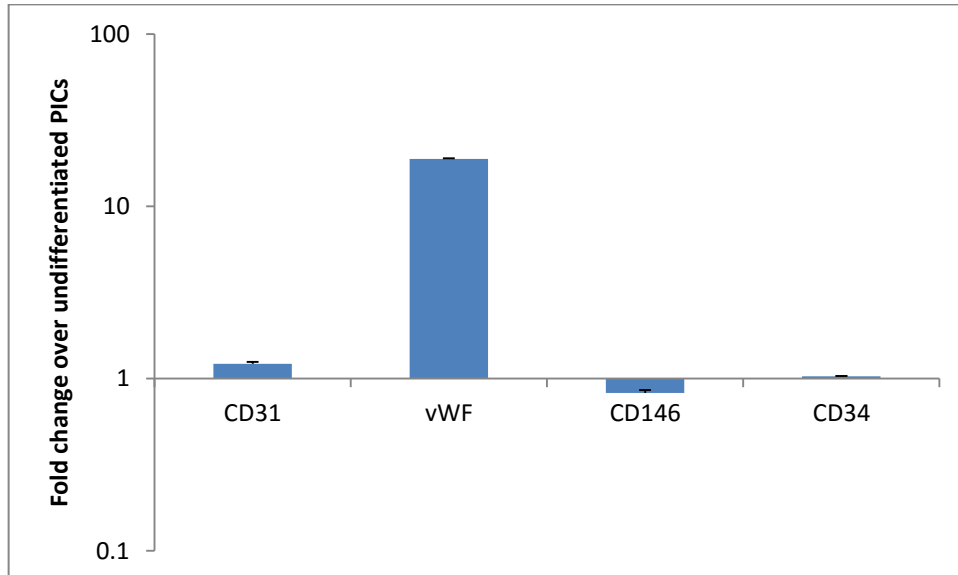
Figure 5.13   Fold change increase in endothelial marker transcripts. The

fold change increase in transcript copy number of CD31, vWF, CD146 and CD34

after 7 days of directed endothelial differentiation of C9 PICs. Bars represent the

fold change over undifferentiated PICs. Error bars represent the standard

deviation of the mean, n=triplicate.

5.2.3 Differentiation into hepatic cells of the Endoderm

To demonstrate cross-lineage differentiation into cell types of the endoderm lineage, C9 PICs were placed in hepatic differentiation media for 14 days, after which they displayed a change in morphology, however this was not consistent with a true hepatic morphology (Figure 5.14). IF Staining showed a small number of cells expressed proteins for cytokeratin's 18 (CK18) (5%) and 19 (CK19) (6%), whilst most cells expressed albumin (92%) and hepatic nuclear factor 1-alpha (HNF1α) (85%) (Figure 5.15). Furthermore, albumin expression was also confirmed by FC (Figure 5.16). It should be noted that HNF1α staining was seen in the cytoplasm, and not in the nucleus as expected. Transcript levels of all four markers increased slightly after differentiation (Figure 5.17; Figure 5.18).
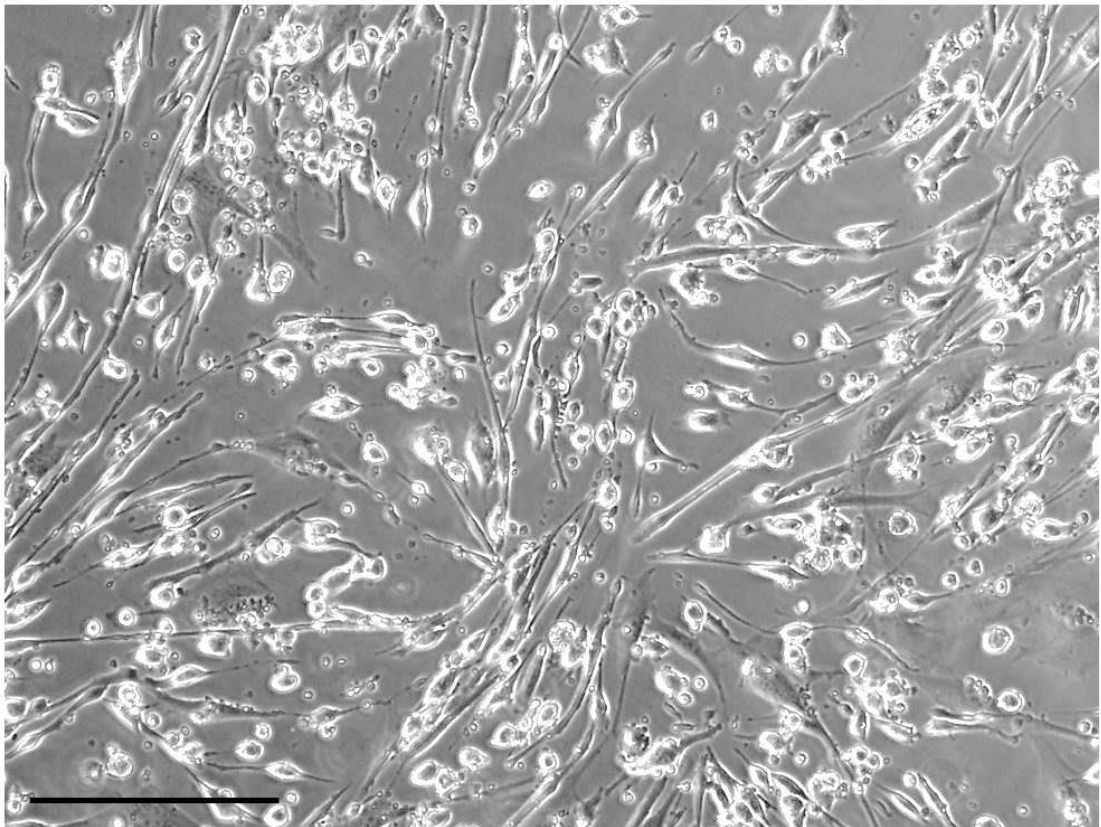
Figure 5.14   Cell morphology after hepatic differentiation. Transmitted light microscope observations after 14 days of hepatic differentiation. Scale = 200µm.
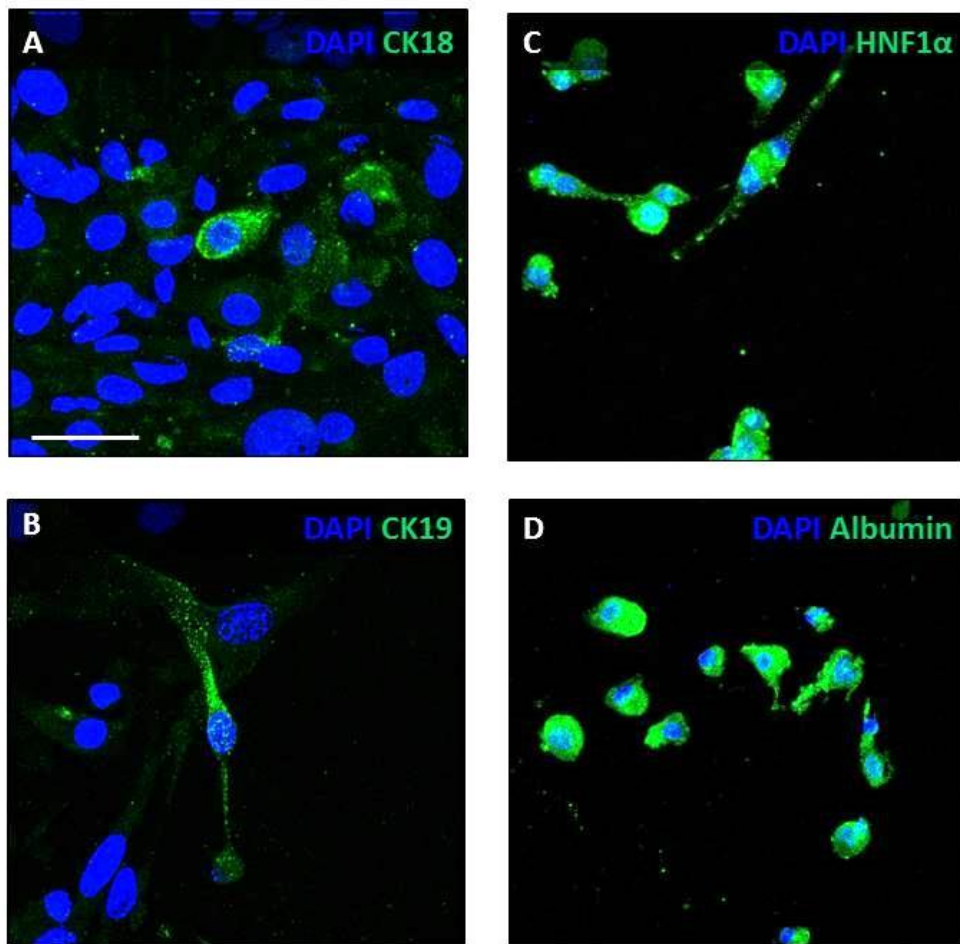
Figure 5.15   Hepatic protein expression. IF staining of C9 PICs after 14 days

of directed hepatic differentiation for surface markers CK18 (**A**); green, CK19 (**B**);

green, HNF1α (**C**);green and Albumin (**D**); green. Nuclei were counterstained

with DAPI (blue). Scale = 50μm.
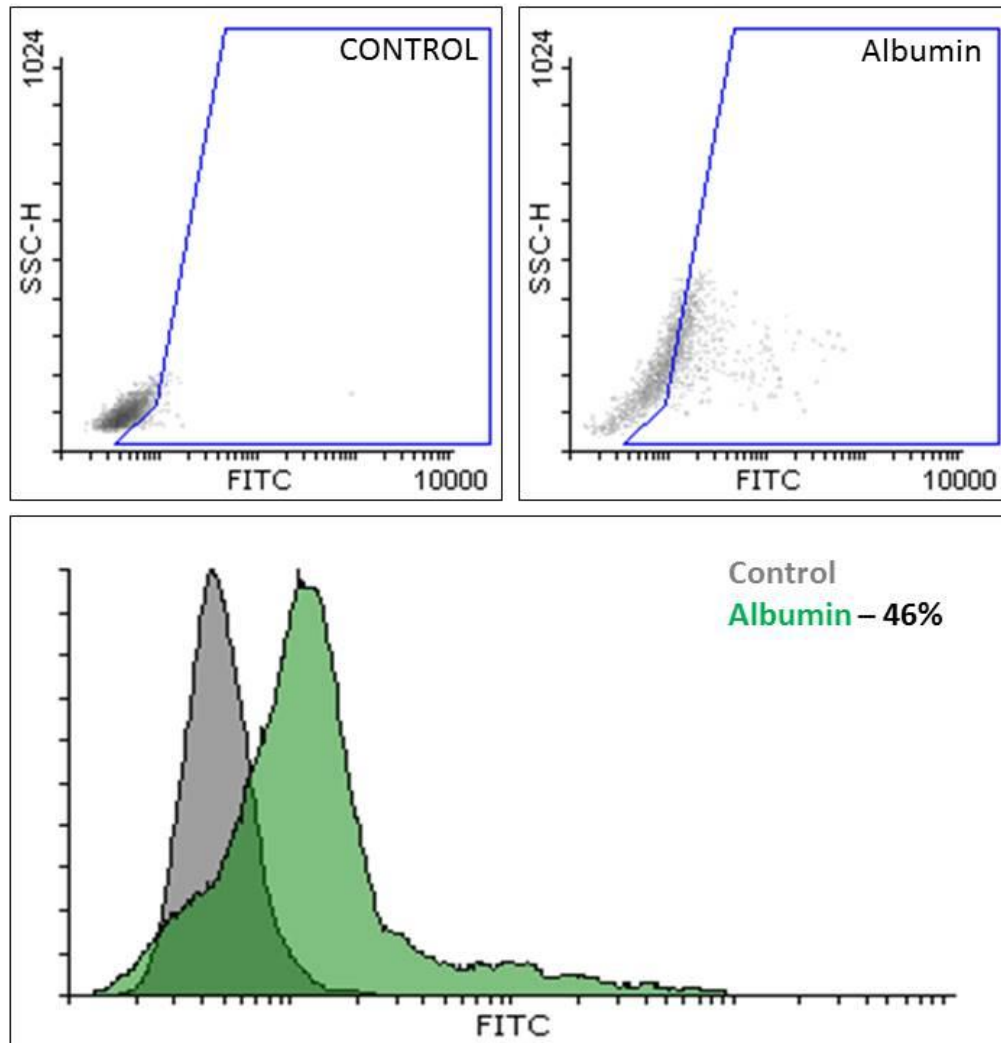
Figure 5.16   Albumin expression. FC analysis for albumin after 14 days of

hepatic differentiation of C9 PICs. Control is undifferentiated C9 PICs.
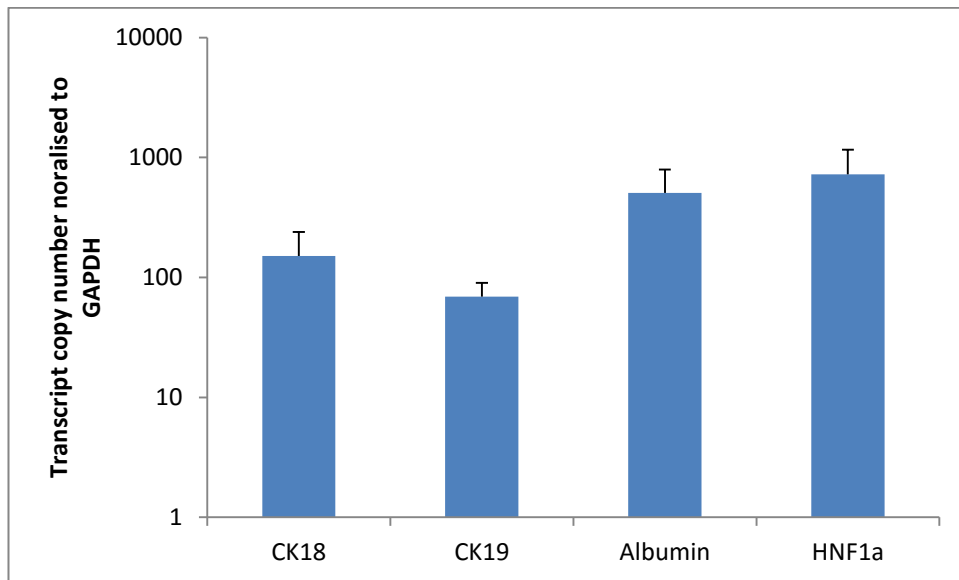
Figure 5.17 **Hepatic transcript expression.** Transcript analysis by qRT-PCR

for endothelial markers CK18, CK19, Albumin and HNF1α after 14 days of

directed hepatic differentiation of C9 PICs. Bars represent the transcript copy

number normalised to GAPDH. Error bars represent the standard deviation of the

mean, n=triplicate.
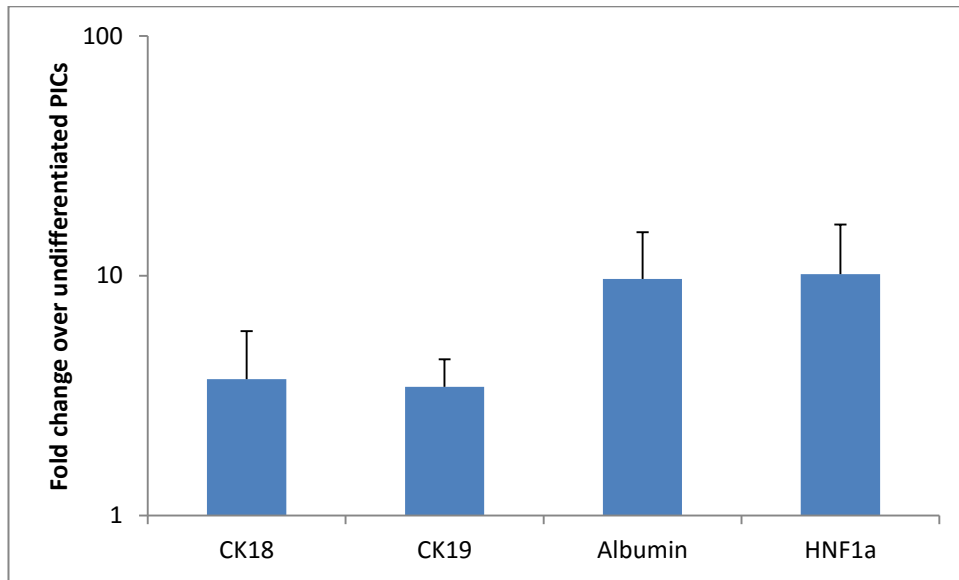
Figure 5.18   Fold change increase in hepatic marker transcripts. The fold change in transcript copy number of CK18, CK19, Albumin and HNF1α, after 14 days of directed hepatic differentiation of C9 PICs. Bars represent the fold change over undifferentiated PICs. Error bars represent the standard deviation of the mean, n=triplicate.

5.2.4 Differentiation into neuronal cells of the Ectoderm

Finally neurogenic differentiation was selected to determine differentiation potential of PICs into cell types of the ectoderm lineage.

After 14 days of directed neurogenic differentiation a small number of cells became spindle shaped with dendritic projections as seen in neuronal cell types (Figure 5.19) and were shown to express proteins for choline acetyltransferase (ChAT) (54%) , glial fibrillary acidic protein (GFAP)(96%), class III beta tubulin (β-3-tubulin) (98%) and gamma-Enolase (γ-Enolase) (69%) (Figure 5.20). During the fixation process, dendritic cells morphology changed as seen in Figure 5.20.

qRT-PCR revealed high levels of transcripts for these markers (Figure 5.21) and moderate (<2) fold changes over undifferentiated controls (Figure 5.22).
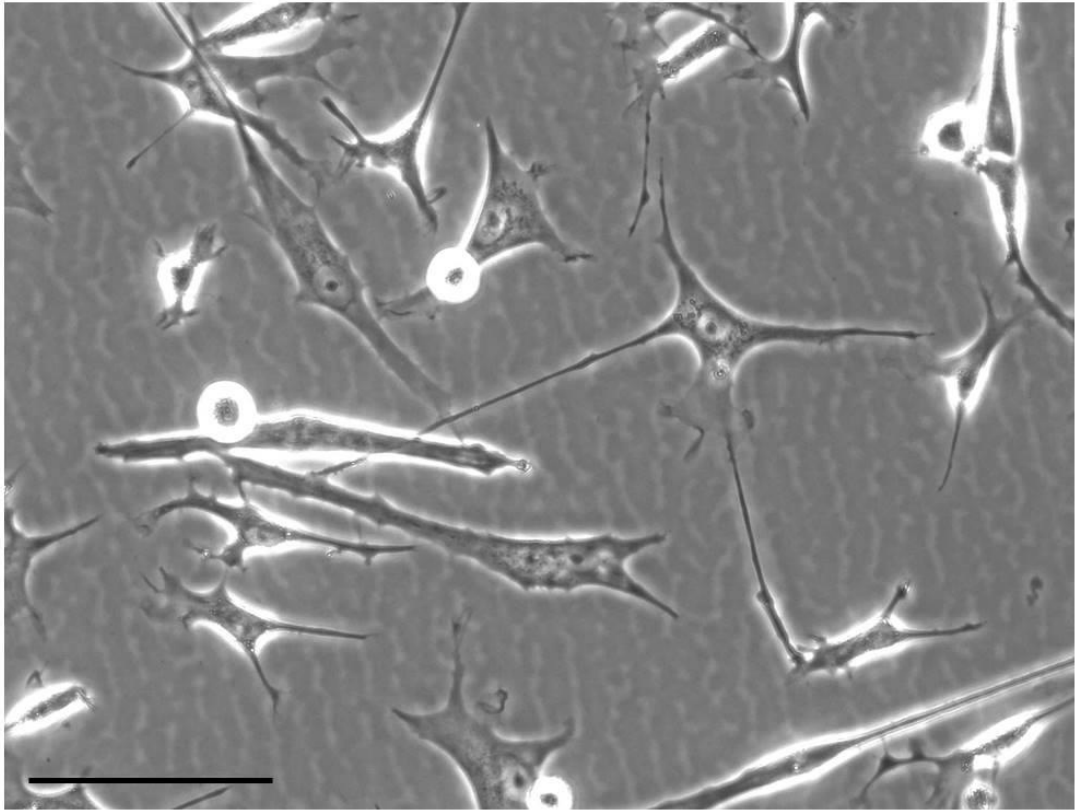
Figure 5.19   Cell morphology after neuronal differentiation. Transmitted

light microscope observations after 14 days of neuronal differentiation of C9 PICs.

Scale = 100µm
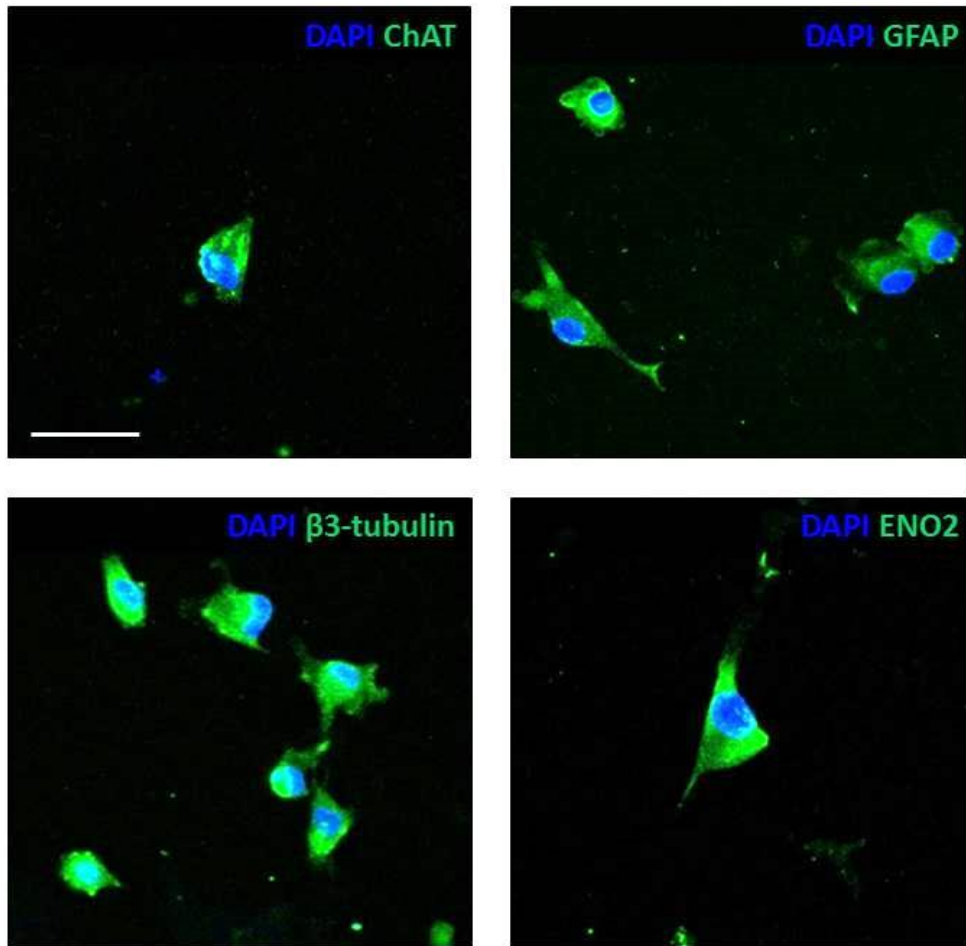
Figure 5.20   Neuronal protein expression. IF staining of cells of C9 PICs after

14 days of directed neuronal differentiation for surface markers ChAT (**A**); green,

β-3-tubulin (**B**); green, GFAP (**C**); green and ENO2 (**D**); green. Nuclei were

counterstained with DAPI (blue). Scale = 50µm.
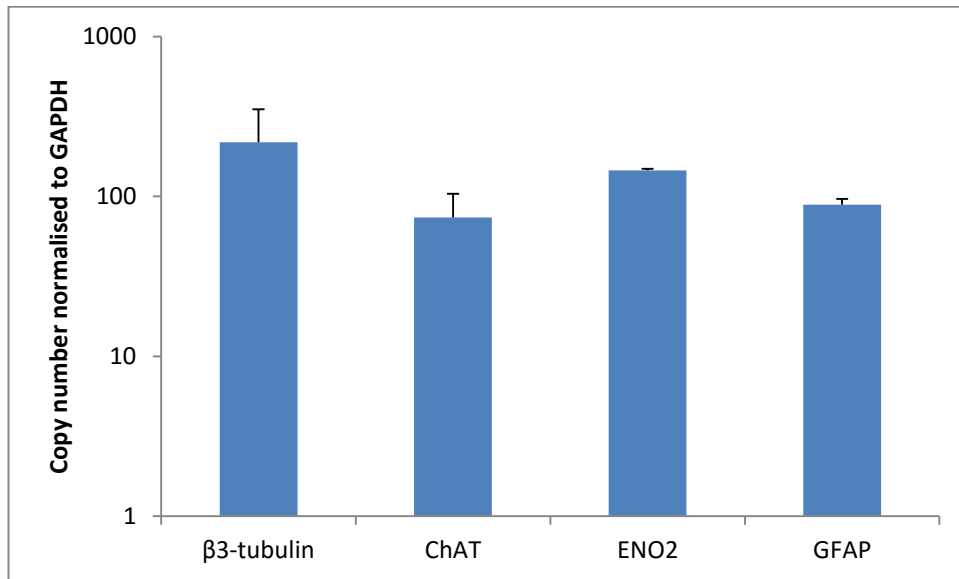
Figure 5.21 **Neuronal transcript expression.** Transcript analysis by qRT-PCR for eneuronal markers β-3-tubulin, ChAT, ENO2 and GFAP, after 14 days of directed neuronal differentiation of C9 PICs. Bars represent the transcript copy number normalised to GAPDH. Error bars represent the standard deviation of the mean, n=triplicate.
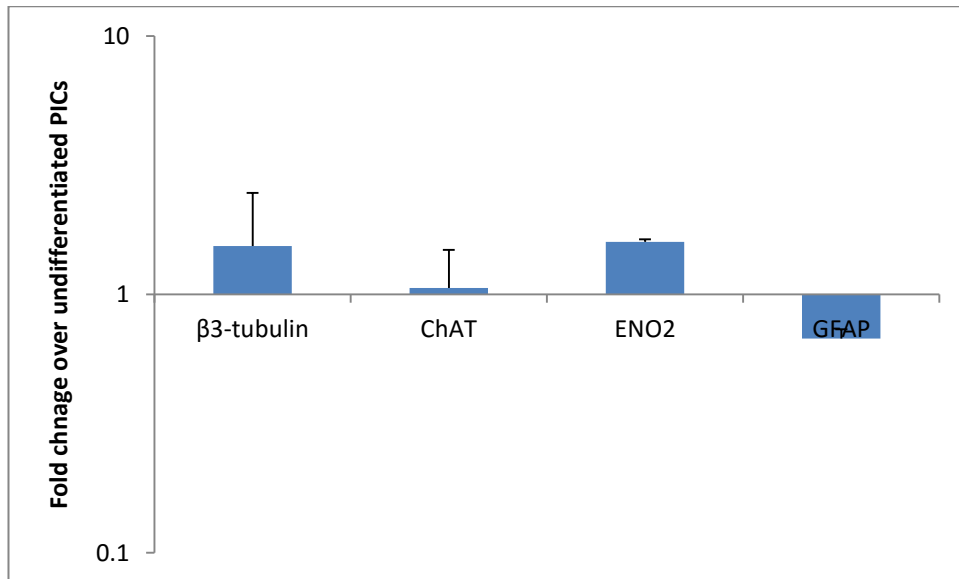
Figure 5.22 **Fold change increase in neuronal marker transcripts.** The fold change in transcript copy number of β-3-tubulin, ChAT, ENO2 and GFAP after 14 days of directed neuronal differentiation of C9 PICs. Bars represent the fold change over undifferentiated PICs. Error bars represent the standard deviation of the mean, n=triplicate.

Whilst calculating fold changes in transcripts, a transcript profile of undifferentiated PICS revealed that they expressed transcripts for genes associated with multiple cell fates (Figure 5.23) with the highest being for myogenic and neuronal lineages.
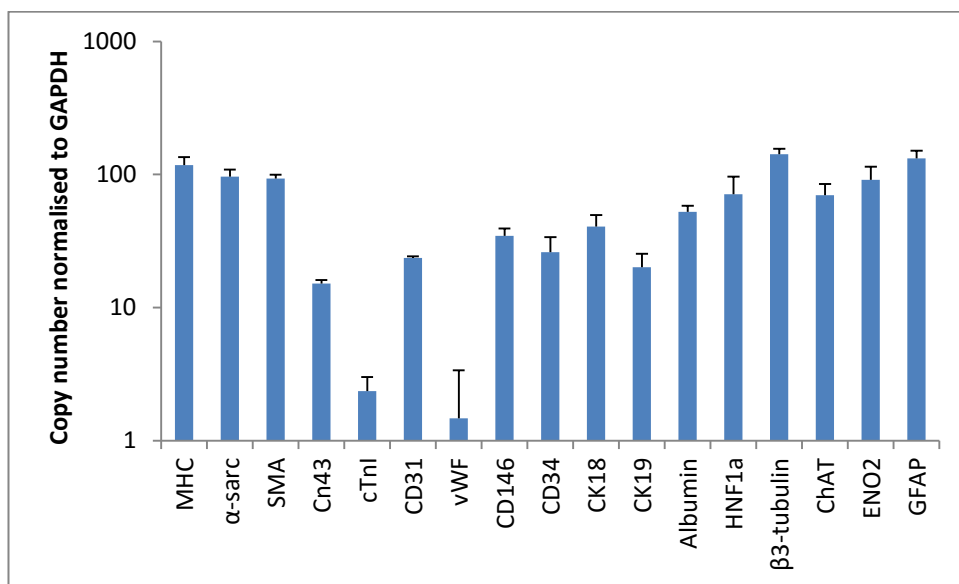
Figure 5.23   Multi-lineage transcript expression of PICs. Transcript analysis by qRT-PCR for: myogenic, cardiomyogenic, endothelial, hepatic, and neuronal genes of C9 PICs. Bars represent the transcript copy number normalised to GAPDH. Error bars represent the standard deviation of the mean, n=triplicate.

5.2.5 Multipotency of PICs in vivo.

To test whether PICs displayed a similar multipotency in an *in vivo* environment, PICs were transplanted under the kidney capsule alongside ESC's in a tumour formation assay (see section 2.14). To distinguish between cells that arose from ESC's or PICs, C9 PICs (P10) were transduced with a GFP construct prior to injection (see section 2.14.1).

Post-transduction, GFP$^+$ PICs demonstrated normal PIC morphology and their GFP expression was confirmed by FC at P2-post transduction (Figure 5.24; Figure 5.25). Furthermore, GFP$^+$ PICs (P8) retained a similar transcript profile to their non-GFP$^+$ counterparts (Figure 5.26). GFP$^+$ PICs were propagated for 8 passages to obtain enough cells to perform the assay. Mouse ESC's were cultured feeder-free prior to transplantation to prevent MEF contamination (Figure 5.27).

Mice injected with PBS (no cells), and those injected with only GFP$^+$ PICs did not form a tumour demonstrating that PICs are not tumorigenic. In contrast mice injected with ESC's, and those injected with a mix of ESCs and GFP PICs displayed hair loss, and tumour formation (Figure 5.28). Tumours contained a variety of cells with different morphologies (Figure 5.29).

Upon staining, ESC-only derived tumours did not contain any GFP whilst tumours formed from co-cultures of ESC's and GFP$^+$ PICS did (Figure 5.30). GFP was co-localised with cells from all 3 germ layers (Figure 5.31, denoted by arrows), however the majority of GFP$^+$ cells expressed mesodermal markers (not quantified).
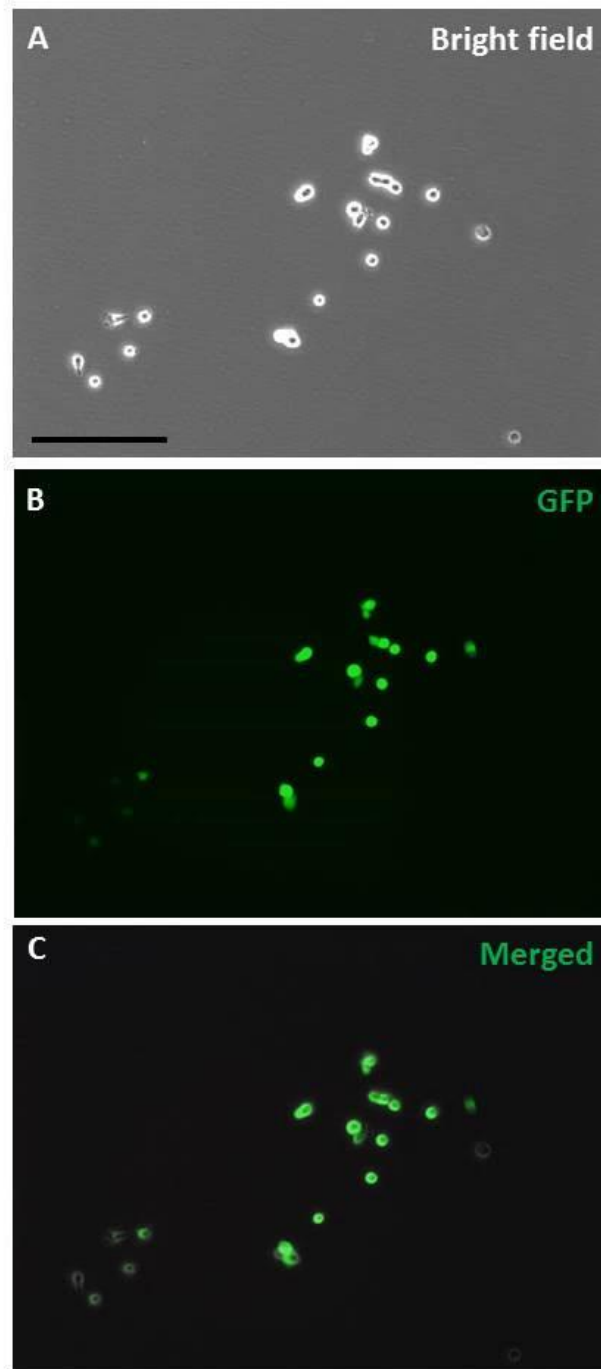
Figure 5.24   GFP⁺ PIC morphology. Transmitted light microscope observation (**A**), fluorescence (**B**) and merged image (**C**) of GFP⁺ transfected C9 PICs. Scale = 200μm.
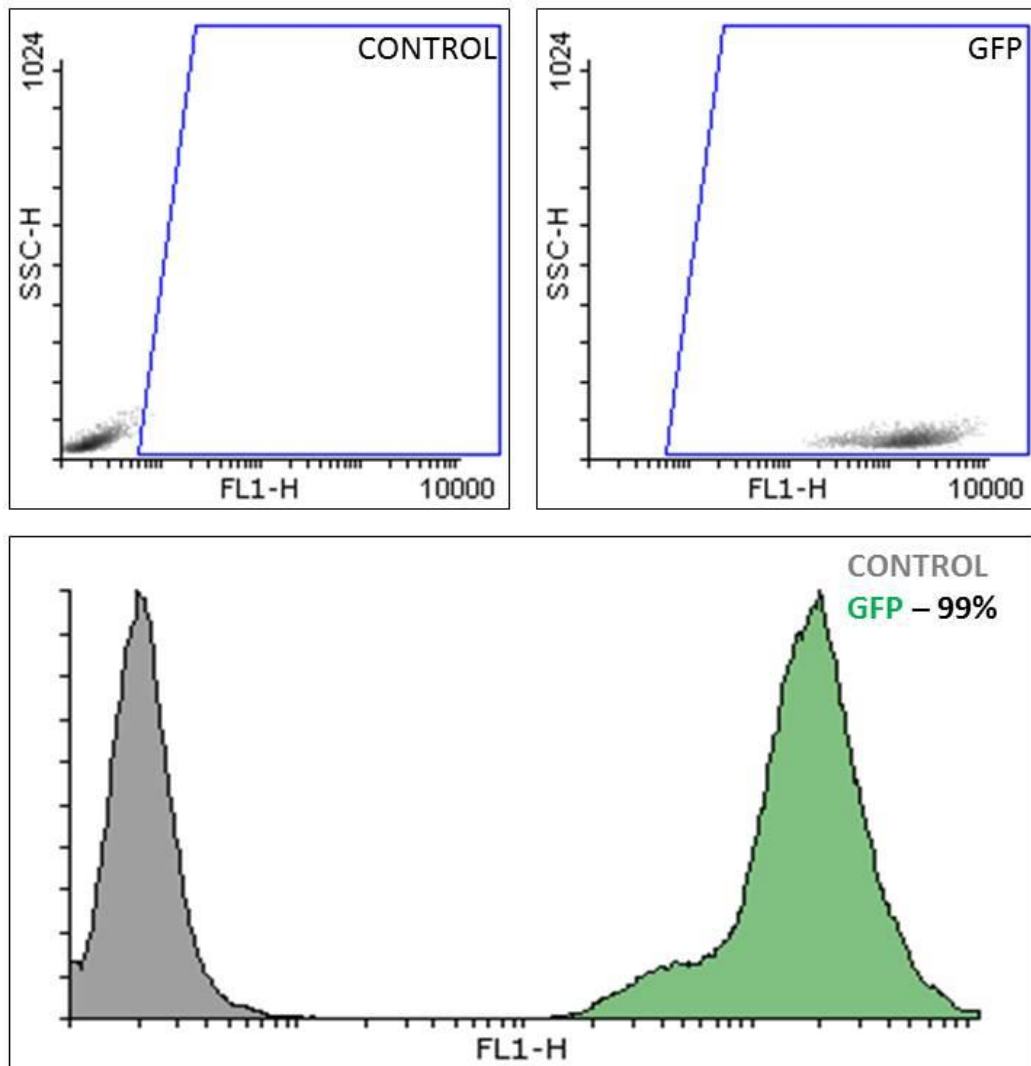
Figure 5.25   GFP expression of transfected PICs. FC analysis of GFP

expression in transfected C9 PICs.
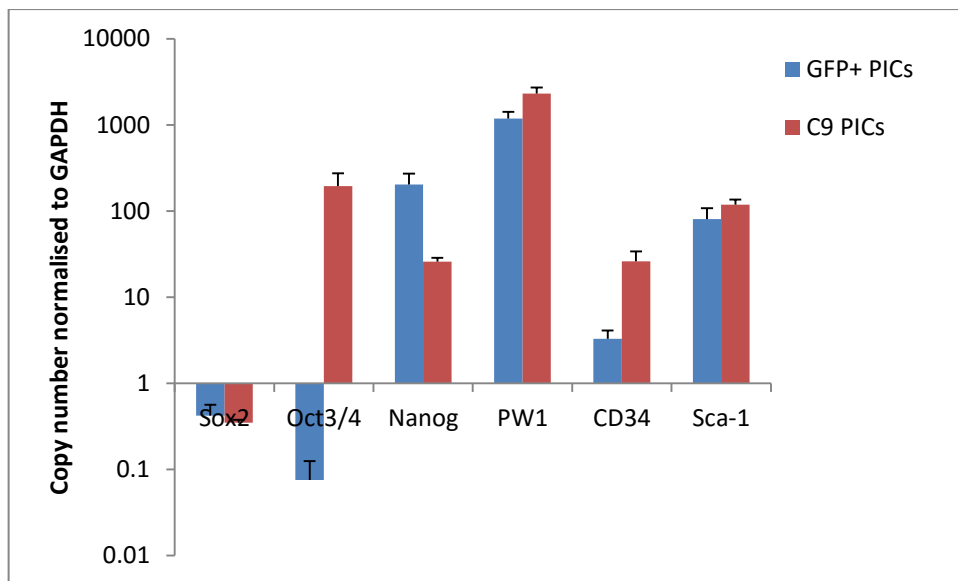
Figure 5.26   Transcription profile of GFP transfected PICs. Transcript analysis by qRT-PCR of GFP$^+$ PICs (P8) vs. C9 PICs (P10). Bars represent the transcript copy number normalised to GAPDH. Error bars represent the standard deviation of the mean, n=triplicate.
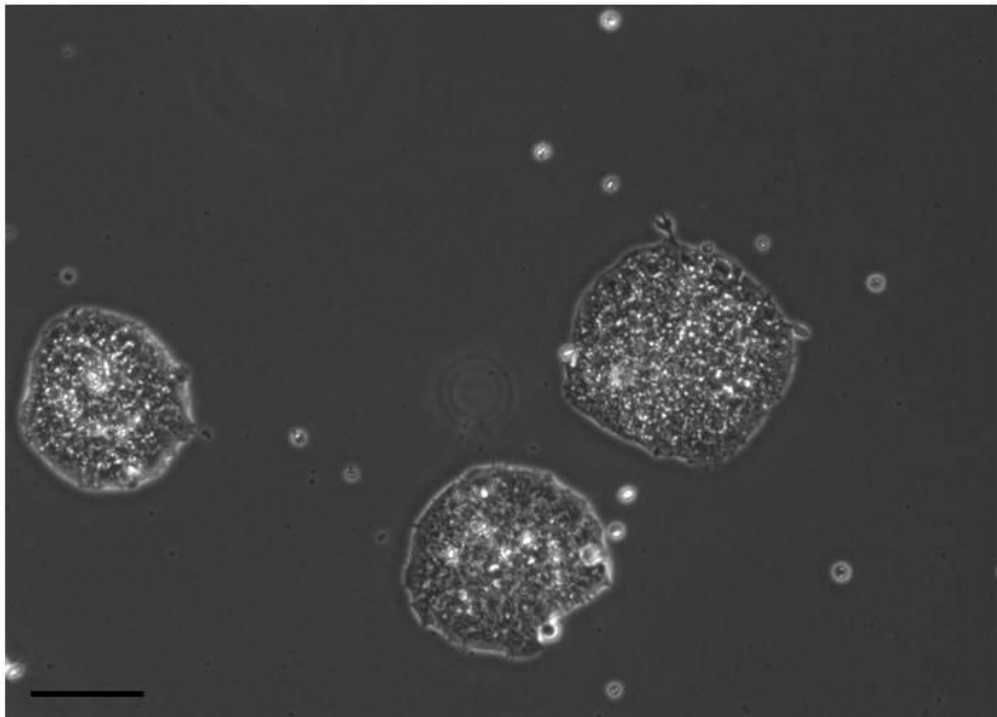
Figure 5.27   ESC morphology. Transmitted light microscope observations of
ESCs colonies prior to transplantation. Scale = 100μm
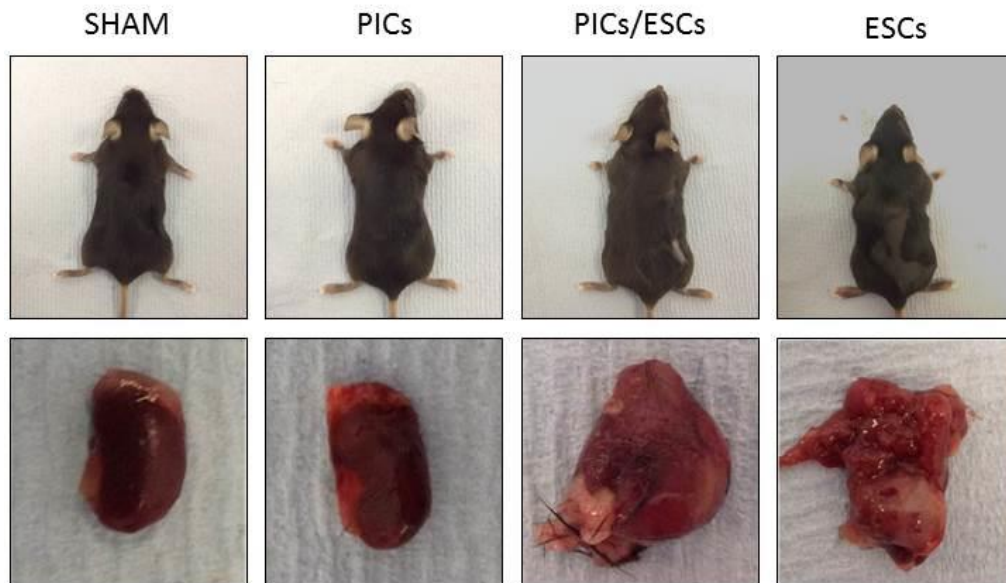
Figure 5.28   Teratoma formation in mice. Hair loss and teratomas viewed on

the kidney of mice after 4 weeks. No teratomas found in SHAM (n=2) or PIC only

(n=3) treated animals. Hair loss and teratoma formation seen in PIC/ESC (n=3)

and ESC only (n=2) treated animals.
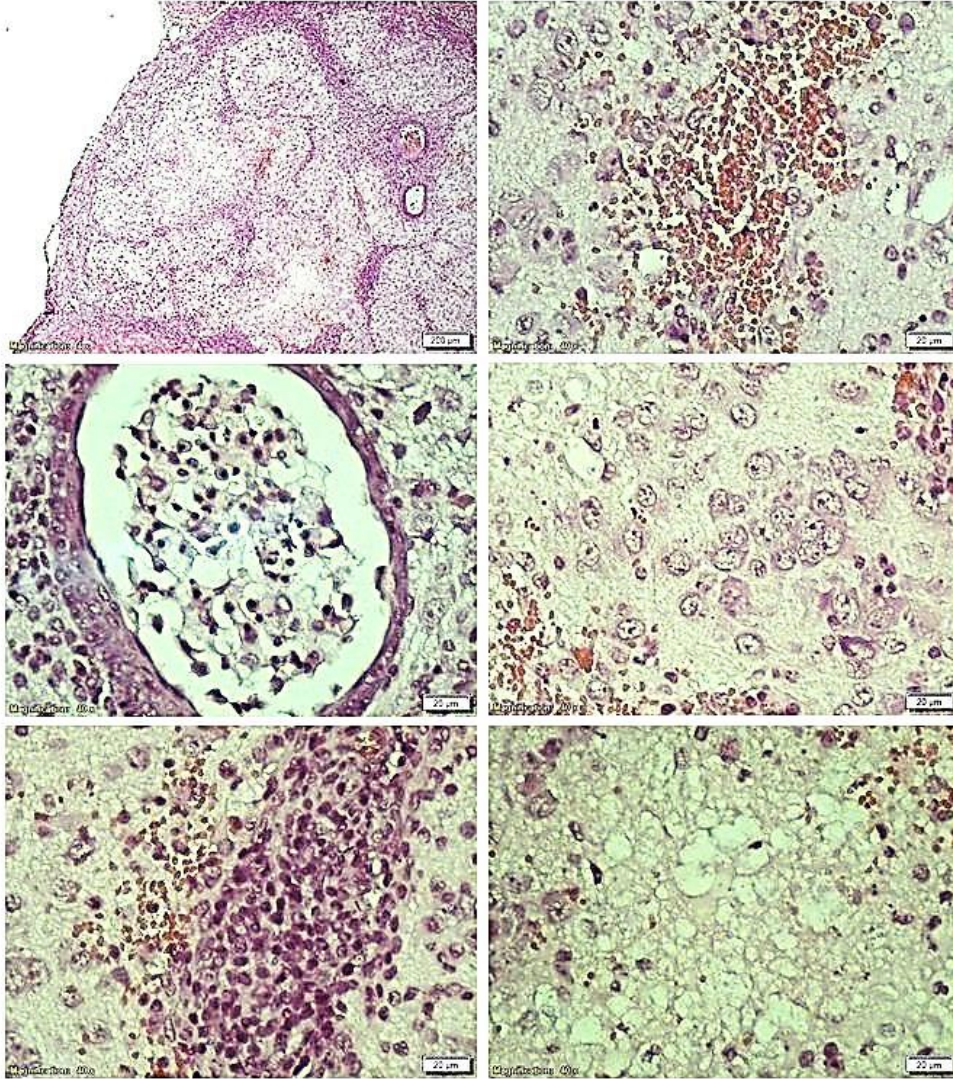
Figure 5.29 **Tumour morphology.** Variety of morphologies seen in teratomas; visualised by haematoxylin and eosin staining. Scale = 200μm (top left) and 20μm in all other images.
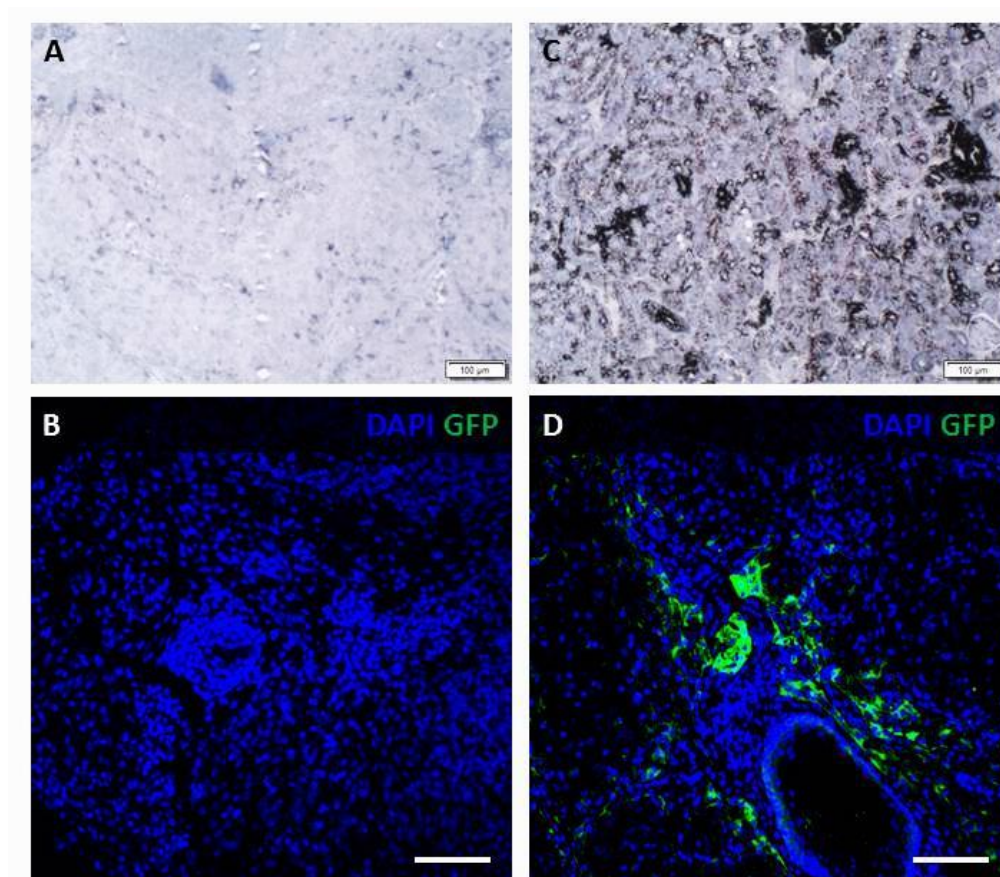
Figure 5.30   GFP staining of teratomas. No GFP was detected in teratomas generated in ESC only treated mice by DAB (**A**) or IHC (**B**); green. GFP was detected by DAB staining (**C**) and IHC (**D**); green in tumours from GFP$^+$ PIC/ESC treated mice. Nuclei were counterstained with DAPI (blue), scale = 100μm.
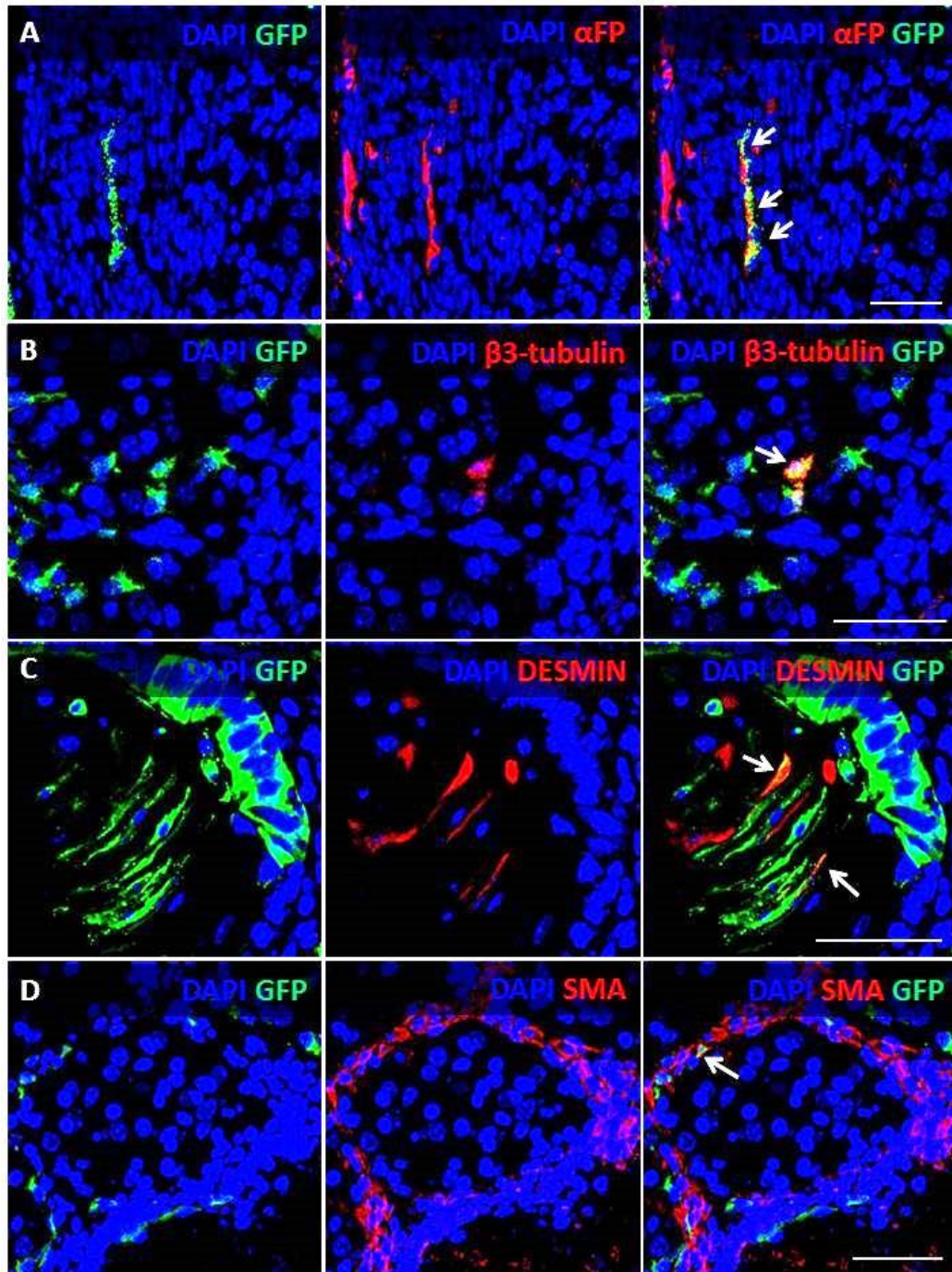
Figure 5.31   Teratomas from PIC/ESC treated mice display GFP$^+$ cells from the 3 germ layers. GFP staining (green) by IHC co-expressed (arrows) with αFP (**A**); red, β3-tubulin (**B**); red, DESMIN (**C**); red and SMA (**D**); red. Nuclei were counterstained with DAPI (blue), scale = 50µm. Arrows indicate co-localisation with GFP.

173

5.3 Discussion

The main findings to emerge from this study are:

1. For the first time, it is shown that single-cell derived PICs can generate both skeletal and smooth muscle *in vitro,* and display differentiation potential into cardiomyocytes.

2. PICs can be driven to express proteins and transcripts of multiple cell types from the mesoderm.

3. PICs display multipotent potential expressing proteins and transcripts from cells of the 3 germ layers *in vitro* and *in vivo,* but are primarily driven towards a mesodermal and specifically skeletal muscle lineage.

4. PICs are not tumorigenic.

5.3.1 PICs can generate skeletal, cardiac and smooth muscle

Mitchell et al (2010) previously described PICs giving rise to new muscle fibres *in vivo*, which was the cell fate of the majority of PICs placed in myogenic differentiation media this study. The ratio of skeletal/smooth muscle of 80/20 is directly opposite to that found in the previous studies by Mitchell et al. (2010), Pannérec et al. (2013) and Lewis et al. (2014), whom all reported that PICs predominantly formed smooth muscle *in vitro* with a fusion index of only 20-30% skeletal muscle.

Both Mitchell et al. (2010) and Pannérec et al. (2013) assessed myogenic differentiation after 24-48 hours, once the formation of muscle fibres was observed. This study, in line with Lewis et al. (2014) assessed myogenic

differentiation after 5 days, however the ratio of skeletal to smooth muscle in pPICs was similar to that previously reported in the mouse, and therefore the time point of assessment for differentiation would not seem to cause the change in ratio. Furthermore, myogenic differentiation of pPICs at P3 and P40 yielded similar results and therefore implies that time in culture before differentiation is not a factor (Lewis et al. 2014).

All three previous studies (Mitchell et al.2010; Pannérec et al. 2013; Lewis et al. 2014) used heterogeneous populations whilst this study used a clonal cell line, this study is therefore the first to demonstrate that a single PIC is capable of generating both types of muscle. This may also account for the difference in ratio with the clonal cell line used displaying an affinity towards skeletal muscle, whilst the previously described heterogenous populations harbour cells that form both. Aside from the differences in ratio, all studies are in agreement that PICs are capable of forming both skeletal and smooth muscle. Importantly, the observation of twitching fibres at 5 days of differentiation indicates some functionality of the muscle fibres and not just phenotypic and biochemical expression.

Lewis et al. (2014) demonstrated directed differentiation into a cardiac muscle type, with the formation of cardiospheres and cardiomyogenic differentiation. In agreement with this, C9 PICs were able to form cardiosphere like aggregates, in which a small number were positive for cardiac specific markers (Cx43, cTnI). Cx43 is a cardiac gap junction protein, whilst cTnI binds exclusively to actin filaments in cardiomyocytes, both of these proteins were found post-differentiation with an increase in transcription over un-differentiated cells, in agreement with Lewis et al. (2014). However, cardiospheres in this study were not

seen to beat, and the low expression of Cx43 would suggest sufficient gap junctions had not formed between cells. Therefore, whilst these data indicate that PICs can form cardiomyocyte-like cells, what is not shown is whether they are capable of full maturation and functionality of *bona fide* cardiomyocytes. This lack of maturity could be a result of non-optimal culture conditions, or it may be that while PICs can be manipulated to start expressing proteins and transcripts associated with cardiomyocytes, intrinsic processes prevent them from full differentiation and maturation.

5.3.2 PICs display differentiation potential into multiple mesodermal cell types.

It was previously shown that PICs have adipogenic differentiation potential (Pannérec et al. 2013; Lewis et al. 2014), however previous differentiation was solely reported in PDGFRα^+ PICs; Sca-1$^+$/PDGFRα^+ cells in skeletal muscle have been described as adipogenic progenitors (Uezumi et al. 2010). This study used clonal PICs, which were negative for PDGFRα by FC analysis, and found that while intracellular lipid droplets were observed, cells did not adopt full adipocyte morphology. Adipogenic differentiation of pPICs also failed to differentiate fully (Lewis et al. 2014) using the same protocol, however ~33% of pPICs expressed PDGFRα. Similarly, PDGFRα^+ bone marrow derived cells possess adipogenic differentiation potential whilst their PDGFRα^- counterparts do not (Rostovskaya and Anastassiadis 2012).

It should be noted that previous studies used different differentiation medias; Pannérec et al. (2013) used DMEM, 20% FBS, 0.25µM dexamethasone, 0.5mM

isobutylmethylxanthine, 1μg/ml insulin and 5μM troglitazone for 5 days, whilst this study and Lewis et al. (2014) used low-glucose DMEM (1 g/l), 10% FBS, 1 mM dexamethasone, 50 mM hydrocortisone for 7 days. Therefore it may be that the protocol was not sufficient to drive full differentiation.

Further to myogenic and cardiomyogenic differentiation, Lewis et al. (2014) also demonstrated endothelial differentiation of cardiospheres derived from pPICs; this present study is the first to show direct endothelial differentiation potential. However, full differentiation and maturity was not displayed.

These data suggest that PICs are capable of expressing proteins and transcripts from multiple cell types of mesodermal tissues, further work would be needed to determine whether they are capable of full differentiation.

Promisingly other similar skeletal muscle derived stem cells (Sca1$^+$/CD45$^-$/c-kit$^+$) have been shown to contribute to all 3 major blood lineages, 3 months post-transplant after bone marrow irradiation (Jackson et al. 1999).

A similar ability is also seen in embryonic mesoangioblasts which are capable of generating endothelial cells, adipocytes, smooth muscle, osteoblasts, cartilage, myotubes and cardiomyocytes *in vitro* and/or *in vivo* (Minasi et al. 2002).

5.3.3 PICs have multipotent potential *in vitro* and *in vivo*

For the first time, this study demonstrated that PICs can cross the germ layer barrier *in vitro* and contribute to the formation of cell types from all three lineages *in vivo.* However, whilst these assays suggest a broad differentiation potential with up regulation of lineage specific markers for all 3 germ layers, they do not demonstrate any functionality of PIC derived cells. In both differentiation assays

PICs showed an affinity towards the mesodermal lineage, with higher transcript levels and fold changes *in vivo*, and more GFP[+] PICs co-expressing mesodermal proteins, than endodermal or ectodermal ones *in vivo.* Furthermore, *in vitro* differentiation resulted in immature cells suggesting that either PICs are not capable of full differentiation due to intrinsic processes, or a more efficient differentiation protocol is needed to drive full maturation.

The ability to cross the germ-layer barrier is rare but not unknown in ASC populations; In 2007, Beltrami et al. demonstrated that Oct3/4[+]/Nanog[+]/REX1^{+} human multipotent adult stem cells (hMASCs), isolated from the liver, heart and bone marrow, were capable of cross-lineage differentiation *in vitro*, each demonstrating differentiation into neuron (ectoderm), osteoblast (mesoderm) and hepatocyte (endoderm) like cells.

Similarly, murine PDGFRα[+] cardiac resident cCFU stem cells are capable of hepatic, endoderm and neuronal differentiation *in vitro.* Furthermore, when GFP labelled cCFUs cells were transplanted alongside unlabelled ESCs under the kidney capsule of a mouse, resulting teratomas contained GFP expressing cells from all 3 germ layer lineages (Chong et al. 2011).

Furthermore, Muscle-derived stem cells, obtained via pre-plating, have previously been shown to differentiate into hepatocyte-like cells when co-cultured with hepatocytes, expressing albumin and HNF1α (Bellayr et al. 2010). When injected into liver tissue following partial hepatectomy, they engraft and persist >3 months post transplantation (Bellayr et al. 2010).

The functionality of cells generated *in vitro* is hard to determine, and behaviour *in vitro* does not necessarily encapsulate the behaviour of their *in vivo* counterparts. Importantly, DiI labelled adult neural stem cells have shown transdermal differentiation, contributing to the formation of chimeric chick and mouse embryos, and to cell formation of all 3 germ layers (Clarke et al. 2000). This suggests that some ASC populations are capable of generating functional cells of multiple lineages.

In agreement with this study; Pannérec et al. (2013) previously reported that PICs express genes for multiple cell fates: PW1 is most widely expressed in skeletal muscle and the CNS in postnatal tissue (Besson et al. 2011), interestingly PICs demonstrated the highest transcripts for genes associated with these two lineages.

This raises the question; Are PW1 cells in skeletal muscle the same population as found in the CNS? If so, it may be that PICs are primed for multiple cell fates dependent of their niche.

5.3.4 PICs are not tumorigenic

PICs did not form teratomas *in vivo* suggesting they have multipotent potential, but are not pluripotent, as also seen in PDGFRα$^+$ cardiac resident MSC-like stem cells (Chong et al. 2011). Importantly, the inability of PICs to form teratomas independently means they are good candidates to be used in cellular therapies.

6. PW1 Expression in the Heart

6.1 Introduction

PW1 has previously been described as being expressed in the heart during embryological development. The heart is the first mesodermal derivative to down regulate PW1 between 8-10 days post coitum (p.c), however PW1 is later expressed in the atria by 16 days p.c (Relaix et al. 1996; Besson et al. 2011). Furthermore, PW1 mRNA has been detected in postnatal mouse hearts, with a decrease between 1-4 weeks of age (Finkielstain et al. 2009).

PW1 expression has previously been shown to overlap with multiple adult stem cell populations including Lrg5^{+} intestinal stem cells, spermatogonia, Runx2^{+} osteogenic progenitors, Sox9^{+} chondrogenic progenitors, CNS stem cells, HSCs and Epidermal stem cells (Besson et al. 2011). In line with this it would be expected that PW1 could also be expressed in adult cardiac stem cell populations: Yaniz-Galende et al. (2014) reported that 1.5±1.4 % of murine cardiac cells express PW1, located mainly in the epicardium and myocardial interstitium. When PW1^{+} cells were isolated from mice 52±22% co-expressed Sca-1 and 43±14% co-expressed PDGFRα, whilst only ~6±5% expressed c-kit. Furthermore, after MI there is a 3 fold increase in the number of PW1^{+} cells.

This study will quantify overall PW1 expression in cardiac tissue during postnatal development and in aged tissue. Furthermore, isolated Sca-1^{+} CSCs will be tested for PW1 expression.

6.2 Methods

6.2.1 Quantitative Immunohistochemistry

Cardiac sections of 3, 10, 21 day and 2 year old mice (n=3 per age group) were stained as described in methods (Section 2.3), for antibodies listed in Table 6.1. Total nuclei, PW1$^+$ nuclei and total cardiomyocytes were counted (n=60 fields of view per animal in all groups, 20 per region: endocardium, epicardium and mid-wall). Cardiomyocytes were identified as having a fully intact cell membrane and central nuclei; PW1 staining was nuclear. Standard deviation was calculated from the mean of each animal per group (n=3 per group).

Table 6.1   Antibodies used on paraffin embedded cardiac tissue sections.

Primary Antibody	Dilution	Incubation	Secondary Antibody
PW1 (Gifted by David Sassoon, Inserm, Paris)	1:3000	Overnight at 4°C	Alexa Fluor 488 Donkey anti-Rabbit (Stratech)
Laminin (Sigma)	1:50	1 Hour at 37°C	Alexa Fluor 594 Donkey anti-Chicken (Stratech)

CSCs were isolated and cultured as described (see Sections 2.5.2 and 2.6) and their phenotype confirmed by immunocytochemistry, flow cytometry and qRT-PCR.

6.2.2 Immunocytochemistry

Immunocytochemistry was conducted as per methods (Section 2.8) for antibodies

and their applications listed in table 4.1. The number of positive cells/nuclei was

quantified as a percentage of total nuclei (n=100 cells per marker).

Table 6.2   Antibodies used in immunocytochemistry of cytospin slides.

Primary Antibody	Dilution	Incubation	Secondary Antibody
Sca-1 (Abcam)	1/50	1 hour at 37°	Alexa Fluor 488 Donkey anti-Rat (Stratech)
PW1 (Gifted by David Sassoon, Inserm, Paris)	1/3000	1 hour at 37°	Cy 3 Donkey anti-Rabbit (Stratech)
CD45 (Santa Cruz)	1/50	1 hour at 37°	Alexa Fluor 594 Donkey anti-Rat (Stratech)
c-kit (RnD Systems)	1/50	1 hour at 37°	Alexa Fluor 488 Donkey anti-Rabbit (Stratech)
LRG5 (Santa Cruz)	1/50	1 hour at 37°	Alexa Fluor 488 Donkey anti-Goat (Stratech)

6.2.3 Flow Cytometry

Flow cytometry was conducted as per methods (Section 2.6) using antibodies and

relevant controls described in Table 6.3.

Table 6.3   Antibodies used in Flow Cytometry

Antibody	Conjugate/ Secondary	Control	Dilution	Incubation
PW1 (Gifted by David Sassoon, Inserm, Paris)	Alexa Fluor 488 Donkey anti-Rabbit (Stratech)	Alexa Fluor 488 Donkey anti-Rabbit (Stratech)	1/20	15 minutes at 4°C
CD31 (eBioscience)	FITC Conjugated	FITC Rat IgG isotype Control (Abcam)	1/20	15 minutes at 4°C
Pdgfrα (Santa Cruz)	Dylight 488 Donkey anti-Goat (Stratech)	Dylight 488 Donkey anti-Goat (Stratech)	1/20	15 minutes at 4°C

6.2.4 qRT-PCR

qRT-PCR was conducted as per methods (Section 2.8) using the primers listed in

Table 6.4.

Table 6.4   Primer sequences

Gene	Accession Number	Forward	Reverse
Sox2	NM_011443.3	CACAACTCGGAGATCAGCAA	CTCCGGGAAGCGTGTACTTA
Oct3/4	NM_013633.2	CCAATCAGCTTGGGCTAGAG	CTGGGAAAGGTGTCCCTGTA
Nanog	NM_028016.2	TACCTCAGCCTCCAGCAGAT	GTGCTGAGCCCTTCTGAATC
c-kit	NM_021099.3	TTATCCTTTAGGCCGTGTGG	TGTGGCCCCTTAAGTACCTG
PW1	NM_008817.2	TTTTGGTGAGTTGCTTGCAG	ACGTTCTTGGGCATAACTGG
CD34	NM_133654.3	GGGTAGCTCTCTGCCTGATG	TCTCTGAGATGGCTGGTGTG
SCA1	NM_001271446.1	CCATCAATTACCTGCCCCTA	AAGGTCTGCAGGAGGACTGA
CD45	NM_011210.3	CCTGCTCCTCAAACTTCGAC	GACACCTCTGTCGCCTTAGC
CD31	NM_001032378.1	GCCTCACCAAGAGAACGGAAGGC	TGGGCCTTCGGCATGGAACG
GAPDH	NM_008084.2	ACCCAGAAGACTGTGGATGG	CACATTGGGGGTAGGAACAC

6.2 Results

6.2.1 PW1 Expression and Distribution in Cardiac Tissue

First the nuclei expression of PW1 in cardiac longitudinal cross sections was assessed at 3, 10 and 21 days and 2 years; PW1$^+$ cells were observed in interstitial spaces, no cardiomyocyte nuclei expressed PW1 (Figure 6.1).

The abundance of PW1 expression decreased ($p<0.05$) during the first 3 weeks postnatal, there was no further decrease in aged mice (Figure 6.2). PW1$^+$ cells were predominantly found in the epicardium in all ages (Figure 6.3).

In line with this, numbers of PW1$^+$ cells per 10^4 cardiomyocytes reduced between 3-21 days (Figure 6.4) with greater PW1$^+$ cells per cardiomyocyte in epicardial regions (Figure 6.5).
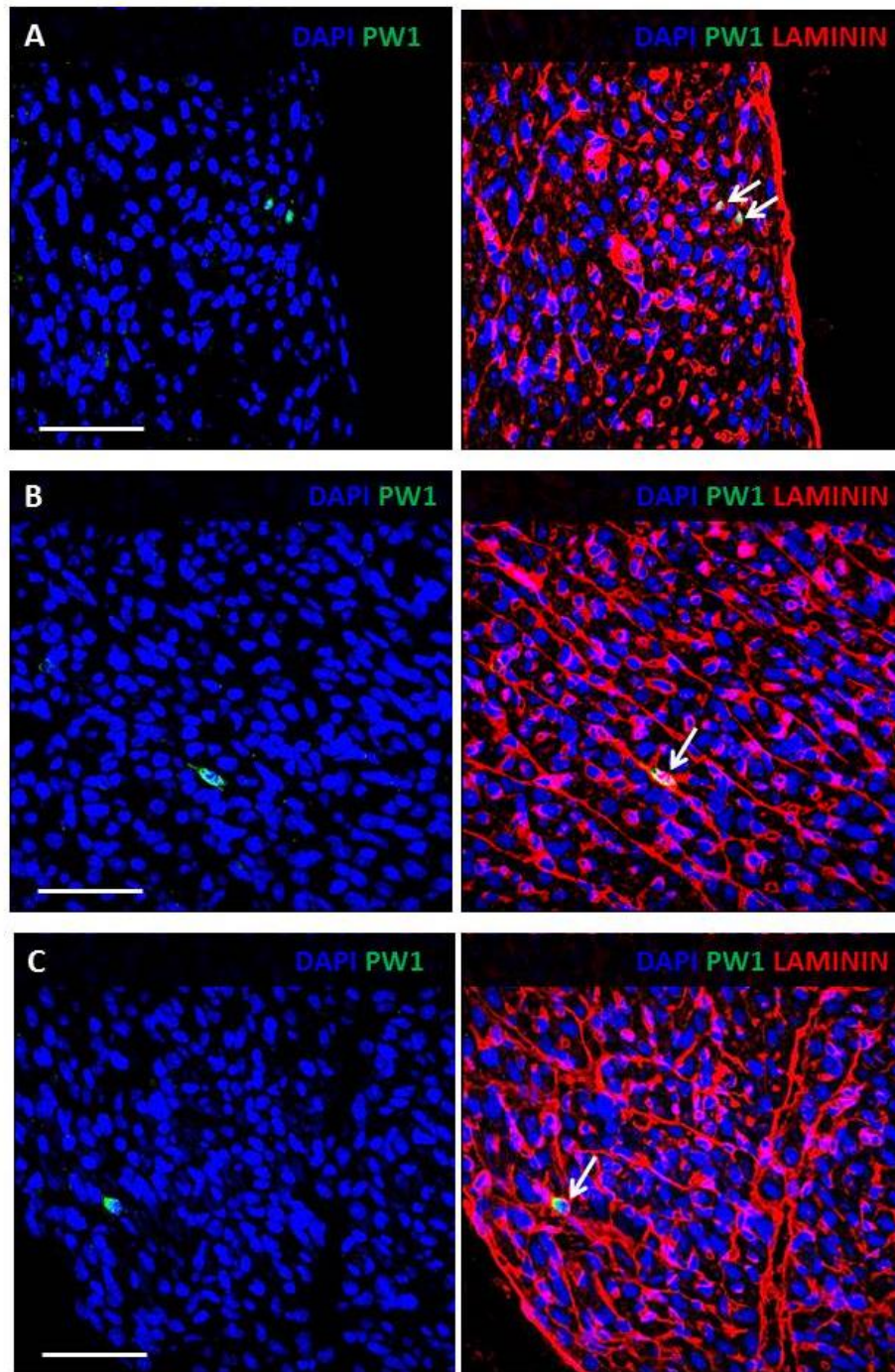
Figure 6.1   Identification of PW1 in murine cardiac tissue. 10 day old

mouse epicardium (**A**), mid-wall (**B**) and endocardium (**C**); stained for PW1 (red),

laminin (green) and nuclei identified by DAPI (blue). Scale = 50µm.
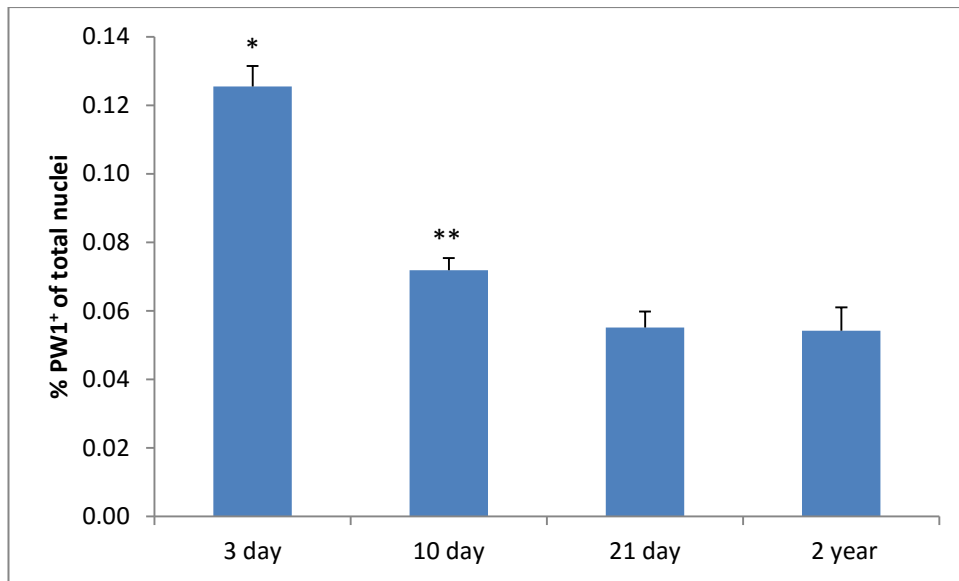
Figure 6.2   PW1 abundance in cardiac tissue with age. PW1 expression as a percentage of total nuclei in 3, 10 and 21 day, and 2 year old mice. Data is mean ±SD, n=3 per group. * denotes significant differences (p<0.05) vs 10, 21 day and 2 year; ** denotes significant differences (p<0.05) vs 21 day and 2 year.
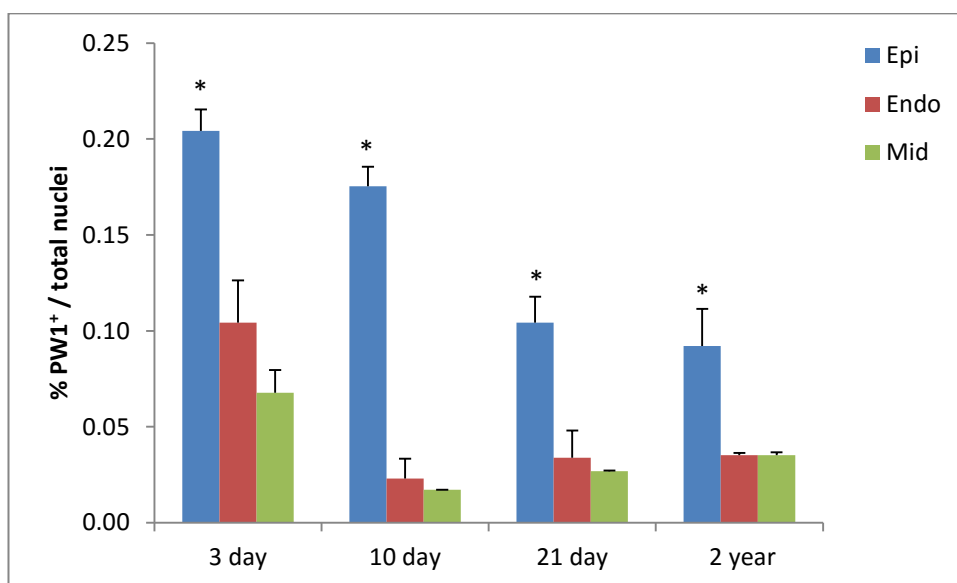
Figure 6.3   PW1 abundance in the three cardiac layers. PW1 expression as

a percentage of total nuclei in 3, 10 and 21 day, and 2 year old mice for each layer:

epicardium (Epi), endocardium (Endo) and mid-wall (Mid). Data is Mean ±SD,

n=3 per group. * denotes significant differences (p<0.05) vs. Endo and Mid for

that time point.
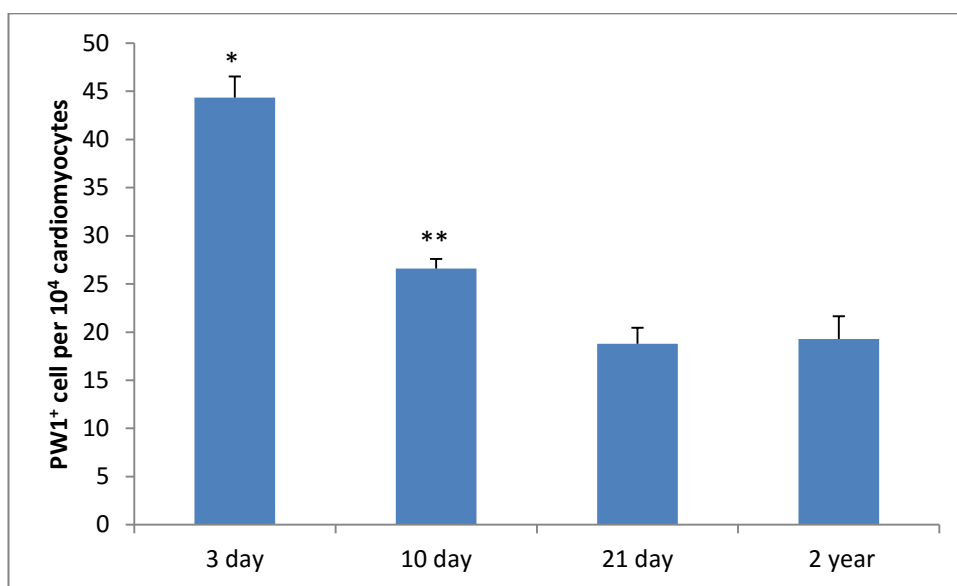
Figure 6.4 **The number of PW1 nuclei per 10^4 cardiomyocytes between 3 days and 2 years.** The number of PW1$^+$ nuclei per 10^4 cardiomyocytes in 3, 10, and 21 day and 2 year old mice. Data is Mean ±SD, n=3 per group. * denotes significant differences (p<0.05) vs. 10 day, 21 day and 2 year; ** denotes significant differences (p<0.05) vs. 21 day and 2 year.
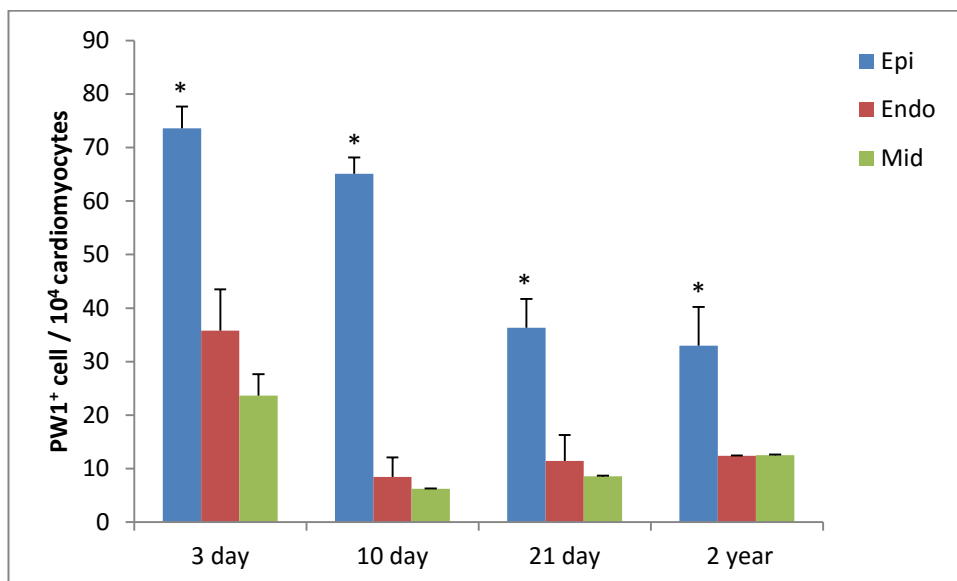
Figure 6.5   The number of PW1 nuclei per 10^4 cardiomyocytes in the three

cardiac layers. The number of PW1$^+$ nuclei per 10^4 cardiomyocytes in 3, 10 and

21 day, and 2 year old mice in each layer: epicardium (Epi), endocardium (Endo)

and mid-wall (Mid). Data is mean ±SD, n=3 per group. * denotes significant

differences ($p<0.05$) vs Endo and Mid for each time point.

6.2.2 Isolation of CD45⁻ /Sca-1⁺ cardiac stem cells (CSCs)

Murine hearts from 21 day old mice were perfused and enzymatically digested. The CD45⁻/Sca-1⁺ fraction was obtained via MACS technology and propagated in culture (Figure 6.6) (see Methods 2.4.2).

ICC of cytospin slides of P3 Sca-1⁺ CSCs confirmed they were CD45⁻/Sca-1⁺ and were negative for CD45, positive for Sca-1 and also positive for PW1 (Figure 6.7). Furthermore, this Sca-1⁺ cell population contained a subset of c-kit+ (7%) and LRG5⁺ (15%) cells (Figure 6.8).

FC analysis quantified PW1 expression (83%) whilst determining the Sca-1⁺ CSCs were also negative for CD31 and PDGFRα (Figure 6.9).

The transcriptome profile of P3 Sca-1⁺ CSCs was assessed by qRT-PCR; They expressed Sca-1, PW1, CD34 and the pluripotency marker Nanog. Transcript levels of Sox2, Oct3/4 and c-kit were negligible (Figure 6.10).

The clonogenicity of Sca-1⁺ CSCs assessed at P5 was 38±7% (Figure 6.11) and they maintained a stable population doubling time of 37±2 hours over 20 passages (Figure 6.12).
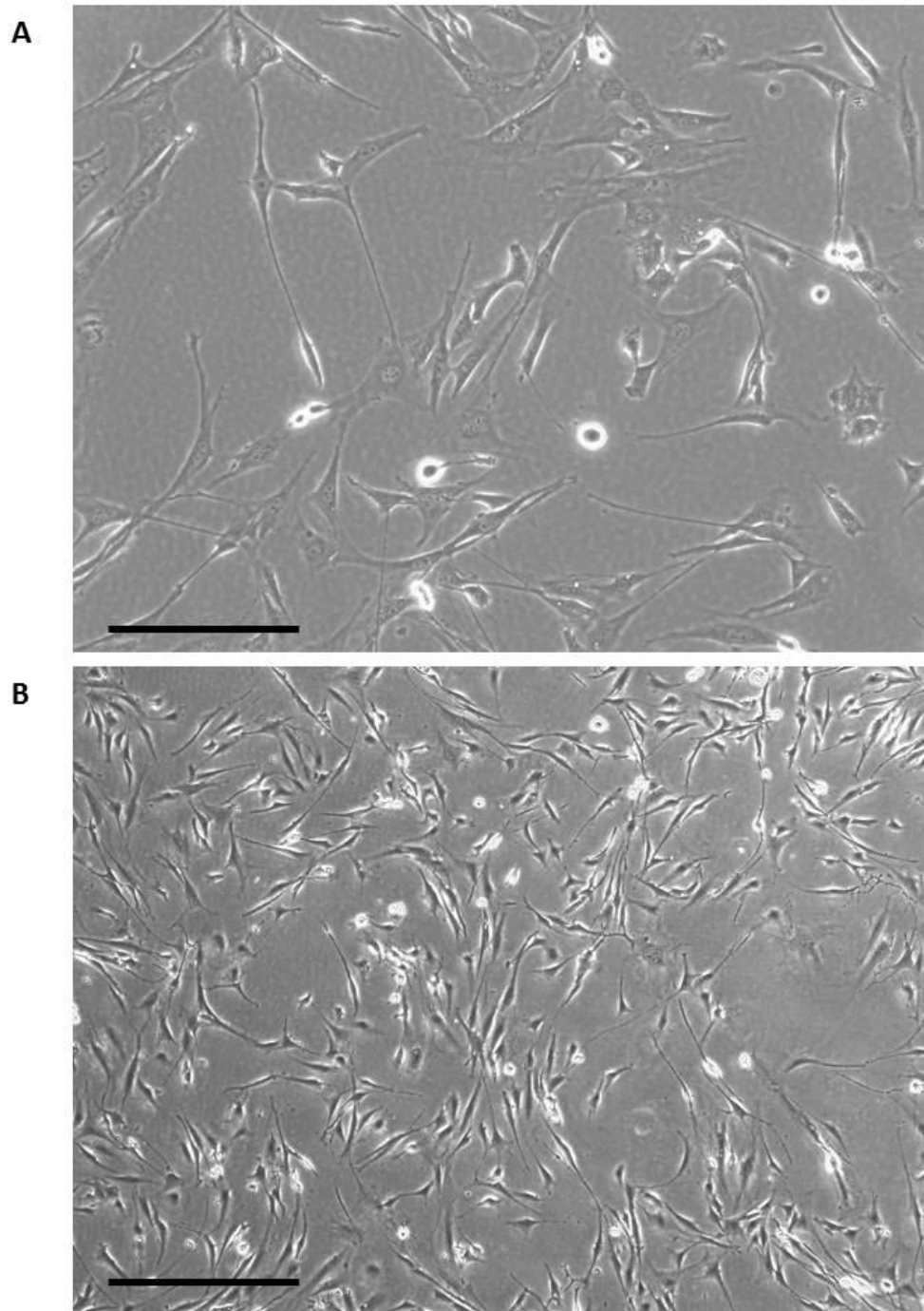
Figure 6.6**Isolated cell morphology.** Transmitted light microscope observation of CD45^{-}/Sca-1^{+} CSC's isolated from 21 day old mice hearts at P0 (**A**) and P3 (**B**). Scale =200µm.
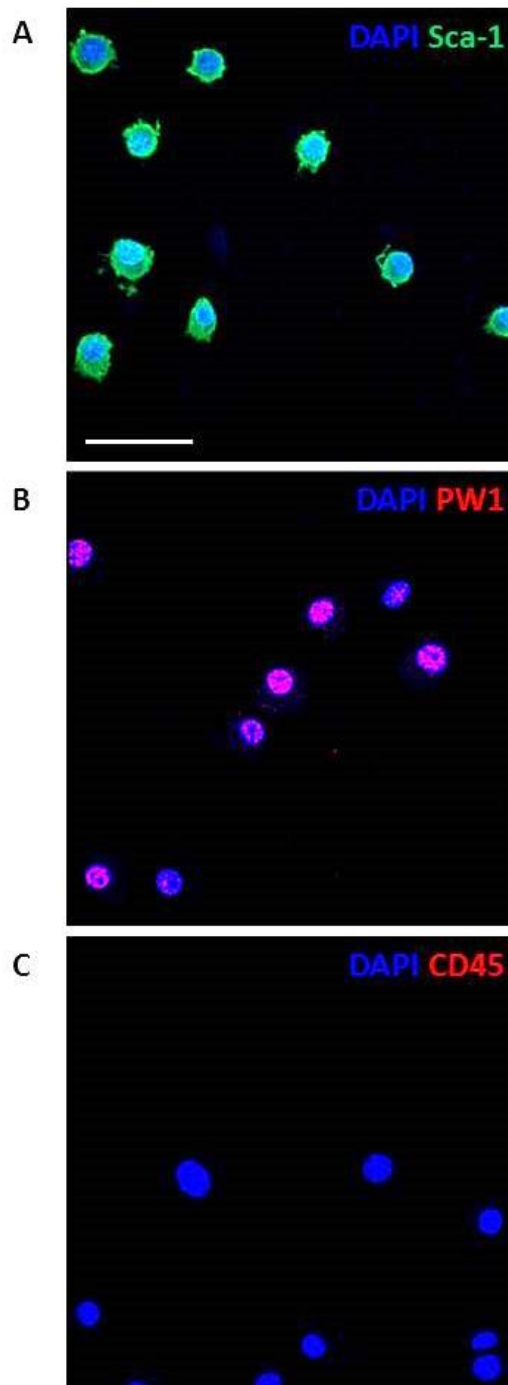
Figure 6.7   Phenotype by ICC. Expression of CD45⁻/Sca-1⁺ CSCs by ICC at

P3: showing positivity for Sca-1 (green; **A**), PW1 (red; **B**) and negativity for

CD45 (red; **C**). Nuclei visualised with DAPI (blue). Scale =50μm.
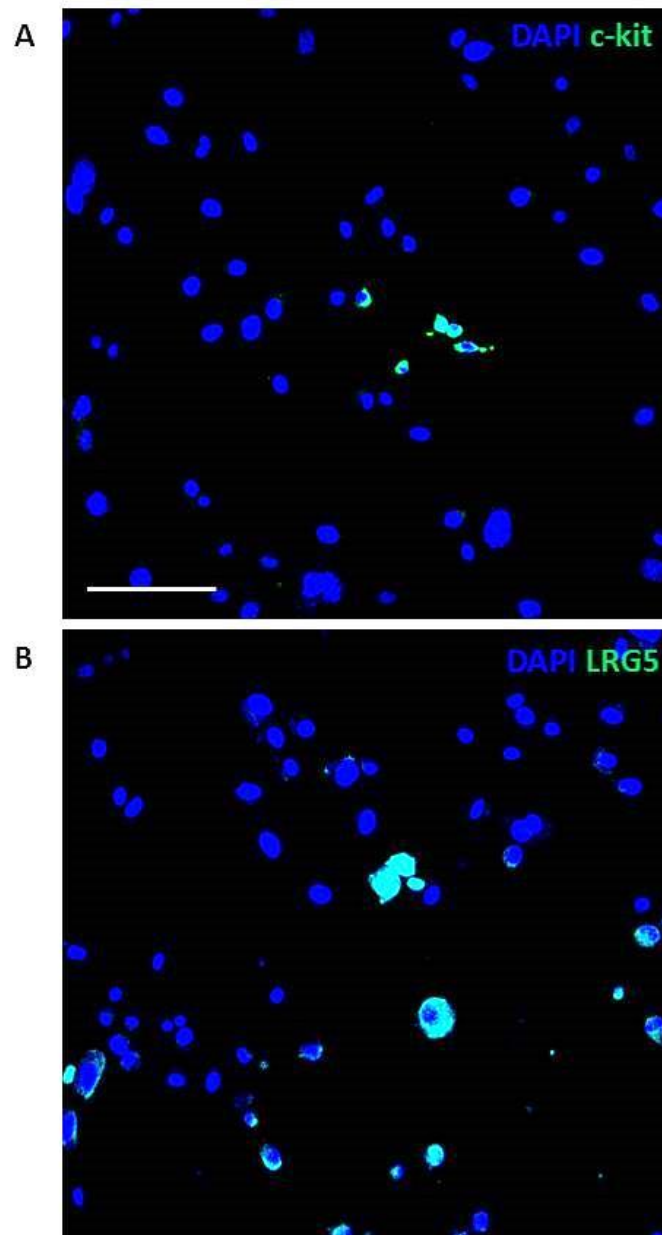
Figure 6.8   **Sca-1$^+$ CSCs contain c-kit$^+$ and LRG5$^+$ fractions.** Expression of

CD45$^-$/Sca-1$^+$ CSCs by ICC at P3: showing positivity for c-kit (green; **A**) and

LRG5 (green; **B**). Nuclei visualised with DAPI (blue). Scale =100µm.
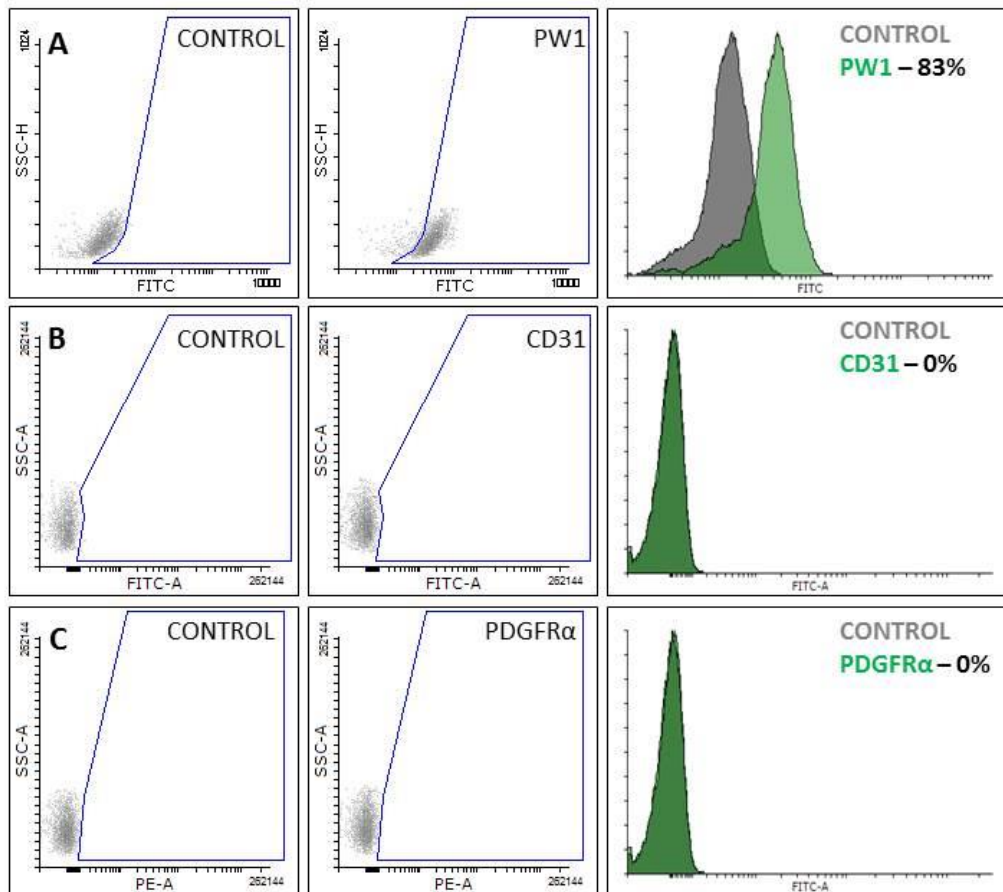
Figure 6.9 **Phenotype by FC.** Phenotyping of CD45⁻/Sca-1⁺ cells by FC at P3: showing positivity for PW1 (**A**) and negativity for CD31 (B) and PDGFRα (**C**). Control are cells stained with isotype controls.
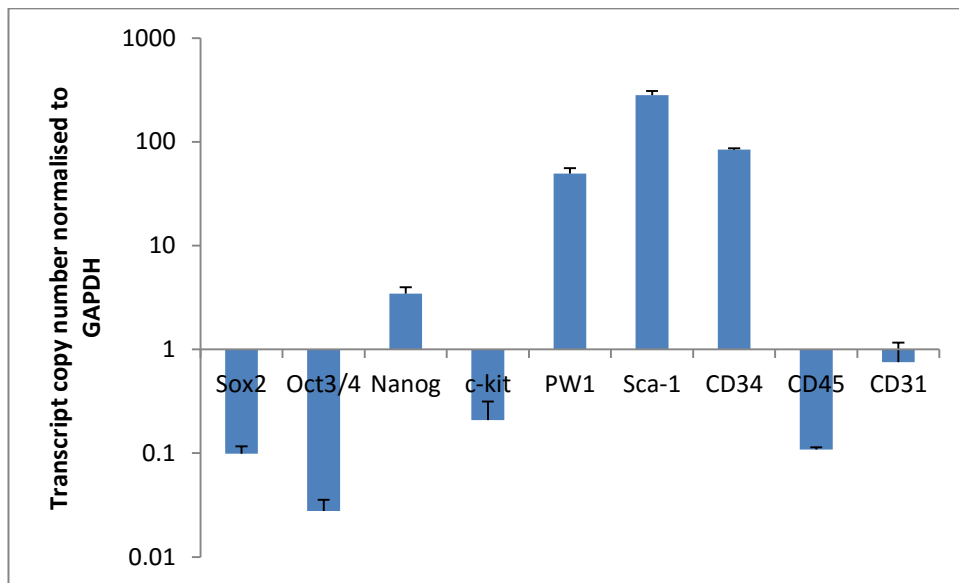
Figure 6.10   Sca-1$^+$/PW1$^+$ CSC transcript profile. qRT-PCR of CSCs at P3.

Bars represent the transcript copy number normalised to GAPDH. Error bars

represent the standard deviation of the mean, n=triplicate.
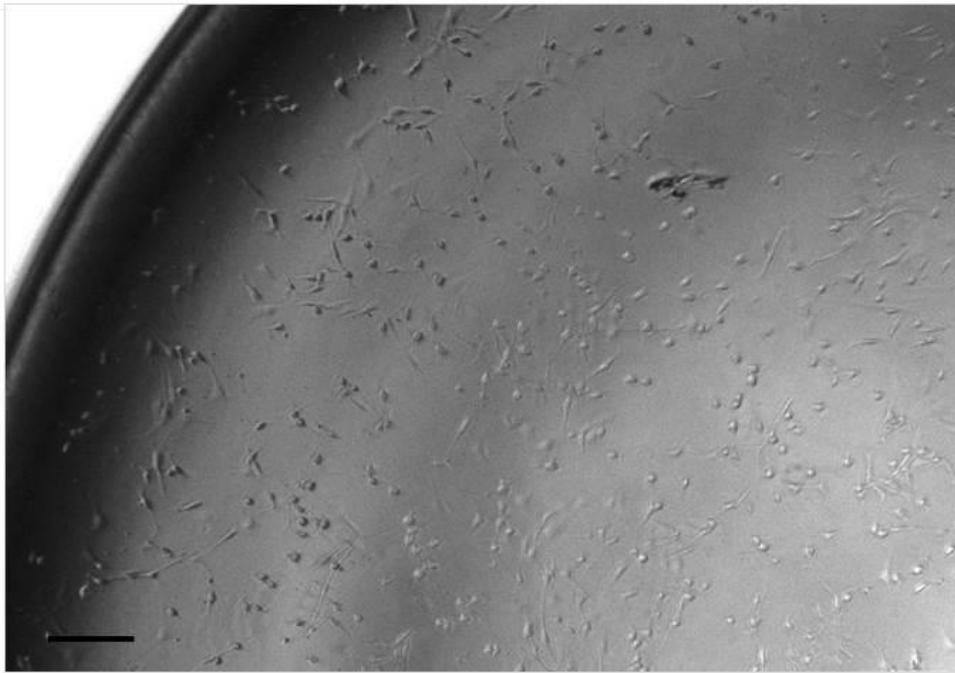
Figure 6.11 **Sca-1$^+$/PW1$^+$ CSCs are clonogenic.** Transmitted light microscope observation of a clonal population after 14 days in a 96 well plate. Scale =200µm.
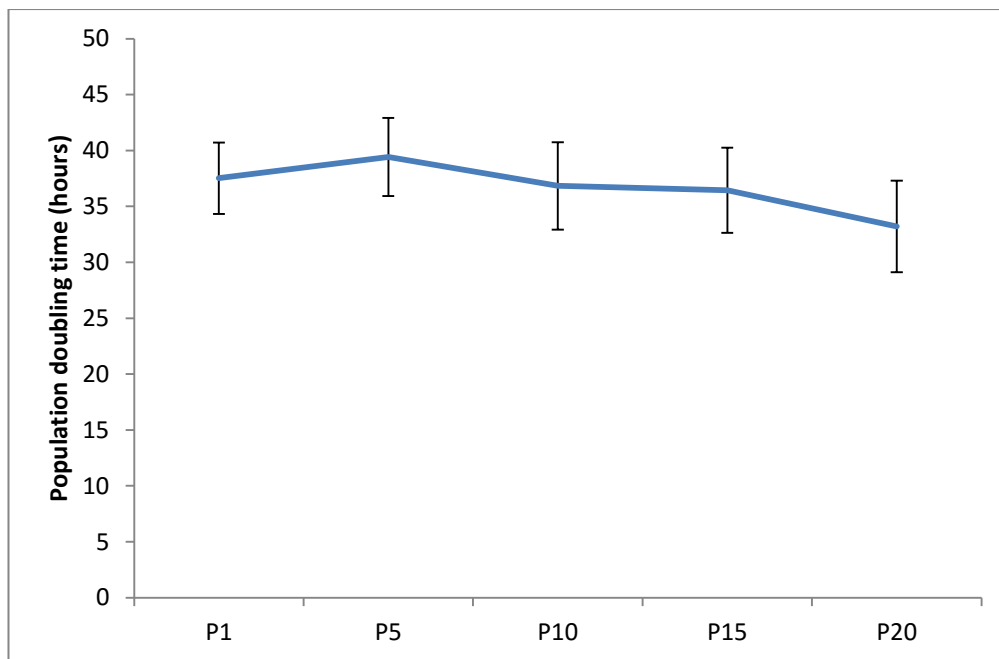
Figure 6.12 **Sca-1$^+$/PW1$^+$ CSC population doubling time.** Doubling time between P1 and P20. Data are the Mean $\pm$ SD, n=3.

6.3 Discussion

The main findings that emanated from this study were:

1. PW1 cells are present in the heart.

2. $PW1^+$ cells decreased for the first 3 weeks of postnatal development, and maintained their number at 2 years.

3. $PW1^+$ cells are mostly expressed in the epicardium.

4. $CD45^-/Sca-1^+$ CSCs express PW1.

6.3.1 PW1 expression in the heart

The expression of PW1 in cardiac tissue and the decline in PW1 abundance over the first 3 weeks of postnatal development corroborated previous data; Indeed, Finkielstain et al. (2009) reported a ~5 fold decline in PW1 mRNA in mice between 1-4 weeks of age, with a lesser ~2 fold reduction seen in rats between 3-9 weeks. Furthermore, the percentage of $PW1^+$ nuclei in the present study was similar to that described by Yaniz-Galande et al. (2014). PW1 expression in cardiac tissue of aged animals had not previously been described. Interestingly, unlike in skeletal muscle, in the present study PW1 expression was not reduced in aged animals. As PW1 marks stem cell populations, it would be expected that the abundance of PW1 would mirror the abundance of stem cells in aged tissue.

6.3.2 PW1 marks CSC populations

To date the abundance of most cardiac stem/progenitor cells, including $Sca-1^+$ CSCs in aged animals has not been quantified. However, the abundance of $c-kit^+$ CSCs has been shown to increase in aged hearts, with a ~2 fold increase between 4 and 22 months old rats (Torella et al. 2004); In the present study there was no

difference between 21 days and 2 years, however it is possible that PW1 declines further than 21 days into adulthood before increasing in aged animals. Further time points during adult life would be needed to support this theory.

Matsuura et al. (2004) reported that Sca-1$^+$ cells are found at a frequency of 33 per 10^4 cardiomyocytes in 10-12 week old mice. The present study reported ~19 PW1$^+$ nuclei per 1 x 10^4 cardiomyocytes, at both 21 days and 2 years. Tomita et al. (2005) described Sca-1$^+$ SP cells in the heart which account for 3.5% of all cells at 2 days of age. In this present study PW1 was seen in ~0.1% of cells at 3 days. These data suggest that not all Sca-1$^+$ cells within the heart express PW1. In this present study, PW1 was expressed in 83% of isolated CD45$^-$/Sca-1$^+$ cells, however this was after culture and therefore may not be representative of freshly isolated cells and the percentage found *in vivo*.

In the present study, Sca-1$^+$/PW1$^+$ CSCs were low or negative for c-kit expression. Matsuura et al. (2004) reported that ~9% of Sca-1 cells from the heart co-express c-kit, and this also included CD45$^+$ (40%) mast cells. In contrast ~45% of c-kit$^+$ CSCs express Sca-1 (Smith et al. 2014). It was not determined here whether the c-kit$^+$ CSCs express PW1.

The majority of PW1$^+$ cells were situated in epicardial regions; which are similar to that reported by Yaniz-Galende et al. (2014). These data support an epicardial origin, and could be similar to the previously described Sca-1$^+$ cardiac derived cCFU population, which similar to PICs in this present study, demonstrated multi lineage differentiation potential *in vitro* and *in vivo* (Chong et al. 2011), however isolated Sca-1$^+$/PW1$^+$ CSCs did not express PDGFRα.

These data suggests that PW1 does indeed mark a proportion of cardiac stem/progenitor cells. However, whether this proportion corresponds to an independent population, or is comprised of subsets from multiple populations remains to be determined (see Section 7). Indeed, it is known that PW1 marks skeletal mesoangioblasts, and may therefore also mark MABs of cardiac origin.

Isolated Sca-1$^+$/PW1$^+$ CSCs maintained a stable doubling time over 20 passages and were clonogenic, which together with their phenotype suggest the cells demonstrated properties of cardiac stem/progenitor cells. Sca-1$^+$ CSCs in the study by Wang et al. (2014) had a similar phenotype, with a comparable morphology and were stable *in vitro* over >50 passages. From these data it may be deduced that Sca-1$^+$ /PW1$^+$ cells isolated here represent the same Sca-1$^+$ cells as described by Wang et al. (2014); which were also shown to differentiate into the three cardiac lineages; cardiomyocyte, endothelial and smooth muscle cells *in vitro*. Furthermore, they were not tumourigenic when injected into SCID (severe combined immune deficiency) mice (Wang et al. 2014).

In summary, these data suggest PW1 is not expressed by all cardiac derived stem/progenitor cells. However, its abundance mostly co-insides with cells from epicardium regions and it is highly expressed in CD45$^-$/Sca-1$^+$ CSCs.

7. DISCUSSION

PW1[+] PICs are found within interstitial spaces of skeletal muscle at a similar frequency to satellite cells, declining in abundance with age. Isolated PICs display stem cell properties of self-renewal, clonogenicity and multipotency *in vitro*; they can be propagated over long term culture whilst maintaining their phenotype, and are multipotent but not tumourigenic *in vivo*. PW1 also marks an epicardial derived Sca-1^{+} stem cell population in the heart.

7.1 PW1 expression with ageing

PW1 marks multiple stem cell populations found throughout the mammalian body (Besson et al. 2011) inclusive of PICs, SC's and a subset of CSC's. Most recently, PW1 has also been identified in mesoangioblasts from the mouse, dog and human (Bonfanti et al. 2015).

Bonfanti et al. (2015) postulated that PW1 expression may be linked to stem cell competence, as PW1^{-} MABs displayed inhibited myogenic potential compared to their PW1^{+} counterparts. Furthermore, silencing PW1 inhibited the ability of MABs to cross the endothelium (Bonfanti et al. 2015). Moreover, PW1 has previously been implicated as a mediator of embryonic and post-natal growth (Finkielstain et al. 2009), and the decline in PW1 in both skeletal and cardiac muscle with age would seem to be linked to the decrease in growth velocity post-natally.

The decrease in PW1 expression in skeletal muscle of aged animals, seen as a decrease in both PICs and SC's, was not mirrored in cardiac tissue. However, the

cellular turnover of these two muscles is vastly different; skeletal muscle demonstrates a higher rate of cell proliferation and regenerative capacity then cardiac tissue. Indeed, c-kit[+] CSC's are maintained within their niche, and increase in aged animals (Torella et al. 2004). However it is not yet conclusively determined if the c-kit[+] CSC population also express PW1. . The present study showed low/negative c-kit expression in Sca-1^{+}/PW1^{+} CSCs in the heart. Lewis et al. (2014) showed that 17% of PW1^{+} PICS isolated from porcine skeletal muscle and propogated in culture expressed c-kit. Further analysis of heart sections for PW1 and c-kit expressing cells are warranted. The mechanism behind why some ASC populations decrease in abundance with age, but others do not is not yet known; however, it may be linked to stem cell aging. Other ASC populations that have previously been shown to decline in abundance with age; include SP cells of the bone marrow (Garvin et al. 2007), keratinocytes (Blanpain and Fuchs 2009) and neuronal stem cells (Kuhn et al. 1996).

The decline in PICs and SC abundance may be due to replicative aging, causing them to become senescent and drop out of the cell compartment. The remaining PICs and SC's, may be chronologically aged; however, aged satellite cells have been shown to regain their function when transplanted into a 'younger' environment, suggesting that chronological aging processes may be reversible (Conboy et al. 2005).

Chronologically aged cells such as CSCs which have undergone minimal replicative aging do not drop out of the compartment; thus their abundance is maintained. However, this does not mean they will have the same regenerative capacity as their younger counterparts. It should be noted that chronological and

replicative aging are not exclusive of each other, and many cells will be aged by both processes.

In light of this, when deriving stem cell therapies the following question should be considered: Does the stimulation of endogenous ASCs to proliferate *in vivo* speed up the aging process?

7.2 PICs vs. CSCs

PICs and CSC's share multiple characteristics and phenotypic properties. Indeed, both are negative for the hematopoietic marker CD45 and positive for Sca-1, with sub-sets also expressing c-kit (Lewis et al. 2014). PICs and CSCs have been shown to efficiently contribute to new skeletal or cardiomyocyte formation *in vivo* (Mitchell et al. 2010; Beltrami et al. 2003; Oh et al. 2004; Takamiya et al. 2011). The present study shows for the first time the self-renewing and clonogenic potential of $PW1^+/Sca-1^+$ PICs isolated from skeletal and cardiac muscle. Similar properties have been shown for $Sca-1^+$ CSCs (Pfister et al. 2005; Tomita et al. 2005; Chong et al. 2011). Furthermore, colony forming $Sca-1^+$ cells isolated from 12 week old mice hearts have shown osteogenic, chondrogenic, smooth muscle, endothelial and cardiac differentiation *in vitro* (Takamiya et al. 2011). Moreover, a subset of $Sca-1^+$ cardiac CFU cells originated from the epicardium have shown similar multipotent differentiation potential as the $PW1^+$ PICs in this study when transplanted in a teratoma formation assay (Chong et al. 2011). Whether this multipotent potential results in functional regeneration of multiple tissues *in vivo* remains to be tested. Finally, the cardiac $PW1^+/Sca-1^+$ cells in the present study were located in the epicardium, which together with their multipotent

differentiation potential in vivo, suggests they are the same or a derivative cell of the Sca-1$^+$ cCFU cells, described by Chong et al. (2011).

The similarities between skeletal muscle and cardiac derived PW1$^+$ cells raise the possibility that they are tissue specific counterparts of the same universal ASC population.

7.3 The overlap of ASC populations within the body

There are a plethora of purported ASC populations, many share similar phenotypes, differentiation potential, and reside within the same niche e.g. pericytes and PICs both form SC's and subsequent myotubes (Cappellari and Cossu. 2013; Mitchell et al. 2010). It may be that these cell types describe sub-sets of a single population, displaying various phenotypic markers dependent on their location and differentiation state. Indeed, this is apparent in the heart, which was previously thought to be post-mitotic; since the first discovery of CSCs a number of different cardiac progenitor cells have been described. If the heart did indeed contain multiple stem cell populations we would expect it to have a higher regenerative capacity than it demonstrates (Ellison et al. 2014). Further to this, some ASC's such as SP cells and pericytes are found in multiple tissues and organs throughout the body suggesting they represent a 'global' cell population and are not tissue specific (Armulik et al. 2011; Unno et al. 2011; Asakura et al. 2002; Preffer et al. 2002). Moreover, ASC's from a variety of different tissues express similar markers such as PW1 (Besson et al 2011; Mitchell et al. 2010; Bonfanti et al. 2015); Whether PW1 is independently expressed by multiple stem cell populations, or indicates that these ASC populations originate from the same lineage remains to be determined. The multipotent potential of purported ASC's

varies, from progenitor cells such as SC's, which are capable of limited differentiation into myotubes; to stem cells which are capable of generating several cell types within their germ layer (e.g pericytes of the mesoderm and PW1$^+$ PICs in the present study). Interestingly, a small number of ASC populations have demonstrated broad developmental plasticity; generating cell types form multiple germ layers, such as neuronal stem cells (Clarke et al. 2000), cCFUs (Chong et al. 2011) and hMASCs (Beltrami et al. 2007).

In the present study we showed that PW1$^+$ PICs have the potential to give rise to cells from the 3 germ layers, both *in vitro* and *in vivo*. However, the number of PW1$^+$ PICs that generated endo- and ecto-derm cells was minimal in the teratoma assay, and their functional competence was not validated. Further investigation into whether PICs can regenerate damaged tissue (such as brain and heart) *in vivo* is warranted.

It could be hypothesized that the adult mammalian body harbors a small number of truly multipotent ASC's that are responsible for the replenishment and homeostasis of germ layer specific ASCs (Figure 7.2). These germ-lineage specific ASC's would in turn maintain tissue specific progenitor cell populations (e.g SC's), to facilitate the regeneration of tissues with injury or age in a cascade effect. Thus a stem cells multipotent potential is greater the higher up the hierarchy they are (Figure 7.2).

Whilst many ASC populations have been extensively characterized, there is not yet an exclusive marker of a truly multipotent ASC. If they do exist, these cells would represent a tiny percentage of all cells within the mammalian body; thus,

they have so far eluded detection and subsequent characterization. If an exclusive

marker can be found, lineage tracing studies could then be used to track these

cells and their progeny, testing this hypothesis (Figure 7.2).
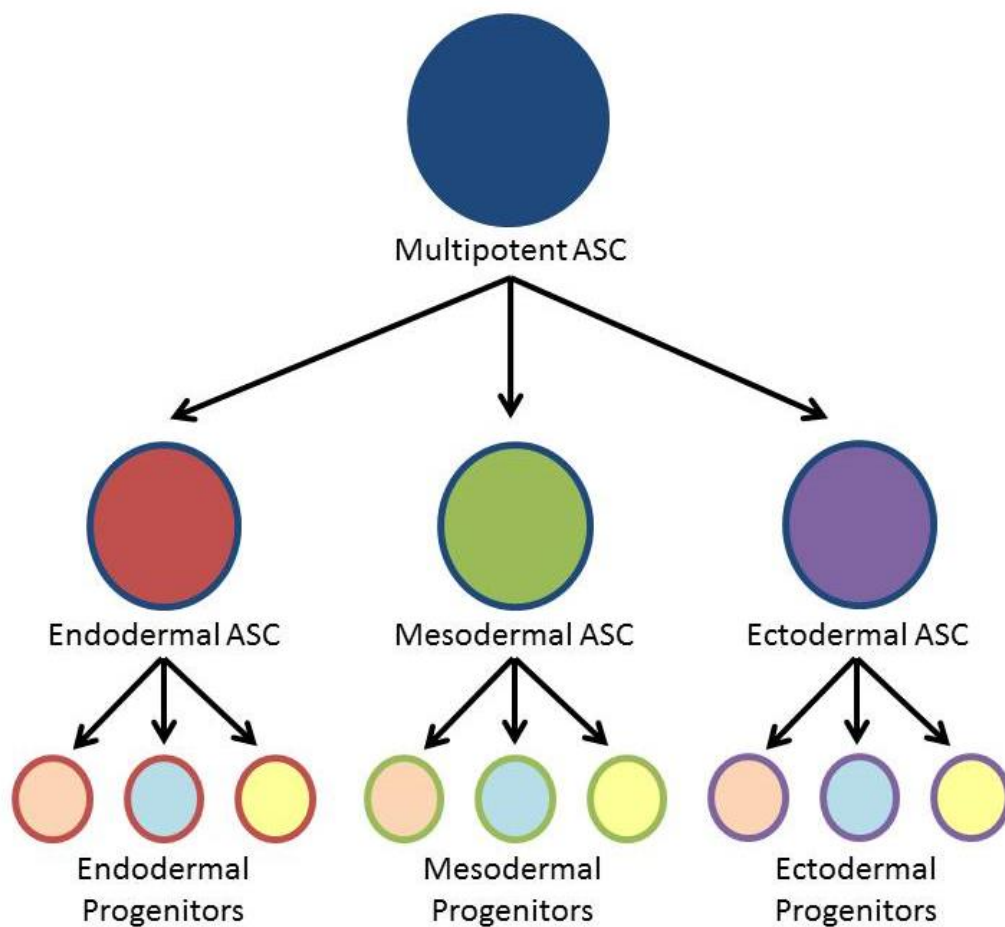
Figure 7.2   Schematic to show proposed hierarchy of ASC populations.

Size of circle indicates level of potency**.**

7.4 PICs are candidates for a multipotent ASC population.

The present study has demonstrated that's PICs express genes for multiple cell fates and have true stem cell characteristics of self-renewal, clonogenicity and multipotency *in vitro* and *in vivo*. They are also present in the heart. They have been shown to restore muscle after injury (Mitchell et al. 2010), however their ability to contribute to functional and sufficient regeneration of other tissues is yet to be determined. If PICs are found to be capable of such functional regeneration of other tissues, they would be representative of a truly multipotent ASC.

7.5 PICs in regenerative medicine.

PICs are candidates for stem cell therapy for regeneration of skeletal muscle, as demonstrated by Mitchell et al. (2010). Furthermore, as the present study has shown, their self-renewal, proliferation and phenotype preservation in culture allows large numbers to be propagated. These can be used in cellular therapies where large numbers are required for transplantation. Importantly, the present study also showed that PICs do not form teratomas allowing for safe transplantation. However, immunological responses following transplantation might need to be determined.

Although normal homeostasis of skeletal muscle is generally efficient throughout adult life, PICs may be of use in treating age related diseases such as sarcopenia, or improving muscle regeneration and limiting fibrosis after major injury.

7.5.1 Muscular dystrophies

It has not yet been described if PICs are capable of functional repair of muscle in diseases such as DMD. However, it may be hypothesized that allogenic

transplantation of PICs from a healthy individual into a DMD patient would result in the formation of SC's and myofibres that do not contain malfunctions in the dystrophin gene. Whether transplanted PICs and their progeny would temporarily ameliorate muscle wastage, or could persist to provide long-term regenerative benefits is unknown. However, allogeneic transplantation of WT mesoangioblasts into α-sarcoglycan null mice (limb girdle muscular dystrophy model) has been shown to reconstitute skeletal muscle; with labelled cells and their progeny still present after 4 months (Sampaolesi et al. 2003). Furthermore, when transplanted into golden retrievers with muscular dystrophy, allogeneic WT mesoangioblasts resulted in the recovery of dystrophin expression, muscle morphology and function. However, 50% of dogs deteriorated after immunosuppression was stopped (Sampaolesi et al. 2006). An early phase I/II clinical trials is currently underway in Italy (EudraCT number: 2011-000176-33) to determine the safety of intra-arterial delivery of HLA-identical allogeneic mesoangioblasts in DMD patients.

7.5.2 Regeneration of other tissues

PICs are located in an easily accessible and abundant tissue within the body, with a higher concentration of cells per tissue than other rare populations, such as CSC's in the heart. Therefore, if PICs are capable of both cardiac and skeletal muscle regeneration then they may provide a source of patient-specific stem-progenitor cells in individuals with heart disease.

Furthermore, if PICs are truly representatives of a *bona fide* multipotent ASC population, regenerating multiple tissues of different lineages, then they may also potentially be used to regenerate other organs or tissues, from which their tissue

specific ASC are either a) rare or b) inaccessible or c) senescent, such as the heart or brain.

It is not known whether PICs would demonstrate an affinity to home to skeletal muscle, or whether transplanted PICs would home to other sites of injury throughout the body. However, PICs express CXCR4, which is associated with homing: Indeed, c-kit$^+$ CSCs, which display an affinity to home to the heart following injury, lose this ability when CXCR4 is knocked down, and are found in other tissues such as the spleen and lungs (Ellison et al. 2013). CXCR4 has also been implicated in the homing of other stem cells population after injury including renal stem cells of the kidney (Tögel et al. 2005) and MSCs in fracture repair (Yellowley 2013).

Although these data are promising, there are many obstacles to be overcome to determine if PICs are amenable with multiple systemic cellular therapies.

7.6 Limitations of the study.

There are several limitations to this study:

1) PICs were isolated from 21 day old mice. Thus, it is not known if the *in vitro* characteristics and multipotent potential are representative of PICs found in adult muscle (6-8 week old mice).

2) C9 PICs were used for all *in vitro* assays to demonstrate the multipotent potential of a single PIC: therefore it is not known what percentage of the bulk PIC population demonstrates these characteristics and phenotype.

3) PICs were not sorted for CD34 expression as previously described in the literature and this was due to the selection method used. MACS sorting

only allows for positive enrichment of one marker because after the first

positive enrichment all cells would continue to be labelled with magnetic

beads, preventing a second positive enrichment. MACS sorting was

utilized because as FACS sorting was not available, but also because

MACS sorting results in higher cell viability which is crucial for sorting

rare cell populations (Li et al. 2013).

This study would also benefit from the following additions:

1) PW1 and PIC abundance in different ages throughout adulthood.

2) Phenotyping of the multiple previously described CSC populations, to
   determine if PW1 is expressed in all CSC populations, or if not, which
   ones specifically. This work is now ongoing in the Ellison Laboratory.

3) To extrapolate these data to humans, PICs should be isolated and
   characterized in human skeletal and cardiac muscle.

8. CONCLUSIONS

PW1 is expressed in PICs, SC's and CSCs, declining in abundance during postnatal development. Furthermore, PICs decline at a faster rate than SC's in skeletal muscle, whilst PW1 abundance in cardiac tissue is comparable between 21 days and 2 years.

Here, it is shown for the first time that murine PICs isolated from skeletal muscle display true stem cell properties of clonogenicity, self-renewal and express pluripotency markers Oct3/4, Sox2 and Nanog. They show a small capacity for multipotency displaying proteins and transcripts of cell types from all 3 germ layers both *in vitro* and *in vivo,* although the maturity and functionality of these cells was not assessed. However, most PICs display a strong preference towards the skeletal muscle lineage from which they originate.

PICs maintain their phenotype and morphology over long-term culture, together with their clonogenicity, and without evidence of growth arrest or senescence. Furthermore, PICs are not tumorigenic. These data validate the ability of isolated PICs to undergo *in vitro* propagation in the prospect of generating large numbers of these cells to be used in cellular regenerative therapies.

9. FUTURE DIRECTIONS

Following on from these findings, a number of questions are raised that warrant further investigation:

• Do all SC's originate from PICs?

• Does PIC abundance increase following exercise or injury?

• Do PICs isolated from aged mice have the same regenerative capability as their younger counterparts?

 • Are PICs present, and in what abundance in diseased muscle?

• Can PICs regenerate cardiac tissue following an MI?

10. REFERENCES

Abdel-Latif, A., Bolli, R., Tleyjeh, I.M., Montori, V.M., Perin, E.C., Hornung, C.A., Zuba-Surma, E.K., Al-Mallah, M., Dawn, B. (2007) Adult bone marrow-derived cells for cardiac repair: a systematic review and meta-analysis. *Archives of internal medicine*, 167 (10), 989-97.

Agley, C.C., Rowlerson, A.M., Velloso, C.P., Lazarus, N., Harridge, S.D.R. (2013) Human skeletal muscle fibroblasts, but not myogenic cells, readily undergo 1 adipogenic differentiation. Journal of Cell Science, 126 (Pt24), 5610-25.

Amit, M., Carpenter, M.K., Inokuma, M.S., Chiu, C.P., Harris, C.P., Waknitz, M.A., Itskovitz-Eldor, J., Thomson, J.A. (2000) Clonally derived human embryonic stem cell lines maintain pluripotency and proliferative potential for prolonged periods of culture. *Developmental Biology*, 227(2), 271-278

Anversa, P., Kajstura, J. (1998) Ventricular Myocytes Are Not Terminally Differentiated in the Adult Mammalian Heart. Circulation Research, 83 (1), 1-14.

Armulik, A., Genové, G., Betsholtz, C. (2011) Pericytes: developmental, physiological, and pathological perspectives, problems, and promises. *Developmental Cell*, 21 (2), 193-215.

Arsalan, M., Woitek, F., Adams, V., Linke, A., Barten, M.J., Dhein, S., Walther, T., Mohr, F.W., Garbade, J. (2012) Distribution of cardiac stem cells in the human heart. *ISRN Cardiology*, 2012:483407.

Asakura, A., Komaki, M., Rudnicki, M. (2001) Muscle satellite cells are multipotential stem cells that exhibit myogenic, osteogenic, and adipogenic differentiation. *Differentiation*, 68 (4-5), 245-53.

Asakura, A., Seale, P., Girgis-Gabardo, A., Rudnicki, M.A. (2002) Myogenic specification of side population cells in skeletal muscle. *The Journal of Cell Biology*, 159(1), 123-134.

Avilion, A.A., Nicolis, S.K., Pevny, L.H., Perez, L., Vivian, N., Lovell-Badge, R. (2003) Multipotent cell lineages in early mouse development depend on SOX2 function. *Genes and Development*, 17(1), 126-140

Bakker, E., Veenema, H., Den Dunnen, J.T., van Broeckhoven, C., Grootscholten, P.M., Bonten, E.J., van Ommen, G.J.B., Pearson, P.L. (1989) Germinal mosaicism increases the recurrence risk for 'new' Duchenne muscular dystrophy mutations. *Journal of Medical Genetics*, 26 (9), 553-9.

Balsam, L.B., Wager, A.J., Christensen, J.L., Kofidis, T., Weissman, I.L., Robbins, R.C. (2004) Haematopoietic stem cells adopt mature haematopoietic fates in ischaemic myocardium. Nature, 428 (6983), 668-73.

Bartosh, T.J., Wang, Z., Rosales, A.A., Dimitrijevich, S.D., Roque, R.S. (2008) 3D-model of adult cardiac stem cells promotes cardiac differentiation and resistance to oxidative stress. *Journal of Cellular Biochemistry*, 105(2), 612-623.

Beauchamp, J.R., Heslop, L., Yu, D.S., Tajbakhsh, S., Kelly, R.G., Wernig, A., Buckingham, M.E., Partridge, T.A., Zammit, P.S. (2000) Expression of CD34 and Myf5 defines the majority of quiescent adult skeletal muscle satellite cells. *The Journal of Cell Biology*, 151(6), 1221-1234

Bellayr, I.H., Gharaibeh, B., Huard, J., Li, Y. (2010) Skeletal muscle-derived stem cells differentiate into hepatocyte-like cells and aid in liver regeneration. *International Journal of clinical and experimental pathology,* 3(7), 681-90.

Beltrami, A.P., Barlucchi, L., Torell, D., Baker, M., Limana, F., Chimenti, S., Kasahara, H., Rota, M., Musso, E., Urbanek, K., Leri, A., Kajstura, J., Nadal-

Ginard, .B., Anversa, .P. (2003) Adult Cardiac Stem Cells Are Multipotent and Support Myocardial Regeneration. *Cell*, 114, 763-776.

Beltrami, A.P., Cesselli, D., Bergamin, N., Marcon, P., Rigo, S., Puppato, E., D'Aurizio, F., Verardo, R., Piazza, S., Pignatelli, A., Poz, A., Baccarani, U., Damiani, D., Fanin, R.,Mariuzzi, L., Finato, N., Masolini, P., Burelli, S., Belluzzi, O., Schneider, C., Beltrami, CA. (2007) Multipotent cells can be generated in vitro from several adult human organs (heart, liver, and bone marrow). *Blood*, 110(9), 3438-3446

Berger, M.J., Doherty, T.J. (2010) Sarcopenia: prevalence, mechanisms, and functional consequences. *Interdisciplinary Topics in Gerontology*, 37, 94-114.

Bergmann, O., Bhardwaj, R.D., Bernard, S., Zdunek, S., Barnabé-Heider, F., Walsh, S., Zupicich, J., Alkass, K., Buchholz, B.A., Druid, H., Jovinge, S., Frisén, J. (2009) Evidence for cardiomyocyte renewal in humans. *Science,* 324(5923), 98-102.

Bertoni, C. (2014) Emerging gene editing strategies for Duchenne muscular dystrophy targeting stem cells. *Frontiers in Physiology*, 5, 148.

Besson, V., Smeriglio, P., Wegener, A., Relaix, F., Nait Oumesmar, B., Sassoon, D., Marazzi, G. (2011) PW1 gene/paternally expressed gene 3 (PW1/Peg3) identifies multiple adult stem and progenitor cell populations. *Proceedings of the national academy of sciences of the united states of America*, 108(28), 11470-5.

Bischoff, R. (1974) Enzymatic liberation of myogenic cells from adult rat muscle. *The Anatomical Record*, 180(4), 645-661

Blake, D.J., Weir, A., Newey, S.E., Davies, K.E. (2002) Function and Genetics of Dystrophin and Dystrophin-Related Proteins in Muscle. Physiological Reviews, 82 (2), 291-329.

Blanpain, C., Fuchs, E. (2009) Epidermal homeostasis: a balancing act of stem cells in the skin. Nature Reviews: *Molecular Cell Biology*, 10 (36), 201-17.

Bolli, R., Chugh, A.R., D'Amario, D., Loughran, J.H., Stoddard, M.F., Ikram, S., Beache, G.M., Wagner, S.G., Leri, A., Hosoda, T., Sanada, F., Elmore, J.B., Goichberg, P., Cappetta, D., Solankhi, N.K., Fahsah, I., Rokosh, D.G., Slaughter, M.S., Kajstura, J., Anversa, P. (2011) Cardiac stem cells in patients with ischaemic cardiomyopathy (SCIPIO): initial results of a randomised phase 1 trial. *Lancet*, 378(9806),1847-1857.

Bondue, A., Tännler, S., Chiapparo, G., Chabab, S., Ramialison, M., Paulissen, C., Beck, B., Harvey, R., Blanpain, C. (2011) Defining the earliest step of cardiovascular progenitor specification during embryonic stem cell differentiation. *The Journal of Cell Biology*, 192(5), 751-765.

Bonfanti, C., Rossi, G., Tedesco, F.S., Giannotta, M., Benedetti, S., Tonlorenzi, R., Antonini, S., Marazzi, G., Dejana, E., Sassoon, D., Cossu, G., Messina, G. (2015) PW1/Peg3 expression regulates key properties that determine mesoangioblast stem cell competence. *Nature Communications,* 6:6364. doi: 10.1038/ncomms7364.

Bosnali, M., Münst, B. Their, M., Edenhofer, F. (2009) Deciphering the stem cell machinery as a basis for understanding the molecular mechanism underlying reprogramming. *Cellular and molecular life sciences*, 66(21), 3403-3420.

Cappellari, O., Cossu, G. (2013) Pericytes in development and pathology of skeletal muscle. *Circulation Research*, 133 (3), 341-7.

Cardasis, C.A., Cooper, G.W. (1975) An analysis of nuclear numbers in individual muscle fibers during differentiation and growth: a satellite cell-muscle fiber growth unit. *The Journal of Experimental Zoology*, 191 (3), 347-58.

Carlson, B. M., Faulkner, J. A. (1989) Muscle transplantation between young and old rats: age of host determines recovery. *The American Journal of Physiology*, 256, C1262–C1266.

Carr, C.A., Stuckey, D.J., Tan, J.J., Tan, S.C., Gomes, R.S., Camelliti, P., Messina, E., Giacomello, A., Ellison, G.M., Clarke, K. (2011) Cardiosphere-derived cells improve function in the infarcted rat heart for at least 16 weeks--an MRI study. *PLoS One,* 6(10),e25669.

Chamberlain, J.S., (2002) Gene therapy of muscular dystrophy. *Human Molecular Genetics*, 11 (20), 2355-62.

Chambers, I., Colby, D., Robertson, M., Nichols, J., Lee, S., Tweedie, S., Smith, A. (2003) Functional expression cloning of Nanog, a pluripotency sustaining factor in embryonic stem cells. *Cell*, 113(5), 643-655

Chien, K.R., Olson, E.N. (2002) Converging pathways and principles in heart development and disease: CV@CSH. *Cell,* 110(2),153-162.

Chong, J.J., Chandrakanthan, V., Xaymardan, M., Asli, N.S., Li, J., Ahmed, I., Heffernan, C., Menon, M.K., Scarlett, C.J., Rashidianfar, A., Biben, C., Zoellner, H., Colvin, E.K.,Pimanda, J.E, Biankin, A.V., Zhou, B., Pu, W.T., Prall, O.W., Harvey, R.P. (2011) Adult cardiac-resident MSC-like stem cells with a proepicardial origin. *Cell Stem Cell*, 9(6), 527-540

Chugh, A.R., Beache, G.M., Loughran, J.H., Mewton, N., Elmore, J.B., Kajstura, J., Pappas, P., Tatooles, A., Stoddard, M.F., Lima, J.A.C., Slaughter, M.S., Anversa, P., Bolli, R. (2012) Administration of cardiac stem cells in patients with ischemic cardiomyopathy: the SCIPIO trial: surgical aspects and interim analysis of myocardial function and viability by magnetic resonance. *Circulation*, 126 (11 suppl 1), s54-64.

Clarke, D.L., Johansson, C.B., Wilbertz, J., Veress, B., Nilsson, E., Karlström, H., Lendahl, U., Frisén, J. (2000) Generalized potential of adult neural stem cells. *Science*, 228, 1660-1663

Collins, C.A., Olsen, I., Zammit, P.S., Heslop, L., Petrie, A., Partridge, T.A., Morgan, J.E. (2005) Stem cell function, self-renewal, and behavioral heterogeneity of cells from the adult muscle satellite cell niche. *Cell*, 122(2), 289-301.

Conboy, I.M., Rando, T.A. (2002) The regulation of Notch signaling controls satellite cell activation and cell fate determination in postnatal myogenesis. *Developmental Cell*, 3 (3), 397-409.

Conboy, I.M., Conboy, M.J., Wagers, A.J., Girma, E.R., Weissman, I.L., Rando, T.A. (2005) Rejuvenation of aged progenitor cells by exposure to a young systemic environment. *Nature*, 433 (7027), 760-4.

Cornetta, K., Morgan, R.A., Anderson, W.F. (1991) Safety issues related to retroviral-mediated gene transfer in humans. *Human Gene Therapy*, 2(1), 5-14

Cosgrove, B.D., Sacco, A., Gilbert, P.M., Blau, H.M. (2009) A home away from home: challenges and opportunities in engineering in vitro muscle satellite cell niches. *Differentiation*, 78 (2-3), 185-94.

Cossu, G., Bianco, P. (2003) Mesoangioblasts - vascular progenitors for extravascular mesodermal tissues. *Current Opinion in Genetics & Development. 13, 537-542.*

Cossu, G., Sampaolesi, M. (2007) New therapies for Duchenne muscular dystrophy: challenges, prospects and clinical trials. Trends in Molecular medicine, 13 (12), 520-6.

Davis, D.R., Zhang, Y., Smith, R.R., Cheng, K., Terrovitis, J., Malliaras, K., Li, T.S., White, A., Makkar, R., Marbán, E. (2009) Validation of the cardiosphere method to culture cardiac progenitor cells from myocardial tissue. *PLoS One*, 4(9):e7195.

Day, K., Shefer, G., Shearer, A., Yablonka-Reuveni Z. (2010) The depletion of skeletal muscle satellite cells with age is concomitant with reduced capacity of single progenitors to produce reserve progeny. *Developmental Biology*, 340 (2), 330-43

Dellavalle, A., Sampaolesi, M., Tonlorenzi, R., Tagliafico, E., Sacchetti, B., Perani, L., Innocenzi, A., Galvez, B.G., Messina, G., Morosetti, R., Li, S., Belicchi, M., Peretti, G., Chamberlain, J.S., Wright, W.E., Torrente, Y., Ferrari, S., Bianco, P., Cossu, G. (2007) Pericytes of human skeletal muscle are myogenic precursors distinct from satellite cells. *Nature Cell Biology*, 9 (3), 255-67.

Dellavalle, A., Maroli, G., Covarello, D., Azzoni, E., Innocenzi, A., Perani, L., Antonini, S., Sambasivan, R., Brunelli, S., Tajbakhsh, S., Cossu, G. (2011) Pericytes resident in postnatal skeletal muscle differentiate into muscle fibres and generate satellite cells. *Nature Communications*, 2, 499.

Dyce, P.W., Zhu, H., Craig, J., Li, J.(2004) Stem cells with multilineage potential derived from porcine skin. *Biochemical and Biophysical Research Communications*, 316 (3), 651-8.

Eglitis, M.A., Mezey, E. (1997) Hematopoietic cells differentiate into both microglia and macroglia in the brains of adult mice. *Proceedings of the national academy of sciences of the united states of America*, 96 (8), 4080-5.

Ellison, G.M., Torella, D., Karakikes, I., Nadal-Ginard, B. (2007) Myocyte death and renewal: modern concepts of cardiac cellular homeostasis. *Nature Clinical Practice, Cardiovascular Medicine*. 4 Suppl 1, s52-59.

Ellison, G.M., Torella, D., Dellegrottaglie, S., Perez-Martinez, C., Perez de Prado, A., Vicinanza, C., Purushothaman, S., Galuppo, V., Iaconetti, C., Waring, C.D., Smith, A., Torella, M., Cuellas, Ramon, C., Gonzalo-Orden, J.M., Agosti, V., Indolfi, C., Galiñanes, M., Fernandez-Vazquez, F., Nadal-Ginard, B. (2011) Endogenous cardiac stem cell activation by insulin-like growth factor-1/hepatocyte growth factor intracoronary injection fosters survival and regeneration of the infarcted pig heart. *Journal of the American College of Cardiology*, 58(9), 977-986.

Ellison, G.M., Vicinanza, C., Smith, A.J., Aquila, I., Leone, A., Waring, C.D., Henning, B.J., Stirparo, G.G., Papait, R., Scarfò, M., Agosti, V., Viglietto, G., Condorelli, G., Indolfi, C., Ottolenghi, S., Torella, D., Nadal-Ginard, B. (2013) Adult c-kit(pos) cardiac stem cells are necessary and sufficient for functional cardiac regeneration and repair. *Cell,* 154(4):827-42.

Ellison, G.M., Smith, A.J., Waring, C.D., Henning, B.J., Burdina, A.O., Polydorou, J., Vicinanza, C., Lewis, F.C., Nadal-Ginard, B., Torella, D. (2014) Adult Cardiac Stem Cells: Identity, Location and Potential. *Adult Stem Cells: Stem Cell Biology and Regenerative Medicine*, pp 47-90.

Evans, M.J., Kaufman, M.H. (1981) Establishment in culture of pluripotential cells from mouse embryos. *Nature*, 292, 154-156

Ezashi, T., Telugu, B.P., Alexenko, A.P., Sachdev, S., Sinha, S., Roberts, R.M. (2009) Derivation of induced pluripotent stem cells from pig somatic cells. *Proceedings of the National Academy of Sciences of the United States of America*, 106(27), 10993-10998

Faulkner, J.A., Brooks, S.V., Zerba, E. (1995) Muscle atrophy and weakness with aging: contraction-induced injury as an underlying mechanism. *The journals of gerontology. Series A, Biological sciences and medical sc*iences, 50, 124-129

Finkielstain G.P., Forcinito, P., Lui, J.C., Barnes, K.M., Marino, R., Makaroun, S., Nguyen, V., Lazarus, J.E., Nilsson, O., Baron, J. (2009) An extensive genetic program occurring during postnatal growth in multiple tissues. *Endocrinology*, 150 (4), 1791-800.

Formicola, L., Marazzi, G., Sassoon, D.A. (2014), The extraocular muscle stem cell niche is resistant to ageing and disease. *Frontiers in Ageing Neuroscience*, 6, 328.

Fransioli, J., Bailey, B., Gude, N.A., Cottage, C.T., Muraski, J.A., Emmanuel, G., Wu, W., Alvarez, R., Rubio, M., Ottolenghi, S., Schaefer, E., Sussman, M.A. (2008) Evolution of the c-kit-positive cell response to pathological challenge in the myocardium. *Stem Cells* 26(5), 1315-1324.

Fuchs, E. (2008) Skin stem cells: rising to the surface. *The Journal of Cell Biology*, 80 (2), 273-284.

Garvin, K., Feschuk, C., Sharp, J.G., Berger, A. (2007) Does the number or quality of pluripotent bone marrow stem cells decrease with age? *Clinical Orthopedics and Related Research*, 465, 202-7

Gao, L., Thilakavathy, K., Nordin, N. (2013) A Plethora of Human Pluripotent Stem Cells. *Cell Biology International*. 37(9), 875-887.

Genead, R., Danielsson, C., Andersson, A.B., Corbascio, M., Franco-Cereceda, A., Sylvén, C., Grinnemo, K.H. (2010) Islet-1 cells are cardiac progenitors present during the entire lifespan: from the embryonic stage to adulthood. *Stem Cells and Development*, 19(10), 1601-1615.

Goldstein, S. (1974) Agine in vitro: Growth of cultured cells from the Galapagos tortoise. *Experimental Cell research*, 83 (2), 297-302.

Gupta, S., Verfaillie, C., Chmielewski, D., Kren, S., Eidman, K., Connaire, J., Heremans, Y., Lund, T., Blackstad, M., Jiang, Y., Luttun, A., Rosenberg, M.E. (2006) Isolations and characterization of kidney-derived stem cells. *Journal of the American Society of Nephrology*, 17 (11), 3028-40.

Gussoni, E., Soneoka, Y., Strickland, C.D., Buzney, E.A., Khan, M.K., Flint, A.F., Kunkel, L.M., Mulligan, R.C. (1999) Dystrophin expression in the mdx mouse restored by stem cell transplantation. *Nature*, 401 (6751), 390-4.

Hardy, K., Hooper, M.A., Handyside, A.H., Rutherford, A.J., Winston, R.M., Leese, H.J. (1989) Non-invasive measurement of glucose and pyruvate uptake by individual human oocytes and preimplantation embryos. *Human Reproduction*, 4(2), 188-191.

Hart, A.H., Hartley, L., Ibrahim, M., Robb, L. (2004) Identification, cloning and expression analysis of the pluripotency promoting Nanog genes in mouse and human. *Developmental Dynamics*, 230(1), 187-198

Hawke, T.J., Garry, D.J. (2001) Myogenic satellite cells: physiology to molecular biology. *Journal of Applied Physiology*, 91(2), 534-551

Hayflick, L., Moorhead, P.S. (1961) The serial cultivation of human diploid cell strains. *Experimental Cell Research*, 25, 585-621.

Hayflick, L. (1973) The biology of human ageing. *The American Journal of the Medical Sciences*, 265 (6), 432-45

Hayflick, L. (1979) The cell biology of ageing. *The Journal of Investigative Dermatology*, 73 (1), 8-14.

Hierlihy, A.M., Seale, P., Lobe, C.G., Rudnicki, M.A., Megeney, L.A. (2002) The post-natal heart contains a myocardial stem cell population. *FEBS Letters,* 530(1-3), 239-243.

Holmes, C., Stanford, W.L. (2007) Concise review: stem cell antigen-1: expression, function, and enigma. *Stem Cells*, 25 (6), 1339-47.

Hsieh, P.C., Segers, V.F., Davis, M.E., MacGillivray, C., Gannon, J., Molkentin, J.D., Robbins, J., Lee, R.T. (2007) Evidence from a genetic fate-mapping study that stem cells refresh adult mammalian cardiomyocytes after injury. *Nature Medicine*, 13(8), 970-974.

Hunter, J.J., Chien, K.R. (1999) Signaling pathways for cardiac hypertrophy and failure. *The New England Journal of Medicine*, 341(17), 1276-1283.

Iwasaki, H., Akashi, K. (2007) Myeloid lineage commitment from the hematopoietic stem cell. *Immunity*, 26(6), 726-740.

Jackson, K.A., Mi, T., Goodell, M.A. (1999) Hematopoietic potential of stem cells isolated from murine skeletal muscle. *Proceedings of the National Academy of Sciences of the United States of America*, 96 (25), 14482-6.

Jessup, M., Brozena, S. (2003) Heart failure. *The New England Journal of Medicine*, 348 (20), 2007-18.

Joe, A.W., Yi, L., Natarajan, A., Le Grand, F., So, L., Wang, J., Rudnicki, MA., Rossi, F.M. (2010) Muscle injury activates resident fibro/adipogenic progenitors that facilitate myogenesis. *Nature Cell Biology*, 12(2), 153-163.

Jones, D.A., Round, J.M. (1990) *Skeletal Muscle in health and Disease: A Textbook of Muscle Physiology*: Manchester University Press.

Jones, J.C., Kroscher, K.A., Dilger, A.C. (2014) Reductions in expression of growth regulating genes in skeletal muscle with age in wild type and myostatin null mice. *BMC Pysiology*, 14:3. doi: 10.1186/1472-6793-14-3.

Judson, R.N., Zhang, R.H., Rossi, F.M. (2013) Tissue-resident mesenchymal stem/progenitor cells in skeletal muscle: collaborators or saboteurs? *The FEBS Journal*, 280 (17), 4100-8.

Kallestad, K.M, McLoon, L.K. (2010) Defining the heterogeneity of skeletal muscle-derived side and main population cells isolated immediately ex vivo. *Journal of Cellular Physiology*, 222 (3), 676-84.

Kajstura, J., Leri, A., Finato, N., Di Lorento, C., Beltrami, C.A., Anversa, P. (1998) Myocyte proliferation in end-stage cardiac failure in humans. *Proceedings of the National Academy of Sciences of the United States of America,* 95 (15), 8801-5.

Kang, S., Yang, Y.J., Li, C.J., Gao, R.L. (2008) Effects of intracoronary autologous bone marrow cells on left ventricular function in acute myocardial infarction: a systematic review and meta-analysis for randomized controlled trials. *Coronary Artery Disease*, 19 (5), 327-35.

Knoepfler, P.S. (2009) Deconstructing Stem Cell Tumorigenicity: A roadmap to safe regenerative medicine. *Stem Cells*, 27(5), 1050-1056.

Kordes, C., Häussinger, D. (2013) Hepatic stem cell niches. *The Journal of Clinical Investigation*, 123 (5), 1874-80.

Koudstaal, S., Jansen Of Lorkeers, S.J., Gaetani, R., Gho, J.M., van Slochteren, F.J., Sluijter, J.P., Doevendans, P.A., Ellison, G.M., Chamuleau, S.A. (2013) Concise review: heart regeneration and the role of cardiac stem cells. *Stem Cells Translational Medicine*, 2 (6), 434-43.

Koudstaal, S., Bastings, M.M., Feyen, D.A., Waring, C.D., van Slochteren, F.J., Dankers, P.Y., Torella, D., Sluijter, J.P., Nadal-Ginard B,, Doevendans, P.A., Ellison, G.M., Chamuleau, S.A. (2014) Sustained delivery of insulin-like growth factor-1/hepatocyte growth factor stimulates endogenous cardiac repair in the chronic infarcted pig heart. *Journal of Cardiovascular Translational Research*, 7 (2), 232-41.

Kuhn, H.G., Dickinson-Anson, H., Gage, F.H. (1996) Neurogenesis in the dentate gyrus of the adult rat: age-related decrease of neuronal progenitor proliferation. *The Journal of Neuroscience*, 16 (6), 2027-33.

Kuroiwa, Y., Kaneko-Ishino, T., Kagitani, F., Kohda, T., Li, L.L., Tada, M., Suzuki, R., Yokoyama, M., Shiroishi, T., Wakana, S., Barton, S.C., Ishino, F., Surani, M.A. (1996) Peg3 imprinted gene on proximal chromosome 7 encodes for a zinc finger protein. *Nature Genetics*, 12 (2), 186-90.

Laflamme, M.A., Murry, C.E .(2011) Heart regeneration. *Nature,* 473(7347), 326-335.

Laugwitz, K.L., Moretti, A., Lam, J., Gruber, P., Chen, Y., Woodard, S., Lin, L.Z., Cai, C.L., Lu, M.M., Reth, M., Platoshyn, O., Yuan, J.X., Evans, differentiated cardiomyocyte lineages. *Nature,* 433(7026), 647-653.

Lewis, F.C., Henning, B.J., Marazzi, G., Sassoon, D., Ellison, G.M., Nadal-Ginard, B. (2014) Porcine skeletal muscle-derived multipotent PW1pos/Pax7neg interstitial cells: isolation, characterization, and long-term culture. *Stem Cells Translational Medicine*, 3 (6), 702-12.

Li, L., Keverne, E.B., Aparicio, S.A., Ishino, F., Barton, S.C., Surani, M.A. (1999) Regulation of maternal behavior and offspring growth by paternally expressed Peg3. *Science*, 284 (5412), 330-3.

Li, W., Wei, W., Zhu, S., Zhu, J., Shi, Y., Lin, T., Hao, E., Hayek, A., Deng, H., Ding, S. (2009) Generation of rat and human induced pluripotent stem cells by combining genetic reprogramming and chemical inhibitors. *Cell Stem Cell*, 4(1), 16-19

Li, T.S., Cheng, K., Lee, S.T., Matsushita, S., Davis, D., Malliaras, K., Zhang, Y., Matsushita, N., Smith, R.R., Marbán, E. (2010) Cardiospheres recapitulate a niche-like microenvironment rich in stemness and cell-matrix interactions, rationalizing their enhanced functional potency for myocardial repair. *Stem Cells,* 28(11), 2088-2098.

Li, Q., Zhang, X., Peng, Y., Chai, H., Xu, Y., Wei, J., Ren, X., Wang, X., Liu, W., Chen, M., Huang, D. (2013) Comparison of the sorting efficiency and influence on cell function between the sterile flow cytometry and immunomagnetic bead purification methods. *Preparative Biochemistry and Biotechnology*, 43 (2), 197-206.

Liberman, J., Sartelet, H., Flahaut, M., Mühlethaler-Mottet, A., Coulon, A., Nyalendo, C., Vassal, G., Joseph, J.M., Gross, N. (2012) Involvement of the CXCR7/CXCR4/CXCL12 axis in the malignant progression of human neuroblastoma. *PLoS One*, 7 (8), e43665.

Limana, F., Zacheo, A., Mocini, D., Mangoni, A., Borsellino, G., Diamantini, A., De Mori, R., Battistini, L., Vigna, E., Santini, M., Loiaconi, V., Pompilio, G., Germani, A., Capogrossi, M.C. (2007) Identification of myocardial and vascular precursor cells in human and mouse epicardium. *Circulation Research*, 101(12), 1255-1265.

Linke, A., Müller, P., Nurzynska, D., Casarsa, C., Torella, D., Nascimbene, A., Castaldo, C., Cascapera, S., Böhm, M., Quaini, F., Urbanek, K., Leri, A., Hintze, T.H., Kajstura, J., Anversa, P. (2005) Stem cells in the dog heart are self-renewing, clonogenic, and multipotent and regenerate infarcted myocardium, improving

cardiac function. *Proceedings of the National Academy of Sciences of the United States of America,* 102(25), 8966-8971.

Lipinski, M.J., Biondi-Zoccai, G.G., Abbate, A., Khianey, R., Sheiban, I., Bartunek, J., Vanderheyden, M., Kim, H.S., Kang, H.J., Strauer, B.E., Vetrovec, G.W. (2007) Impact of intracoronary cell therapy on left ventricular function in the setting of acute myocardial infarction: a collaborative systematic review and meta-analysis of controlled clinical trials. *Journal of the American College of Cardiology*, 50 (18), 1761-7.

Liu, X., Driskell, R.R., Engelhardt, J.F. (2006) Stem cell in the lung. *Methods in Enzymology*, 419, 285-321.

Liu, H., Zhu, F., Yong, J., Zhang, P., Hou, P., Li, H., Jiang, W., Cai, J., Liu, M., Cui, K., Qu, X., Xiang, T., Lu, D., Chi, X., Gao, G., Ji, W., Ding, M., Deng, H. (2008) Generation of induced pluripotent stem cells from adult rhesus monkey fibroblasts. *Cell Stem Cell*, 3 (6), 587-92.

Liu, L., Rando, T.A. (2011) Manifestations and mechanisms of stem cell aging. *The Journal of Cell Biology*, 193 (2), 257-66.

Lui, J.C., Baron, J. (2011) Mechanisms Limiting Body Growth in Mammal. *Endocrine Reviews*, 32 (3), 422-440.

Maegawa, S., Yoshioka, H., Itaba, N., Kubota, N., Nishihara, S., Shirayoshi, Y., Nanba, E., Oshimura, M. (2001) Epigenetic silencing of PEG3 gene expression in human glioma cell lines. *Molecular Carcinogenesis*, 31 (1), 1-9.

Makkar, R.R., Smith, R.R., Cheng, K., Malliaras, K., Thomson, L.E., Berman, D., Czer, L.S., Marbán, L., Mendizabal, A., Johnston, P.V., Russell, S.D., Schuleri, K.H., Lardo, A.C., Gerstenblith, G., Marbán, E. (2012) Intracoronary cardiosphere-derived cells for heart regeneration after myocardial infarction

(CADUCEUS): a prospective, randomised phase 1 trial. *Lancet,* 379(9819), 895-904.

Malliaras, K., Makkar, R.R., Smith, R.R., Cheng, K., Wu, E., Bonow, R.O., Marbán, L., Mendizabal, A., Cingolani, E., Johnston, P.V., Gerstenblith, G., Schuleri, K.H., Lardo, A.C., Marbán, E. (2014) Intracoronary cardiosphere-derived cells after myocardial infarction: evidence of therapeutic regeneration in the final 1-year results of the CADUCEUS trial (CArdiosphere-Derived aUtologous stem CElls to reverse ventricUlar dySfunction). *Journal of the American College of Cardiology*, 63 (2), 110-22.

Martin, C.M., Meeson, A.P., Robertson, S.M., Hawke, T.J., Richardson, J.A., Bates, S., Goetsch, S.C., Gallardo, T.D., Garry, D.J. (2004) Persistent expression of the ATP-binding cassette transporter, Abcg2, identifies cardiac SP cells in the developing and adult heart. *Developmental Biology,* 265(1), 262-275.

Malmqvist, U.P., Aronshtam, A., Lowey, S. (2004) Cardiac myosin isoforms from different species have unique enzymatic and mechanical properties. *Biochemistry*, 43 (47), 15058-65.

Matsuura, K., Nagai ,T., Nishigaki, N., Oyama, T., Nishi, J., Wada, H., Sano, M., Toko, H., Akazawa, H., Sato, T., Nakaya, H., Kasanuki, H., Komuro, I. (2004) Adult cardiac Sca-1-positive cells differentiate into beating cardiomyocytes. *The Journal of Biological Chemistry*, 279(12), 11384-11391.

Mauro, A. (1961) Satellite cell of skeletal muscle fibers. *The Journal of Biophysical and Biochemical Cytology*, 9, 493-495.

Messina, E., De Angelis, L., Frati, G., Morrone, S., Chimenti, S., Fiordaliso, F., Salio, M., Battaglia, M., Latronico, M.V., Coletta, M., Vivarelli, E., Frati, L., Cossu, G., Giacomello, A. (2004) Isolation and expansion of adult cardiac stem cells from human and murine heart. *Circulation Research*, 95(9), 911-921.

Minasi, M.G., Riminucci, M., De Angelis, L., Borello, U., Berarducci, B., Innocenzi, A., Caprioli, A., Sirabella, D., Baiocchi, M., De Maria, R., Boratto, R., Jaffredo, T., Broccoli, V., Bianco, P., Cossu, G. (2002) The meso-angioblast: a multipotent, self-renewing cell that originates from the dorsal aorta and differentiates into most mesodermal tissues. *Development*, 129 (11), 2773-83.

Mitchell, K.J., Pannérec, A., Cadot, B., Parlakian, A., Besson, V., Gomes, E.R., Marazzi, G., Sassoon, D.A. (2010) Identification and characterization of a non-satellite cell muscle resident progenitor during postnatal development. *Nature Cell Biology*, 12(3), 257-266

Mitsui, K., Tokuzawa, Y., Itoh, H., Segawa, K., Murakami, M., Takahashi, K., Maruyama, M., Maeda, M., Yamanaka, S. (2003) The homeoprotein Nanog is required for maintenance of pluripotency in mouse epiblast and ES cells. *Cell*, 113(5), 631-642

Montarras, D., Morgan, J., Collins, C., Relaix, F., Zaffran, S., Cumano, A., Partridge, T., Buckingham, M. (2005) Direct isolation of satellite cells for skeletal muscle regeneration. *Science*, 309(5743), 2067-2067.

Moretti, A., Caron, L., Nakano, A., Lam, J.T., Bernshausen, A., Chen, Y., Qyang, Y., Bu, L., Sasaki, M., Martin-Puig, S., Sun, Y., Evans, S.M., Laugwitz, K.L., Chien, K.R. (2006) Multipotent embryonic isl1+ progenitor cells lead to cardiac, smooth muscle, and endothelial cell diversification. *Cell*, 127 (6), 1151-65.

Morrison, S.J., Kimble, J. (2006) Asymmetric and symmetric stem-cell divisions in development and cancer. *Nature*, 441 (7097), 1068-74.

Morton, J.P., Kayani, A.C., McArdle, A., Drust, B. (2009) The exercise-induced stress response of skeletal muscle, with specific emphasis on humans. *Sports Medicine*, 39 (8), 643-62.

Müller, T., Fleischmann, G., Eildermann, K., Mätz-Rensing, K., Horn, P.A., Sasaki, E., Behr, R. (2009) A novel embryonic stem cell line derived from the common marmoset monkey (Callithrix jacchus) exhibiting germ cell-like characteristics. *Human Reproduction*, 24(6), 1359-1372

Murphy, M.M., Lawson, J.A., Mathew, S.J., Hutcheson, D.A., Kardon, G. (2011) Satellite cells, connective tissue fibroblasts and their interactions are crucial for muscle regeneration. *Development*, 138(17), 3625-3637.

Murry, C.E., Soonpaa, M.H., Reinecke, H., Nakajima, H., Nakajima, H.O., Rubart, M., Pasumarthi, K.B., Virag, J.I., Bartelmez, S.H., Poppa, V., Bradford, G., Dowell, J.D., Williams, D.A., Field, L.J. (2004) Haematopoietic stem cells do not transdifferentiate into cardiac myocytes in myocardial infarcts. *Nature*, 428 (6983), 664-8.

Nadal-Ginard, B. (1978) Commitment, fusion and biochemical differentiation of a myogenic cell line in the absence of DNA synthesis. *Cell.* 15(3), 855-864.

Nadal-Ginard, B., Kajstura, J., Leri, A., Anversa, P. (2003) Myocyte death, growth, and regeneration in cardiac hypertrophy and failure. *Circulation Research*, 92(2), 139-150.

Nadal-Ginard, B., Torella, D., Ellison, G.M. (2006) Cardiovascular regenerative medicine at the crossroads. Clinical trials of cellular therapy must now be based on reliable experimental data from animals with characteristics similar to human's, *Revista española de cardiologiá*, 59 (11), 1175-89.

Neal, A., Boldrin, L., Morgan, J.E. (2012) The satellite cell in male and female, developing and adult mouse muscle: distinct stem cells for growth and regeneration. *PLoS One*, 7 (5), e37950.

Nichols, J., Zevnik, B., Anastassiadis, K., Niwa, H., Klewe-Nebenius, D., Chambers, I., Schöler, H., Smith, A. (1998) Formation of pluripotent stem cells in the mammalian embryo depends on the POU transcription factor Oct4. *Cell*, 95(3), 379-391

Niwa, H., Miyazaki, J., Smith, A.G. (2000) Quantitative expression of Oct-3/4 defines differentiation, dedifferentiation or self-renewal of ES cells. *Nature Genetics*, 24(4), 372-376.

O'Connor, T.P., Crystal, R.G. (2006) Genetic medicines: treatment strategies for hereditary disorders. *Nature Reviews: Genetics*, 7 (4), 261-76.

Ogawa, T., Dobrinski, I., Avarbock, M.R., Brinster, R.L. (2000) Transplantation of male germ line stem cells restores fertility in infertile mice. *Nature Medicine*, 6(1), 29-34.

Oh, H., Taffet, G.E., Youker, K.A., Entman, M.L., Overbeek, P.A., Michael, L.H., Schneider, M.D. (2001) Telomerase reverse transcriptase promotes cardiac muscle cell proliferation, hypertrophy, and survival. *Proceedings of the National Academy of Sciences of the United States of America*, 98(18), 10308-10313.

Oh, H., Bradfute, S.B., Gallardo, T.D., Nakamura, T., Gaussin, V., Mishina, Y., Pocius, J., Michael, L.H., Behringer, R.R., Garry, D.J., Entman, M.L., Schneider, M.D. (2003) Cardiac progenitor cells from adult myocardium: homing, differentiation, and fusion after infarction. *Proceedings of the National Academy of Sciences of the United States of America*, 100(21), 12313-12318.

Oh, H., Chi, X., Bradfute, S.B., Mishina, Y., Pocius, J., Michael, L.H., Behringer, R.R., Schwartz, R.J., Entman, M.L., Schneider, M.D. (2004) Cardiac muscle plasticity in adult and embryo by heart-derived progenitor cells. *Annals of the New York Academy of Sciences*, 1015, 182-9.

Oishi, T., Uezumi, A., Kanaji, A., Yamamoto, N., Yamaguchi, A., Yamada, H., Tsuchida, K. (2013) Osteogenic differentiation capacity of human skeletal muscle-derived progenitor cells. *PLoS One*, 8(2), e56641.

Orlic, D., Kajstura, J., Chimenti, S., Jakoniuk, I., Anderson, S.M., Li, B., Pickel, J., McKay, R., Nadal-Ginard, B., Bodine, D.M., Leri, A., Anversa, P. (2001) Bone marrow cells regenerate infarcted myocardium. *Nature* , 410 (6829), 701-5.

Osawa, M., Hanada, K., Hamada, H., Nakauchi, H. (1996) Long-term lymphohematopoietic reconstitution by a single CD34-low/negative hematopoietic stem cell. *Science*, 273, 242-245.

Oustanina, S., Hause, G., Braun, T. (2004) Pax7 directs postnatal renewal and propagation of myogenic satellite cells but not their specification. *The EMBO Journal*, 23 (16), 3430-9.

Overy, H.R., Priest, R.E. (1966) Mitotic cell division in postnatal cardiac growth. *Laboratory Investigation*, 15 (6), 1100-3.

Oyama, T., Nagai, T., Wada, H., Naito, A.T., Matsuura, K., Iwanaga, K., Takahashi, T., Goto, M., Mikami, Y., Yasuda, N., Akazawa, H., Uezumi, A., Takeda, S., Komuro, I. (2007) Cardiac side population cells have a potential to migrate and differentiate into cardiomyocytes in vitro and in vivo. *The Journal of Cell Biology*, 176(3), 329-341.

Pagliuca, F.W., Millman, J.R., Gürtler, M., Segel ,M., Van Dervort, A., Ryu, J.H., Peterson, Q.P., Greiner, D., Melton, D.A. (2014) Generation of functional human pancreatic β cells in vitro. *Cell*, 159 (2), 428-39.

Pannérec, A., Formicola, L., Besson, V., Marazzi, G., Sassoon, D.A. (2013) Defining skeletal muscle resident progenitors and their cell fate potentials. *Development*, 140 (14), 2879-91.

Paspala, S.A., Murthy, T.V., Mahaboob, V.S., Habeeb, M.A. (2011) Pluripotent stem cells - a review of the current status in neural regeneration. *Neurology India*, 59 (4), 558-65.

Pauklin, S., Pedersen, R.A., Vallier, L. (2011) Mouse pluripotent stem cells at a glance. *Journal of Cell Science,* 124 (22), 3727-32.

Pearson, C.M. (1963) Muscular Dystrophy. Review and recent observations. *The American Journal of Medicine*, 35, 632-45.

Péault, B., Rudnicki, M., Torrente, Y., Cossu, G., Tremblay, J.P., Partridge, T., Gussoni, E., Kunkel, L.M., Huard, J. (2007) Stem and progenitor cells in skeletal muscle development, maintenance, and therapy. *Molecular Therapy: the Journal of the American Society of Gene Therapy*, 15(5), 867-877

Pfister, O., Mouquet, F., Jain, M., Summer, R., Helmes, M., Fine, A., Colucci, W.S., Liao, R. (2005) CD31- but Not CD31+ cardiac side population cells exhibit functional cardiomyogenic differentiation. *Circulation Research*, 97(1), 52-61.

Preffer ,F.I., Dombkowski, D., Sykes, M., Scadden, D., Yang, Y.G. (2002) Lineage-Negative Side-Population (SP) Cells with Restricted Hematopoietic Capacity Circulate in Normal Human Adult Blood: Immunophenotypic and Functional Characterization. Stem Cells, 20 (5). 417-427.

Preisler, H.D., Lutton, J.D., Giladi, M., Goldstein, K., Zanjani, E.D. (1975) Loss of clonogenicity in agar by differentiating erythroleukemic cells. *Life Sciences*, 16(8), 1241-1251.

Price, F.D., Kuroda, K., Rudnicki, M.A. (2007) Stem cell based therapies to treat muscular dystrophy. *Biochimica et Biophysica Acta*, 1772(2), 272-283.

Rando, T.A. (2006) Stem cells, ageing and the quest for immortality. *Nature*, 441, 1080-1086.

Relaix, F., Weng, X., Marazzi, G., Yang, E., Copeland, N., Jenkins, N., Spence, S.E., Sassoon, D. (1996) Pw1, a novel zinc finger gene implicated in the myogenic and neuronal lineages. *Developmental Biology*, 177 (2), 383-96.

Relaix, F., Montarras, D., Zaffran, S., Gayraud-Morel, B., Rocancourt, D., Tajbakhsh, S., Mansouri, A., Cumano, A., Buckingham, M. (2005) Pax3 and Pax7 have distinct and overlapping functions in adult muscle progenitor cells. *The Journal of Cell Biology*, 172 (1), 91-102.

Renault, V., Thorne, L.E., Eriksson, P.O., Butler-Browne, G.,Mouly, V. (2002) Regenerative potential of human skeletal muscle during aging. Aging Cell, 1 (2), 132-9.

Rizzino, A. (2009) Sox2 and Oct-3/4: a versatile pair of master regulators that orchestrate the self-renewal and pluripotency of embryonic stem cells. Wiley Interdisciplinary Reviews. Systems Biology and Medicine, 1 (2), 228-36.

Roskoski, R. Jr. (2005) Signaling by Kit protein-tyrosine kinase-the stem cell factor receptor. *Biochemical and Biophysical Research Communications*, 337(1), 1-13.

Rostovskaya,M., Anastassiadis, K. (2012) Differential expression of surface markers in mouse bone marrow mesenchymal stromal cell subpopulations with distinct lineage commitment. *PLoS One,* 7 (12), e51221.

Samal, R., Ameling, S., Wenzel, K., Dhople, V., Völker, U., Felix, S.B., Könemann, S., Hammer, E. (2012) OMICS-based exploration of the molecular phenotype of resident cardiac progenitor cells from adult murine heart. *Journal of Proteomics*, 75(17), 5304-5315.

Sampaolesi, M., Torrente, Y., Innocenzi, A., Tonlorenzi, R., D'Antona, G., Pellegrino, M.A., Barresi, R., Bresolin, N., De Angelis, M.G., Campbell, K.P., Bottinelli, R., Cossu, G. (2003) Cell therapy of alpha-sarcoglycan null dystrophic mice through intra-arterial delivery of mesoangioblasts. Science, 301 (5632), 487-92.

Sampaolesi, M., Blot, S., D'Antona, G., Granger, N., Tonlorenzi, R., Innocenzi, A., Mognol, P., Thibaud, J.L., Galvez, B.G., Barthélémy, I., Perani, L., Mantero, S., Guttinger, M., Pansarasa, O., Rinaldi, C., Cusella De Angelis, M.G., Torrente, Y., Bordignon, C., Bottinelli, R., Cossu, G. (2006) Mesoangioblast stem cells ameliorate muscle function in dystrophic dogs. *Nature*, 444 (7119), 574-9.

Sampaziotis, F., Cardoso de Brito, M., Madrigal, P., Bertero, A., Saeb-Parsy, K., Soares, F.A., Schrumpf, E., Melum, E., Karlsen, T.H., Bradley, J.A., Gelson, W.T., Davies, S., Baker, A., Kaser, A., Alexander, G.J., Hannan, N.R., Vallier, L.. (2015) Cholangiocytes derived from human induced pluripotent stem cells for disease modeling and drug validation. *Nature Biotechnology*, doi: 10.1038/nbt.3275.

Schmalbruch, H., Lewis, D.M. (2000) Dynamics of nuclei of muscle fibers and connective tissue cells in normal and denervated rat muscles. *Muscle Nerve*, 23 (4), 617-26.

Schöler, H.R., Dressler, G.R., Balling, R., Rohdewohld, H., Gruss, P. (1990) Oct-4: a germline-specific transcription factor mapping to the mouse t-complex. *The EMBO Journal*, 9(7), 2185-2195.

Schultz, E., Lipton, B.H. (1982) Skeletal muscle satellite cells: changes in proliferation potential as a function of age. *Mechanisms of Ageing and Development*, 20(4), 377-383.

Seale, P., Sabourin, L.A., Girgis-Gabardo, A., Mansouri, A., Gruss, P., Rudnicki, M.A. (2000) Pax7 is required for the specification of myogenic satellite cells. *Cell*, 102(6), 777-786.

Secker, G.A, Daniels, J.T. (2009) Limbal epithelial stem cells of the cornea. *StemBook, The Stem Cell Research Community*, doi/10.3824/stembook.1.48.1,

Senyo, S.E., Steinhauser, M.L., Pizzimenti, C.L., Yang, V.K., Cai, L., Wang, M., Wu, T.D., Guerquin-Kern, J.L., Lechene, C.P., Lee, R.T. (2013) Mammalian heart renewal by pre-existing cardiomyocytes. *Nature*, 493 (7432), 433-6.

Shadrach, J.L., Wagers, A.J. (2011) Stem cells for skeletal muscle repair. *Philosophical transactions of the Royal Society of London. Series B, Biological sciences*, 366(1575), 2297-2306.

Sharma, M., Afrin, F., Satija, N., Tripathi, R.P., Gangenahalli, G.U. (2011) Stromal-derived factor-1/CXCR4 signaling: indispensable role in homing and engraftment of hematopoietic stem cells in bone marrow. *Stem Cells and Development*, 20 (6), 933-46.

Shefer, G., Rauner, G., Yablonka-Reuveni, Z., Benayahu, D. (2010) Reduced satellite cell numbers and myogenic capacity in aging can be alleviated by endurance exercise. *PLoS One*, 5 (10), e13307.

Shi, M., Li, J., Liao, L., Chen, B., Li, B., Chen, L., Jia, H., Zhao, R.C. (2007) Regulation of CXCR4 expression in human mesenchymal stem cells by cytokine treatment: role in homing efficiency in NOD/SCID mice. Haematologica, 92 (7), 897-904.

Shih, C.C., Forman, S.J., Chu, P., Slovak, M. (2007) Embryonic stem cells are prone to generate primitive, undifferentiated tumors in engrafted human fetal

tissues in severe combined immunodeficient mice. *Stem Cells and Development*, 16, 893–902

Sigurjonsson, O.E., Perreault, M.C., Egeland, T., Glover, J.C.. (2005) Adult human hematopoietic stem cells produce neurons efficiently in the regenerating chicken embryo spinal cord. *Proceedings of the National Academy of Sciences of the United States of America*, 102 (14), 5227-32.

Smith, R.R., Barile, L., Cho, H.C., Leppo, M.K., Hare, J.M., Messina, E., Giacomello, A., Abraham, M.R., Marbán, E. (2007) Regenerative potential of cardiosphere-derived cells expanded from percutaneous endomyocardial biopsy specimens. *Circulation*, 115(7), 896-908.

Smith, A.J., Lewis, F.C., Aquila, I., Waring, C.D., Nocera, A., Agosti, V., Nadal-Ginard, B., Torella, D., Ellison, G.M. (2014) Isolation and characterization of resident endogenous c-Kit+ cardiac stem cells from the adult mouse and rat heart. *Nature Protocols*, 9(7), 1662-81.

Snippert, H.J., Clevers, H. (2011) Tracking adult stem cells. *EMBO Reports*, 12(2), 113-122.

Soonpaa, M.H., Field, L.J. (1998) Survey of studies examining mammalian cardiomyocyte DNA synthesis. *Circulation Research*, 83(1), 15-26.

Stuermer, E.K., Lipenksy, A., Thamm, O., Neugebauer, E., Schaefer, N., Fuchs, P., Bouillon, B., Koenen, P. (2015) The role of SDF-1 in homing of human adipose-derived stem cells. *Wound Repair and Regeneration*, 23 (1), 82-9.

Suzuki, T., Takaishi, H., Sakata, T., Do, M.K., Hara, M., Sato, A., Mizunoya, W., Nishimura, T., Hattori, A., Ikeuchi, Y., Tatsumi, R. (2010) In vitro measurement of post-natal changes in proliferating satellite cell frequency during rat muscle growth. *Animal Science Journal*, 81 (2), 245-51.

Syed, B.A., Evans, J.B. (2013) Stem Cell Therapy Market. Nature Reviews: *Drug Discovery*, 12 (3), 185-6.

Takahashi, K., Yamanaka, S. (2006) Induction of pluripotent stem cells from mouse embryonic and adult fibroblast cultures by defined factors. *Cell*, 126, 663–676.

Takahashi, K., Tanabe, K., Ohnuki, M., Narita, M., Ichisaka, T., Tomoda, K., Yamanaka, S. (2007) Induction of pluripotent stem cells from adult human fibroblasts by defined factors. *Cell*, 131, 861-872.

Takamiya, M., Haider, K.H., Ashraf, M. (2011) Identification and characterization of a novel multipotent sub-population of Sca-1$^+$ cardiac progenitor cells for myocardial regeneration. *PLoS One,* 6(9), e25265.

Takebe, T., Sekine, K., Enomura, M., Koike, H., Kimura, M., Ogaeri, T., Zhang, R.R., Ueno, Y., Zheng, Y.W., Koike, N., Aoyama, S., Adachi, Y., Taniguchi, H. (2013) Vascularized and functional human liver from an iPSC-derived organ bud transplant. *Nature*, 449 (7459), 481-4.

Taylor, C.J., Bolton, E.M., Bradley, J.A. (2011) Immunological considerations for embryonic and induced pluripotent stem cell banking. *Philosophical transactions of the Royal Society of London. Series B, Biological sciences*, 366, 2312-2322

Tedesco, F.S., Dellavalle, A., Diaz-Manera, J., Messina, G., Cossu, G. (2010) Repairing skeletal muscle: regenerative potential of skeletal muscle stem cells. *The Journal of Clinical Investigation*, 120(1), 11-9.

Thomas, E.D. (1999) A history of haemopoietic cell transplantation. *British Journal of Haematology*, 105(2), 330-339.

Thomson, J.A., Itskovitz-Eldor, J., Shapiro, S.S., Waknitz, M.A., Swiergiel, J.J., Marshall, V.S., Jones, J.M. (1998) Embryonic stem cell lines derived from human blastocysts. *Science*, 282(5391), 1145-1147.

Till, J.E., McCulloch, E.A. (1961) A direct measurement of the radiation sensitivity of normal mouse bone marrow cells. *Radiation Research*, 14, 213-222.

Tögel, F., Isaac, J., Hu, Z., Weiss, K., Westenfelder, C. (2005) Renal SDF-1 signals mobilization and homing of CXCR4-positive cells to the kidney after ischemic injury. *Kidney International*, 67(5):1772-84.

Tomita, Y., Matsumura, K., Wakamatsu, Y., Matsuzaki, Y., Shibuya, I., Kawaguchi, H., Ieda, M., Kanakubo, S., Shimazaki, T., Ogawa, S., Osumi, N., Okano, H., Fukuda, K. (2005) Cardiac neural crest cells contribute to the dormant multipotent stem cell in the mammalian heart. *The Journal of Cell Biology*, 170 (7), 1135-46.

Tonlorenzi, R., Dellavalle, A., Schnapp, E., Cossu, G., Sampaolesi, M. (2007) Isolation and characterization of mesoangioblasts from mouse, dog, and human tissues. *Current Protocols in Stem Cell Biology*, Chapter 2:Unit 2B.1. doi: 10.1002/9780470151808.sc02b01s3

Torella, D., Rota, M., Nurzynska, D., Musso, E., Monsen, A., Shiraishi, I., Zias, E., Walsh, K., Rosenzweig, A., Sussman, M.A., Urbanek, K., Nadal-Ginard, B., Kajstura, J., Anversa, P., Leri, A. (2004) Cardiac stem cell and myocyte aging, heart failure, and insulin-like growth factor-1 overexpression. Circulation Research, 94 (4), 514-24.

Torella, D., Ellison, G.M., Méndez-Ferrer, S., Ibanez, B., Nadal-Ginard, B. (2006a) Resident human cardiac stem cells: role in cardiac cellular homeostasis and potential for myocardial regeneration. *Nature Clinical Practice. Cardiovascular Medicine*, 3 Suppl 1, s8-13.

Torella, D., Ellison, G.M., Karakikes, I., Galuppo, V., De Serio, D., Onorati, F., Mastroroberto, P., Renzulli, A., Indolfi, C., Nadal-Ginard, B. (2006b) Biological properties and regenerative potential, in vitro and in vivo, of human cardiac stem cells isolated from each of the four chambers of the adult human heart. *Circulation,* 114: 87.

Torella, D., Ellison, G.M., Karakikes, I., Nadal-Ginard, B. (2007) Resident cardiac stem cells. *Cellular and Molecular Life Sciences*, 64(6), 661-673.
Uezumi, A., Fukada, S., Yamamoto, N., Takeda, S., Tsuchida, K. (2010) Mesenchymal progenitors distinct from satellite cells contribute to ectopic fat cell formation in skeletal muscle. *Nature cell Biology*, 12(2), 143-152

Uezumi, A., Fukada, S., Yamamoto, N., Takeda, S., Tsuchida, K. (2010) Mesenchymal progenitors distinct from satellite cells contribute to ectopic fat cell formation in skeletal muscle. *Nature Cell Biology*, 12 (2), 143-52.

Unno, K., Jain, M., Liao, R. (2012) Cardiac side population cells: moving toward the center stage in cardiac regeneration. *Circulation Research*, 110 (10), 1355-63.

van Tuyn, J., Atsma, D.E., Winter, E.M., van der Velde-van Dijke, I., Pijnappels, D.A., Baxm N.A., Knaän-Shanzer, S., Gittenberger-de Groot, A.C., Poelmann, R.E., van der Laarse, A., van der Wall, E.E., Schalij, M.J., de Vries, A.A. (2007) Epicardial cells of human adults can undergo an epithelial-to-mesenchymal transition and obtain characteristics of smooth muscle cells in vitro. *Stem Cells*, 25(2), 271-278.

von Zglinicki, T., Saretzki, G., Döcke, W., Lotze, C. (1995) Mild hyperoxia shortens telomeres and inhibits proliferation of fibroblasts: a model for senescence? Experimental Cell Research, 220 (1), 186-96.

Wang, X., Hu, Q., Nakamura, Y., Lee, J., Zhang, G., From, A.H., Zhang, J. (2006) The role of the sca-1+/CD31- cardiac progenitor cell population in postinfarction left ventricular remodeling. *Stem Cells,* 24(7), 1779-1788.

Wang, F., Scoville, D., He, X.C., Mahe, M.M., Box, A., Perry, J.M., Smith, N.R., Lei, N.Y., Davies, P.S., Fuller, M.K., Haug, J.S., McClain, M., Gracz, A.D., Ding, S., Stelzner, M., Dunn, J.C., Magness, S.T., Wong, M.H., Martin, M.G., Helmrath, M., Li, L. (2013) Isolation and characterization of intestinal stem cells based on surface marker combinations and colony-formation assay. Gastroenterology, 145 (2), 383-95.

Waring, C.D., Vicinanza, C., Papalamprou, A., Smith, A.J., Purushothaman, S., Goldspink, D.F., Nadal-Ginard, B., Torella, D., Ellison, G.M. (2012) The adult heart responds to increased workload with physiologic hypertrophy, cardiac stem cell activation, and new myocyte formation. European Heart Journal. 35 (39), 2722-31

Winter, E.M., Grauss, R.W., Hogers, B., van Tuyn, J., van der Geest, R., Lie-Venema, H., Steijn, R.V., Maas, S., DeRuiter, M.C., deVries, A.A., Steendijk, P., Doevendans, P.A., van der Laarse, A., Poelmann, R.E., Schalij, M.J., Atsma, D.E., Gittenberger-de Groot, A.C .(2007) Preservation of left ventricular function and attenuation of remodeling after transplantation of human epicardium-derived cells into the infarcted mouse heart. *Circulation*, 116(8), 917-927.

Winter, E.M., van Oorschot, A.A., Hogers, B., van der Graaf, L.M., Doevendans, P.A., Poelmann, R.E., Atsma, D.E., Gittenberger-de Groot, A.C., Goumans, M.J. (2009) A new direction for cardiac regeneration therapy: application of synergistically acting epicardium-derived cells and cardiomyocyte progenitor cells. *Circulation: Heart Failure*, 2(6), 643-653.

Yang, C.C., Cotsarelis, G. (2011) Review of hair follicle dermal cells. *Journal of Dermatological Science*, 57(1), 2-11.

Yaniz-Galende, E., Formicola, L., Mougenot, N., Legrand, L., Chen, J., Hajjar, R.J., Marazzi, G., Sassoon, D., Hulot, J.S. (2014) Identification of a Novel Cardiac Progenitor Population Expressing Pw1/peg3 in the Murine Heart. Circulation, 130-A18698.

Ye, J., Boyle, A., Shih, H., Sievers, R.E., Zhang, Y., Prasad, M., Su, H., Zhou, Y., Grossman, W., Bernstein, H.S., Yeghiazarians, Y. (2012) Sca-1+ cardiosphere-derived cells are enriched for Isl1-expressing cardiac precursors and improve cardiac function after myocardial injury. *PLoS One,* 7(1), e30329.

Yellowley, C. (2013) CXCL12/CXCR4 signaling and other recruitment and homing pathways in fracture repair. BoneKEy Reports, 2, 300.

Yu, J., Vodyanik, M.A., Smuga-Otto, K., Antosiewicz-Bourget, J., Frane, J..L, Tian, S., Nie, J., Jonsdottir, G.A., Ruotti, V., Stewart, R., Slukvin, I.I., Thomson, J.A. (2007) Induced pluripotent stem cell lines derived from human somatic cells. *Science*, 318, 1917-1920

Zammit, P.S., Partridge, T.A., Yablonka-Reuveni, Z. (2006) The skeletal muscle satellite cell: the stem cell that came in from the cold. *The Journal of Histochemistry and Cytochemistry*, 54(11), 1177-1191.

Zhang, J., Wang, X., Chen, B., Suo, G., Zhao, Y., Duan, Z., Dai, J. (2005) Expression of Nanog gene promotes NIH3T3 cell proliferation. *Biochemical and Biophysical Research Communications*, 338(2), 1098-1102.

Zhao, T., Zhang, Z.N., Rong, Z., Xu, Y. (2011) Immunogenicity of induced pluripotent stem cells. *Nature*, 474, 212-215.

Zhu, B., Murthy, S.K. (2013) Stem Cell Separation Technologies. *Current opinion in chemical engineering*, 2(1), 3-7.

11. APPENDIX

Table 11.1   **qRT-PCR CT values of bulk PICs**

Gene	Bulk PICs
	Mean CT ± SD
GAPDH	19.79 ± 0.15
Sox2	28.75 ± 0.10
Oct3/4	25.71 ± 0.81
Nanog	24.96 ± 0.10
PW1	19.92 ± 0.19
CD34	27.20 ± 0.76
Sca-1	25.82 ± 0.45
CD45	34.73 ± 0.65
CD146	24.13 ± 0.07

Table 11.2   qRT-PCR CT values of clonal PICs

Gene	C1	C2	C3
	Mean CT ± SD	Mean CT ± SD	Mean CT ± SD
GAPDH	18.50 ± 0.06	17.26 ± 0.03	16.65 ± 0.2
Sox2	33.85 ± 0.90	33.00 ± 0.24	33.39 ± 0.52
Oct3/4	26.83 ± 0.13	24.63 ± 0.52	24.20 ± 0.23
Nanog	25.52 ± 0.69	24.61 ± 0.21	24.89 ± 0.22
PW1	23.45 ± 0.87	20.35 ± 0.5	20.78 ± 0.88
CD34	32.42 ± 0.35	27.47 ± 0.49	27.88 ± 0.88
Sca-1	30.07 ± 0.27	25.82 ± 0.45	25.70 ± 0.39
Gene	**C4**	**C5**	**C12**
	Mean CT ± SD	Mean CT ± SD	Mean CT ± SD
GAPDH	16.25 ± 0.58	16.88 ± 0.06	17.95 ± 0.00
Sox2	33.10 ± 0.28	33.50 ± 0.16	35.25 ±1.82
Oct3/4	25.83 0.68	24.23 ± 0.58	26.04 ± 1.69
Nanog	24.82 0.35	24.55 ± 0.17	24.83 ± 0.11
PW1	19.85 0.10	19.55 ± 0.86	19.47 ± 0.58
CD34	27.67 0.34	26.06 ± 0.19	26.91 ± 0.31
Sca-1	24.49 0.36	24.45 ± 0.13	25.30 ± 0.10
Gene	**C9**	**C9 P10**	**C9 P20**
	Mean CT ± SD	Mean CT ± SD	Mean CT ± SD
GAPDH	18.50 ± 0.06	19.28 ± 0.53	18.37 ± 0.07
Sox2	29.12 ± 0.70	37.78 ± 0.12	33.07 ± 0.37
Oct3/4	25.75 ± 0.54	23.27 ± 0.72	23.04 ± 0.62
Nanog	25.15 ± 0.20	26.23 ± 0.17	27.20 ± 0.63
PW1	19.55 ± 0.22	19.42 ± 0.28	20.44 ± 0.20
CD34	28.40 ± 0.75	26.26 ± 0.47	25.22 ± 0.93
Sca-1	25.34 ± 0.89	23.93 ± 0.22	24.55 ± 0.30

Table 11.3   qRT-PCR CT values of myogenic differentiation

Gene	Myogenic Mean CT ± SD	Gene	Undifferentiated Mean CT ± SD
GAPDH	27.56 ± 0.61	GAPDH	19.28 ± 0.53
β-actin	27.12 ± 0.90	n/a	n/a
MHC	29.42 ± 0.37	MHC	23.94 ± 0.23
α-sarc	27.88 ± 0.13	a-sarc	24.24 ± 0.20
SMA	27.14 ± 0.64	SMA	24.28 ± 0.10

Table 11.4   qRT-PCR CT values of cardiomyogenic differentiation

Gene	Cardiomyogenic Mean CT ± SD	Gene	Undifferentiated Mean CT ± SD
GAPDH	14.83 ± 0.25	GAPDH	16.98 ± 0.29
β-actin	15.36 ± 0.19	Cx43	27.61 ± 0.47
Cx43	21.97 ± 0.26	cTnI	27.61 ± 0.47
α-sarc	12.73 ± 0.14	GAPDH	19.28 ± 0.53
GAPDH	21.58 ± 0.84	a-sarc	24.24 ± 0.20
β-actin	22.39 ± 0.37	n/a	n/a
cTnI	27.50 ± 0.75	n/a	n/a

Table 11.5   qRT-PCR CT values of endothlial differentiation

Gene	Endothelial Mean CT ± SD	Gene	Undifferentiated Mean CT ± SD
GAPDH	19.26 ± 0.14	GAPDH	19.28 ± 0.53
β-actin	23.26 ± 0.34	n/a	n/a
CD31	28.67 ± 0.72	CD31	26.37 ± 0.04
vWF	27.67 ± 0.26	vWF	30.27 ± 3.76
CD146	28.61 ± 1.01	CD146	25.79 ± 0.20
CD34	26.90 ± 0.13	CD34	26.26 ± 0.47

Table 11.6   qRT-PCR CT values of hepatic differentiation

Gene	Hepatic	Gene	Undifferentiated
	Mean CT ± SD		Mean CT ± SD
GAPDH	24.19 ± 0.24	**GAPDH**	19.28 ± 0.53
β-actin	23.24 ± 0.44	n/a	n/a
CK18	28.23 ± 1.21	**CK18**	25.57 ± 0.35
CK19	29.21 ± 0.43	**CK19**	26.65 ± 0.39
Albumin	26.29 ± 0.84	**Albumin**	25.16 ± 0.17
HNF1α	25.86 ± 1.20	**HNF1α**	24.76 ± 0.59

Table 11.7   qRT-PCR CT values of neuronal differentiation

Gene	Neuronal	Gene	Undifferentiated
	Mean CT ± SD		Mean CT ± SD
GAPDH	19.78 ± 0.74	**GAPDH**	19.28 ± 0.53
β-actin	19.90 ± 0.27	n/a	n/a
β3-tubulin	24.08 ± 0.32	**β3-tubulin**	23.64 ± 0.16
ChAT	25.26 ± 0.63	**ChAT**	24.74 ± 0.33
ENO2	24.17 ± 0.04	**ENO2**	24.34 ± 0.40
GFAP	24.92 ± 0.13	**GFAP**	23.76 ± 0.23

Table 11.8   qRT-PCR CT values of GFP PICs

Gene	GFP PICs
	Average CT ± SD
GAPDH	20.04 ± 0.33
Sox2	33.32 ±0.59
Oct3/4	36.10 ± 1.07
Nanog	23.90 ± 0.48
CD34	30.17 ± 0.42
PW1	21.20 ± 0.33
Sca-1	25.32 ± 0.54

Table 11.9   qRT-PCR CT values of CSCs

Gene	CSCs Average CT ± SD
GAPDH	17.76 ± 0.37
Sox2	33.19 ± 0.27
Oct3/4	35.14 ± 0.40
Nanog	27.79 ± 0.23
c-kit	32.16 ± 0.75
GAPDH	17.50 ± 0.08
CD31	29.33 ± 1.26
GAPDH	17.65 ± 0.54
CD34	22.81 ± 0.05
CD45	32.92 ± 0.07
GAPDH	17.00 ± 0.08
PW1	22.98 ± 0.19